



The
University
Of
Sheffield.

EngD: The performance of stormwater treatment
devices and methods for measuring maintenance
requirements.

By:

Mr Matthew F Mahoney

A thesis submitted in partial fulfilment
of the requirements for the degree of
Doctor of Engineering

University of Sheffield
Faculty of Engineering

STREAM IDC

December 2018

To my Fiancé Michael

ABSTRACT

With the UK urban based population growing, and separate drainage systems increasingly utilised, surface water bodies will become increasingly polluted by urban stormwater run-off. The Up-Flo[®] Filter System is a stormwater treatment device designed by Hydro International Ltd, which utilises sedimentation and filtration. This EngD project was formed to understand the systems performance and to optimise its maintenance, whilst also developing knowledge about porous media, including its use as a filter media and sound propagation through it. A bespoke made rig containing the Up-Flo[®] Filter System was constructed. Numerous experiments were conducted, with measurements of; filter media permeability, sediment removal efficiency and sediment particle size. Additionally, bench scale and in-situ experiments were conducted to assess acoustic and conductance techniques to develop a filter media monitoring system.

Full scale rig experiments provided in-depth information regarding the Up-Flo[®] Filter System's removal mechanisms. A key finding was that the filter media's permeability experiences a long term decline due to stratification, reducing the maximum treatment capacity of the system. This stratification effect was found to be a greater impact on permeability than typical sediment capture. Additionally, recommendations are made to optimise the performance and maintenance routines.

Acoustic sensor development suffered from low signal-to-noise issues identified in the bench scale experiments. However, measured attenuation in deaired samples were similar to previously published data. The effect of sediment caused greater attenuation than observed in clean media samples. This, and the in-situ experimental results, show acoustics is a possible technique for monitoring, but requires work to overcome the air effects within the filter media. Additionally, in-situ testing of a bespoke made novel multi-probe conductance device found it was capable of monitoring flow rate through the media, water level, saturation, and permeability.

ACKNOWLEDGMENTS


I would like to thank my supervisors, Prof. Simon Tait, Prof. Kirill Horoshenkov and Dr Andrew Nichols at the University of Sheffield for their invaluable guidance and support throughout this EngD research project. I wish to also say thank you to the technicians in the University of Sheffield Civil Engineering Department for all their help in constructing the equipment and all their help in the project. I am also grateful to Dr. Daniel Jarman and others at Hydro International Ltd for their support in this project.

I would like to also express my gratitude towards STREAM IDC for providing me opportunities for personal development and for their support throughout the project. I would also like to thank EPSRC and Hydro International Ltd for funding this research project, as well as UKCRIC for funding the Malvern Mastersizer which allowed for in-depth measurements to be conducted.

Furthermore, I would like to thank Jack Wreathall for his help in completing the sediment dosed experiments in this project. I would also like to thank Fran Pick, Sally Weston and Luke Peters for proof-reading my work. Finally, I would like to thank all my friends and family for their support throughout this project, in particular my Fiancé Michael for his continued support and encouragement.

STATEMENT OF ORIGINALITY

Unless otherwise stated in the text, the work described in this thesis was carried out solely by the candidate. None of this work has already been accepted for any degree, nor is it concurrently submitted in candidature for any degree.

Candidate: M. 

Mr Matthew F Mahoney

CONTENTS

List of Figures	xi
List of Tables	xvi
List of Acronyms	xvii
Nomenclature	xviii
Chapter 1: Introduction	1
1.1 Background	1
1.2 The Up-Flo® Filter System	3
1.3 Research Motive and Aims	7
1.4 Contributions	9
1.5 Thesis Formation	10
Chapter 2: Literature Review	11
2.1 Urban Stormwater Pollution	12
2.2 Urban Stormwater Treatment in the United Kingdom	15
2.3 Particle Settlement	20
2.4 Filter Media Capture	24
2.5 Acoustical Techniques	32
2.6 Electrical Techniques	51
2.7 Chapter Summary	56
Chapter 3: Up-Flo® Filter System Experiments	59
3.1 Experiment Identification Table	61
3.2 Material Information Table	63
3.3 Experimental Strategy	64
3.4 Experimental Methodology	66

3.5	Post Measurement Processing	84
3.6	Results	95
3.7	Clean Water Experiment Permeability Results	97
3.8	ST01 Permeability Results	106
3.9	ST02 Permeability Results	108
3.10	ST03 Permeability Results	112
3.11	Permeability Results Comparison	114
3.12	Up-Flo® Filter Total Suspended Solids Results	116
3.13	Mass Balance Results	127
3.14	Filter Media Efficiency Results	134
3.15	Chapter Discussion	140
3.16	Chapter Summary	151
Chapter 4:	Filter Media Monitoring Experiments	153
4.1	Acoustic Experiment Identification Table	154
4.2	Acoustic Experimental Strategy	156
4.3	Acoustic Experimental Method	158
4.4	Clogged Media Preparation	170
4.5	Acoustic Data Analysis Techniques	170
4.6	Acoustic Results	171
4.7	Acoustic Distance Experimental Results	185
4.8	Conductance Probe Experimental Method	186
4.9	Conductance Probe Data Analysis Techniques	188
4.10	Conductance Probe Experimental Results	190
4.11	Chapter Discussion	197
4.12	Chapter Summary	200
Chapter 5:	Regulatory Compliance & Maintenance	202
5.1	The Up-Flo® and Treatment Regulations	203
5.2	Regulation Discussion	215
5.3	Maintenance Guidelines	219
5.4	Chapter Summary	221

Chapter 6: Discussion	222
6.1 Up-Flo® Filter System Experiments	224
6.2 Filter Media Monitoring	234
6.3 Conclusion	239
Chapter 7: Thesis Summary	241
References	245
Appendix A: Permeability Experiment Identification Table	262
Appendix B: Permeability Chapter Appendix	265
B.1 VT.jpg	265
B.2 Hydro UpFlo Installation Blueprint.pdf	265
B.3 Flow control.vi	265
B.4 Error propagation.pdf	265
B.5 ST02 M4 Camera Calibration.pdf	265
B.6 ST03 M4 Calibration.pdf	265
B.7 PERMCOMPLETE v2.m	265
B.8 PSA Settings.pdf	265
B.9 Sand.pdf	265
Appendix C: Acoustic Experiment Identification Table	266
Appendix D: Filter Monitoring Appendix	270
D.1 Olympus Transducer Calibration Sheets.pdf	270
D.2 Oscilloscope Settings.set	270
D.3 Transducer LabVIEW Continuous Signal Programme.vi	270
D.4 AT42 to AT82 FFT Analysis.m	270
D.5 AT83 to AT92 FFT Analysis.m	270
D.6 AT93 to AT99 Integral Code.m	270
D.7 Conductance Probe Design.pdf	270
D.8 Sediment Conductance Control File.vi	270
D.9 Conductance Analysis File.m	270

Appendix E: Filter Guidelines Appendix	271
E.1 China Standards.pdf	271

LIST OF FIGURES

1.1	Cross-sectional view of the MCTT developed at the University of Alabama-Birmingham by Pitt <i>et al</i> [10].	3
1.2	Annotated CGI Cross Section of Hydro International Ltds Up-Flo [®] Filter System [12] [Not to scale].	5
1.3	Annotated CGI Cross Section of Hydro International Ltds Up-Flo [®] Filters Module [12] [Not to scale].	6
2.1	Particle Sieve analyses for sediment samples from different urban catchments. With the benchmark ranges for stormwater pond sediment and street/road dust [9].	13
2.2	Particle types in sedimentation [37].	20
2.3	Streamlines of water flow [50].	27
2.4	Schematic of radii of a rough sediment particle [70].	37
2.5	Buckingham’s wave speed and Wood’s Equation vs mean grain diameter using Hamilton’s previous published data. vfs = very fine sands, fs = fine sands, ms = medium sand, and cs = coarse sand [70].	39
2.6	Hickey, et al. Graph of phase velocity for type 1 (circle) and type 2 (triangle) waves with different bulk moduli. Solid lines are Chotiros values of bulk modulus and dashed are calculated values [82].	43
2.7	Damascenco and Fratta figure showing arrangement of ERT and the two different schemes possible; (a) Basic 16 electrode ERT system with simulated inclusion, and electric potential lines for (b) adjacent and (c) opposing excitation scheme [96].	51
2.8	Multi-probe array by Nichols [99].	54
2.9	Plot of probe length and voltage per probe [99].	54
3.1	Annotated image of the collection box.	67

3.2	Experimental set-up for Clean Water Experiments, T01 to T23 (Not to scale).	69
3.3	Particle size analysis of Fraction B Sand, using Malvern Mastersizer 3000.	69
3.4	Location Numbers for Modules in the Up-Flo [®] Rig.	70
3.5	Approximate Location of Pressure Tappings in Up-Flo [®] Module 4 (Original image from [102]) [Not to scale].	71
3.6	Experimental set-up for sediment experiments with sampling points highlighted in red (Not to Scale).	73
3.7	Picture of sediment mixer and pump during ST01.	74
3.8	Particle Size Analysis of silica flour and Sil-Co-Sil 106 samples, using Malvern Mastersizer 3000.	75
3.9	Plan View of Collection Tank with 1 Micron Polyester Felt Filter Socks (Not to Scale).	76
3.10	Picture of installed Filter Socks in ST01.	77
3.11	Particle Size Analysis of Garside Sand, using Malvern Mastersizer 3000.	80
3.12	PSA of Fraction E sediment.	84
3.13	Reynolds Number against Flow Rate for Fraction B and Garside Sand with various particle sizes.	87
3.14	Core Sample Locations from ST02 Bag H (Bottom Bag).	92
3.15	Module 4 T11 permeability and flow rate against time. 2 Stage (2S) at 2 Ls^{-1}	97
3.16	Method Analysis of the Final Permeability Values across Module 4 Filter Media during the Clean Water Experiments. 1S is 1 Stage, 2S is 2 Stage and WM is Whole Module.	98
3.17	Final permeability values against experiment flow rate. 1S is 1 Stage, 2S is 2 Stage and WM is Whole Module.	99
3.18	Permeability against number of days from T04. 1S is 1 Stage, 2S is 2 Stage and WM is Whole Module.	100
3.19	T04 and T16 images of water level in the rig, demonstrating the rise in water level through the experimental program indicating a long term decrease in permeability.	100

3.20	Final permeability readings across the Whole Module for M4 Clean Water Experiments against Test Number. 1S is 1 Stage, 2S is 2 Stage and WM is Whole Module.	101
3.21	Percentage changes in Whole Module 4 Final Permeability Value from last recorded experiment Final Permeability Value with outliers removed.(T05, T17 and T22).	102
3.22	Final permeability readings across the Top Bag for Module 4 Clean Water Experiments against Test Number. 1S is 1 Stage, 2S is 2 Stage and TB is Top Bag.	103
3.23	Final permeability readings across the Bottom Bag for Module 4 Clean Water Experiments against Test Number. 1S is 1 Stage, 2S is 2 Stage and BB is Bottom Bag.	103
3.24	Exponential constant against test number from Whole Module 4 permeability results.	105
3.25	Permeability results for ST01 for Module 4 across the Whole Module (WM).	106
3.26	Permeability across Modules 4 (M4), 2 (M2) and 1 (M1) during ST02 T29.	108
3.27	Water head comparison in each module during T29. M4 is Module 4, M2 is Module 2 and M1 is Module 1.	110
3.28	Permeability across Module 4 (M4) over ST02 at $2 Ls^{-1}$ 2 Stage.	111
3.29	Permeability across Module 4 over ST03. WM is Whole Module.	112
3.30	TSS values during ST01 T28 against time with Influent being $501 mgL^{-1} \pm 2.8 mgL^{-1}$. T28 Sediment start time at 45 mins, experiment ended at 152 mins due to Filter Sock clogging.	117
3.31	TSS values during ST02 T33 & T34 against time with influent being $569.6 mgL^{-1} \pm 3.1 mgL^{-1}$. T33 sediment dosing start time 45 mins. T34 sediment dosing start time 0 mins.	118
3.32	TSS Values during ST03 T39 & T40 against time. Influent TSS estimated to be $561.21 mgL^{-1} \pm 3.1 mgL^{-1}$. Sediment dosing began at 45 mins in T39 and 0 mins in T40.	120

3.33 Sediment Experiment Up-Flo [®] Filter System overall removal efficiencies against time. Sediment start time; T28, T33 and T39 was 45 mins, T34 and T40 was 0 mins.	121
3.34 ST01 T28 Up-Flo [®] Filter System removal efficiency of particle sizes.	123
3.35 ST02 T33 Up-Flo [®] Filter System removal efficiency of particle sizes.	124
3.36 ST02 T34 Up-Flo [®] Filter System removal efficiency of particle sizes.	125
3.37 ST01 Mass Balance.	127
3.38 ST02 Mass Balance.	128
3.39 ST03 Mass Balance.	129
3.40 ST01 Sediment Mass collected by the Up-Flo [®] sump.	130
3.41 ST02 Sediment Mass collected by the Up-Flo [®] sump.	131
3.42 ST03 Sediment Mass collected by the Up-Flo [®] sump.	132
3.43 PSA using the Malvern Mastersizer 3000 of Fraction E and a sample from the Up-Flo [®] sump.	133
3.44 ST02 Core Sample Particle Size Analysis of Module 2 Top Bag and Bottom Bags.	134
3.45 Flow distributing top matallas after ST02.	136
3.46 ST03 Core Sample Particle Size Analysis of Module 2 Top and Bottom Bags.	136
3.47 ST02 filter media capture estimate against particle size.	138
3.48 Max treatment capacity against permeability. Using T14 pressure data where overflow was used.	142
4.1 Aluminium Acoustic Test Vessel, measurements in <i>mm</i>	158
4.2 Aluminium Test Vessel.	159
4.3 The final transducer holder made using a 3D printer.	160
4.4 Photo of Acoustic Transducer in 3D printed holder.	161
4.5 Experimental set-up used for experiments AT42 to AT53 [Not to scale].	162
4.6 Partition in the media.	163
4.7 Image of experiment AT42 500 <i>kHz</i> sent pulse, with a duration of 1.52 μs	163
4.8 Hydrophone experimental set-up [Not to scale].	166
4.9 Acoustic transducers in bottom bag of Module 3 for experiments ST02 and ST03.	169

4.10	FFT results of the received 350 kHz pulse in various vacuumed media samples.	171
4.11	FFT results of the received 350 kHz pulse in various non-vacuumed media.	173
4.12	FFT analysis of 500 kHz pulse in water and water in bag.	174
4.13	FFT results of the received 500 kHz pulse in various clogged media in bag.	175
4.14	FFT results of the received 500 kHz pulse in various deaired clogged media.	176
4.15	FFT results of the received 500 kHz pulse in various deaired Fraction B media.	177
4.16	FFT results of the received 500 kHz pulse in various deaired 10% clogged media.	177
4.17	FFT results of the received 500 kHz pulse in various 16 hour deaired media.	178
4.18	Attenuation of 500 kHz pulse in various media.	179
4.19	FFT of Hydrophone Data.	180
4.20	Pulse energy against experimental time for ST02.	181
4.21	Pulse energy against experimental time for ST03.	183
4.22	Multi-probe conductance device after ST03.	186
4.23	Conductance profile recorded in Module 4 during ST02 T32 clean water experiment.	188
4.24	Conductance profiles in Module 4 of Up-Flo [®] Filter System at various flow rates, with the modules regions highlighted. Points A, B and C denote the approximate locations of the pressure tappings.	191
4.25	ST02 Gradient Comparison. (Sediment start times: T33 45 mins, T34 0 mins).	192
4.26	ST03 Gradient Comparison. (Sediment start times: T39 45 mins, T40 0 mins).	194
4.27	Conductance gradient across both filter media bags against recorded permeability during experiments ST02 and ST03 at $2 Ls^{-1}$. Experimental times taken: 30 mins then every 15 mins until end of experiment.	195

LIST OF TABLES

2.1	Biot-Stoll geophysical inputs [69].	33
3.1	Permeability Experiment Number Identification Table.	62
3.2	Key information of materials used in the experimental work presented.	63
3.3	Average Percentage Errors in PSA.	91
3.4	Errors in Removal Efficiency.	94
4.1	Acoustic Experiment Number Identification Table.	154
5.1	China case study heavy metal concentrations in Beijing road run-off and the limits of receiving water bodies.	211
5.2	Heavy metal size ranges with the average removal efficiency of Up-Flo [®] Filter from ST02. (Range of metal TSS using distribution and Beijing case study [mgL^{-1}] * down to $1.056\mu m$	212
5.3	Estimate of treated Beijing run-off using the weightings and removal effi- ciencies in Table 5.2. With the regulatory targets for reference.	213
A.1	Permeability Experiment Number Identification Table. (Long)	262
C.1	Acoustic Experiment Number Identification Table. (Long)	266

LIST OF ACRONYMS

CWE Clean Water Experiments

DWA The German Association for Water, Wastewater and Waste

EA Environmental Agency

EPA Environmental Protection Agency

EU European Union

FFT Fast Fourier Transform

NJCAT New Jersey Corporation for Advance Technology

NJDEP New Jersey Department of Environmental Protection

PPA Performance Partnership Agreement

PSA Particle Size Analysis

STREAM IDC Skills Technology, Research and Management Industrial Doctoral Centre

TSS Total Suspended Solids

UK United Kingdom of Great Britain and Northern Ireland

USA United States of America

WFD Water Framework Directive

NOMENCLATURE

Symbol	Meaning	Units
α_p	Attenuation coefficient	Np/m or dB/m
α_b	Bubble attenuation coefficient	Np/cm
β_{cg}	Compressibility of solid materials	Pa^{-1}
β_{cw}	Compressibility of water	Pa^{-1}
Γ	Compressional loss tangent	Dimensionless
γ	Ratio of specific heats of the gas	Dimensionless
γ_g	Volume ratio of smaller to larger grains	Dimensionless
δ	Particle roughness single statistical parameter	μm
ζ	Rigidity (Shear Modulus)	Pa
ζ_0	Scaling factor for frictional-rigidity modulus ($=2 \times 10^9 Pa$)	Pa
θ	Angle of divergence	<i>Radians</i>
κ	Intrinsic permeability	m^2
κ_F	Forcheimer permeability	m^2
Λ	Lamé's First Parameter	Pa
λ	Filtration coefficient	m^{-1}
μ	Dynamic viscosity of the fluid	$Pa.s$
ν	Poissons ratio for particle material	Dimensionless
Ξ	Acoustic wave number	Dimensionless
π	Pi constant = 3.14159	Dimensionless
ρ	Bulk Density of porous media	kg/m^3
ρ_{eff}	Effective density	kg/m^3
ρ_g	Density of media	kg/m^3

Continuation of Nomenclature

Symbol	Meaning	Units
ρ_w	Density of fluid	kg/m^3
ϱ	Deviation from Poiseuille flow	Dimensionless
τ	Tortuosity	Dimensionless
Υ	Mass or number concentration of particles	mg/L
ϕ	Water potential	kPa
ϕ_t	Total potential	kPa
ϕ_s	Solid potential	kPa
χ_f	Compressional dissipation coefficient	Dimensionless
ω	Angular frequency	rad/s
A	Area	m^2
A_P	Polytropic coefficient	Dimensionless
$A_{quality}$	Air Quality	Dimensionless
B	Bulk modulus of porous media	Pa
B_w	Bulk modulus of water	Pa
B_g	Bulk modulus of media grains	Pa
C	Kozeny-Carmen Constant	Dimensionless
C_1	Porous media constant	Dimensionless
C_2	Porous media constant (turbulent regime)	Dimensionless
c_b	Compressional wave speed with intergranular friction	m/s
c_g	Compressional wave speed in gassy saturated media	m/s
c_p	Compressional wave speed	m/s
d	Grain diameter	m
d_0	Reference grain diameter = $1000\mu m$	μm
d_{pore}	Pore diameter	m

Continuation of Nomenclature

Symbol	Meaning	Units
E_A	Ergun Coefficient A	Dimensionless
E_B	Ergun Coefficient B	Dimensionless
F	Forcheimer coefficient	Dimensionless
f	Frequency	kHz
f_b	Bubble resonance frequency	Hz
f_c	Biot characteristic frequency	Hz
G	Constant	$m/skPa$
g_a	Acceleration due to gravity	m/s^2
ΔH	Head change	m
I	Damping constant	Dimensionless
J	Constant	m/s
K_b	Boltzmann's constant (1.38×10^{-23})	J/K
K_p	Constant	$dB/m/kHz$
k	Kinematic viscosity	m^2/s
L	Litres	L
m	Moles of vapour adsorbed	mol
m_m	Moles to cover a monolayer	mol
N	Number of contacts per head	Dimensionless
N_{mod}	Number of modules	Dimensionless
n	Porosity	Dimensionless
n_g	Gas porosity	Dimensionless
P_F	Packing factor	Dimensionless
p	Pressure	Pa
p_c	Vapour pressure above curved surface	Pa
p_f	Vapour pressure above flat surface	Pa
Q	Volumetric flow	m^3/s
q	Flow rate per unit cross-sectional area (fluid velocity)	m/s

Continuation of Nomenclature

Symbol	Meaning	Units
R	Reynolds Number	Dimensionless
r_b	Body radius	m
r_c	Contact radius	m
r_g	Gas bubble radius	m
r_m	Mean radius	m
$S_{contamination}$	Surface contamination	Dimensionless
T	Temperature	$^{\circ}C$ or K
$T_{admissible}$	Admissible value	Dimensionless
$T_{emission}$	Emission value	Dimensionless
t	Time	s
V	Voltage	V
v_s	Settling velocity	m/s
w	Monolayer coverage	m
x	Length/Thickness of the Media	m
x_b	Distance caused by Brownian motion	m
x_d	Submergence depth	m
x_i	Probe length	m
x_w	Depth of water	m

End of Nomenclature

Chapter 1

INTRODUCTION

1.1 Background

An estimated 82% of the UK population lived in urban areas in 2013 [1]. Numerous problems are associated with urban areas, one main issue is that of surface water pollution that occurs in water bodies such as rivers, canals, lakes, estuaries and coastal waters [2]. A number of potential pollutants can cause this type of pollution, however they can all fit within two main sources of pollution: point-source and diffuse.

Point-source pollution arises from discharges from man-made discrete outlets, for example pipes and effluent outfalls which are also mediated by man-made devices. Whilst diffuse pollution is resultant from when there are no discrete point of discharge and there are numerous paths the pollution can enter the water body. The diffuse pollution more generally arises from land use activities and can be difficult to control [3]. This project worked on improving treatment of diffuse pollution from urban stormwater.

A problem currently associated with the management of stormwater, is that a significant amount goes into watercourses without any treatment or undergoes treatment at a water treatment plant, through the use of a combined sewage system. The combined sewage system combines stormwater, diffuse pollution, with domestic sewage waste, non-point source, for treatment at a water treatment plant [4]. The areas drained by combined sewer systems are treated during dry weather, but during wet weather events these systems have a problem of lack of capacity to treat such large volumes. Meaning that in the case of large storm events, both the untreated stormwater and the untreated domestic sewage may have to bypass the treatment plant to discharge straight to a watercourse [5]. Targeting the diffuse pollution before it enters the watercourse reduces the impact on the environment, and by treating the diffuse pollution separately from the point-source there

will be less strain on the treatment plant. With a projected increase in rainfall of up to 10% by 2100 for some parts of the UK, and a 5% decrease in other parts due to climate change [6], it is clear that a treatment device that can handle high loads and a wide variance in pollutant concentrations is essential. Especially when considering that diffuse urban pollution accounted for 23 UK bathing water failures in 2011 [7].

A key source of diffuse urban stormwater pollution is sediment, such as that which arises from cars resultant from the wear of tires and the roads. Other sources can include chunks of pavement, dust, sand, flakes of metal and brake lining [8]. These sediment particles in urban stormwater run-off have also shown to have absorption properties, with some chemical pollutants and are also associated with other pollutants [9]. This means that through primarily targeting the sediment particles other pollutants can also be treated. Hydro International Ltd developed a stormwater treatment device, called the Up-Flo[®] Filter, which is capable of removing sediment in urban stormwater run-off.

1.2 The Up-Flo® Filter System

The Up-Flo® Filter System began at the University of Alabama-Birmingham when researchers developed the Multi Chamber Treatment Train (MCTT) device, shown in Figure 1.1, which aimed to treat stormwater pollution [10]. It contained 3 chambers that provided key functions in the treatment of the stormwater, the first chamber removed the grit and large suspended solids to protect the following chambers. The second chamber settled suspended solids and removed hydrocarbons and 8 other volatile compounds. In the final chamber a mixed media filter allowed for final polishing of the water. The device was designed to accommodate all run-off from 6 to 10 *mm* whilst removing 83 to 98% of suspended solids [10].

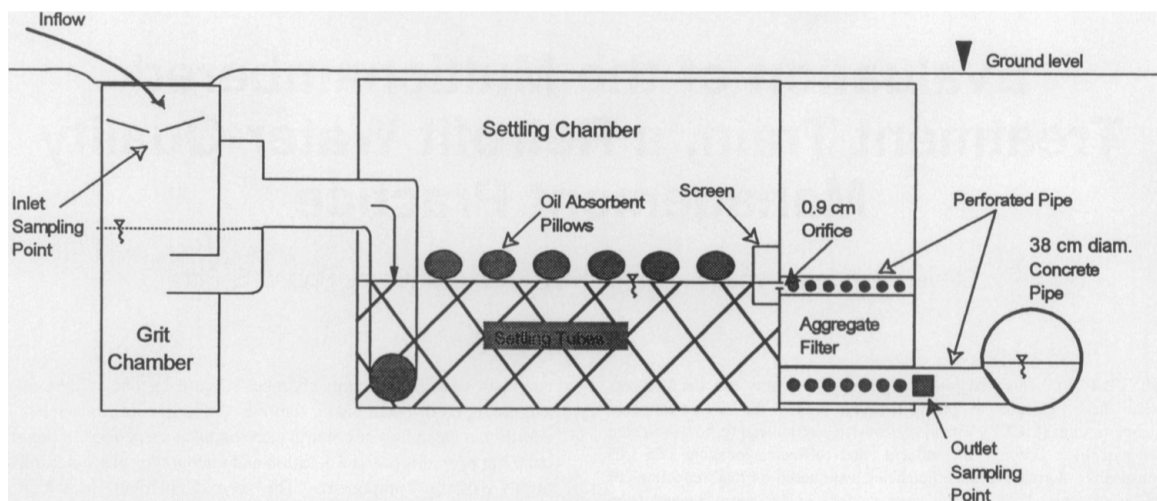


Figure 1.1: Cross-sectional view of the MCTT developed at the University of Alabama-Birmingham by Pitt *et al* [10].

Whilst the MCTT was highly effective in the aspect of treatment the cost was prohibitive, with the trial cost \$72,000, and there were problems associated with retrofitting manholes. Hydro International Ltd worked to develop a commercially viable product, the Up-Flo® Filter System, shown in Figure 1.2. This device is a simplified MCTT design with one chamber and 2-6 filter modules, shown in Figure 1.3. This device has a reduced size and reduced retrofitting requirements, due to the ease in installing into

preexisting manholes. In this set-up, the urban run-off enters the chamber via an inlet pipe which is directed between the filter modules to the sump of the chamber. In the sump the debris and large sediment settle whilst the oil and floatables rise to the surface of the water. Whilst the water fills the chamber the flow is directed through an angled screen that prevents the larger material entering the filter media. A flow distributing media, the matalla, then spreads the flow evenly across the filter media whilst the water level increases within the chamber. Once treated, the flow enters a conveyance channel to the outlet module which is connected to the outlet pipe. Each module has a treatment flow rate capacity of 1.3 Ls^{-1} [11] and in the event of a large storm event there is a designed bypass that discharges the water out, allowing a maximum hydraulic capacity of 170 Ls^{-1} [12]. Due to the unique shape of the filter modules, they could also be arranged in a rectangular shape, which allows for the Up-Flo[®] Filter System to be used in differently shaped environments. The Up-Flo[®] Filter System removed fine particles by more than 80%, heavy metals by more than 70% whilst nutrients removal efficiency was greater than 70% [13].

The improvements were needed and allowed the treatment device to be commercially viable, meaning treatment of stormwater is more likely to be taken up in developments. But problems remain with the Up-Flo[®] Filter System, particularly in regards to its maintenance routine, as the replacement of the filter media is done on a timed basis. The problem with this approach is that at the time of filter media replenishment, there is no way to measure in the field whether the filter media is in fact clogged. There is also a problem with the filter media clogging before a maintenance cycle. Both of these are problematic for the environment and for the sustainability of the Up-Flo[®] Filter System [12], due to the potential waste and discharge bypassing.

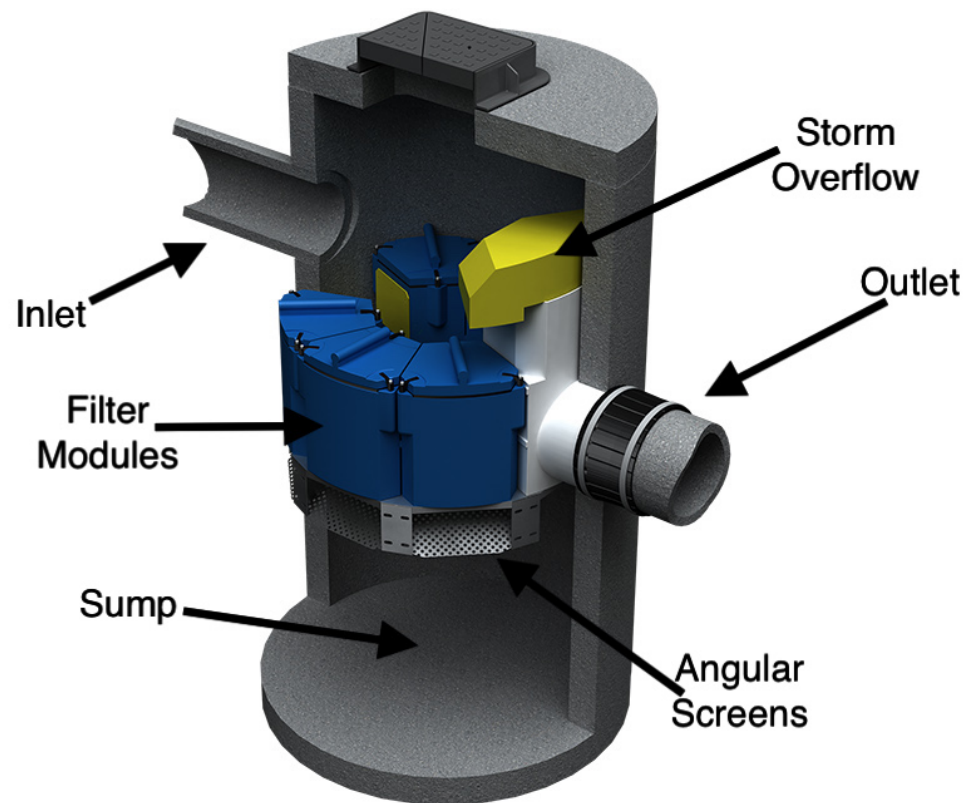


Figure 1.2: Annotated CGI Cross Section of Hydro International Ltd's Up-Flo® Filter System [12] [Not to scale].

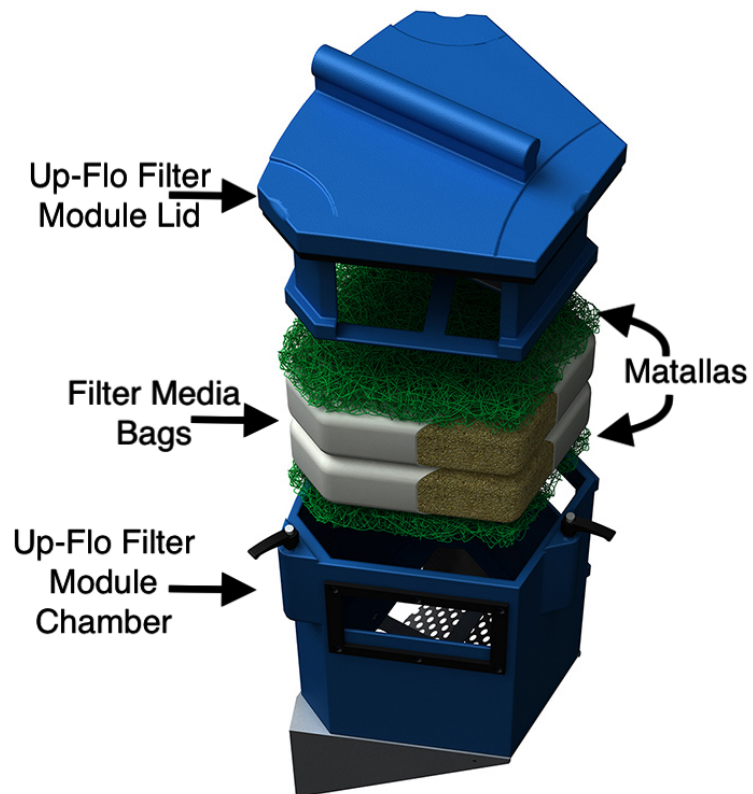


Figure 1.3: Annotated CGI Cross Section of Hydro International Ltds Up-Flo[®] Filters Module [12] [Not to scale].

1.3 Research Motive and Aims

Due to the problems outlined with the Up-Flo[®] Filter System and the impact this would have on the environment, this research project was formed to study the Up-Flo[®] Filter System in greater detail and to enhance the sustainability through the development of a sensor system. This allowed for a more in-depth understanding regarding the problems associated and possible solutions to be outlined.

To undertake this research, an EngD project was conducted within the STREAM IDC at the University of Sheffield, sponsored by EPSRC and Hydro International Ltd. This arrangement allowed a close working relationship between the industry and academia.

A PhD and a EngD is very similar with both requiring a distinct contribution to knowledge. However, there are a number of differences which have impacted this project. Primarily a PhD is aimed towards academia whilst a EngD is more aimed to industrial and non-academic research. EngD projects usually relate to the sponsor companies activities, presenting a more real world impact. With a PhD project the work is more theoretical or abstract. These differences result in the outcomes of the project being related to Hydro International Ltd products, whilst highly related the learnings can be applied elsewhere.

The aim of the industrial side of the project was the optimisation of the Up-Flo[®] Filter Systems maintenance protocols and the improvement of the system's performance. That was to be completed through developing in-depth information on the removal mechanisms of the system, and to recommend ways to improve it. Additionally, it was to be completed by researching the viability of an effective sensor system, that was capable of monitoring the state of the filter and report the findings back to the relevant party. That allowed for Hydro International Ltd to improve performance, make a more sustainable product and provide a potential decrease in long term maintenance costs.

The aim of the academic side was increased physical knowledge of granular media. This included sediment removal mechanisms and effect of flow through it. Additionally it included developing knowledge on how filter media properties, such as media saturation

and saturation cycles, influenced acoustic and electrical signals.

Throughout this research project, these aims were achieved through completing the following objectives:

1. Research the background theory and form a review of the current research literature.
2. Design and build the experimental set-up and equipment for the project, including an experimental rig for the Up-Flo[®] Filter System and a testing vessel for the acoustic transducers and electrical conductance probes.
3. Run experiments which measures various parameters such as acoustic attenuation, permeability and removal efficiency.
4. Interpret and analyse the data to provide an understanding of the removal mechanisms of the system and the acoustic and electrical techniques for monitoring filter media.
5. Form an analysis of different legal frameworks the Up-Flo[®] Filter System may operate in, and how the results of this project can be used to optimise it use.
6. Form an EngD Thesis.

1.4 Contributions

This projects research findings have been presented in various formats at STREAM IDC Challenge Weeks, Institute of Water 2017 Conference, Departmental Water Seminar and ReNUWit Industrial Advisory Board Meeting. Results from this research has also previously aided in Hydro International Ltd meeting project requirement specifications in New Zealand. It is anticipated that the results from this research will influence Hydro International Ltd product design and maintenance procedures.

1.5 Thesis Formation

This thesis has been organised into 7 distinct chapters. This chapter provides the background, motivation, and the aims & objectives of the project, whilst also presenting the Up-Flo[®] Filter System.

In Chapter 2 a review of related literature is presented. This includes: the regulatory frameworks, stormwater studies, sediment removal techniques, hydraulics, acoustics, and conductance.

Chapter 3 and 4 present the experimental work undertaken throughout the research. Chapter 3 presents the experimental work and results from the hydraulic and sediment experiments conducted on the Up-Flo[®] Filter. Whilst Chapter 4 presents the work to develop a sensor system including the acoustics and the conductance experimental work.

Based on information in Chapters 3 and 4, Chapter 5 presents an analysis of the Up-Flo[®] Filter Systems use in various regulatory environments, and guidelines on how to optimise maintenance protocols.

Chapter 6 presents a discussion of the obtained experimental results, and explains how the aims were met and recommendations on product development.

Finally, Chapter 7 presents the conclusions of this research, key findings and further recommendations for future work.

Chapter 2

LITERATURE REVIEW

This chapter presents a review of the literature which was used to structure and inform the research project. Section 2.1 outlines what problems are associated with pollution in urban stormwater and why it is necessary to treat it. The approach to the treatment of urban stormwater pollution in the United Kingdom (UK) and how it has developed and continues to develop, is presented in Section 2.2.

As Chapter 1 outlines, the Up-Flo[®] Filter System utilises a number of treatment techniques. Section 2.3 presents the first treatment technique of particle settlement, with an outline of the theory behind it and what influences it. Then Section 2.4 outlines the second treatment technique of filtration of non-settled particles through the use of a filter media. The theory behind the capture is presented, and how water flows through and what influences it.

Chapter 1 highlights the aim and objectives of the research project, objective 5 was to design and build a filter media monitoring system. Section 2.5 of this chapter outlines how acoustics could be used for this purpose and the problems associated with it. Then Section 2.6 presents how electrical resistivity could be utilised and its limitations.

Section 2.7 then summarises this review of literature to indicate to the reader the key information that has been used to structure the research project activities.

2.1 Urban Stormwater Pollution

As Chapter 1 discusses, sediment is a key source of diffuse pollution in urban stormwater [8] and sediment composition from catchment surfaces can vary significantly, due to its dependence on land use and catchment characteristics. This makes a general definition of sediment from catchment surfaces difficult, but can include fine to medium grained soil particles, particulate heavy metals, phosphorus and nitrogen [14]. Additionally, in urban areas it can also include chunks of pavement, dust, sand, flakes of metal and brake lining [8].

Whilst the exact effects of sediment is dependent on its volume, particle size distribution and chemical composition, and the receiving waters characteristics there are a number of significant effects on watercourses. Firstly, sediment can cause changes to aquatic habitats and impact the aquatic flora and fauna [14]. This is because it can cause the water body to become murky, which then prevents light to reach the depths needed for the habitats to survive. Additionally, organic matter bound to sediment degrades which utilises oxygen, lowering dissolved oxygen concentration in the watercourse impacting aquatic life [15].

Secondly, as a pollutant, sediment can impact the economic use of rivers, waterways and reservoirs. Resultant from multiple effects of sediment; such as sedimentation and reduced conveyance capacity [14].

Thirdly, as Chapter 1 outlines, sediment has adsorption capabilities resulting in it containing an array of other dangerous contaminants. These can include; pesticides, toxic metals, faecal pathogens and nutrients (such as nitrogen and phosphorus) [14]. Which is especially common with flocculated fine-grain sediment, which also can include *Salmonella* and *Cryptosporidium* which cause illness in humans [14] [16].

An important characteristic of sediment is size. Researchers at Hydro International Ltd [9] conducted a study to measure the sediment diameter at sites with different land use, the results are shown in Figure 2.1. It shows that different sites gave different values of diameter. Even similar sites such as the Residential Development Sites A and B were

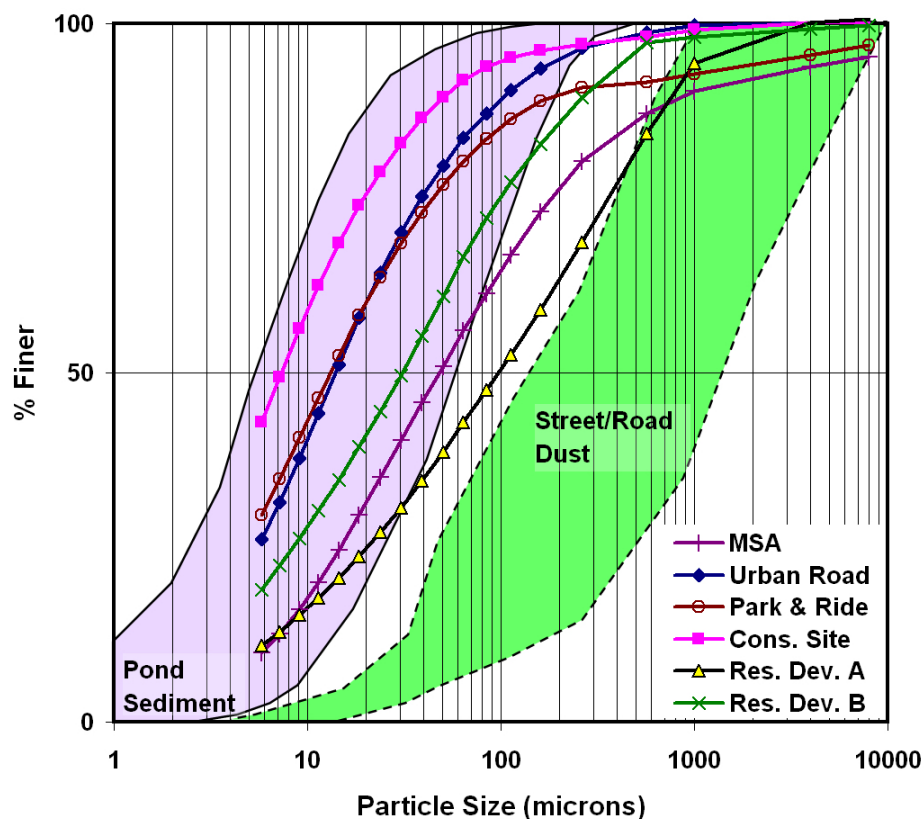


Figure 2.1: Particle Sieve analyses for sediment samples from different urban catchments. With the benchmark ranges for stormwater pond sediment and street/road dust [9].

different. The sizes varied from 7 to 112 μm [9]. In addition seasonal changes impact the sediment size characteristics washed off the catchment surfaces [17].

This was further evidenced by research conducted by Ellis [18] where the concentrations of pollutants for various sites were reported. Sediment in UK urban stormwater run-off was reported to have a typical event concentration of 190 mgL^{-1} however the range varied from 21 to 2582 mgL^{-1} [18]. As with sediment size, the site characteristics influence the typical event concentration. Ellis [19] reports the event mean characteristic ranges from 100 mgL^{-1} for low density residential sites to 280 mgL^{-1} for commercial sites [14][19]. Seasonal changes are also shown to impact sediment concentrations in urban run-off, for example gritting during winter causes additional sediment [20].

The literature shows that the concentrations and sizes of sediment particles are highly

dependent on the site condition and the seasonal changes. This results in the different effects discussed. Which means that in-depth information regarding the site characteristics and seasonal changes is required. This information would allow better urban stormwater treatment planning and better preparation to mitigate the effects of sediment pollution on the receiving water body.

2.2 Urban Stormwater Treatment in the United Kingdom

As outlined in Chapter 1, there are two types of drainage systems in the UK; combined and separate. The combined system combines stormwater with domestic sewage waste for treatment at a water treatment plant [4]. The separate system discharges stormwater straight to a watercourse [21]. The discharge of untreated stormwater, containing diffuse pollutants, would impact the environment of surface water bodies as outlined in Section 2.1.

The UK approach to stormwater treatment, in separate drainage systems, to protect surface water bodies from diffuse pollution is reviewed in this section. The UK is chosen for the review, as the UK is a key market for Hydro International Ltd's Up-Flo[®] Filter System, the UK's regulatory approach continuing to develop, and the majority of newly constructed sewerage systems since 1945 being separate drainage systems [21]. Chapter 5 presents a summary of different approaches, taken by four different countries, for stormwater management and treatment.

Numerous initiatives to highlight the problem of surface water pollution and to bring about potential solutions have been undertaken. One key initiative is the European Union (EU) Water Framework Directive (WFD), which the UK is currently bound by. This integrates water quality, water resources, physical habitat and river basin management to ensure that surface waters eventually reach good ecological status. Numerous objectives help form the WFD. Including preventing further deterioration, and protecting and enhancing the status of aquatic ecosystems. Additionally, promoting sustainable water use based on the long-term protection of available water resources and ensure the progressive reduction of surface water pollution, whilst also helping to limit the effects of floods and droughts [22].

With these objectives, the WFD attempts to provide a framework for reducing the impact of diffuse pollution. In Article 1 of the WFD a strong emphasis is placed on diffuse pollution, though this article does not explicitly define what is meant by diffuse pollution. However, Articles 11.3(h) and 11 outline the need to identify and quantify the diffuse sources. This allows for the framework to be easily adapted to the needs of the local

environment and the time, without being locked into specific diffuse pollution requirements. Further framework in Articles 4 and 7 is provided where it is required for estimates and a programme of measures to monitor and control diffuse sources within the future River Basin Management Plans (RBMPs) [23].

Many actions and initiatives were born out of the introduction of the WFD. Such as RBMPs, mentioned above, where all river catchments in member states of the EU are assigned to administrative River Basin Districts (RBDs). Within each RBD the water bodies are identified as to whether they are groundwater or as a significant type of surface water (river, lake, canal, etc.). Which has managed to improve the management of UK water bodies [24].

A key development of the management and treatment of urban stormwater was the development of the Sustainable Drainage Systems (SuDS) approach. This is an attempt to manage run-off from rainfall on roofs and other catchment surfaces through a sequence of actions with key objectives to manage the flow rate and volume of the stormwater. This is to reduce the risk of flooding and water pollution, it also helped to reduce pressure on the sewage network and to improve the biodiversity and local amenity. Two types of SuDS solutions are available, which are characterised as soft and hard solutions [25]. Hard SuDS solutions are manufactured and used above or below ground to treat stormwater, whilst soft SuDS use more natural routes to treat the stormwater [25].

Using these definitions examples of soft SuDS solutions would be retention ponds and wetlands, which retain stormwater to control the flow and provide treatment releasing it slowly to surface water bodies. Settling of solids is used to remove the pollutants in the water, biological uptake reduces nutrients, and adhesion to aquatic vegetation (where present) [26]. Examples of hard SuDS solutions include hydrodynamic separators, that are built below ground and utilise sedimentation and separation to remove sediment. They are designed for the water to move in a circular manner increasing residence time, this circular movement also creates a vortex which causes sediment to move to the centre of the device where it settles quicker. This device is capable of removing large sediments and floatables however it has problems removing small solids that have poor settling velocities [26]. Another example of a hard SuDS device is the Up-Flo[®] Filter System,

described in Chapter 1, which is a multi-process system which removes through sedimentation and separation as a vortex system does. However, it utilises a filter media to increase residence time within its sump and filters particles that do not settle or separate [26].

Both types of SuDS have their own benefits and drawbacks. Soft SuDS can be easily constructed at a low cost, can be built to create a landscape feature, and can encourage biodiversity. However these benefits come with a cost, typically to achieve these benefits it takes a large amount of land, needs regular maintenance so it doesn't become a health and safety hazard and to prevent public flytipping, and reduces the potential for water reuse [27]. These costs can limit the use of soft SuDS, especially within already built up urban areas. Hard SuDS can overcome some of the soft SuDS problems as it can be; built below ground limiting land use and maintenance requirements, allow potential water reuse, and can be potentially retrofitted. Whilst these overcome some of the issues of soft SuDS, hard SuDS can result in high construction costs. The maintenance that is required is more specialist due to the confined space, and additional components are required to discharge the treated effluent to surface water bodies [27].

The Up-Flo[®] Filter System is a good hard SuDS solution. As it can be used in built up areas, where soft SuDS can not be, but also overcomes some of the issues typically associated with hard SuDS. It can be installed into pre-existing manholes, reducing construction cost, and as it is pressure driven system only pipe is required to discharge to surface water bodies. Additionally, it has multiple treatment techniques reducing the need for further treatment, as other hard SuDS options may require.

Kirby [25] highlighted the past difficulties in the implementation of SuDS in England and Wales. The difficulties in implementing SuDS principles were believed to be partly due to the regulatory authorities and partly due to the legislation which meant it was problematic to interpret the law regarding SuDS use at the time. However, another stumbling block at the time was the lack of viable information about the techniques [25]. These difficulties have been highlighted elsewhere, in the Pitt review [28] following the UK 2007 floods one of the recommendations was that the Government should resolve who has responsibility for ownership and maintenance of SuDS. Further, in a Institute of Civil

Engineers briefing Goodson highlighted that there was a lack of viable information about SuDS longevity and their maintenance and management implications [29].

Recent UK legislation and policies have attempted to address some of the problems associated with SuDS. In England, Schedule 3 of the UKs 2010 Flood Water and Management Act outlines the need to manage stormwater run-off [30]. To implement Schedule 3, the Department for Environment, Food and Rural Affairs (Defra) in 2011/12 consulted on National Standards that could be used in England. These standards set out what to design and construct in order to obtain approval from a SuDS Approving body (SAB) and the standards which operate and maintain SuDS. The main exemption from this was if the cost was to be disproportionate [31].

However, the outcome from the consultation resulted in the National Standards approach not being implemented. In 2014 a further consultation was held on an alternate approach to that set by Schedule 3. This approach sought to implement SuDS through changes to the planning system [32]. This has led to the local planning systems being responsible for the implementation of SuDS with the Lead Local Flood Authorities being a statutory consultee [33] [34].

To fill the gap in regulatory guidance on SuDS, CIRIA has produced a guide covering its planning, design, construction and maintenance. Using existing guidance and research best practice is outlined [26].

To further aid in the uptake of manufactured treatment devices for SuDS, the water supply chain body British Water in 2017 published a code of practice for SuDS technologies. This was developed with both the Environmental Agency (EA) and manufacturers [35]. This code of practice seeks to allow for manufactured treatment devices to be tested with an agreed protocol. The test protocol aims to acquire three fundamental requirements of the manufactured treatment devices [36]:

1. "Typical pollutant capture efficiency for frequent, sub-annual rainfall events."
2. "Sediment retention capability for up to 1:2 year rainfall events likely to cause washout."

3. “Capability of filter media to retain dissolved pollutants under the influence of de-icing salt.”

Approval and certification under this code of practice allow for the manufacturers published removal capabilities to be independently proven. Whilst it is a voluntary code of practice, it has been designed to fulfil the requirements within the CIRIA SuDS Manual [36].

The regulatory development in the UK, the Best Practice Manual developed by CIRIA and the Code of Practice by British Water allows for the problems highlighted by Kirby in SuDS early development to be addressed. However, as the Best Practice Manual and Code of Practice are voluntary and the fact regulation is devolved there may be issues in ensuring SuDS is fully utilised.

The devolved nature in the management of urban stormwater in the UK is seen in other countries, as Chapter 5 highlights. As the UK approach continues to develop, learning from other regulatory regimes will allow for the best techniques to be utilised.

2.3 Particle Settlement

A key process utilised by the Up-Flo[®] Filter System for treatment of urban stormwater is the settlement of sediment within its sump. This process is typically known as sedimentation or gravity separation, which is a widely used technique in water treatment and one of the oldest. Sedimentation uses gravitational attraction to separate suspended sediment from the water, by allowing the sediment to settle to the bottom of the treatment basin [37].

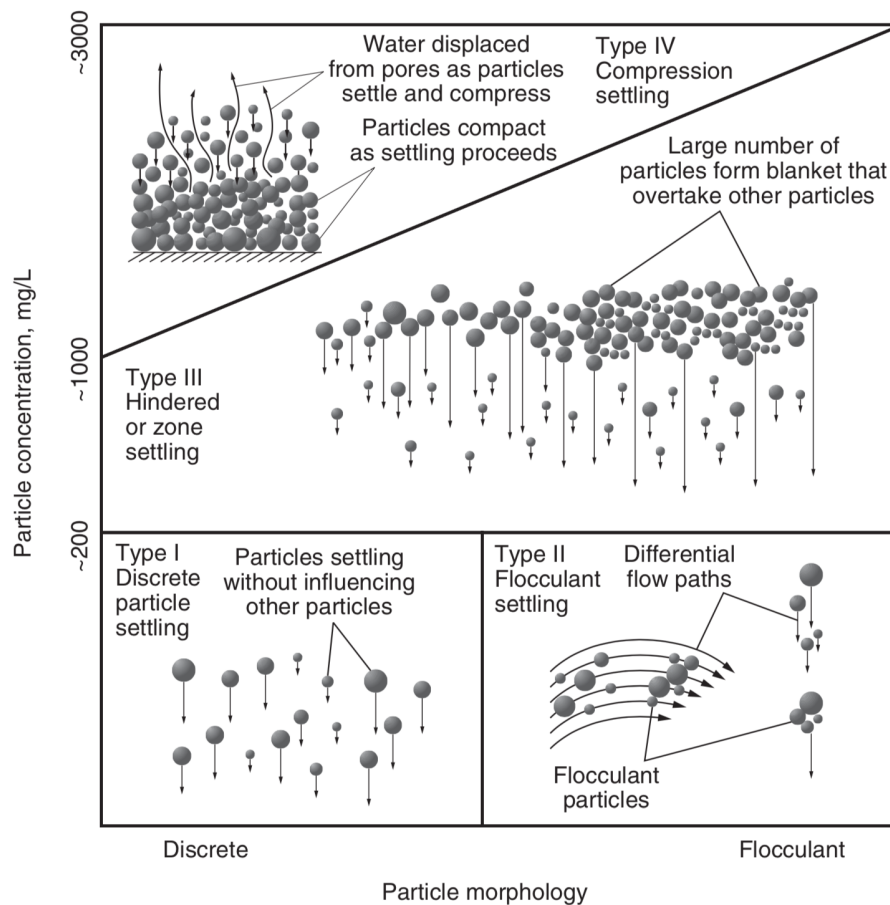


Figure 2.2: Particle types in sedimentation [37].

The type of sedimentation process depends on the particles concentration and morphology. Figure 2.2 outlines the four different classifications of settlement. Type 1 is

discrete settlement where particles are surrounded by water and do not interact with other particles settle. Type 2 is flocculent settlement where particles interact with one another during settlement and form larger particles resulting in increased settlement velocity. Type 3 is hindered settlement where particles interact and slow down the settlement of other nearby particles. This results in the formation of a layer that settles and overtakes other particles. Lastly, type 4 is compression settlement where a particle blanket contains a high concentration of particles compresses as water moves up through the voids within the blanket due to the weight of the particles [37].

As Section 2.1 outlines, urban stormwater typically has a large TSS range which potentially results in all four types of settlement processes being utilised in the Up-Flo[®] Filter System. However, as the typical mean concentration is less than 200 mgL^{-1} , and the dilution effect of the Up-Flo[®] Filter System, primary settlement of particles would be due to either type 1 or 2 settlement processes.

In type 1, settlement under gravity is influenced by the sediments drag coefficient. In laminar flow, the settling velocity is determined by Stoke's Law which is shown in Equation 2.1 [37].

$$v_s = \frac{1}{18} \frac{\rho_g - \rho_w}{\mu} g_a d^2 \quad (2.1)$$

Here the settling velocity, v_s , is determined by the density of the sediment, ρ_g , density of the water, ρ_w , the dynamic viscosity of the fluid, μ , the acceleration due to gravity, g_a , and the sediment particle diameter, d . For sand particles and a temperature of 20°C Stoke's law is applicable for particles up to a diameter of 0.13 mm [37].

For transitional flow the settling velocity is described by Equation 2.2 [37].

$$v_s = \left[\frac{g_a(\rho_g - \rho_w)d^{1.6}}{13.9\rho_w^{0.4}\mu^{0.6}} \right]^{1/1.4} \quad (2.2)$$

Equation 2.2 is valid while the system is in transitional flow. This is valid up to a particle size of 1.7 mm , for sand particles at a temperature of 20°C .

The Reynolds Number defines whether the flow is laminar or transitional, Section 2.4 outlines this. Reynolds Number is used as the drag coefficient in the settling of a particle cannot be predicted theoretically, but the drag coefficient depends on the Reynolds

Number.

The sediment will settle as long as the particles are large enough for the settling velocity to be greater than that caused by Brownian motion. Brownian motion is caused by the collisions with fluid particles, Equation 2.3 provides the mean squared distance travelled caused by Brownian motion [37].

$$\overline{x_b^2} = \frac{2K_bT}{3\pi\mu d}t \quad (2.3)$$

Here the mean squared distance caused by the collision, x_b , is impacted by the Boltzmann constant, K_b , diameter of the particle, d , time, t , and the temperature in Kelvin, T [37].

When there is an upward flow in the tank, as would be in the Up-Flo[®] Filter System, the particles will settle as long as the settling velocity is greater than the liquids upwards velocity [38].

Additionally, settlement only occurs when the density of the sediment is greater than the density of the fluid. If the density is lower then the sediment will float, in what is called flotation [39]. This flotation process would still capture sediment within the sump of the Up-Flo[®] Filter System.

An additional sedimentation process is Flocculant settling. This sedimentation process typically occurs after coagulation [37]. In Flocculant settlement, particles collide and adhere to form larger particles, *flocs*, these then have a larger settling velocity allowing them to settle [37] [40].

Flocculation can also occur naturally without the coagulation step [41]. This occurs as the principle electrical property of fine particulate matter in water is the particles surface charge. This surface charge prevents the particles from aggregating and forming flocs, however, it is thermodynamically unstable. This results in the particles flocculating, when given sufficient time [37]. This can occur between several to 12 hours from the initial run-off, dependent on the mixing, pH, ionic strength and particle properties [41].

This could be seen in the Up-Flo[®] Filter System as smaller particles which have a small settling velocity would rise through the filter media, but some particles may collide resulting in the particles potentially adhering and increasing the settling velocity. If the

newly formed flocs have a large enough settling velocity these will then settle to the bottom of the Up-Flo[®] Filter System.

2.4 Filter Media Capture

Particles that are not captured in the sump of the Up-Flo[®] Filter System, will pass through a filter media bed. Developing knowledge on the properties of granular filter media and the changes they undergo under the effect of clogging and other factors is a key area in this project. This would allow for knowledge of the Up-Flo[®] Filter System's filter media performance over time to be improved. Numerous studies into the phenomena of clogging in a fluidised granular media and other types of media have been conducted that is used to form appropriate experiments. However, there were three types of research into the clogging effects that was needed, the effect of the sediment characteristics, flow regimes and the effect of the filter media characteristics and its susceptibility to clogging.

Sediment particles are removed by a number of different mechanisms in filter media filtration. If the particle is larger than void spaces in the media then the particle is removed by straining. This forms a cake at the entrance of the filter media bed, which improves sediment removal but leads to a reduced flow through the filter media [37].

For smaller sized particles the only removal technique of filter media is through adhesion of the particles to the filter media grains. This occurs through close-range molecular forces, for example, the van der Waals force [37]. The van der Waals force is a short-range force that exists within both gas and liquid phases resultant from the fluctuations in electron clouds [42]. In this process, particles are removed throughout the filter bed and is dependent on the particle concentration. This is described by Equation 2.4 [37]:

$$\frac{\partial \Upsilon}{\partial x} = -\lambda \Upsilon \quad (2.4)$$

where λ is the filtration coefficient, m^{-1} , Υ is the mass concentration of the particles, mgL^{-1} , and x is the filter media depth (thickness), m .

As the sump in the Up-Flo[®] Filter System settles larger sized particles, the primary filtration technique of the filter media is expected to be due to particle-grain adhesion. The effectiveness of the filter media is impacted by a number of variables including material density, material hardness, porosity and grain shape. Which makes material selection important when designing a filter media bed.

A prominent design factor in filter media design is that of packing density, i.e. the fraction of the space taken up by the media [43]. This is due to the dependence of the porosity on the packing density [44]. A highly packed filter bed results in a reduced porosity and permeability, resulting in reduced flow through the media and increased straining, increasing filter media removal efficiency. The constraints on the filter media in the Up-Flo[®] Filter System will impact this as well, as a more constrained filter media results in a lower porosity caused by fluidisation.

Kandra, et al. [45] assessed the clogging phenomena in granular filter media used in urban stormwater treatment and the factors that affect it. The researchers dosed five identical columns containing filter media with a semi-synthetic urban stormwater, made from tap water and stormwater pond sediment, to study the influences of clogging. The sediment size, d_{50} was $34.5 \mu m$ with a d_{10} and d_{90} of $5.1 \mu m$ and $301 \mu m$, which was close to the particle size distribution observed from city urban roads in Australia. Targeted concentration was between $100-300 mgL^{-1}$, which was based on typical concentrations from international data. The columns were dosed manually at a controlled pace and a constant head was maintained on top of the media. Results from the study found that the shape and smoothness of filter media grains had a limited effect on clogging and sediment removal. It was found that the volume of stormwater and flow-rate had more of an effect on the filtering performance of the filter media instead. This was found to be very surprising as previous studies quoted by Kandra, et al. suggest that the shape and smoothness of the particles did play a substantial role in filtration. In this study, it was found that the clogging rate was found to be inversely proportional to flow rate. Using the experimental technique presented by Kandra, et al. an experiment to investigate whether these results are in fact reproducible would be useful and the possibility to provide more reliable results for mean time till clogging for different sites [45]. This inverse relationship was also observed by Hamoda, et al. [46] in their study granular media filtration in wastewater reclamation and reuse. The study found the highest removal efficiency was at the lowest filtration rates [46].

The reduced clogging rate with a higher flow rate observed by Kandra is to be expected. As if the main removal mechanism is the adhesion of the particles to the filter media

grains then an increased flow rate would result in a reduced residence time. This reduced time within the filter media would result in a decline of successful adhesion. Additionally, a higher flow rate may cause increased bed expansion, resulting in less straining and less opportunities for adhesion.

Flow through filter media both impacts and is impacted by sediment capture. Due to this, it is important to fully understand the basics of flow through a granular media. One of the first major works in this area was Darcy's empirical flow law, which was the first extension of classical fluid dynamics principles into the field of fluid flow through granular media [47]. Through adapting Darcy's empirical flow law, to take into account cross-sectional area and expanding on the saturated hydraulic conductivity a flow equation is provided [48] [49].

$$Q = \frac{\kappa A (p_B - p_A)}{\mu x} \quad (2.5)$$

Here Q is the volumetric flow, $(p_B - p_A)$ is the pressure drop across the granular media, κ is intrinsic permeability, A is the area of the media, μ is the dynamic viscosity and x is the thickness of the media.

This version of Darcy's law allows for the effect on the flow of the different variables to be clearly identified. It can be easily seen that given a fluid of constant temperature and pressure drop across a granular media the flow is highly dependent on the properties of the granular medium. In particular, the intrinsic permeability will play a significant role.

The intrinsic permeability has been expressed using other parameters that make up the properties of the granular media through the Kozeny-Carmen equation [48]:

$$\kappa = C d_{pore}^2 \frac{n^3}{(1 - n)^2} \quad (2.6)$$

Here C is a constant to account for the effects of the irregularities in the geometry of the pore spacing, d_{pore} is the effective pore diameter and n is the porosity. An additional expression is through the Hazen equation [48]:

$$\kappa = C d^2 \quad (2.7)$$

Here the intrinsic permeability is related to the average grain diameter, d , rather than the pore diameter.

These equations show that as expected porosity, irregularities of pore spacing, pore diameter and average grain diameter of the granular medium have a large effect on the ability of the granular media to transmit fluid. Understanding these effects will allow for a thorough understanding of the filtration process and how to optimise the media for flow [48]. Chapter 3 outlines which permeability is used in this project analysis, based on media type and flow rates used. Whilst the Darcy equation is hugely beneficial, research over time has shown numerous problems associated with it, particularly when fluid velocity increases over a certain point, which is dependent on media properties [49].

What defines the nature of the flow and is important in understanding the flow through the granular media is the Reynolds Number, R . The Reynolds Number determines whether a flow will be laminar or turbulent, it is determined by four factors; fluid density, ρ_w , fluid velocity, q , diameter of the passageway through which the fluid moves, d , and the fluid viscosity, μ , in Equation 2.8. The variable d is difficult to define as various different particle diameters are used, Section 3.5.2 explores the different diameters and estimates the Reynolds Number for the filter media used in this project.

$$R = \frac{qd\rho_w}{\mu} \quad (2.8)$$

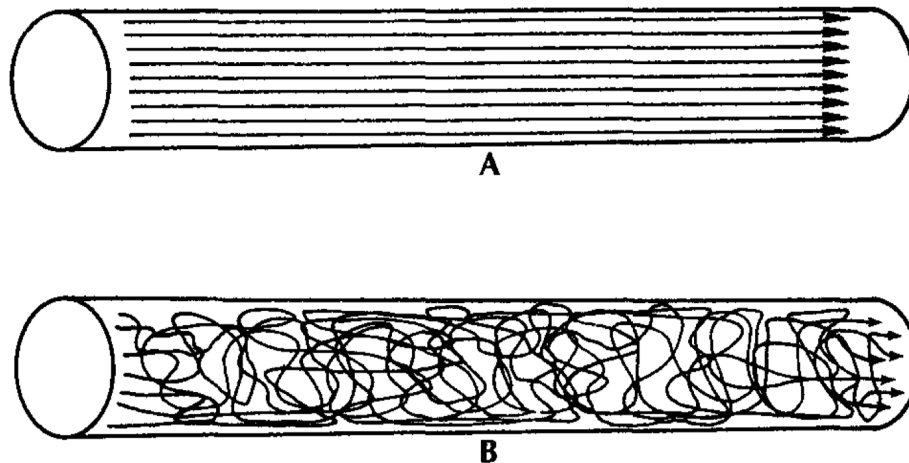


Figure 2.3: Streamlines of water flow [50].

In laminar flow, water molecules follow streamlines, in this type of flow the viscous forces

are dominant, this is visualised in Figure 2.3.A. However, as the velocity of the flow increases inertial forces due to the chaotic movement of the water transferring momentum internally becomes more dominant than that of the viscous forces. This will cause the water particles to rush past each other in an erratic behaviour, this is shown in Figure 2.3.B. This is known as turbulent flow, at this stage, Darcy's law becomes invalid leading to the need for new relationships to be developed to predict water flow through the granular medium. When considering flow in a pipe the Reynolds Number is widely reported, however, in granular media it is less so. Experimentation [51][52][53] has shown that Darcy's law is valid only when resistive forces of viscosity predominate, this is when the Reynolds Number is less than 1 to 10 [50]. Whilst it has been reported [54][55] that the Reynolds Number for turbulent flow in granular media ranges from 60 to 600 [50]. This means Darcy's law is only valid for slow-moving laminar flow, which has certain laminar flow conditions and all turbulent flow is incompatible with Darcy's law [50].

This presents an issue, as although most groundwater flows in granular media are primarily in the range at which Darcy's law is valid. The Up-Flo[®] Filter System could be in all three ranges; Darcy's range, fast moving laminar flow and turbulent flow. Section 3.5.2 outlines this in more detail and estimates the Reynolds Numbers the filter media in the Up-Flo[®] Filter System experiences. To account for flow outside of the Darcy range additional equations are required.

Dukhan, et al. [56] attempted to find a solution for those ranges where Darcy's law is invalid. Conducting experiments with a range of granular media laws which have been formulated in response to this problem were tested and two widely-used equations in this region were reconciled through the use of hydraulic radius theory. Dukhan, et al. outlined the two major equations of the post-Darcy range; Forchheimer and Ergun. The Forchheimer equation is an empirical formula but one that can be arrived at analytically as well. Forchheimer used the analogy of pipe flow to postulate his equation which is shown below in Equation 2.9 [56]:

$$\frac{\Delta p}{x} = \frac{\mu}{\kappa_F} q + \frac{\rho_w F}{\sqrt{\kappa_F}} q^2 \quad (2.9)$$

Here x is the thickness of the granular medium, κ_F is the permeability while F is a dimensionless constant known as the Forchheimer coefficient. The variables that have a

large impact on the Darcy's equation also have a big impact in Equation 2.9, but with the addition of the Forchheimer coefficient which is fixed for a certain class of granular media. The internal structure of the granular medium strongly influences the Forchheimer coefficient. In the previous work referenced by Dukhan, et al. it has been found that the permeability is constant in the Darcy regime whilst in the Forchheimer regime it decreases with the increasing velocity. This indicates that the velocity of the flow will have a significant effect on understanding the effects of flow through a granular medium [56].

An alternative widely used equation discussed by Dukhan, et al. is the Ergun equation, Equation 2.10, which was formed to link the pressure drop to the structural characteristics of the granular medium [56].

$$\frac{\Delta p}{x} = E_A \frac{(1-n)^2 \mu}{n^3 d^2} q + E_B \frac{(1-n) \rho_w}{n^3 d} q^2 \quad (2.10)$$

Equation 2.10 links the pressure drop to the structural characteristics of the granular medium. Here E_A and E_B are the Ergun constants. These constants were thought to be universal, but further experiments by Fand et al. [56], [57] proved they varied with the diameter of the grain. This has led some researchers to suggest modifications to this equation. McDonald et al. have suggested replacing n^3 by $n^{3.6}$ and using $E_A=180$ and dependent on the roughness of the particles using 1.8 to 4.0 for the values for E_B . The Ergun constants are viewed as correction factors which account for the geometrical difference between flow paths through the packed spheres [56].

Dukhan et al. discussed the differences between the Forchheimer and Ergun equations. The main differences are in the multipliers. Dukhan et al reconciled these differences through the use of Kozeny-Carman hydraulic radius theory, which slightly modified form is stated in Equation 2.6, Dukhan et al argued that the permeability is the same permeability utilised in the Ergun equation. The dependence of the permeability on the porosity and the particle diameter is stressed as an important point by Dukhan et al. [56].

One problem that Dukhan et al. attempted to rectify was that the permeability used in Forchheimer equation is not the same as the one used in Equation 2.6 and the existence

of constant E_A and its relationship for constant E_B . One step to rectify this was to present the Forchheimer permeability in terms of Darcy's intrinsic permeability [56]:

$$\kappa_F = \frac{\kappa}{C_1} \quad (2.11)$$

Equation 2.11 links Forchheimer permeability with the Darcy intrinsic permeability where C_1 is a constant for the granular media. Substituting into Equation 2.9 and converting the Forchheimer and Ergun equation into a non-dimensional form then comparing the equations the following equations are found:

$$C_1 = \frac{E_A}{36C} \quad (2.12)$$

$$\sqrt{C_1}F = \frac{E_B}{6n^{\frac{3}{2}}\sqrt{C}} \quad (2.13)$$

Through this Dukhan et al. [56] demonstrated the two multipliers of the viscous and drag terms are connected and the multiplier of the drag term is dependent entirely on the porosity. When looking at the turbulent flow regime the Forchheimer Equation 2.11 had to be rewritten. Mainly in regards to the permeability coefficient which uses a different constant now C_2 . This is because of the new nature of the flow. Dukhan et al. finished by looking at real data of turbulent flow, a major problem lies in the lack of data within this area of 1 mm spheres however for other media the laws investigated and reconciled by the researchers seemed to be accurate [56].

As these relationships show, the filter medias permeability is linked to its porosity. As sediment is caught, through either straining or adhesion, the porosity declines leading to a declining permeability. This results in flow through the filter media becoming more difficult. Whilst this may increase the removal efficiency of the filter media, untreated urban stormwater may bypass the Up-Flo[®] Filter System as the maximum treatable flow rate reduces. By monitoring the medias permeability, the maintenance procedures could be optimised.

Although the media properties have a significant effect on the removal efficiency of the filter media, other factors have been identified that may impact the removal efficiency as outlined in a study by Hsiau, et al [58]. It was found that the velocity of individual filter media grains impacted the performance of the filter. However, the velocity was largely

dependent on the geometry of the filter itself. Whilst the fluid in this study was gas rather than water, it raises interesting questions on whether the internal geometry of the Up-Flo[®] Filter System modules is optimal for the performance of the Up-Flo[®] Filter System [58].

As discussed earlier, particle concentration is important for removal by the filter media. This results in the size range, TSS and density of the urban stormwater sediment being important considerations when choosing an appropriate filter media for the Up-Flo[®] Filter System. This is because these properties impact the particle concentration that would enter the filter media. The sediment type would also impact the filtration efficiency, as if the sediment is positively charged then the sediment may attach to filter media grains through stronger opposite attract forces. However, negatively charged particles would utilise van der Waals forces and neutral particles would adhere through weaker double layer forces. The pH of the influent water would also impact the filtration efficiency of the filter media [59].

While the influent conditions cannot be controlled, having a more comprehensive picture of the conditions allows for a more accurate estimate of filtration efficiency. This allows for more appropriate filter options to be explored.

One significant part of the project was to complete the objective to design and build a sensor system so as to objectively decide whether the filter media would need replacement so as to maintain an acceptable level of hydraulic and filtering performance. There are numerous requirements on a sensing system as well as the clear need to detect the physical parameters that determine the state of the filter. These include low power requirements, low cost, robust and the ease of acquiring and transmitting data. These are essential as if they are not met the sensor system will not be considered an appropriate way to optimise some of the Up-Flo[®] Filter System's maintenance issues. As although if they are not met the system could still reduce the waste of the filter media it may become too cost prohibitive for it to be implemented. Additionally, if the low power and robust conditions are not met it could lead to more waste in other areas. Numerous techniques were considered, the following sections explore these.

2.5 Acoustical Techniques

Acoustics is one method that was considered as part of the sensor development. This was due to the potential information that can be acquired from the granular media and due to the low cost and power requirements. It was important to first understand how the characteristics of the media can impact the acoustic wave transmission through the media.

A number of different models throughout the years have been formed to understand the transmission of acoustic waves through a fully saturated granular media. A key model that is currently utilised is the Biot-Stoll model, this model relates a media's geoacoustic properties to its physical properties. To do this it utilises Biot [60], [61] theories of propagation of elastic waves in a fluid granular solids and is based on physical principles.

The Biot-Stoll model was formed when Stoll [62]–[66] applied the Biot theory to marine sediments and introduced complex bulk and rigidity for the sediment to account for grain contact losses [64]. The model found that when an acoustic wave is applied to a granular media, there are 3 resulting waves, not 1. There are 2 types of compressional (dilatational) waves and 1 type of shear (rotational) wave [67], [68]. Type 1 of the 2 types of compressional waves is similar to the shear wave in that attenuation due to viscous losses is relatively low as the skeletal frame and pore fluid move nearly in phase. The type 2 compressional wave, however, becomes highly attenuated due to out of phase movement [68].

This model requires 13 geophysical inputs to acquire both the wave speed and attenuation for each type of wave [69], shown in Table 2.1.

The developed model predicts the phase velocity and attenuation as functions of the frequency of the wave. There are two distinct frequency limits: (i) low; and (ii) high. These limits are separated by the Biot characteristic frequency, f_c , shown in Equation 2.14 [60], [61]. At low frequencies, $f \ll f_c$, the attenuation scales with the square of the frequency. At higher frequencies, $f \gg f_c$, the attenuation scales with the square root of the frequency [60], [61], [70]. The losses are resultant from intergranular friction and

Table 2.1: Biot-Stoll geophysical inputs [69].

Sediment grain bulk modulus	Permeability
Sediment grain density	Pore size parameter
Fluid density	Real dry frame rigidity
Fluid bulk modulus	Imaginary dry frame rigidity
Fluid viscosity	Real dry frame bulk modulus
Structure factor	Imaginary dry frame bulk modulus
Porosity	

viscous friction as a result of the motion of the frame relative to the fluid [71]. These losses are taken into account by the geophysical inputs in Table 2.1. The intergranular friction losses are represented by the imaginary dry frame rigidity and the imaginary dry frame bulk modulus, both of which can be calculated. The viscous friction losses are represented by the measurable values of permeability, porosity and fluid viscosity.

$$f_c = \frac{\mu n}{2\pi\kappa\rho_w} \quad (2.14)$$

Where: μ is the fluid viscosity, n is porosity, κ is intrinsic permeability, and ρ_w is density of fluid.

Due to the complexities of the model it is not presented mathematically in this thesis, references [60]–[66] outline the theory in detail and its mathematical basis. The Biot-Stoll model has been one of the dominant models for understanding the interaction between acoustic waves and fully saturated granular media. Holland and Brunson [69] assessed the model experimentally, they found that broadly model predictions were in excellent agreement with their experimental data. However, they found that the Type 1 compressional wave attenuation predictions to be the least accurate, this was seen especially in clay-sized sediments [69].

This is a similar criticism outlined by Buckingham [70] as the characteristic attenuation caused by the granular materials over a broad frequency range was not easily accounted for [70]. Additional criticisms have been highlighted in numerous works on the models

complexity and the number of inputs needed.

Over the years, an alternative more practical model has been developed by Hamilton [72] which relates the geophysical and geoacoustical properties but it is empirically based. Hamilton looked at the relationship between saturated media properties and acoustic transmission, reflection and losses by studying the relationships between sound velocity and density [72]. This is important to the research due to the density changes that will occur with the filter media clogging. Hamilton [72] presented an equation to relate the compressional wave speed, c_p with the media's bulk density, ρ , this is shown below in Equation 2.15.

$$c_p = [(B + \frac{4}{3}\zeta)/\rho]^{\frac{1}{2}} \quad (2.15)$$

The equation shows that as density increases the compressional wave speed would decrease. However the compressional wave speed is also related to the bulk modulus of the media, B , and the rigidity of the media, ζ . If these could be accurately measured Hamilton suggested that the impedance could be calculated, which would allow for more information of the media to be acquired [72]. As with density, these variables are also impacted by the porosity of the material. This results in filter media clogging impacting all the variables in Equation 2.15, with the bulk modulus and rigidity both increasing.

Hamilton [73] further developed this study into marine seabeds. If the compressional and shear wave velocities and density are known, then elastic material properties such as dynamic rigidity and Lamé's first parameter, Λ , can be calculated [73].

Hamilton stated in this research that there was a first-power dependence of attenuation on frequency f^1 , but the Biot-Stoll model had indicated a f^2 dependence for low frequencies and a $f^{\frac{1}{2}}$ for high frequencies. Hamilton presented the following equation which relates the attenuation of the wave with sediment porosity and grain sizes.

$$\alpha_p = K_p f \quad (2.16)$$

Equation 2.16 relates the attenuation of the compressional wave, α_p , in dBm^{-1} with the frequency, f , in kHz through the use of the constant K_p which have units of $dBm^{-1}kHz^{-1}$. This constant varied with sediment type and is related to porosity and

mean grain diameter. Hamilton, however, points out that the equations to calculate this constant is problematic with different values calculated dependent on whether porosity or grain size is used [73].

The relationship between sound velocity and marine sediment properties was further developed by Hamilton [74]. It found that due to the high dependence on the environment there are issues in relating bulk density and mean grain size of the sediment. Additionally, Hamilton analysed the Wood Equation at modelling compressional wave speed.

$$c_p = \left(\frac{1}{[n\beta_{cw} + (1-n)\beta_{cg}][n\rho_w + (1-n)\rho_g]} \right)^{1/2} \quad (2.17)$$

Equation 2.17 relates the compressional wave speed, c_p , with the compressibility of the mineral solids and water, β_{cg} and β_{cw} , and the density of the mineral solids and water, ρ_w and ρ_g . n represents the porosity, occupied by the water [74].

Hamilton found that Equation 2.17 is useful for high-porosity silt-clays which have low rigidities, realistically all marine sediments have high rigidities resulting in the Wood Equation underestimating compressional wave speed. Hamilton argued that due to this issue the Wood Equation should not be used and Hamiltons Equation 2.15 was more applicable [74].

Hamilton has had significant success with this empirically based model. However, problems have been encountered, in terms of whether the observed attenuation dependence on f^1 is correct. Kibblewhite [75] argues in his review that in saturated media there appears to be an additional frequency dependent absorption at low frequencies resulting in it being closer to a f^2 relationship with attenuation [75].

An attempt to solve some of the issues regarding the Biot-Stoll and Hamilton approaches was made by Buckingham [70] in developing his own theory regarding acoustic transmission through saturated granular media, based on a linear wave equation, formed by linearized Navier-Stokes equations. The attenuation in Buckingham's theory was resultant from intergranular dissipation, e.g. grain-to-grain friction. Buckingham attempted to link equations describing an acoustic wave with the mechanical properties

such as particle size, porosity and the density of the media. As these are shown to have an important effect on compressional wave speed.

Buckingham related the attenuation coefficient in nepers, α_p , to the angular frequency, ω , of the wave, the compressional wave speed with intergranular friction, c_b , and the compressional loss tangent, Γ . This equation allows for the calculation of the attenuation of a wave travelling through the granular media.

$$\alpha_p = \frac{\omega}{c_b} \Gamma \quad (2.18)$$

Buckingham noted that intergranular friction gives rise to a f^1 relationship, as argued by Hamilton. Buckingham additionally explored topics of pulse propagation and pore-fluid viscosity. Buckingham found that the velocity was causal in the media and the pressure was well behaved whilst the pore fluid viscosity was found to have a negligible effect on attenuation. This may be the case with most marine sediments, however, any effects due to viscosity is important to consider within this research project as the viscosity is dependent on temperature.

Buckingham then described the importance of having an accurate density for the two-phase medium, due to the inaccurate modelling of the wave if the density is not accurate. A key equation for bulk density is:

$$\rho = n\rho_w + (1 - n)\rho_g \quad (2.19)$$

Here the bulk density of the media is equal to the porosity, n , multiplied by the density of the water, ρ_w , and added to the density of the grains, ρ_g , multiplied by the difference between one and the porosity. This allows for the accurate calculation of the bulk density of the media, with the porosity representing the the ratio of the volume of water to the total volume of water and grains. However, this equation could also be used for different types of fluid other than water.

As grains are not perfectly spherical the porosity term needs to be adapted for this.

Buckingham presented the following equation.

$$n = 1 - P_F \frac{r_m^3}{r_c^3} = 1 - P_F \left\{ \frac{d + 2\delta}{d + 4\delta} \right\}^3 \quad (2.20)$$

Where $d = 2r_b$ where r_b is body radius. This equation calculates a modified porosity which takes into account the roughness of the spheres, it is made up of the packing factor, P_F , the mean radius, r_m , the contact radius, r_c , the body diameter, d and a single statistical parameter that represents grain roughness, δ . The radii of the grain are illustrated below in Figure 2.4:

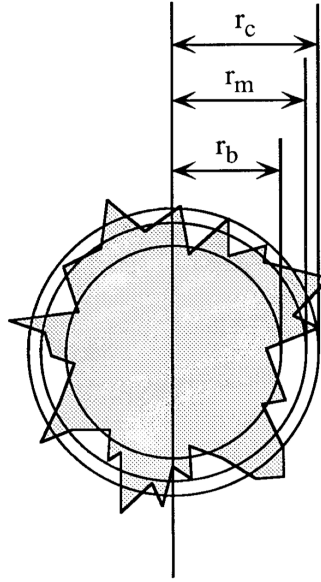


Figure 2.4: Schematic of radii of a rough sediment particle [70].

Buckingham used this equation and compared the results to previously reported data by Hamilton. It was found that the equations for porosity and density match reported data over a range of grain sizes. This indicates that this equation may be beneficial for both the acoustic and the hydraulics work in later sections.

Buckingham noted that when the grain size is not unimodal then Equation 2.20 needs adapting to account for the difference in particle size distribution. Assuming that the smaller sized particles fill up the pore spaces of the larger particles and do not impact the random packing then the new porosity equation is shown below, where γ_g is volume ratio of smaller to larger grain sizes and d is the larger grain size.

$$n = 1 - P_F \frac{r_m^3}{r_c^3} = 1 - P_F \left\{ \frac{d + 2\delta}{d + 4\delta} \right\}^3 (1 + \gamma_g) \quad (2.21)$$

The developed Buckingham equations describing wave speed and compressional loss tangent in terms of grain properties are shown below in Equations 2.22 - 2.25.

$$c_b = \sqrt{c_p^2 + \left(\frac{d}{d_0}\right)^{\frac{1}{3}} \frac{\zeta_0}{\rho}} \quad (2.22)$$

Equation 2.22 presents the phase speed in relation to the speed of sound in the absence of intergranular losses, c_p . This is calculated by the Wood equation shown in Equation 2.17 with the body diameter of the grains, d , and the reference grain diameter, $d_0 = 1000\mu m$, the bulk density, ρ , and the scaling constant for the rigidity of the media, ζ_0 .

$$\Gamma = \frac{n\pi}{4} \frac{d^{\frac{1}{3}}}{d^{\frac{1}{3}} + W} \quad (2.23)$$

where:

$$W = \frac{d_0^{\frac{1}{3}} \rho c_p^2}{\zeta_0} \quad (2.24)$$

Buckingham presented Equation 2.23 and Equation 2.24 which calculates the compressional loss tangent, Γ , with the intergranular theory being taking into account. This allows for the attenuation to be calculated using Equation 2.18, and takes into account the new bulk porosity and the media properties.

$$\chi_f = \frac{\zeta}{\rho c_p^2} = \left(\frac{d}{d_0}\right)^{\frac{1}{3}} \frac{\zeta_0}{\rho c_p^3} \quad (2.25)$$

Equation 2.25 provided a fractional power-law relationship giving the compressional dissipation coefficient, χ_f , which governs the wave speed and attenuation of the compressional wave. These laws combined allowed for an accurate model of the acoustic wave with different media variables.

Buckingham plotted his theory against a range of previously published data, it was found the intergranular theory matches sound speed well with recorded results, as shown in Figure 2.5. This seems to suggest these equations are appropriate in this study. However, there are issues regarding the attenuation coefficients matching measured data, but suggestion is made that this could be due to the memory function of the material. Due to the previous data showing that the intergranular theory providing a good indicator for sound speed with regards to sound speed and grain diameter it will be important for the understanding of the acoustic response in saturated filter media. There remain questions

about attenuation calculations and the need for the collection of real data, the effect of layering and fluid velocity, which will be an interesting area to study in this project [70].

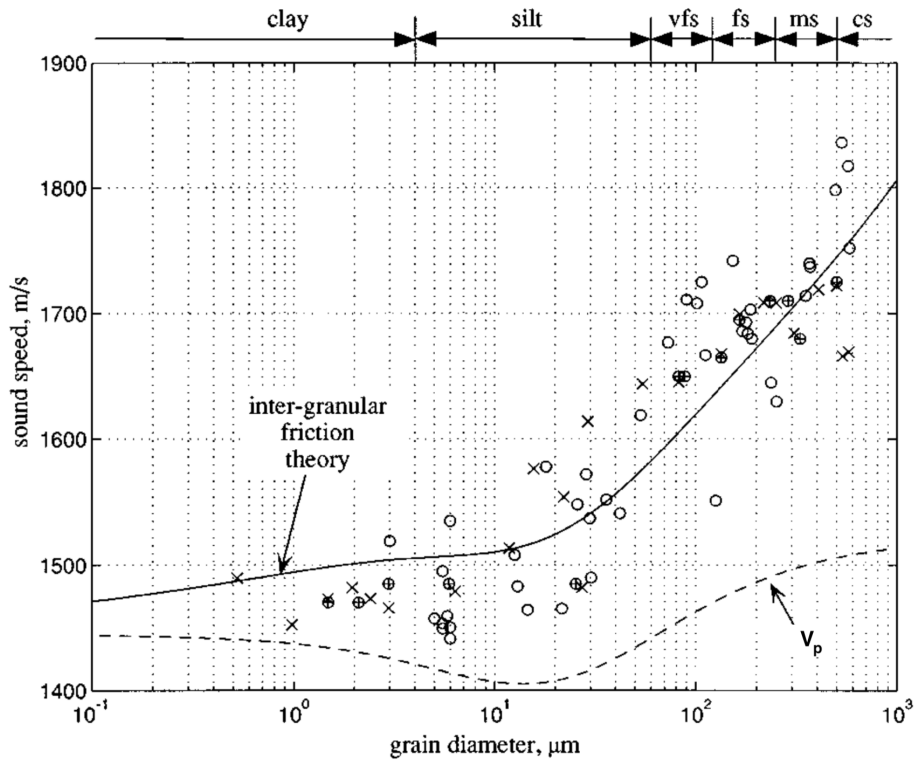


Figure 2.5: Buckingham's wave speed and Wood's Equation vs mean grain diameter using Hamilton's previous published data. vfs = very fine sands, fs = fine sands, ms = medium sand, and cs = coarse sand [70].

Buckingham's theory is one of interest as it is simpler than Biot-Stoll and concludes an attenuation relationship of f^1 as Hamilton has found. Buchanan [71] in a review of Biot-Stoll and Buckingham models, highlights previous research found the Buckingham model attenuation calculation is in good agreement over a broad frequency range, whilst Biot-Stoll struggled with frequencies above 100 kHz . However, Buchanan noted that in predicting the velocity dispersion the Buckingham model failed and the Biot-Stoll model was more accurate. As of 2005, there were no developed means in correcting the Buckingham model [71].

Another model to describe acoustic propagation through a granular media has been developed by Williams [76]. The Williams model is based on Biot-Stoll theory but is a simplified alternative. Williams model is called the Effective Density Fluid Model (EDFM), and it gives an insight into the environmental parameter that is important in determining the acoustic behaviour in granular media. EDFM treats the granular media as a fluid and assumes the frame bulk and rigidity are zero, which assumes that there are no slow compressional and no shear waves. Williams presented the following equations that define the EDFM:

$$B = \left(\frac{(1-n)}{B_g} + \frac{n}{B_w} \right)^{-1} \quad (2.26)$$

where; B is the bulk modulus of the media when the frame bulk modulus and rigidity is set to zero, n is porosity, B_g is the bulk modulus of the grains, and B_w is the bulk modulus of the fluid.

$$\rho_{eff}(\omega) = \rho_w \left(\frac{\tau(1-n)\rho_g + n(\tau-1)\rho_w + \frac{in\rho g\mu}{\rho_w\omega\kappa}}{n(1-n)\rho_g + (\tau-2n+n^2)\rho_w + \frac{in g\mu}{\omega\kappa}} \right) \quad (2.27)$$

where; $\rho_{eff}(\omega)$ is the effective density as a function of angular frequency ω , τ is tortuosity, g is the deviation from Poiseuille flow as the frequency increases given by equation 5 in [76], μ is the pore fluid viscosity, and κ is the intrinsic permeability.

$$\Xi^2 B \phi_t = \omega^2 \rho_{eff}(\omega) \phi \quad (2.28)$$

where; $\phi_t = \phi + \phi_s$, these are potentials given by Stoll, and Ξ is the acoustic wave number.

Equation 2.26 shows that the compressibility (B^{-1}) is related linearly to the concentration of particles, whilst Equations 2.27 and 2.28 show that the compressibility has a frequency dependence. Equation 2.27 presents the effective density, ρ_{eff} , of the saturated granular media as a function of the angular frequency. As the angular frequency approaches zero, the effective density is equal to the bulk density, ρ . Both terms form part of the fluid equation of motion in Equation 2.28 [76].

Williams' EDFM shows good agreement to the Biot-Stoll method. Which demonstrates that the bulk and rigidity have a minor impact on the energy losses of the acoustic wave [76]. If the bulk and rigidity associated losses can be ignored, the Williams EDFM can be

used as a suitable alternative model to the Biot-Stoll, especially considering its simpler method.

These four models are some of the key ones highlighted by the literature review. It is clear that the properties of the granular media are important in understanding the losses, however all the models differ in how influential granular media properties are on the losses. Differences are also in what the relationship between attenuation and frequency is, empirically Hamilton found a f^1 relationship but Biot-Stoll found a f^2 for low frequencies and $f^{\frac{1}{2}}$ for high frequencies. By looking at the attenuation-frequency relationship in future testing, the appropriate model can be utilised. Further work has been done to develop these models and the relationships between granular media properties and acoustic properties.

Research by Strelitzki, et al. [77] studied the impact of porosity and pore sizes on the ultrasonic properties of bone, they found that higher porosity results in a reduced wave speed but the size of the pores themselves have little impact on the velocity. The researchers also found that the higher porosity caused a reduced attenuation coefficient, but the size of the pore did impact the attenuation as the larger pore size results in a reduced attenuation [77]. This has been seen in other research, such as by Goueygou, et al. [78] where it was found that phase and pulse speed decrease with increased porosity and permeability. The effect of porosity and permeability is more complex though as the relationship depends on the saturation, with dry sample showing an increased attenuation with increased porosity/permeability. The attenuation decreased with greater porosity/permeability in saturated samples [78].

Work undertaken by Sessarego et al [79] shows that attenuation appears to be proportional to the frequency of the wave, as proposed by Hamilton and later on by Buckingham. Other key points to note is that at frequencies above 1.3 MHz the attenuation was so great that the signal could not be measured. Through comparing the data with other researchers Sessarego et al [79] found that the attenuation could be linked to the grain diameter. As those who had experimented with larger grain diameters had higher attenuation. This is an important consideration during this project's research [79].

Work undertaken by Ivakin and Sessarego [80] may explain why there appeared to be a link between attenuation and grain size. It was found that at frequencies below 2 MHz there was a large significant difference in measured backscattered strength. However, this was with the finer sand having a larger backscattering strength [80].

Other work undertaken by Sessarego et al [81] found that the reflection of sound depended strongly on the ratio between the wavelength and the particle size. This further indicates there may be a link between the attenuation and particle size thus it will be important to choose the correct parameters for the particle size [81].

Work conducted by Hickley and Sabatier [82] on the appropriate Biot-Stoll parameters that should be chosen to model water-saturated sand [82]. This work was essentially continued research previously conducted by Chotiros on detecting the Type 2 slow compressional waves [83].

Hickley and Sabatier came to a useful conclusion in that the different values in the bulk modulus, such as Chotiros measuring 7×10^9 Pa rather than the 3×10^{10} Pa, was explained by the inhomogeneity of the solid matrix. This is one of the more important conclusions to take from this as it echoes the research by Shields and Sabatier. It seems that the inhomogeneity of the media will be very important in this project as although it may be inhomogeneous from the start we would expect the inhomogeneity of the media to increase as sediment is captured.

The other key conclusion from the paper is that as the researchers reduced bulk modulus the phase speed of both types of compressional waves are reduced, which is demonstrated in Figure 2.6. Thus it was concluded to obtain the largest speed for the type 2 compressional wave a minimum value of bulk modulus is required [82].

Later work was undertaken by Chotiros and Isakson [84] on wave propagation in a water-saturated sand and grain contact physics, which explored the Biot-Stoll model further. It was found that in sandy ocean sediments when acoustic measurements were taken over a broad range of frequencies the sound speed dispersion was far greater than that predicted by the Biot-Soll model and the sound attenuation did not follow the consistent power law. The researchers made a detailed argument to explain these

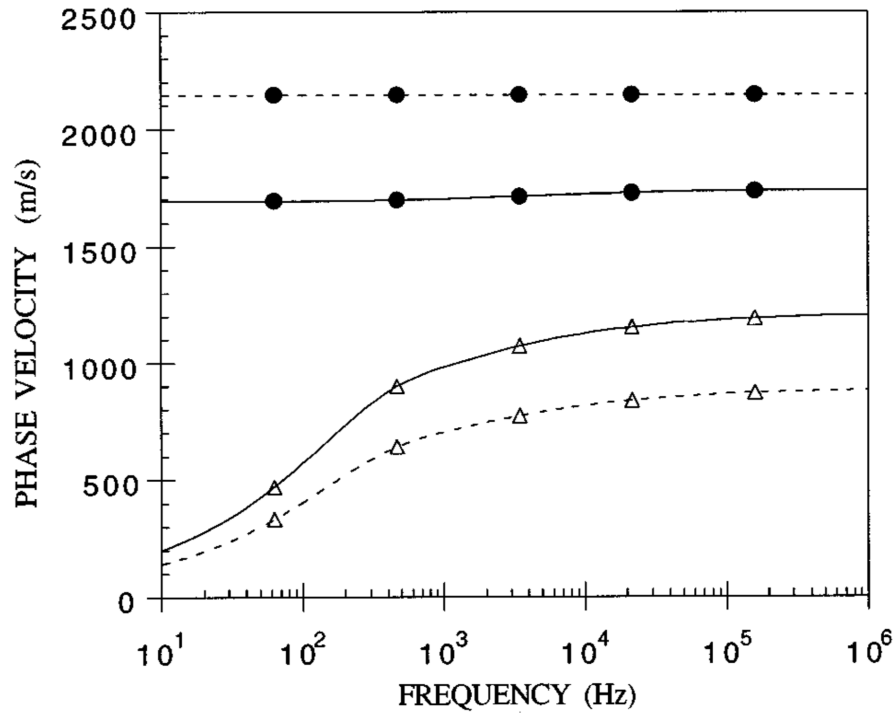


Figure 2.6: Hickey, et al. Graph of phase velocity for type 1 (circle) and type 2 (triangle) waves with different bulk moduli. Solid lines are Chotiros values of bulk modulus and dashed are calculated values [82].

observations [84].

A key factor in the understanding the acoustical response expected in the filter media during operation is the impact of saturation levels. In typical operation, the filter should be at least partially saturated at all times, though this needs to be investigated further. A bulk of research has been conducted within this area, for example, Shields and Sabatier [85] did research into the effect of moisture on wave speeds in a granular medium.

The researchers conducted a series of experiments to determine the effect of moisture on compressional and shear wave speeds in unconsolidated granular material. The researchers conducted these experiments whilst ensuring other effects were minimal, such as the Janssen Effect [85], to ensure repeatable results. The first conclusion the researchers formed was that the Ottawa sand, used as one of the media, had a vapour

pressure isotherm that fit well with Bruauer-Emmett-Teller (BET) theory. One key equation of BET theory describes the amount of water adsorbed on the surface of the grains shown in Equation 2.29.

$$\frac{m}{m_m} = \frac{w(p_c/p_f)}{(1 - p_c/p_f)[1 + (w - 1)(p_c/p_f)]} \quad (2.29)$$

where m is the moles of vapour adsorbed and m_m is the moles to cover a monolayer. The variables needed for this is pressure, p_c , above the curved surface and p_f is the vapour pressure above a flat surface at the same temperature whilst w is the monolayer coverage.

With the circumstance being that the surface area of the grains was assumed to be three times the area calculated. This makes BET theory a potential useful investigation, it also presented an interesting point on what assumption to use for the surface area of the sand. This assumption is due to the fact that Ottawa sand particles are not perfectly spherical and actually vary in size. It is important to take this into account in the project and look to see whether the same assumption is appropriate for the silica sand in this project.

The researchers highlight that the effect of whether the water was flowing or stationary is very small on the acoustical signal due to the low viscosity of the water [85]. This presents a challenge in developing a sensor system as sediment could impact the viscosity of the water.

It was concluded that to understand the acoustic wave passing through a moist granular media it is important to understand the terms contact mechanics due to the moisture of the media having little effect on the wave velocities. Which means that the compressional wave speed for dry material formulated by Shields, Sabatier and Wang presents a potential equation that may be usable to model the acoustic wave, Equation 2.30.

$$c_p = 0.82 \left[\frac{N\zeta x^{\frac{1}{2}}}{(1 - \nu)\rho_g} \right]^{\frac{1}{3}} \quad (2.30)$$

Where; N is the number of contacts per grain, ζ is the rigidity/shear modulus, ν is the Poisson's ratio for the media, ρ_g is the density of the grain, and x is the height of the media.

This means it is important to determine whether filter media ever becomes fully

saturated, which seems unlikely due to the apparent conditions needed to achieve this in the paper [85].

Later research into the effects of soil water potential and moisture content on sound speed, a 2-year monitoring experiment was conducted [86]. The main conclusions from this research show that a power law relationship between the speed of the sound wave and the water potential exists.

$$c_p = J + G\phi^e \quad (2.31)$$

Here the compressional wave speed is equal to the constant, J , and the constant, G , multiplied by the water potential, ϕ , raised to the power of exponent, e . The water potential is the negative pressure caused by internal forces, such as capillary force and absorptive forces, which changes the stiffness and strength of granular media [86].

Lu and Sabatier's results suggested that the impact of moisture content was relatively minor, so it was concluded that a sound speed measurement using the power law equation, can determine the water potential. This is an important value as it results directly from the combination of the capillary and absorptive forces induced by the fluid. As the forces causing a negative pressure, this then influences the granular media's stiffness and water potential[86].

In other work undertaken by Sessarego et al [81] it was found that the reflection of sound depends strongly on the ratio between the wavelength and the particle size. This further indicates there is a link between the attenuation and particle size. Thus it will be important to choose the correct parameters for the particle size [81].

Whilst the level of saturation appears to have little effect on the losses, research has found that gas bubbles within saturated media can significantly impact an acoustic wave. Work by Anderson and Hampton [87], [88] has formed a significant basis for research on bubble effects on acoustics. Anderson and Hampton outlined that the significant bubble characteristics that impact acoustics are internal pressure, size distributions and the ratio of specific heats of the gasses [87], [88].

To understand the impact of gas bubbles in a saturated sediment, Anderson and

Hampton developed an empirical model. Equation 2.32 below presents an equation to calculate a gas bubbles resonance frequency.

$$f_b = \frac{1}{2\pi r_g} \left(\frac{3\gamma p}{A_p \rho} + \frac{4\zeta}{\rho} \right)^{1/2} \quad (2.32)$$

Where; r_g is bubble radius, γ is the ratio of specific heats of the gas, p ambient hydrostatic pressure, A_p is the polytropic coefficient of the gas (see [87]), ρ is the bulk density of the sediment, and ζ is the real part of the sediment shear modulus/rigidity. Equation 2.32 shows that the bubbles resonance frequency is impacted by both the properties of the gas and the surrounding sediment.

Anderson and Hampton then developed an equation that models the sound speed in a large gassy sediment, where the frequency of the wave is below that of the bubbles resonance frequency. Equation 2.33 shows that the sound speed in gassy media, c_g , is primarily impacted by the sediment bulk modulus, B , and the bulk density of the gassy sediment, ρ .

$$c_g = (B/\rho)^{1/2} \quad (2.33)$$

For sediments with a small gas content a different equation is required where the sound speed is now additionally impacted by the sediment rigidity, ζ , as shown in Equation 2.34.

$$c_g = [(B + 4/3\zeta)/\rho]^{1/2} \quad (2.34)$$

Both Equations 2.33 and 2.34 result in the sound speed being lower than in gas-free sediment. When the frequency of the acoustic wave is at and above the bubble resonance frequency given by Equation 2.32, then a different sound speed equation is required.

Anderson and Hampton presented Equation 2.35, which gives the sound speed for frequencies above or equal to the bubble resonance frequency.

$$\left(\frac{c_p}{c_g} \right) = \frac{1}{2} \left(1 + \frac{BX_1}{\gamma p + 4/3\zeta} \right) \times \left\{ 1 \pm \left[1 + \left(\frac{BY_1/(\gamma + p + 4/3\zeta)}{1 + BX_1/(\gamma p + 4/3\zeta)} \right)^2 \right]^{1/2} \right\} \quad (2.35)$$

where $X_1 = \frac{n_g(1-f_*^2)}{(1-f_*^2)^2 + I_*^2}$, $Y_1 = \frac{n_g \cdot I_*^2}{(1-f_*^2)^2 + I_*^2}$, $f_* = f/f_b$, $I_* = I \cdot f_*^2$, n_g is the gas porosity, I is the damping constant given by equations presented in [88].

Anderson and Hampton looked at previously published observations which show that Equation 2.35 agrees well with them. The sound speed calculated through Equation 2.35 shows that just above the bubble resonance frequency the sound speed exceeds that observed in gas-free sediments. However, as the sound frequency increases, the sound speed reduces to approximately the same level seen in gas-free sediments [88].

If the sound speed was the main observation being taken, utilising higher frequencies than the bubble resonance frequency would result in little impact on the observations. However, no matter the model being used, attenuation in a saturated sediment has shown a frequency dependence. Therefore, it may not be practical due to the difficulty of acquiring a good quality signal.

Anderson and Hampton then developed Equation 2.36 which calculates the attenuation, α_b in $Npcm^{-1}$, caused by the presence of gas bubbles. Anderson and Hampton argued that this could explain previously published observations.

$$\alpha_b = \frac{\pi f c_p}{c_g} \frac{BY_1}{c_g \gamma p + 4/3\zeta} \quad (2.36)$$

Anderson and Hampton argued that the attenuation in gassy sediments is primarily resultant from frame friction absorption, loss mechanisms resultant from bubble motion and scattering effects caused by the bubble. Additionally, Anderson and Hampton found that even with relatively low concentrations of gas bubbles in saturated sediment large attenuations can be seen, even if the impact on sound speed is relatively minor.

Herkowitz et al. [89] developed the work by Anderson and Hampton further, by simulating the attenuation caused by microbubbles. They found that the compressibility, bubble size and frequency all varied with the features of the sediment. Herkowitz et al. found that the presence of microbubbles leads to a resonance-type absorption in high-frequency ultrasound. However, low-frequency ultrasound results in a large reduction of sound attenuation [89]. It was found that the Herkowitz et al. simulation correlated well with sound speed data previously published, but problems arose with the lack of data for attenuation as the bubble size and distribution is important.

Leighton [90] summarised the research in acoustic bubbles, and then Leighton [91] further

developed Anderson and Hampton's work on the effect of air bubbles with the development of his theory [91]. Leighton's theory does not assume that the bubble dynamics are linear, steady-state and monochromatic. Instead when an acoustic field drives a gas bubble, the bubble instead acts as a nonlinear oscillator [91]. Equation 11 in [91] forms the main basis to predict the dynamics of a single bubble in a lossy elastic solid.

Leighton [92] developed his 2007 theory further by developing a method for estimating void fractions in sediments using subbottom profiles [92]. The method utilises a first-order technique and is able to assess the sound speed changes caused by bubbles and provide an estimate for the void fraction. However, Leighton highlights that the simplicity of the technique is negated by its limitations [92].

Mantouka et al. [93] further developed Leighton's 2007 theory in their model for nonlinear gas bubble pulsation in marine sediments [93]. Mantouka et al. highlighted that the majority of previous studies on the impact of gas bubbles in sediment have assumed the location of the bubble is within the pore fluid space. Additionally, it was previously assumed that bubbles do not impact the sediment structure [93].

The model developed by Mantouka et al. [93] took this into account. A number of assumptions were made in the development of their model; that the sediment supported one compressional and one shear wave, the first compressional wave dispersion and the dissipation caused by internal friction were neglected [93].

The nonlinear model for bubble pulsations in sediments found that the resonance frequency declined as the size of the bubble increased, as seen in the Anderson and Hampton model. Additionally, the damping of acoustic radiation is found to be the dominant loss mechanism at high frequency. However this is not the only important loss mechanism seen, viscous damping and elastic damping both are significant sources as well. The elastic damping was not identified in the Anderson and Hampton model [93]. At medium frequencies Mantouka et al. highlighted that thermal damping could become a dominant loss mechanisms.

Mantouka et al. model found that as with the Anderson and Hampton model, the smaller

the gas bubble the higher the attenuation at a higher frequency. There is significant difference near the resonant frequency between the results calculated with the Mantouka et al. model and the Anderson and Hampton model. However, Mantouka et al. highlight that the prime advantage of their model is the lack of user intervention required to overcome the sign ambiguity [93].

Dogan et al. [94] continued the work conducted by Montouka et al. by exploring the effects of sediment rheology (shear viscosity and the rigidity) [94]. This work was based on the Williams EDFM, outlined earlier. What the authors found was utilising the Williams EDFM, results in high attenuation near bubble resonance frequencies, as shown in the previous works. However what wasn't caught in previous work was that due to pore fluid viscous dissipation, the attenuation in the high-frequency limit increases to values observed in gas-free sediment [94].

The developed Dogan et al. model also shows that the dispersion of the phase velocity caused by pore fluid and gas bubbles is significant. The enhanced model includes the impact of individual contact surfaces between phases, instead of treating it as a homogeneous medium [94]. Dogan et al. highlight that the general conclusions of the model are that viscous and elastic losses dominate at small bubble sizes with the effect of surface tension at the gas-liquid interface is negligible. Additionally, at mud and clay-like sediment intermediate bubble sizes may cause losses through thermal damping effects. Damping of the acoustic radiation also becomes very effective when the driving frequency and bubble size increases. Multiple bubbles also cause multiple scattering effects, which broadens the attenuation peaks and raises the wave speed at the bubbles resonance frequencies as seen in gassy water [94].

Finally the enhanced model by Dogan et al. takes into account the possible frequency-dependent viscous and elastic behaviour when the gas void fraction is high enough for the linear stress-strain relationship is no longer valid [94].

The work initially developed by Anderson and Hampton, and then developed by others, show that gas bubbles can have significant effects on the acoustic wave. As the Up-Flo[®] Filter System will drain down between storm events, it may experience bubbles within its

filter media. It is important to keep this in mind during sensor development, as it could result in repeatability issues. Especially as bubble size is an important affect, and the size may not be consistent in realistic operation.

From the past research in this area numerous key points and issues have been identified. Firstly, to understand the acoustic wave behaviour in the media, it will be important to establish what the environment and nature of the media are. As factors such as shape, size, porosity and saturation will impact the acoustic signal significantly. However, this is also one of the great benefits of an acoustic system, as through developing knowledge within this area further a robust sensor arrangement can be developed that is highly sensitive to the changes in the media conditions, such as porosity and density which would also impact the hydraulic performance. However, the effect of gas bubbles may cause issues in real life. Requiring further work to take into account the effect.

2.6 Electrical Techniques

One other potential route in monitoring the filter bed condition is through the use of Electrical Resistivity and Conductance techniques. For example, one possible method is through the use of Electrical Resistivity Tomography (ERT). This technique is based on a very simple concept of measuring the resistivity changes to understand the state of the media. It also provides numerous ways to view the data; 1D, 2D or 3D, dependent on the need of the user [95] and the type of sensor used.

Research has shown ERT to be effective in many ways in the monitoring of a fluidised granular media; some potential uses identified clearly show the strengths of ERT. For example Damascenco and Fratta [96] conducted a series of experiments to determine whether the diffusion of chemical fronts in a granular granular media could be monitored through the use of ERT. Using a 2D system, the researchers successfully monitored the diffusion of the chemical front and concluded that in future work a 3D system would be of use. Whilst successfully monitoring the chemical diffusion front, the researchers also characterised the properties in the media that have an effect on ERT and the problems associated with ERT.

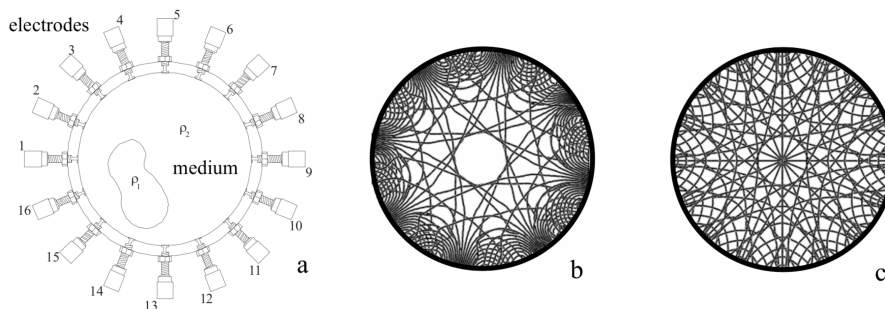


Figure 2.7: Damascenco and Fratta figure showing arrangement of ERT and the two different schemes possible; (a) Basic 16 electrode ERT system with simulated inclusion, and electric potential lines for (b) adjacent and (c) opposing excitation scheme [96].

Firstly, ERT has two different schemes that are important to highlight; the adjacent electrode and opposing electrode schemes, as seen in Figure 2.7. Whilst the adjacent

scheme is very sensitive along the boundaries, it is less sensitive at the centre of the media. The opposing scheme provides a uniform resolution but with less sensitivity. Both schemes though are based on the same method of applying a voltage across electrodes and measuring the voltage drop between them. The resistance between two electrodes is dependent on the electrical resistivity and dielectric permittivity of the mineral, liquid and gas phases, surfaces and distribution of the media. As these properties directly affect the ERT signal, and change as the filter media removes sediment from stormwater, ERT may provide a useful indicator of filter condition [96].

Other work undertaken by Zumar et al [97] demonstrated that ERT could also be used for the observation of water movement in soil. This is of particular interest due to this potentially being a suitable method to determine when the filter clogs as when clogging occurs water movement will, of course, change [97]. Work was also undertaken by Lekmine et al [98] to quantify the evolution of dissolved species in a granular media from 2D resistivity models. The researchers found that they could optimise the measurement protocol with an acceptable compromise between spatial and temporal resolutions. Through dynamics monitoring a reliable estimate can be achieved of the position and thickness of the mixing front. This is of particular significance as it further indicates that ERT may be valuable in the set-up of the present study [98].

Whilst the concept of ERT is simple, the solution of it is quite complex with the calculations that are involved being computationally intensive. This raises questions, due to the low power requirement in the finalised sensor design, as to whether the ERT system is appropriate [96]. Additionally, the number of electrodes required to provide usable data raises the cost resulting in the low cost requirement not being achieved.

Nichols [99], [100] has developed an electrical resistivity technique that could meet this low power and cost requirements, a multi-probe conductance device shown in Figure 2.8. Developed to measure water depth and sediment deposition, due to the usefulness for understanding flow and siltation processes in pipes and channels. It was developed to be cheaper than acoustic and pressure based systems whilst also potentially delivering better accuracy [99], [100].

The multi-probe conductance device developed by Nichols is an extension of the operating method of traditional conductance wave probes. These function through calculating conductance between two partially submerged conductors which output a voltage proportional to the submerged length. With this device the electrical properties, of the substance being tested, determine the ratio of the output voltage to the submergence depth.

The conductance probes output the summation of the conductive effects of the water and the sediment layer. As the ratio of voltage to submergence depth, V/x_d , is different for the water and the sediment layer. The probes are numbered left to right, $i = 1$ to 10. For probes 1 to 3 in the example conditions shown in Figure 2.8 the researchers gave the following probe voltage output, V_i , equation:

$$V_i = [(V/x_d)_{water} \times x_w] + [(V/d)_{sediment} \times x] \quad (2.37)$$

For probes 4 to 7:

$$V_i = [(V/x_d)_{water} \times (x_i - x)][(V/d)_{sediment} \times x] \quad (2.38)$$

For probes 8 to 10:

$$V_i = (V/x_d)_{sediment} \times x_i \quad (2.39)$$

In these equations, x_i represents the probe length. Through plotting the probe length with the corresponding voltage useful data can be acquired.

Figure 2.9 shows an example plot of the output of the multi-probe conductance device. The gradient of line 2 indicates the conductance of the fluid medium, with the gradient affected by changes of the electrical properties of the fluid medium. Allowing for the characterisation of unknown flow substances or detecting pollutants [99]. The gradient of line 1, however, indicates the conductance of the sediment. This allows for the characterisation of the sediment and the degree of saturation, as a more saturated granular media results in a larger conductance [99]. Line 1 shows where the probes are not within wither the fluid medium or the sediment, but within the air where no conductance is possible [99]. Points A and B within the figure, show where the profile changes allowing for the height of the sediment and fluid medium to be calculated.

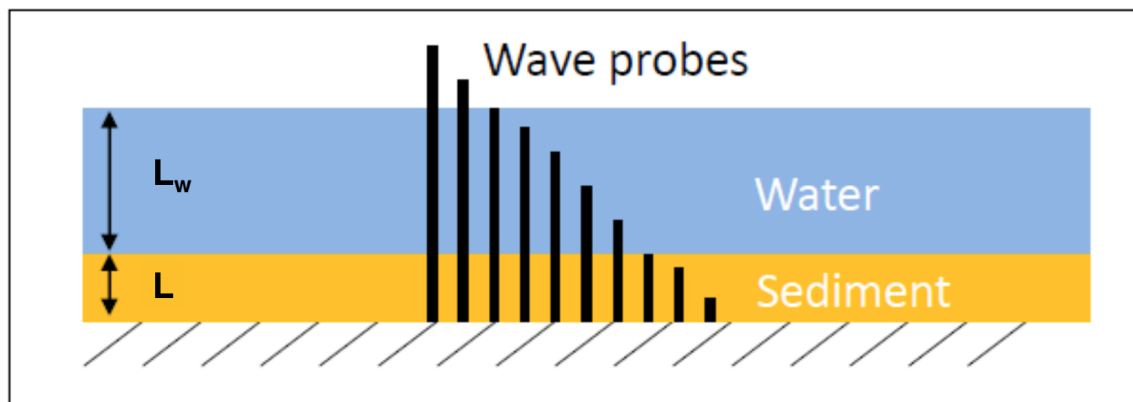


Figure 2.8: Multi-probe array by Nichols [99].

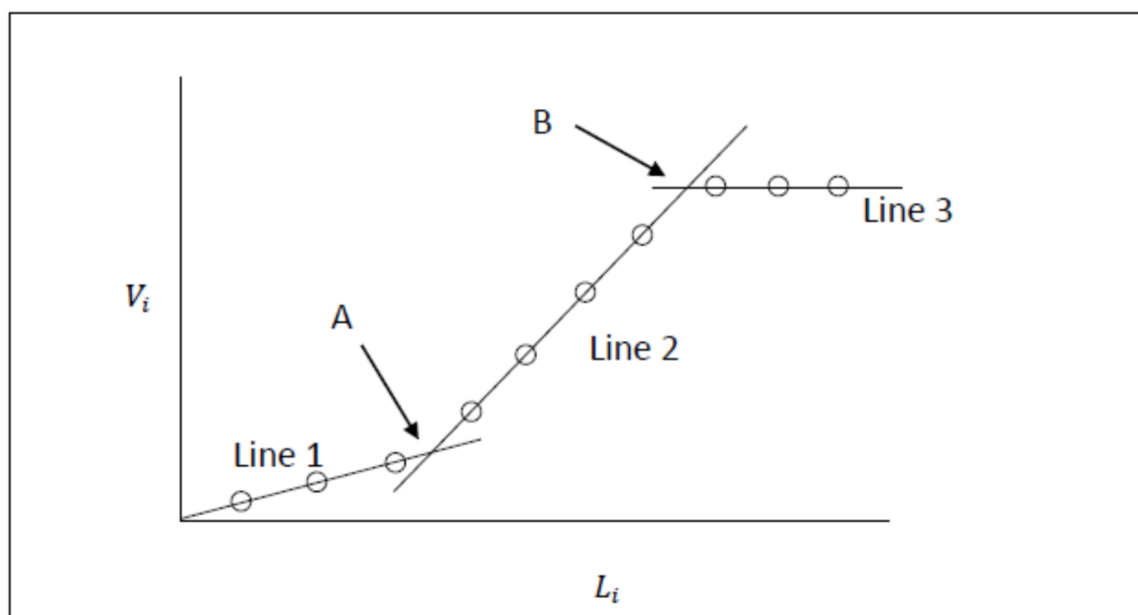


Figure 2.9: Plot of probe length and voltage per probe [99].

These probes are created by printing the electrode strips on a circuit board, 20 strips are printed at 76° which produces an incremented-length array. The way the electrodes are printed can be adapted to the needed scenario [99].

This multi-probe conductance device can be useful in the monitoring of the health of the Up-Flo[®]'s filter media, as the device would be able to monitor the saturation of the media, the height of water on top of the media, and would be impacted by sediment capture as sediment would displace pore fluid. Additionally, the adaptability of the design would be useful in the sensor development as it can be used in different modules, combining with the devices low cost and low power requirements makes this suitable for the sensor development in this project.

However, the design of the electrode strips being printed on a circuit board raises issues regarding the robustness. To ensure the sensor system can be utilised in realistic operation the sensor needs to be robust to withstand poor conditions, this would need to be assessed in this project. Further, whilst the conductivity of the filter media will be changed by sediment capture, the type of sediment would be important information regarding how it will change. As heavy metals may increase the conductivity, but other sediments may decrease it. Finally, one problem is that it would only detect changes in conductance around the edge of the medium, not in the centre. This may result in important changes in the filter media condition being missed.

2.7 Chapter Summary

This literature review has highlighted the key background information, laws and relationships which was necessary to conduct this project. In Section 2.1 the problems of sediment pollution in surface waters caused by diffuse pollution within stormwater was outlined. The pollution arises when stormwater, carried to the surface water body by a separate drainage system, is left untreated. The effects of the pollution is incredibly varied, with impacts to aquatic fauna and flora and to human health. The sediment characteristics, such as size and loading, has also been shown to be highly dependent on the site characteristics and seasonal changes. This requires in-depth knowledge and planning to provide effective treatment and mitigate its effects on the environment.

The United Kingdom's approach to the treatment of stormwater in separate drainage systems was summarised in Section 2.2. The approach was initially born out of the regulations in the European Union's Water Framework Directive. Since the introduction of the directive, the UK approach has continued to evolve, with the introduction of Sustainable Drainage Systems (SuDS). With SuDS there are two types; soft and hard. Soft SuDS use more natural routes for stormwater treatment, such as stormwater detention ponds, and hard SuDS are manufactured treatment systems, of which the Up-Flo[®] Filter System is one. Currently, the local flood authority and local planning systems have responsibility for stormwater treatment and planning, whilst the use of SuDS is encouraged. To fill the lack of national regulation CIRIA has developed a guide on SuDS and British Water have developed a code of practice for manufactured treatment devices.

One of the key processes used by Hydro International Ltd Up-Flo[®] Filter System to treat urban stormwater pollution is the use of settlement within its sump. Section 2.3 highlighted the theory behind it, including the four types of settlement processes. It is anticipated that the Up-Flo[®] Filter System utilises primarily Discrete and Flocculant settlement. The settling velocity is determined by Stokes' Law was given in Equation 2.1, as long as the density is higher than water density and particles are large enough the sediment will settle.

For particles not settled in the sump, the filter media within the Up-Flo[®] Filter System is responsible for removal. Section 2.4 summarised the theory behind how sediment is captured, what influences it and the flow through granular media. The flow is impacted by a media's permeability, which is in turn impacted by its porosity. As the porosity declines with sediment capture, the permeability is a way to monitor the health of the filter media. Determining this permeability is dependent on the nature of the flow, with Darcy's law being utilised for slow-moving flows but additional expressions required for fast moving laminar and turbulent flows.

To develop a functioning monitoring system which is low cost, low power and robust, two techniques were highlighted. Utilising acoustics was one method of interest, Section 2.5 outlined the theory of acoustic transmission in saturated granular media and what influences it. There are a number of developed models to describe acoustic transmission, ranging from empirical to physical based models. This makes it difficult to pick a suitable model for use, however, data from experiments can influence the choice by looking at how attenuation of the signal varies with frequency. No matter the model used to understand the transmission through the media, all models show the property of the media impacts the signal. One of these influencing properties is porosity, which would decrease with the capture of sediment resulting in acoustics being a useful technique for filter media monitoring. However, a growing body of research has shown that gas bubbles within a granular media can have significant impacts on the acoustic transmission, affecting both wave speed and attenuation. As the Up-Flo[®] Filter Systems filter media drains down between storm events, this may result in issues with reliability of the acoustic signal.

Section 2.6 summarised the background to another possible technique of electrical conductance and resistivity. The established technique of Electrical Resistivity Tomography was highlighted as a possible technique, but its power and computational requirements make it an unsuitable monitoring technique for the Up-Flo[®] Filter System. The new resistivity technique developed by Nichols, using a multi-probe conductance device, was summarised and was highlighted as a useful technique in filter media monitoring due to its low cost, adaptability and low power requirements.

This review of the current literature has outlined why it is important to treat urban

stormwater and the current challenges associated with it. The literature helps to form the experimental techniques, which later chapters outline. To fully understand the processes involved in both removal of sediment and filter media monitoring the laws, relationships and observations need to be utilised.

Chapter 3

UP-FLO® FILTER SYSTEM EXPERIMENTS

This chapter presents the method and the results obtained from the experiments of the Up-Flo® Filter System to complete the aims and objectives outlined in Chapter 1. These experiments allowed for the more in-depth knowledge of the removal mechanisms, and recommendations for improving the device and its maintenance protocols.

Sections 3.1 to 3.2 present the experimental conditions and the key variables used for the readers' information.

In Section 3.3 the strategy that was initially formed to achieve the outlined aims and objectives in Section 1.3 is presented. Using this strategy, the experimental method was derived and is outlined in Section 3.4. In this section the experimental layout, operation, and equipment used is discussed in detail.

To analyse the raw data, collected throughout the experiments, a number of methods were used. These methods are outlined for the reader in Section 3.5. The processed results obtained through these methods is then presented in Sections 3.6 - 3.14.

Section 3.7 presents the permeability results from the Clean Water Experiments, to investigate the background permeability changes. Sections 3.8 - 3.11 then present the permeability results of the sediment experiments. Afterwards, the Up-Flo® Filter System removal efficiency is explored using the Total Suspended Solids results in Section 3.12. Section 3.13 then presents the results of the mass balances conducted during the sediment experiments, to explore the Up-Flo® Filter System removal mechanisms further. Finally, Section 3.14 presents the results of the particle size analysis of the filter media bags after the sediment experiments and an estimation of the particles sizes caught in the filter media.

Using the results presented in this chapter, Section 3.15 discusses the removal processes of the Up-Flo® Filter System, the effects of sediment loading on the system, and how maintenance practices could be adapted. Section 3.16 then summarises the chapter and highlights its key findings for the reader.

3.1 Experiment Identification Table

Table 3.1 presents the key information of the experiments and flows that the Up-Flo[®] Filter System had been subjected to during the experimental period. As the table shows the first set of experiments consisted of Clean Water Experiments, this was to study the mechanisms of the Up-Flo[®] Filter System and the impact of clean water flow on the filter media permeability. The second stage of experimentation consisted of sediment dosed experiments on the same filter media used throughout the initial experimentation. This was to study the removal efficiencies of the Up-Flo[®] Filter System and the effect of the sediment on the filter media.

The third stage of experimentation consisted of further sediment experiments on a new filter media, due to supply issues. These sediment experiments consisted of the same sediment as previously used, with adaptations made to the experimental method from the experience of the previous experiments. The fourth and final stage of experimentation consisted of more sediment experiments, with fresh media, using a larger and more realistic sediment size. This was to study the impact of the larger sediment size on the Up-Flo[®] Filter System removal efficiency and its impact on the filter media, in comparison to the smaller sized sediment.

The notes column lists any other information, with definition of the abbreviations shown below.

- CWE: Clean Water Experiments.
- CWC: Clean Water Cycle.
- MC: Filter Media Change.
- VT: Valve Training

Valve training was the exercising of the valve over 10 mins where it was repeatedly opened and closed, to ensure that the valve remained in optimum working condition. See Appendix B.1 for an example flow profile of the valve training.

The reynolds number ranges for each experiment is presented in the final column, this was calculated as shown in Section 3.5, if the value was within the range of 1 and 10 then the flow is applicable to Darcy's Law.

For a less concise table please see Appendix A.

Table 3.1: Permeability Experiment Number Identification Table.

Experiment Number	Date	Flow Rate [Ls^{-1}]	Flow Condition	Notes	Reynolds Number
T01 - T23	23/05/17 - 25/09/17	2 - 5	1 Stage, 2 Stage	CWE, VT	3.47 - 6.94
T24 - T28	23/11/17 - 29/11/17	2	2 Stage	ST01 CWC and ST01	3.47
T29 - T34	03/04/18 - 10/04/18	2	2 Stage	ST02 CWC, MC, ST02	3.47
T35 - T40	25/04/18 - 02/05/18	2	2 Stage	ST03 CWC MC, ST03	3.47
End of Table 3.1					

3.2 Material Information Table

Table 3.2 presents key information regarding the filter media and sediments used throughout the experiments. Section 3.4 presents a more detailed particle size analysis of the filter medias. The d_{10} , d_{50} and d_{90} in the table, was measured using particle size analysis described in Section 3.4.

Table 3.2: Key information of materials used in the experimental work presented.

Media	d_{10} (μm)	d_{50} (μm)	d_{90} (μm)	Particle Density (kgm^{-3})
Fraction B Silica Sand	711	961	1310	2650 [101]
Garside Sand	749	997	1360	2650 [101]
Silica Flour	6.11	38.8	105	2650 [101]
Fraction E	107	150	208	2650 [101]

3.3 *Experimental Strategy*

To improve the sustainability in terms of filter media maintenance of the Up-Flo® Filter System, research was needed to study its removal mechanisms. An experimental strategy was formed to identify the key research questions that required development to accomplish this. To develop an extensive understanding, research was divided into three stages. Initially, fundamental research in idealistic scenarios would be conducted, then in stages 2 and 3 complexity would be added gradually to enhance the knowledge of the Up-Flo® Filter Systems processes.

The first stage of the experimentation was to initially look at clean water flow through the Up-Flo® Filter System. This was to form an in-depth understanding of the mechanisms of the Up-Flo® Filter System. This would be done by studying how the permeability of the filter media changed over repeated clean water flows, with the Up-Flo® Filter System set up in a artificial manhole. This would develop knowledge on how repeated flows affected the filter bed over time. The first stage was also to include a range of flow rates, which would have allowed for the Up-Flo® Filter System's max flow rate to be estimated and extensive knowledge on how the permeability changed with various flow rates.

The second stage of the experimentation was to add complexity through the addition of a experimental sediment to the experiments. This would have allowed for a number of measurements with a known sediment particle size and concentration including; Up-Flo® Filter System removal efficiency, location of sediment capture, and the effect on the permeability of the filter media. This stage would also utilise two distinct sediment size ranges for experimentation so as to study the impact of sediment size on the Up-Flo® Filter System removal efficiency.

The final stage of the experimentation was to add complexity through varying flow rates and sediment load to mimic a realistic storm event. This would have allowed for an in-depth study on how the Up-Flo® Filter System operates in storm conditions. Additionally this would have allowed for the effect of varying flow on the permeability of the media to be studied.

The strategy outlined the approach and primary experimental areas that required development to have an in-depth understanding of the Up-Flo[®] Filter System removal processes. Initial experimentation would be conducted on the Up-Flo[®] Filter System with clean water, so as to develop knowledge on the Up-Flo[®] Filter System processes and the filter media properties. Then through the addition of cumulative complexity, the removal mechanisms could then be examined in detail. With the thorough understanding this strategy would provide, recommendations could then be made to improve the Up-Flo[®] Filter System and its maintenance protocols, allowing for greater protection for the environment. This work would also support the work outlined in Chapter 4.

3.4 Experimental Methodology

The strategy outlined the requirements needed to form an in-depth understanding of the Up-Flo® Filter System and its processes. To accomplish this a experimental methodology was formed, and experimental apparatus designed.

Firstly, Hydro International Ltd provided a version 1.3 model of their Up-Flo® Filter System, which is the current system used commercially by Hydro International Ltd. The Up-Flo® Filter System was installed into an artificial manhole, described below, in a similar set up to current Up-Flo® Filter System installations. The main differences in the set up of the Up-Flo® Filter System was the omission and sealing of the drain-down ports, to ensure no media escaped through it and allow flow to be estimated in each module accurately. Diligence was taken during the installation so as to ensure that there was little to no leaks in the Up-Flo® Filter Modules themselves.

An artificial manhole (known as the “rig”), made from 9 mm thick polypropylene, was designed specifically to house the Up-Flo® Filter System. This was a cylindrical shape with a diameter of 1250 mm and a height of 2370 mm so as to replicate a typical Up-Flo® Filter System manhole installation (blueprint provided by Hydro International Ltd, see Appendix B.2). Due to the difference in strength and thickness between concrete and polypropylene, a lip was made approximately 1040 mm from the base of the cylinder to support the frame of the Up-Flo® Modules. For rig access and to allow a full mass balance to be conducted, a 50.8 mm diameter British Standard Pipe (BSP) outlet was moulded into the bottom of the side of the artificial manhole at the lower end of the reinforced sloping base to drain down the Up-Flo® rig. The 50.8 mm diameter BSP outlet had a valve installed on it and an extension pipe which led to a plastic box, ‘collection box’, with a outlet to the university laboratory sump that could be sealed shut. (Figure 3.1)



Figure 3.1: Annotated image of the collection box.

3.4.1 Clean Water Experiments (CWE)

To complete the first stage outlined in the experimental strategy, the Up-Flo® rig sat within the experimental set-up shown in Figure 3.2 during experiments T01 to T23. Water to the Up-Flo® rig, chlorinated to impede bacterial growth, was supplied by a header tank. This header tank was then resupplied at 40 L s^{-1} ensuring a constant pressure head to the valve, as the maximum flow rate used in the experiments was 7 L s^{-1} . The flow rate into the rig was controlled by an electronic valve which was run by a LabVIEW programme, see Appendix B.3, on the computer which also recorded the flow rate which entered the rig, through the use of an Arkon MAG-910 Electromagnetic Flowmeter.

The water flowed into the Up-Flo® rig sump, increasing the rig's water head which drove water through the Up-Flo® Filter System's 6 filter modules, which contained the filter media. Once passed through the modules, the flow exited the rig through the exit module back to the laboratory sump.

Each Up-Flo® Filter Module contained 2 bags of filter media, weighed to 17.26 kg each, with the filter media being Fraction B Sand from David Ball Sand Group. The filter media particle size analysis is shown in Figure 3.3. This shows that the filter media size ranged from $330 \mu\text{m}$ to $1970 \mu\text{m}$. The d_{10} , d_{50} and d_{90} was $711 \mu\text{m} \pm 13 \mu\text{m}$, $961 \mu\text{m} \pm 12 \mu\text{m}$ and $1310 \mu\text{m} \pm 29 \mu\text{m}$ respectively.

The filter media was placed in 200 micron nylon mono-filament mesh bags from a constant height of 100 mm using a funnel. Once at the set weight, the bags were sealed and then shaken to ensure the media was well distributed, the thickness of each filled bag was approximately 100 mm . The bags were then placed in each module, aided by a technician. To place the media in the module so that the lids could securely close, force was applied on the lid till the module clips closed. This led to possible compaction of the media. A graphic of an Up-Flo® Filter Module and its components is shown in Figure 1.3 in Chapter 1.

During experiments, pressure readings across Up-Flo® Module 4 were recorded, so as to

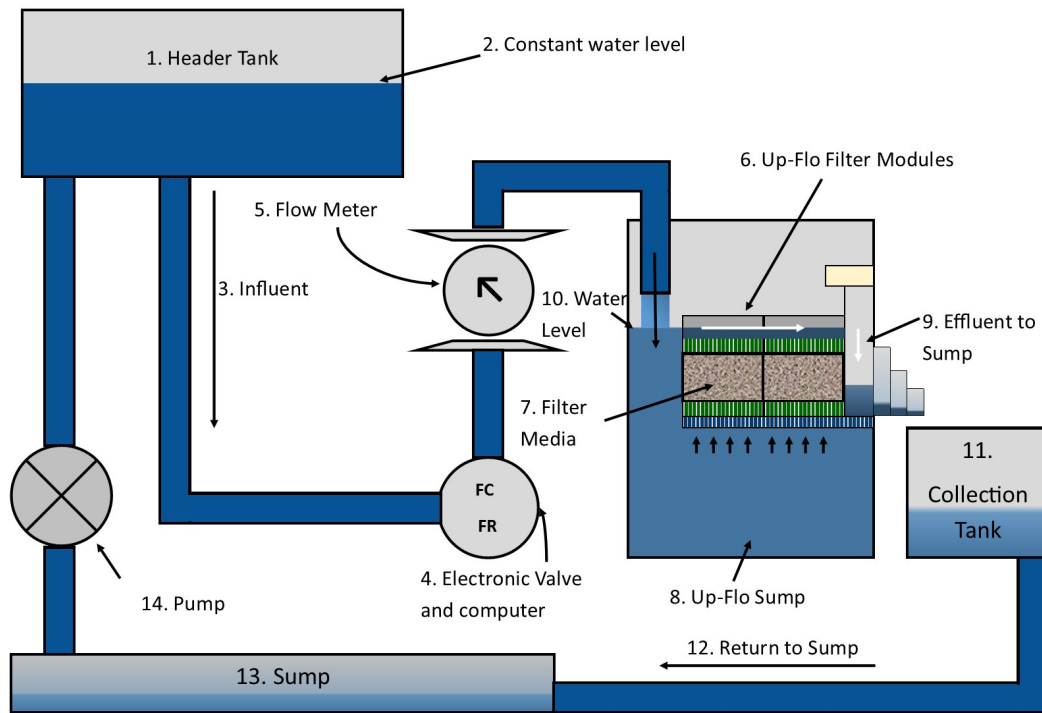


Figure 3.2: Experimental set-up for Clean Water Experiments, T01 to T23 (Not to scale).

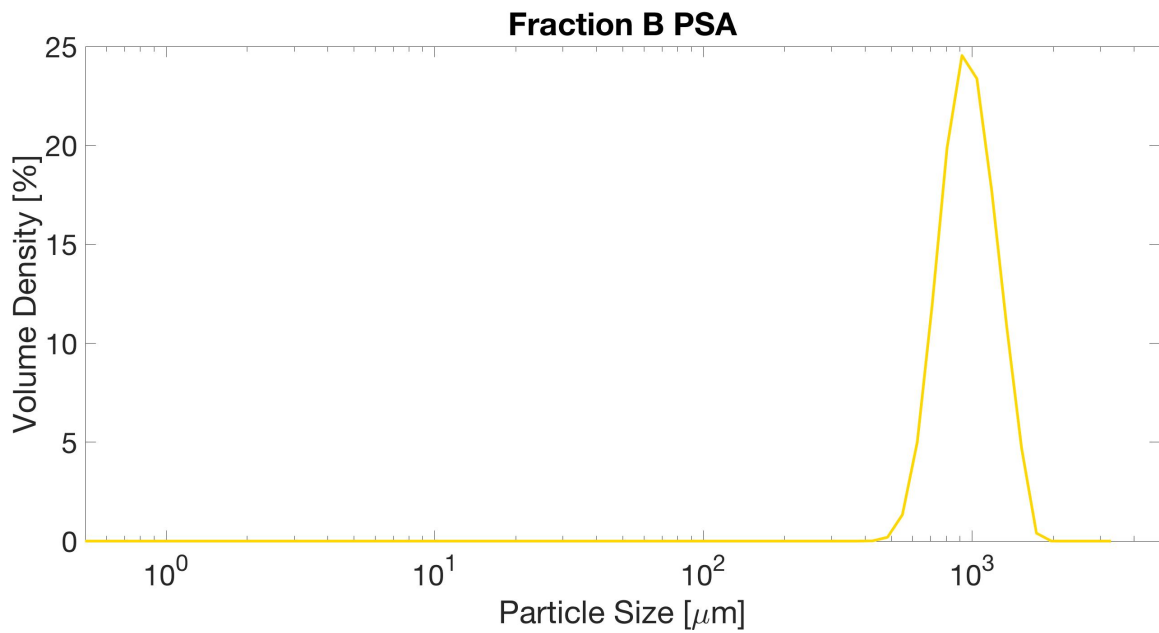


Figure 3.3: Particle size analysis of Fraction B Sand, using Malvern Mastersizer 3000.

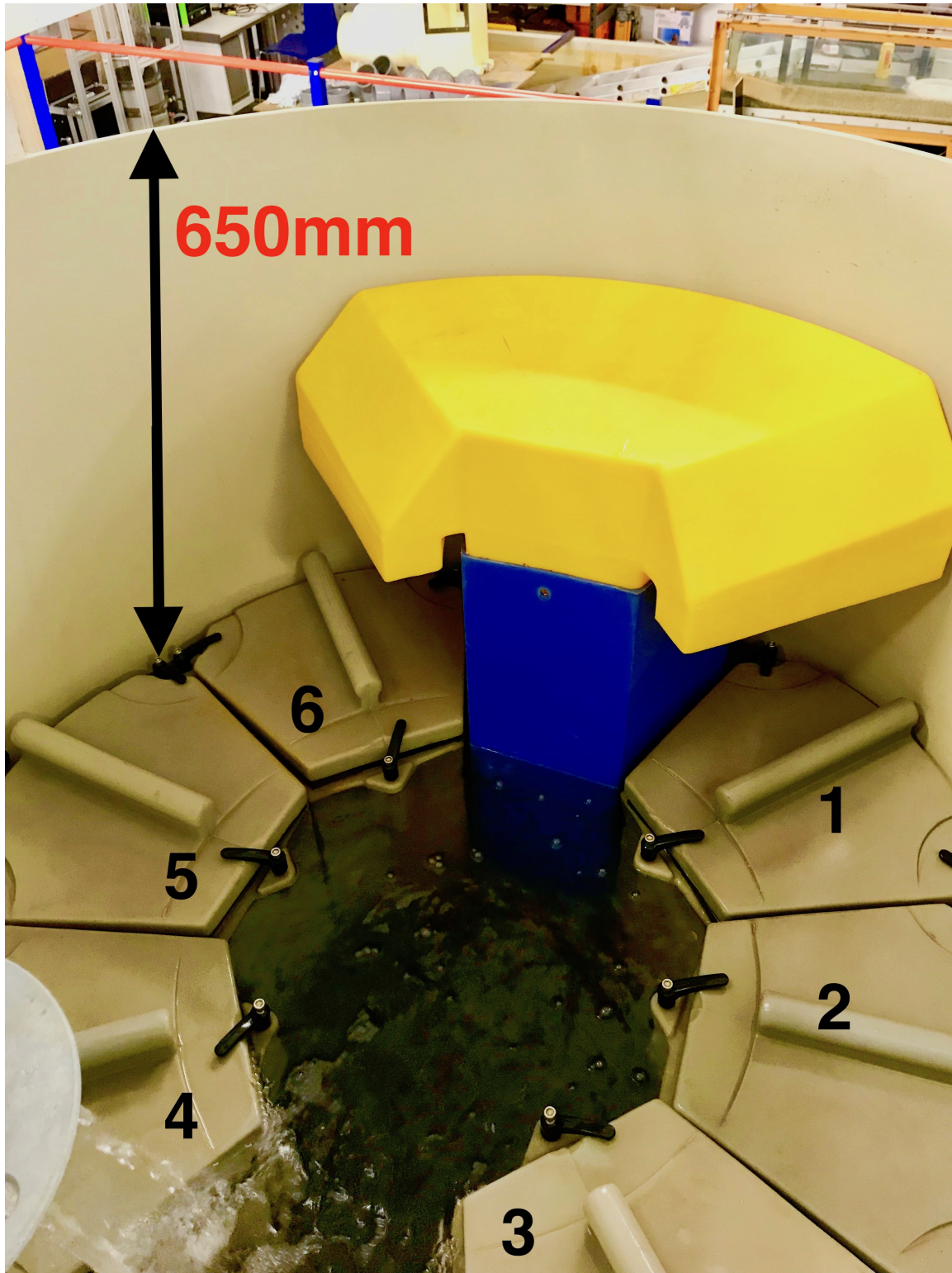


Figure 3.4: Location Numbers for Modules in the Up-Flo® Rig.

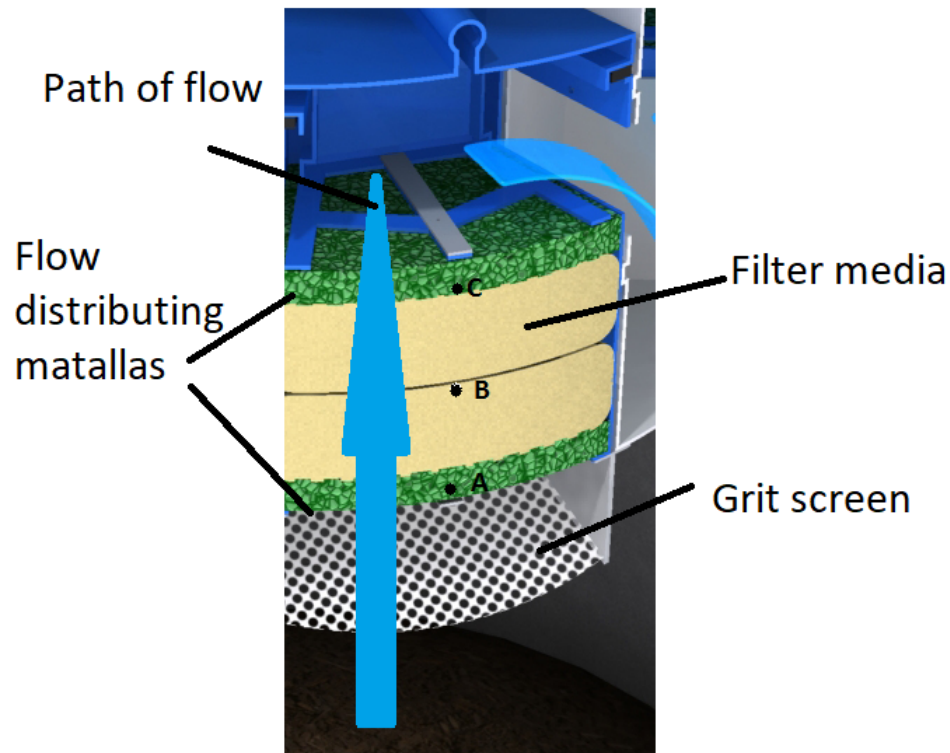


Figure 3.5: Approximate Location of Pressure Tappings in Up-Flo[®] Module 4 (Original image from [102]) [Not to scale].

allow for a calculation of permeability. The location of Module 4 is shown in Figure 3.4 and the approximate locations of these pressure tappings are shown in Figure 3.5.

Pressure point A provided a reading of the pressure at the bottom of the filter media, B provided a pressure reading between the two different filter media bags and C provided a pressure reading on the top of the media where the flow exited the rig and returns to the laboratory sump. The pressure tubes were then drilled through the side of the rig at the same level. The piezometer tubes connected to points A, B and C had an internal diameter of 2.5 *mm*.

A standard 1 metre rule with 1 *mm* divisions was then placed next to the piezometer tubes to measure the water levels to ± 1 *mm*. Testing was then done either by the 1 Stage method or 2 Stage method, explained in the following subsections. Between experiments the rig was not drained, to reduce disturbances on the media and to reduce

air trapped in media.

1 Stage Method

The 1 Stage (1S) method set the flow rate initially to 7 L s^{-1} for 30 minutes, so as to introduce a large flow to the media to uniformly disturb it between experiments. During the 30 minutes the piezometer tubes were dropped down to allow water to flow freely through the tubes, this was to remove any entrapped air from the tubes which may have entered between experiments. At 30 minutes, whilst the flow rate was still 7 L s^{-1} , the tubes were restored to the vertical position and readings were taken for each piezometer tube. Temperature of the sump of the rig was also recorded, these were recorded as 0 minutes. The flow rate required for testing was then set on the computer and the stopwatch was then started. Pressure readings were then started at the 1 minute mark for each of the tappings, with three measurements per tapping being taken. These readings were repeated every minute until the 30 minute mark.

At 30 minutes head measurements were taken once again as well as temperature readings of the sump. The head measurement and temperature readings were then made every 15 minutes until 210 minutes had passed. At 210 minutes the final measurements of head and temperature were taken, then the electronic valve was closed and the experiment was concluded.

2 Stage Method

The 2 Stage (2S) method was broadly similar to the 1 Stage method with the difference being that at the end of the 30 mins at 7 L s^{-1} the pressure tubes were restored but no readings were taken. Instead the flow rate was reduced to 0.3 L s^{-1} for an additional 30 minutes, this allowed for the media to be adequately disturbed but then reduced to allow for it to settle back down. At the end of this 30 mins, pressure measurements and temperature readings were taken and experiment begun in the same way as the 1 Stage method with the flow rate changed to the flow rate required for the experiment.

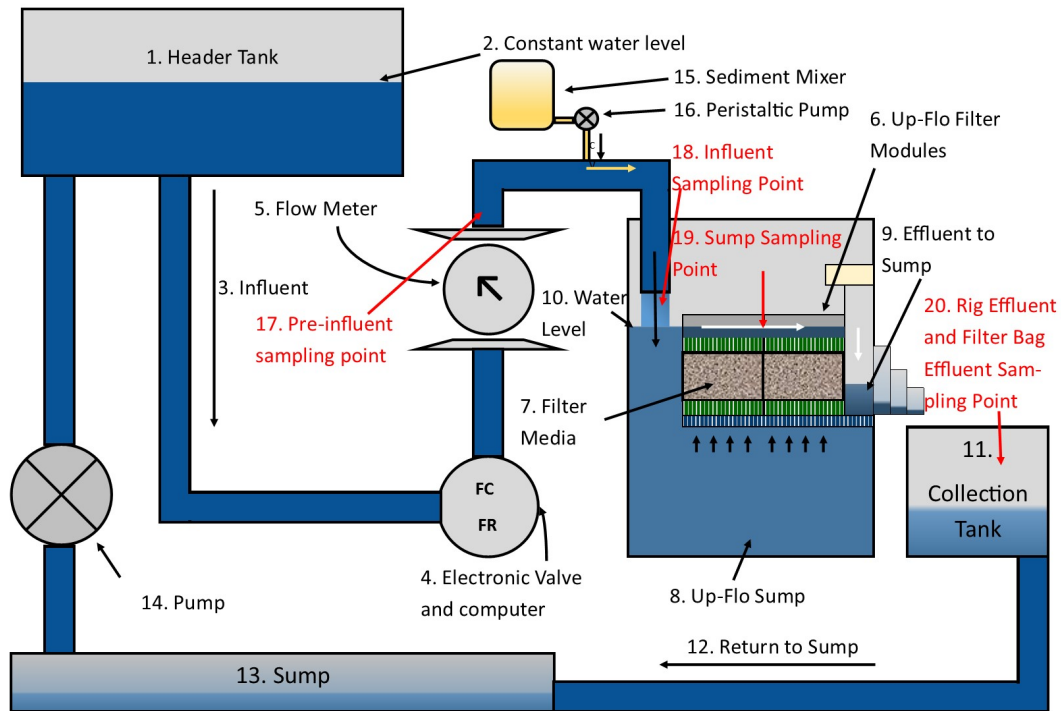


Figure 3.6: Experimental set-up for sediment experiments with sampling points highlighted in red (Not to Scale).

3.4.2 Sediment Test 01 (ST01)

To accomplish the second stage of the strategy, sediment experiments were conducted. Results from T01 to T23 led to the development of the experimental methodology. ST01 ran from T24 to T28, the chosen flow rate was 2 L s^{-1} using the 2 Stage method.

The experimental set-up shown in Figure 3.2 was adapted to introduce a sediment at a constant rate by the use of a 35 x mixer and a peristaltic pump, shown in Figure 3.6. The addition of the mixer and pump, shown in Figure 3.7, allowed the influent water to be dosed at 0.005 L s^{-1} , containing a silica flour mix to provide a total sediment concentration into the rig of 442.34 mg L^{-1} . The sediment inlet into the influent pipe was 390 mm from the outlet of the pipe.

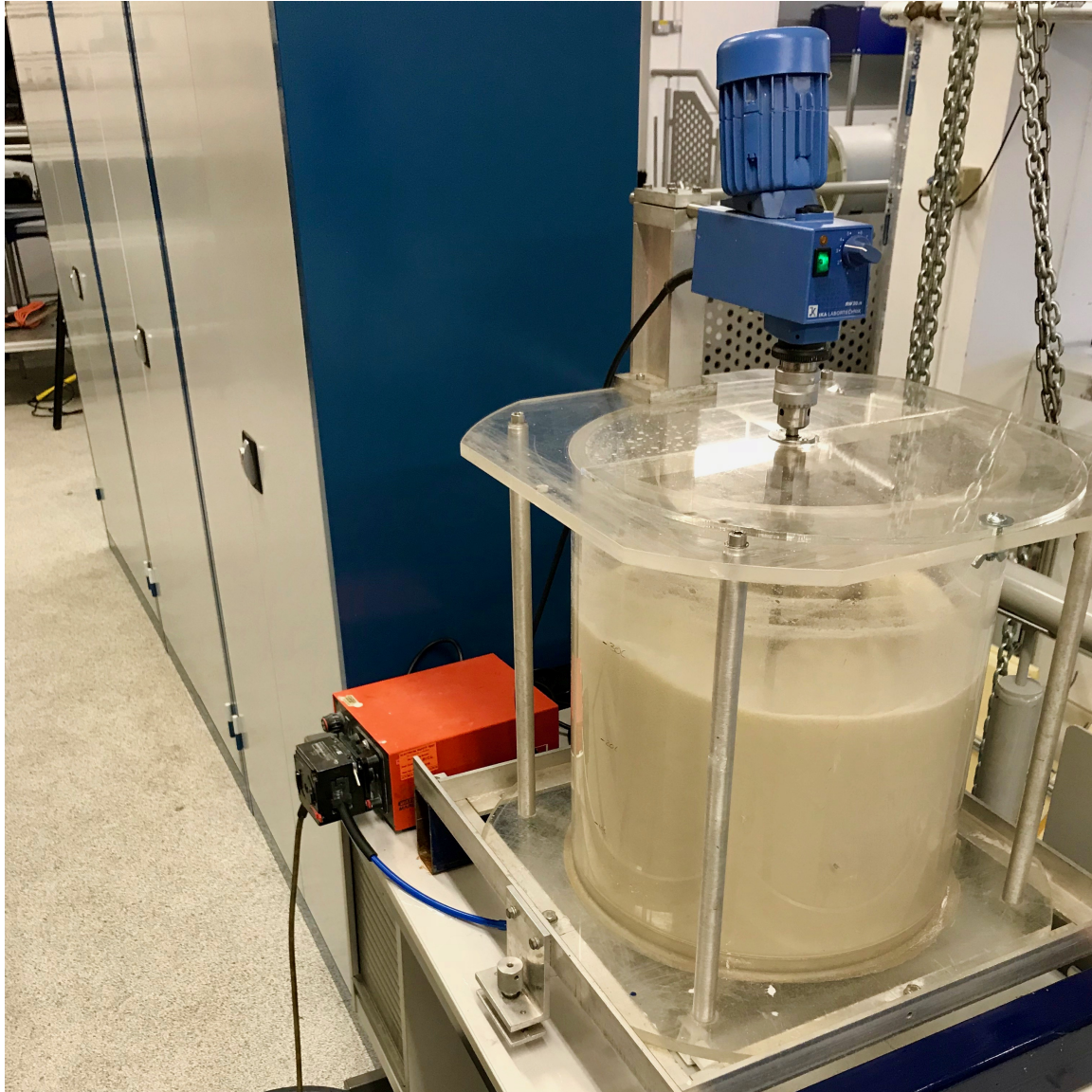


Figure 3.7: Picture of sediment mixer and pump during ST01.

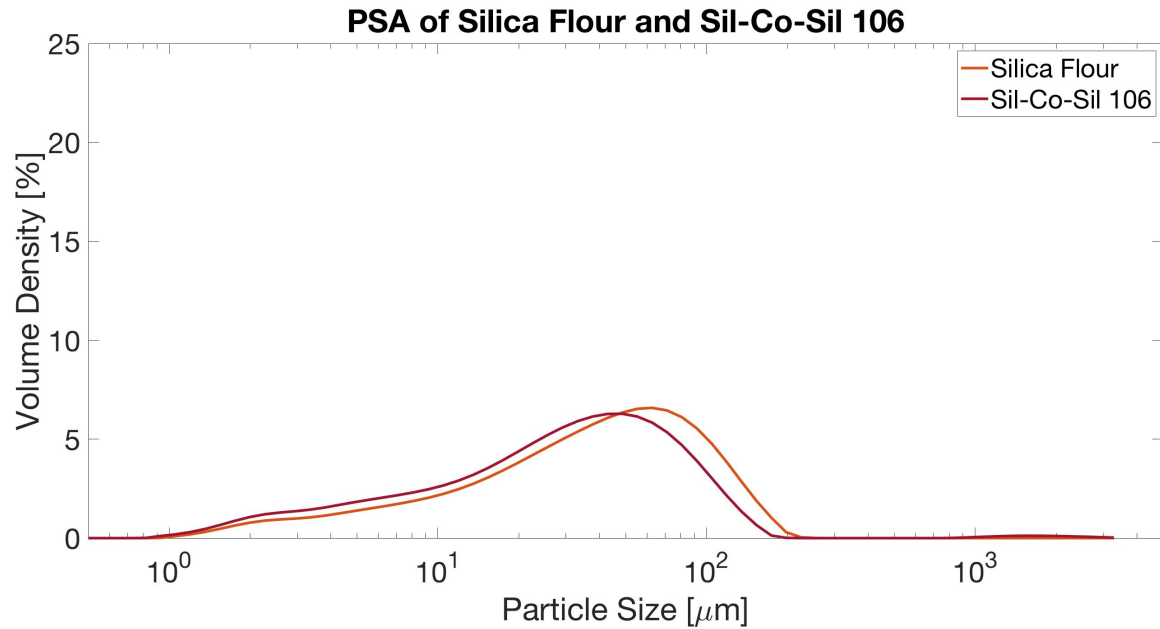


Figure 3.8: Particle Size Analysis of silica flour and Sil-Co-Sil 106 samples, using Malvern Mastersizer 3000.

A targeted dosing of 442.34 mgL^{-1} of silica flour was chosen to reach a 50% clogging of the filter media, assuming a bulk density of 1628 kgm^{-3} and a porosity of 26.05%. Silica flour was chosen as the dosing sediment, due to the similarity with Sil-Co-Sil 106 which is used in internal Hydro International Ltd Up-Flo[®] experiments and NJCAT verification studies. This meant that the results were comparable to previous experiments conducted by Hydro International Ltd. The Particle Size Analysis, of silica flour and Sil-Co-Sil 106 is shown in Figure 3.8.

The d_{50} of silica flour was $38.8 \mu\text{m}$, which was slightly larger than the Sil-Co-Sil 106 d_{50} of $30.2 \mu\text{m}$. Silica flour d_{10} was $6.1 \mu\text{m}$ and the d_{90} was $105 \mu\text{m}$. Whilst Sil-Co-Sil 106 had a d_{10} of $4.52 \mu\text{m}$ and a d_{90} of $86.4 \mu\text{m}$. This shows that the silica flour used was slightly larger than the Sil-Co-Sil 106 used by Hydro International Ltd US labs, also it shows whilst the silica flour is a small sized sediment, it did have a large size range which provided useful analysis of particle size removal in the experiments. The d_{50} of Silica Flour is similar to the residential development site A sediment sizes observed by Hydro International Ltd [9], as shown in Figure 2.1. Additionally the low d_{10} of $6.1 \mu\text{m}$ provides

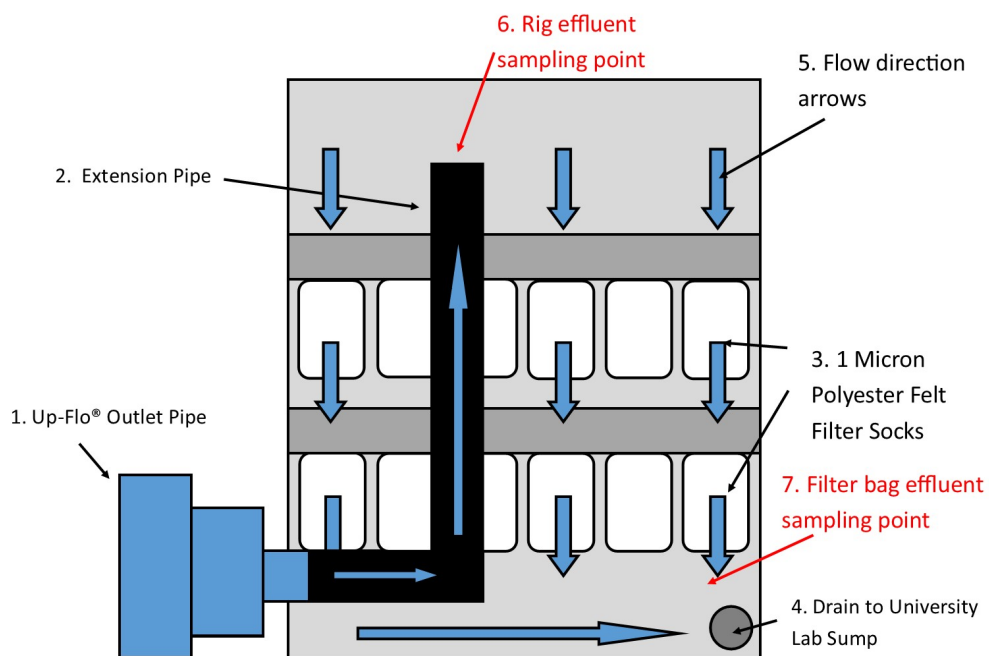


Figure 3.9: Plan View of Collection Tank with 1 Micron Polyester Felt Filter Socks (Not to Scale).

useful analysis, as sizes below this provide significant pollution as outlined in Chapter ?? [103].

The size range of Silica Flour also ensured that it would not be captured by the filter media bag itself, as the pore size was $200 \mu\text{m}$.

The collection tank shown in Figure 3.6 was also adapted to collect any sediment which passed through the Up-Flo® Filter System was captured through the use of 2 rows of 6 SigaFiltration 1 micron polyester felt Filter Socks, as shown in Figures 3.9 and 3.10.

The pre-weighed (dried) 1 micron polyester felt Filter Sock was chosen due to Hydro International Ltd using similar Filter Socks in their experiments, and to allow for the full mass balance to be conducted. Each Filter Socks supported a clean water flow of 2.7



Figure 3.10: Picture of installed Filter Socks in ST01.

Ls^{-1} , information provided by supplier. Each Filter Sock would have also captured more than 90% of silica flour which passed through them, which was calculated through internal experiments by passing 100 g of silica flour through the Filter Sock.

ST01 consisted of 4 Clean Water Experiments (T24 - T27) which followed the method outlined in Sub-section 3.4.1, this allowed for background readings in permeability changes. This was then followed by T28, a 960 mins sediment dosed experiment. Module 4 permeability and temperature readings were taken on T24, first Clean Water Experiment, and T27, the last Clean Water Experiment. During T25 and T26 followed the same Clean Water Experiment method but no measurements were made as the objective of the experiment was to disturb the media.

Experiment T28 was completed over a single day, it began as a standard $2 Ls^{-1}$ 2 Stage experiment, but at 45 mins the sediment feed was started and continued till the end of experiment, 960 mins. To conduct T28, the sediment dosing time was set to 825 mins, the experiment was planned to achieve maximum possible 50% clogging of the filter media. To ensure this the mixer was refilled regularly to ensure dosing rate remained stable. If the overflow operated, or the SigaFiltration Socks became clogged, final measurements and samples were taken and the experiment concluded.

Sampling was conducted throughout T28, locations and timings are discussed below, so that total suspended solids (TSS) and particle size analysis (PSA) could be conducted to provide in depth information on the Up-Flo® removal and filtration efficiencies. For the sampling, $2 \times 250 ml$ sample bottles were used for each sampling point.

Temperature and Permeability Measurements

Temperature readings of the sump were made at 0 mins, 30 mins, 45 mins and 75 mins. At 75 mins the temperature reading interval was 15 mins until the end of the experiment.

Pressure readings in Module 4 was made at 0 mins and occurred every minute for the first 30 mins. At 45 mins additional pressure reading was made, and readings were made every 1 minute until 75 mins. After 75 mins the pressure readings were conducted every 15

mins until end of experimentation.

Pre-Influent and Up-Flo[®] Influent Sampling

Sampling was taken of both the Pre-Influent and Up-Flo[®] Rig Influent. Pre-Influent sampling provided a background sample to the water before sediment dosing occurred, this was taken before the sediment inlet pipe shown in Figure 3.6. Influent sampling was conducted at the opening of the Up-Flo[®] inlet pipe, shown in Figure 3.6.

The timings of both sampling occurred at; 0 mins, 30 mins and 45 mins. Then at 45 mins the sampling interval was increased to every 120 mins until 765 mins, a final sample was taken at 870 mins.

Up-Flo[®] Sump Sampling

Samples of the Up-Flo[®] sump was taken at 0 mins, 30 mins, 45 mins, 75 mins, 285 mins, 525 mins, 765 mins and 870 mins. These samples were taken by placing the sample bottle below the surface of the water, in the centre of the rig.

Rig Effluent Sampling

At 0 mins and 30 mins samples of Up-Flo[®] Rig Effluent was taken, shown in Figure 3.9. At 45 mins the Up-Flo[®] Rig Effluent was then sampled, every 5 mins for 60 mins. At 60 mins the sampling time was reduced to every 30 mins.

Filter Sock Effluent (FSE) Sampling

At 0 mins, 30 mins and 45 mins samples were taken of the effluent passing through the Filter Socks. At 45 mins the sampling interval was increased to 180 mins until 765 mins, an additional sample was taken at 870 mins. The location of this sampling point is shown in Figure 3.9.

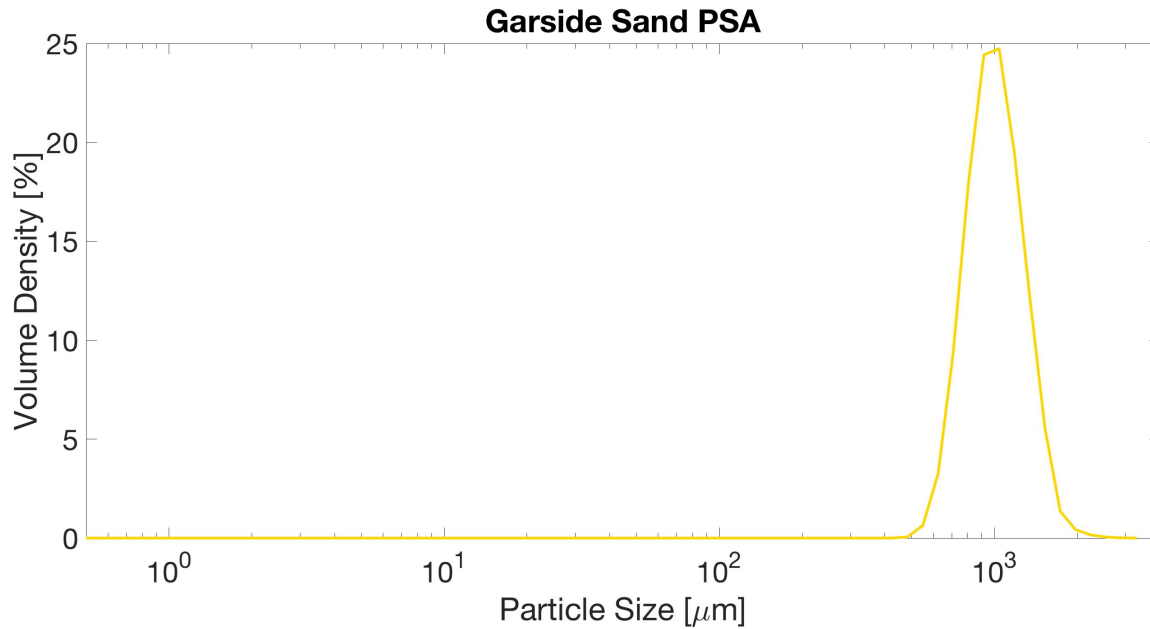


Figure 3.11: Particle Size Analysis of Garside Sand, using Malvern Mastersizer 3000.

3.4.3 Sediment Test 02 (ST02)

ST02 had the same experimental set-up as Figure 3.6 and followed a similar method outlined in ST01, with modifications made from the results from ST01 and the Clean Water Experiments.

Due to the supplier of Fraction B discontinuing the product, a new filter media was sourced. The new supplier was Garside Sands, the grade was similar to Fraction B and is used by Hydro International Ltd now for UK installations of the Up-Flo® Filter System. The new PSA is shown in Figure 3.11.

Figure 3.11 shows that the replacement sand was slightly more coarse than the Fraction B media. The d_{10} , d_{50} and d_{90} of the replacement media was $749 \mu m \pm 11 \mu m$, $997 \mu m \pm 16 \mu m$ and $1360 \mu m \pm 54 \mu m$. This represented an increase in the d_{10} , d_{50} and d_{90} of 5.3% , 3.7% and 3.8% , respectively.

As with ST01 4 Clean Water Experiments were conducted, T29 to T32, these followed the same method as outlined in the Clean Water Experiment and ST01. T33 consisted of a

sediment experiment with a reduced experimental time of 255 mins with a clean water flow for 45 mins, as with ST01. This was reduced as the Filter Socks became clogged in ST01 T28, the reduction in experimental time also made comparison with Clean Water Experiment results better. Due to the reduction of experimental time, an additional sediment experimental day T34, was introduced. This additional sediment experimental day ran for 210 mins without the 2 Stage conditioning method or the 45 mins of clean water flow, with the flow rate increasing to the experimental flow rate of $2 Ls^{-1}$ from $0 Ls^{-1}$. This reduced the possible impact of clean water flow washing out sediment collected the previous day, T33.

The collection tank had seals made, so clogged Filter Socks could be sealed off and replaced mid experiment, which allowed the experiment to continue when a Filter Sock became clogged.

Based on experience from the Clean Water Experiments and ST01, additional permeability tubes were installed. These were installed in Modules 1 and 2, as shown in Figure 3.4, at the same vertical location in each module as Module 4. In addition to this, GoPro Hero 3+ Cameras were installed for more frequent pressure measurements. This automation allowed for the increased sample rate for TSS and PSA, due to the increased productivity.

The following subsections discuss the updated timings that measurements were taken. The Clean Water Cycle experiments T29 and T32 had the same permeability reading interval as that in the Clean Water Experiments.

Temperature and Permeability Measurements

Temperature readings of the sump were made every 15 mins on both T33 and T34 of the sediment experimental days.

Photos were taken of the permeability tube every minute for the entire experimental period, on both sediment experimental days in ST02.

Using these photos pixel readings were made on the Modules 1, 2 & 4 permeability tubes on T33 at 0 mins and occurred every 1 minute for the first 30 mins. At 45 mins another pressure reading was made, and readings were made every 1 minute until 75 mins. After 75 mins the pixel readings were conducted every 15 mins until end of the experiment.

For T34, pixel readings were made at 0 mins and every 1 min for 30 mins. At the end of this the pixel readings were taken at 45 mins and then every 15 mins until the end of the experiment.

Photo calibration readings were taken throughout and at the end of experimentation. By taking manual measurements of the piezometer tubes at a known time. This allowed for a calibration curve to be formed which let the pixel location determine head measurements in the permeability tubes.

Influent, Sump, Rig Effluent & Filter Sock Effluent Sampling

On day 1 of the sediment feed, T33, these were sampled at 0 mins, 30 mins and then 45 mins. At 45 mins these locations was then sampled every 5 mins until 105 mins, where the sampling interval increased to every 15 mins until end of experimentation at 255 mins.

On day 2 of the sediment feed, T34, these were sampled every 5 mins from 0 mins until 60 mins. The sampling interval then increased to every 15 mins until end of experimentation at 210 mins.

Pre-Influent Sampling

On day 1 of the sediment feed, T33, these were sampled at 0 mins, 30 mins and 45 mins. At 45 mins the sampling interval was increased to every 30 mins until end of experimentation at 255mins.

On day 2 of the sediment feed, T34, Pre-Influent was sampled at 0 mins, 30 mins and 45 mins. It was then increased to every 30 mins until 195 mins.

3.4.4 Sediment Test 03 (ST03)

ST03 followed the same methodology outlined for ST02 with the same filter media. But the influent sediment, previously silica flour, was replaced with Fraction E Sand which was supplied by David Ball Sand Group. The PSA of Fraction E is shown in Figure 3.12, Fraction E was chosen due to its coarser profile which was more realistic of sediment pollution in urban stormwater. This also allowed for the estimation of the impact of a coarser sediment on the Up-Flo[®] Filter System. The d_{50} was $150 \mu m$, 3.9x greater than the silica flour. The d_{10} was $107 \mu m$ and the d_{90} was $208 \mu m$, due to the similarity between the d_{10} of Fraction E and d_{90} of silica flour an in depth understanding of the filter removal of a range of sizes was established.

The d_{50} of Fraction E was slightly larger than Residential Site B sediment in Figure 2.1. The larger sized Fraction E also allows analysis of the impact of the larger sized d_{90} site sediments, not covered by Silica Flour.

As the d_{90} of the new sediment was larger than the pore size of the bag containing the filter media, it is possible for the bag to capture some of the sediment. The impact of this shall be assessed in the discussion of the results in Chapter 3.15. If the sediment is captured within the pores of the bag, then a resultant impact on permeability will be seen as flow paths would be blocked.

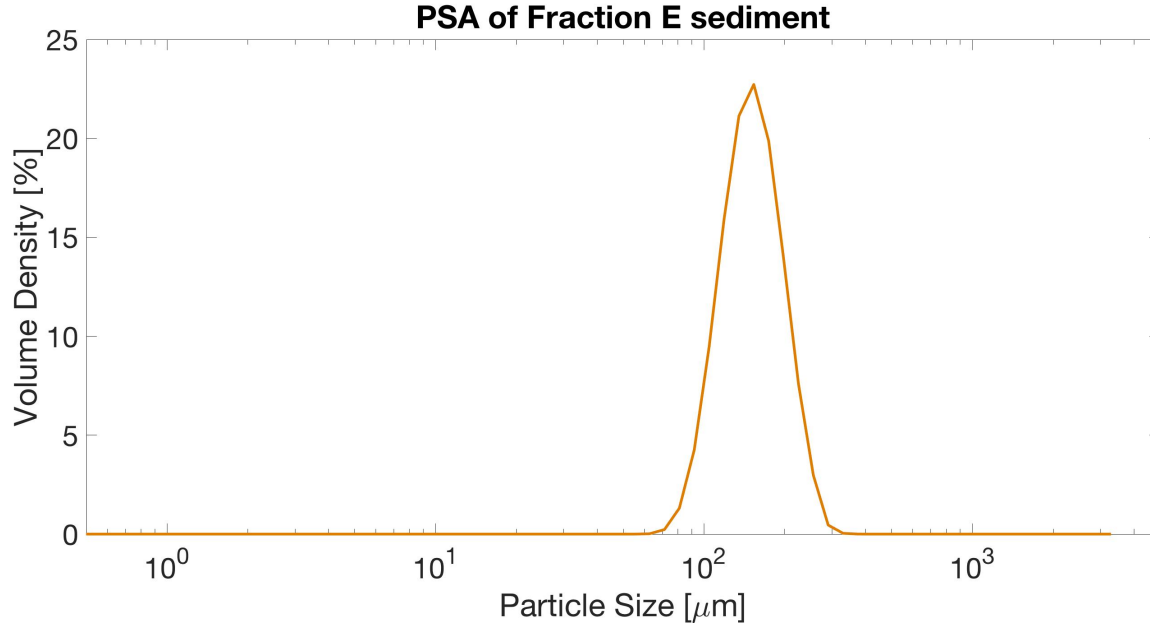


Figure 3.12: PSA of Fraction E sediment.

3.5 Post Measurement Processing

To develop an increased understanding of the removal processes of the Up-Flo® Filter, a number of techniques were utilised to process the raw data and samples collected during the experiment, these are outlined in Sub-sections 3.5.1 to 3.5.6. The errors presented throughout this section were calculated using standard error propagation equations, presented in Appendix B.4 [104].

3.5.1 Camera Results

Using the calibration readings taken in ST02 and ST03 a calibration fit and equation was formed. Once this fit was acquired, the photos used for the permeability readings were analysed for the pixel location. This was then converted using the calibration equation to the water level readings in *mm*. The calibrations are shown in the appendices B.5 and B.6.

3.5.2 Permeability Results

The permeability of the Up-Flo[®] filter media was calculated for Clean Water Experiments, ST01, ST02 and ST03. The results were processed in a MatLAB file, shown in Appendix B.7, the permeability was calculated using the rearranged Darcy Equation shown in 3.1.

$$\kappa = \frac{q\mu x}{\Delta p} \quad (3.1)$$

κ is the permeability, q is the fluid velocity, μ is the dynamic viscosity of water, x is the length of the media, Δp is the change in fluid pressure across the media.

The influent flow rate was converted to fluid velocity by Equation 3.2 below.

$$q = \frac{\frac{Q \times 10^{-3}}{N_{mod}}}{A} \quad (3.2)$$

Here the fluid flow rate was converted from Ls^{-1} to m^3s^{-1} , it was then divided by the number of modules, N_{mod} . This was based on the assumption that flow passed through the modules equally, during the analysis of the results this assumption is tested. This flow rate per module was then divided by the cross-sectional area of one module, A , so to provide the fluid velocity in m/s .

The average temperature, T , during the experiment provided the viscosity of water, shown below in Equation 3.3 [105].

$$\mu = (2.414 \times 10^{-5}) \times 10^{247.8/((T+273.15)-140)} \quad (3.3)$$

The change in fluid pressure from Equation 3.1 was calculated by using the measured head change between pressure tappings in m , ΔH , multiplied by the density of water, ρ_w , and acceleration due to gravity, g_a as shown below in Equation 3.4.

$$\Delta p = \rho_w \times g_a \times \Delta H \quad (3.4)$$

The constants used are listed below.

- N_{mod} was 6.

- x was either; 0.2 m for A to C tapplings, 0.1 m for A to B tapplings or 0.1 m for B to C tapplings. The tapping locations is shown in Figure 3.5.
- A was 0.1025 m^2 .
- g_a was 9.81 ms^{-2} .
- ρ_w was 1000 kgm^{-3}

Darcy's law is valid for slow moving laminar flow, all transitional and turbulent flow are incompatible with Darcy's law. Slow moving laminar flow is valid for a Reynolds Number range of 1 to 10 [49]. Equation 3.5 expresses the Reynolds Number.

$$R = \frac{qd}{k} \quad (3.5)$$

Equation 3.5 was presented by Bear [49], q is the fluid velocity and k is the kinematic viscosity. Placing the equation in terms of dynamic viscosity, as previously used, is presented in Equation 3.6 below.

$$R = \frac{\rho qd}{\mu} \quad (3.6)$$

The variable d is one which was difficult to define, Bear defined d as the length dimension of the granular matrix [49]. Bear observed that it was conventional to use a representative dimension of the grains for d . Bear discussed the divergence in values used for d , it was noted that the mean grain diameter was typically taken. However, some researchers take the grain size that exceeded the diameter of 10% of the material by weight, d_{10} , others also used d_{b0} . Other researchers have not attempted to not describe d in terms of a representative dimension of the grains but in terms of permeability, Bear described how Collins [106] described that $d = (\kappa/n)^{1/2}$, where n is the porosity, and Ward [107] used $d = \kappa^{1/2}$ [49].

Clearly the different values taken by multiple researchers shows a lack of consistency and presents difficulty in describing the nature of the flow through a granular medium. Using d_{10} , d_{50} and d_{90} of the filter medias the estimated Reynolds Number against Flow Rate is shown in Figure 3.13.

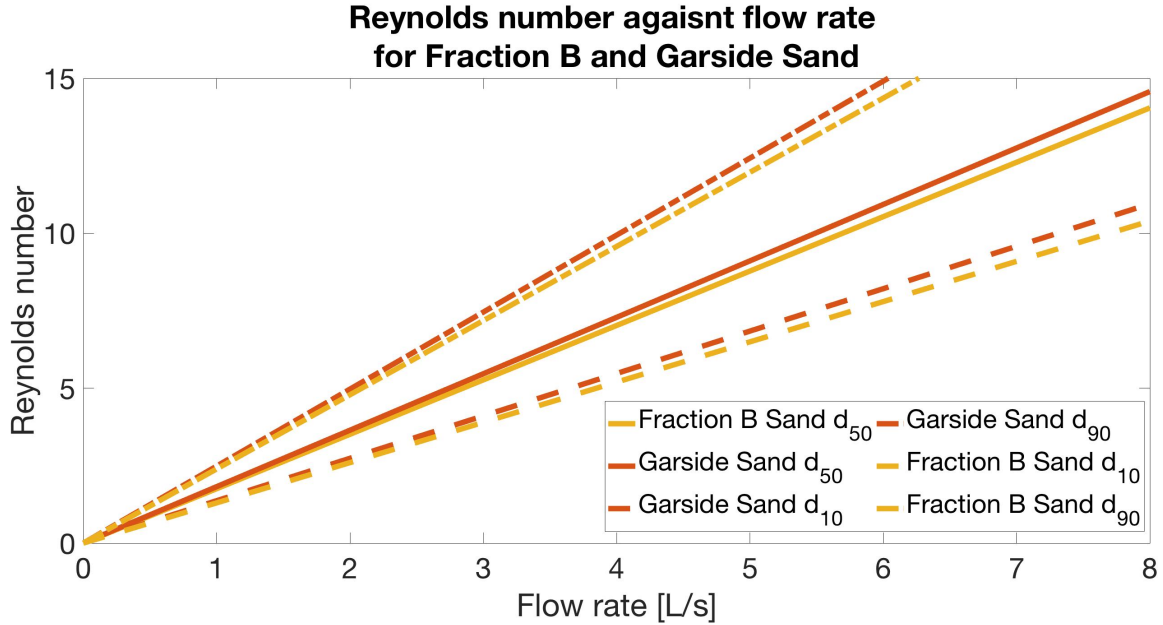


Figure 3.13: Reynolds Number against Flow Rate for Fraction B and Garside Sand with various particle sizes.

From Figure 3.13 the maximum Reynolds Number, using d_{50} which Bear said was typically used, in the Clean Water Experiments and ST01 was 8.779 at 5 L s^{-1} , which suggested that the flow in all experiments was within the Darcy regime and did not enter the Transition Zone or Turbulent Regime. However using d_{90} the maximum Reynolds Number would be 11.97 , suggesting the flow would not be laminar. Using d_{10} would result in the all flow being in the laminar region. If using particle size as the basis for d then Bear said typically d_{10} and d_{50} is used, suggesting the Clean Water Experiments and ST01 would be within the laminar range.

The larger particle sized Garside Sand filter media for ST02 and ST03, resulted in a slightly larger Reynolds Number. With the flow rate being 2 L s^{-1} for both ST02 and ST03 the Reynolds Number would be within the laminar range using all d sizes. The Reynolds Number for d_{10} , d_{50} and d_{90} was 2.737 , 3.643 and 4.969 , respectively.

3.5.3 Permeability Error Sources

This sub-section outlines how the errors were calculated and possible sources of error which could not be quantified accurately. The error in the permeability readings came from the measured parts of the permeability equation shown in Equation 3.1 in Sub-section 3.5.2.

Fluid Velocity

In Equation 3.2 the sources of error resulted from the flow rate and the area. The flow rate was controlled by the computer and electronic valve allowing for a constant flow rate with little variation. To calculate the error in the flow rate, the Standard Deviation was used on the flow rate readings once enough time had passed, 10 mins, for the flow to stabilise. Using the 26/07/17 2 Stage Clean Water Experiment T06 readings the Standard Deviation is $1.1 \times 10^{-5} m^3 s^{-1}$. Whilst the 11/08/17 1 Stage Clean Water Experiment T12 readings the Standard Deviation is also $1.1 \times 10^{-5} m^3 s^{-1}$.

The error from the area came from the difference in the manufactured product and the CAD drawings sent to the manufacturer. Error also resulted from the assumption the sand fills all of the available area in module and no gaps are there. These two errors are difficult to quantify, Hydro International has provided the tolerance in manufacturing as 2%.

Equation 3.7 provides the estimation of the error in fluid velocity.

$$\Delta q = q * \sqrt{\left(\frac{\Delta Q}{Q}\right)^2 + \left(\frac{\Delta A}{A}\right)^2} \quad (3.7)$$

This error was under the assumption that all the flow is passing through the Up-Flo® filter media and the head in the tank was not rising consistently throughout the experiment.

Viscosity

The viscosity was determined by temperature readings in the rig. The temperature measurements were $\pm 0.1^\circ C$. This gave a viscosity error of approximately $\pm 2 \times 10^{-6}$ *Pa.s*.

Length of the media

The length of the media was determined using the distance between the pressure tappings which was measured using a ruler. This provided an error of approximately ± 0.1 *mm*.

Pressure Difference

The pressure difference was calculated using the head change between the pressure tappings. This was measured using a 1 *m* rule with 1 *mm* etchings which provided an error of 1 *mm* in each of the readings. Using Equation 3.8 below the total error is estimated to be ± 8 *Pa*.

$$\Delta p = \rho g_a (1 * 10^{-3})^2 \sqrt{\left[\frac{\sqrt[2]{\Delta BP_1^2 + \Delta BP_2^2 + \Delta BP_3^2}}{3} \right]^2 + \left[\frac{\sqrt[2]{\Delta TP_1^2 + \Delta TP_2^2 + \Delta TP_3^2}}{3} \right]^2} \quad (3.8)$$

Here *BP* is the bottom head reading, *TP* is the top head reading, ρ is the density of water in kgm^3 , g_a is the acceleration due to gravity in ms^{-2} and 1×10^{-3} converts the *mm* into *m*.

Permeability Error Proagation

The total error estimation for permeability was calculated using Equation 3.9 below.

$$\Delta \kappa = \kappa \sqrt{\left(\frac{\Delta q}{q} \right)^2 + \left(\frac{\Delta \mu}{\mu} \right)^2 + \left(\frac{\Delta x}{x} \right)^2 + \left(\frac{\Delta p}{p} \right)^2} \quad (3.9)$$

Using the above equation error in the final permeability values presented throughout this chapter was calculated. These errors typically represented 2.1% of the Whole Module

permeability value, any averaged permeability values were calculated using standard error propagation errors [104].

3.5.4 Total Suspended Solids (TSS)

TSS analysis was conducted on samples from ST01, ST02 and ST03, due to the number of samples every other sample taken was used, with extra samples used between when necessary. British Standard 872:2005 was used for the basis of the analysis. A whole sample bottle was used for the analysis, the sample volume was measured, $\pm 1 \text{ mm}$, and then placed through a pre-washed and pre-weighed $1.5 \mu\text{m}$ Glass Microfibre Filter Paper through the use of a vacuum pump. The sample bottle and measuring cylinder were then flushed with deionised water and passed through the filter paper, so as to ensure all sediment passed through the filter. Finally the crucible internal sides were flushed with deionised water, the pump was then turned off and the TSS filter paper dried in the oven at 105°C overnight.

The TSS filter papers were then cooled in a moisture free box and then weighed using analytical scales, $\pm 0.0001 \text{ g}$. The TSS value in mgL^{-1} was then calculated using Equation 3.10 below.

$$TSS = \frac{W_s - W_f}{V_s} \quad (3.10)$$

Here W_s is the weight of the dried TSS filter paper with sediment, in mg , while W_f is the weight of dried TSS clean filter paper, in mg . V_s is the volume of the sample used, in x .

The maximum error for a result below 10 mgL^{-1} was 33.3% for 1 mgL^{-1} but above 10 mgL^{-1} the maximum error was 3.6% for 10.2 mgL^{-1} .

3.5.5 Particle Size Analysis (PSA)

Using the TSS results, samples were chosen from ST01, ST02 and ST03 with a suitably high (greater than 70 mgL^{-1}) TSS value for PSA. This was done through the use of a Malvern Mastersizer 3000 Hydro R particle sizer, a shaken sample was poured into the mastersizer mixer chamber until either the optimum obscuration of 2-5% is reached or all

Table 3.3: Average Percentage Errors in PSA.

Sample	d ₁₀ [%]	d ₅₀ [%]	d ₉₀ [%]
Garside Sand	1.5	1.6	4.0
Fraction B Sand	1.8	1.3	2.2
Fraction E Sand	0.405	0.169	0.462
Silica Flour	3.23	3.31	2.91
Sil-Co-Sil 106	4.18	3.76	6.22
ST01 T28 Rig Effluent	2.0	3.9	13.7
ST02 T33 Rig Effluent	1.1	1.9	5.6
ST02 T34 Rig Effluent	1.5	2.7	7.7
ST01 Sump Drain Down	4.7	4.7	22.3
ST02 Sump Drain Down	0.4	0.3	0.4
ST03 Sump Drain Down	0.3	0.2	0.3

the sample was used. The mastersizer took 15 measurements, these were then averaged out to provide the particle size analysis of the sample. Additional samples of the silica flour caught within the sump were measured, once dried, three samples were taken. The sample was then mixed and slowly added to the mixer chamber until the optimum obscuration was reached, then 15 measurements were taken. These samples were then averaged out. The settings used for the mastersizer for this analysis is shown in the Appendix B.8.

The average percentage errors, calculated through standard deviation, in the d₁₀, d₅₀ and d₉₀ are shown in Table 3.3. Also included is the percentage errors of the previously presented filter medias and sediments.

In ST02 and ST03 further PSA was conducted on the Up-Flo[®] filter bags from Module 2, see Figure 3.4. This was to study the sediment sizes caught by the filter media. To conduct this PSA the filter bags were removed from the Up-Flo[®] Filter, then the top of the bag was removed and 5 core samples were taken. An example of the location of the

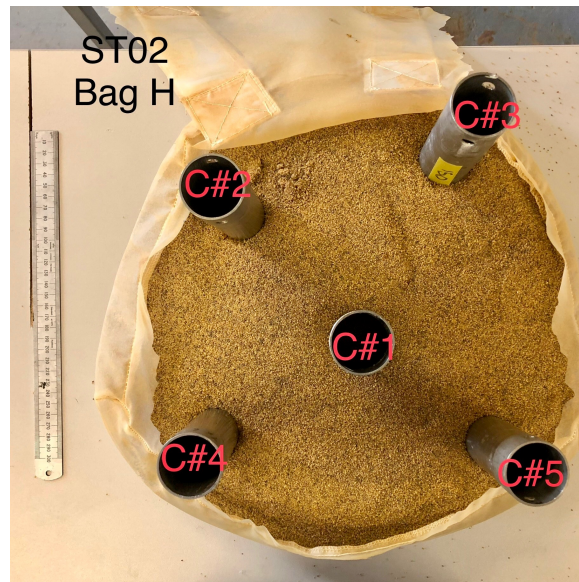


Figure 3.14: Core Sample Locations from ST02 Bag H (Bottom Bag).

core samples is shown in Figure 3.14.

Once the core samples were removed, the core sample was mixed well by hand. Once mixed, a sample (until obscuration level of 2-5% was reached) of the core sample was placed into the mastersizer mixer chamber. Before the mastersizer measured the particle size, the mastersizer's ultrasound was applied for a minimum of 30 s at 30% power. This was to break up bound sediment and filter media particles. After the ultrasound had finished, 15 measurements were taken and averaged out to provide the PSA of the sample. This process was repeated 3 times for each core sample. The settings for the core sample PSA is shown in Appendix B.9. The errors for this was calculated by the standard deviation and then error propagation equations. The maximum errors for the filter bag PSA was as follows d_{10} 0.4%, d_{50} 0.9% and d_{90} 2.3%.

3.5.6 Mass Balance

A mass balance was conducted by weighing the mass of sediment collected by the Filter Socks and the sump of the Up-Flo® rig. To do this the Filter Socks used in ST01, ST02

and ST03 were dried in an oven at $105^{\circ}C$ until constant mass. These were then weighed using weighing scales, with a $\pm 0.1 g$ readability. For ST01, ST02 and ST02 the error in the measured mass of the Filter Socks was 0.08%, 0.03% and 0.04% respectively.

To weigh the mass of sediment in the sump, the Up-Flo[®] rig was drained slowly into the sealed shut collection box. Once the sediment in the box was settled, the water was siphoned out slowly into the lab sump. This process was repeated until the Up-Flo[®] rig was fully drained and the sump cleaned out. Once complete the sediment was placed into pre-weighed drying trays and placed into an oven at $105^{\circ}C$ until constant mass. These were then weighed using weighing scales, with a $\pm 0.1 g$ readability. For ST01, ST02 and ST03 the error in the measured mass of the sump was 0.01%, 0.00% and 0.00% respectively.

The mass of the sediment introduced by the system was calculated by adding the preweighed bags, $\pm 0.001 kg$, used in the experiment then removing the weighed total left in the mixer or missed the mixer. This provided a total error for ST01, ST02 and ST03 of 0.08%, 0.01% and 0.01% respectively.

3.5.7 Removal efficiency equations

The total removal efficiency was calculated through two different methods. One calculation was through using TSS values by the following equation:

$$r_{TSS} = \left[1 - \frac{TSS_{STXXRA} \times Q_{out}}{TSS_{STXXIA} \times Q_{in}} \right] \times 100 \quad (3.11)$$

Here r_{TSS} is the removal efficiency calculated through TSS. The TSS_{STXXRA} is the average TSS value after 10 mins of sediment influent, XX denotes the sediment test number. The flow rates Q_{in} and Q_{out} represent the flow rate entering and leaving the rig, respectively. These flow rates cancelled out in the calculation under the assumption that the flow rate was equal.

As Sections 3.6 to 3.14 explain, the influent TSS samples were too varied to provide a usable result. So TSS_{STXXIA} is the average influent TSS value calculated by the total

influent mass presented to the system. Using the equation below.

$$TSS_{STXXIA} = \frac{MB_{Inf}}{Q \times t} \quad (3.12)$$

Here the total sediment mass added into the system, MB_{Inf} , is divided by the experimental flow rate, Q , multiplied by the experimental time, t . The second method of the Up-Flo® Filter System removal efficiency calculation is through the mass balance.

$$r_{MB} = \left[1 - \frac{MB_{Eff2}}{MB_{Inf}} \right] \times 100 \quad (3.13)$$

Here the removal efficiency, r_{MB} , is calculated using the masses collected through the mass balance, with MB_{Eff2} being the mass collected in the Filter Socks with losses factored in.

$$MB_{Eff2} = \frac{MB_{Eff}}{1 - FS_{loss}} \quad (3.14)$$

Here MB_{Eff} is the total mass collected by the Filter Socks, and FS_{loss} is the loss through the Filter Socks. FS_{loss} was calculated by the average loss through dividing average TSS Filter Sock Effluent value by the average Rig Effluent TSS value, after 10 mins of sediment dosing time. Using the standard error propagation equation from earlier, the estimated measurement error is presented in Table 3.4.

Table 3.4: Errors in Removal Efficiency.

Experiment	r_{TSS} [%]	r_{MB} [%]
ST01	0.2	0.0
ST02	0.2	0.3
ST03	0.1	0.3

3.6 Results

The results collected using the method outlined in Section 3.4 are presented in the following sections. Section 3.7 presents the filter media permeability results of the Clean Water Experiments using the method outlined in Sub-section 3.4.1.

Sections 3.8, 3.9 and 3.10 then present the filter media permeability results from the sediment experiments, ST01, ST02 and ST03 respectively. Then Section 3.11 presents a comparison of the permeability results.

The Up-Flo[®] Filter System TSS results from ST01, ST02 and ST03 are then presented in Section 3.12. Section 3.13 then presents the mass balance results, to explore the removal mechanisms further. Using these results and the Particle Size Analysis of the filter bags an estimation of the filter media removal efficiencies is presented in Section 3.14.

During the experiments important events and deviations were noted. In ST01 at 152 mins the Filter Socks became clogged, which resulted in the experiment being ceased and final results collected as per experimental method. During ST02 the amount of Filter Socks used in the first sediment day, T33, resulted in an insufficient amount for the next sediment experimental day, T34. Due to this, only the last row of Filter Socks were installed to ensure the whole experiment could be completed. This was deemed to have little effect as from the internal experiments on the Filter Socks, there was no significant filtration by passing through another Filter Sock. Additionally, the loss through the bags were estimated using TSS results.

During ST02 T34 a procedural error resulted in an additional 5 mins of lower dosed flow at a higher flow rate (9.1 L s^{-1} max) at the beginning of the experiment. The experiment was stopped and once the system had no running water the experiment was restarted.

Whilst unfortunate, the 5 mins only represent approximately 1% of the total time in T32 and T34, and from the results no impact is seen. Additionally during ST02 T34 the mixer ran out at 205 mins, to allow for a more accurate mass balance the mixer was not refilled and the experiment was ended early.

During ST03 the seal on the drain-down ports became slightly loose. This led to the rig water level over the weekend break to drop below the filter media. This does not appear to have impacted either the permeability or removal efficiency results as the leak was very small.

In ST03 the second sediment dosed day, T40, the filter was exposed to 10 mins of clean water flow, at 2 L s^{-1} , at the start of the experiment. This was resultant from the pipe used for the dosing of the Fraction E being blocked. The experiment was stopped and once the pipe was fixed the experiment was restarted, the results seem to not have been impacted by this problem.

In both ST02 and ST03, due to issues regarding the calibration of the cameras for Modules 1 and 2, only permeability calculated through manual measurements of piezometer tubes are presented for Modules 1 and 2. This has not affected the permeability results presented for Module 4.

3.7 Clean Water Experiment Permeability Results

Permeability results of the Up-Flo[®] filter media provides essential information on the ability of the media to transport water. An example of the permeability over a Clean Water Experiment is shown in Figure 3.15. As the Module 4 T11 results show, the permeability decreased throughout the experiment.

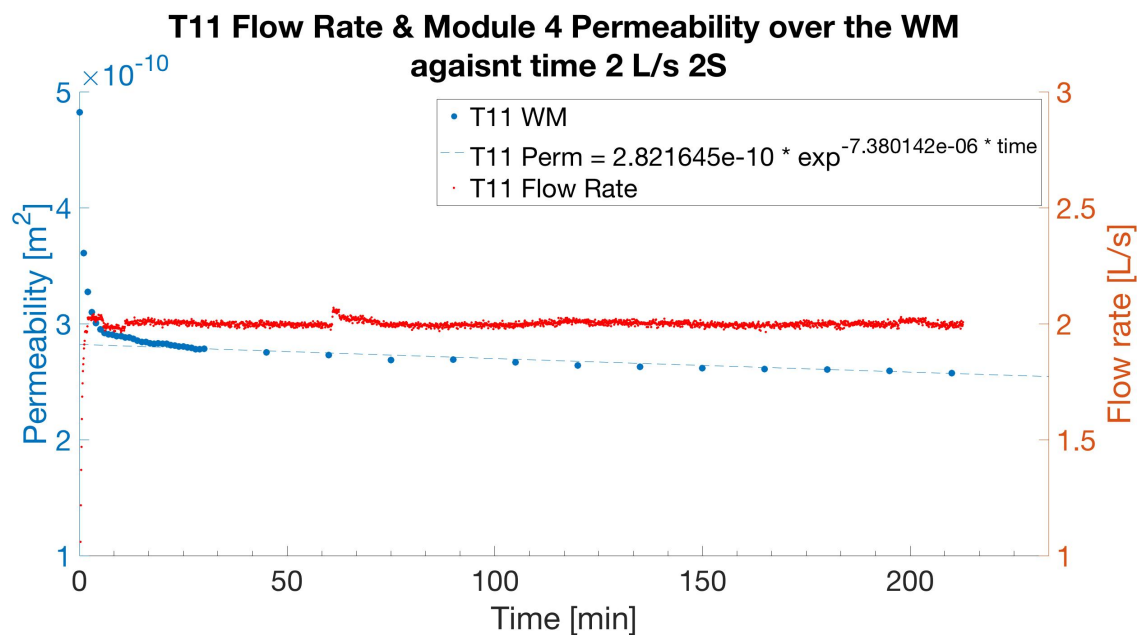


Figure 3.15: Module 4 T11 permeability and flow rate against time. 2 Stage (2S) at 2 Ls^{-1} .

Results from the Clean Water Experiments found a number of findings. Firstly, the difference between the 1 and 2 Stage methods was found to not be significant, as shown in Figure 3.16. The 1 Stage method had the permeability range from $1.78 \times 10^{-10} m^2 \pm 0.04 \times 10^{-10} m^2$ to $2.86 \times 10^{-10} m^2 \pm 0.06 \times 10^{-10} m^2$. Whilst, the 2 Stage ranged from $1.79 \times 10^{-10} m^2 \pm 0.04 \times 10^{-10} m^2$ to $2.69 \times 10^{-10} m^2 \pm 0.06 \times 10^{-10} m^2$.

As the Clean Water Experiment permeability result ranges for 1 Stage and 2 Stage was similar, the 2 Stage method was chosen for ST01, ST02 and ST03. This was due to the closer replication of a realistic storm event. The similarity between the 1 and 2 Stages

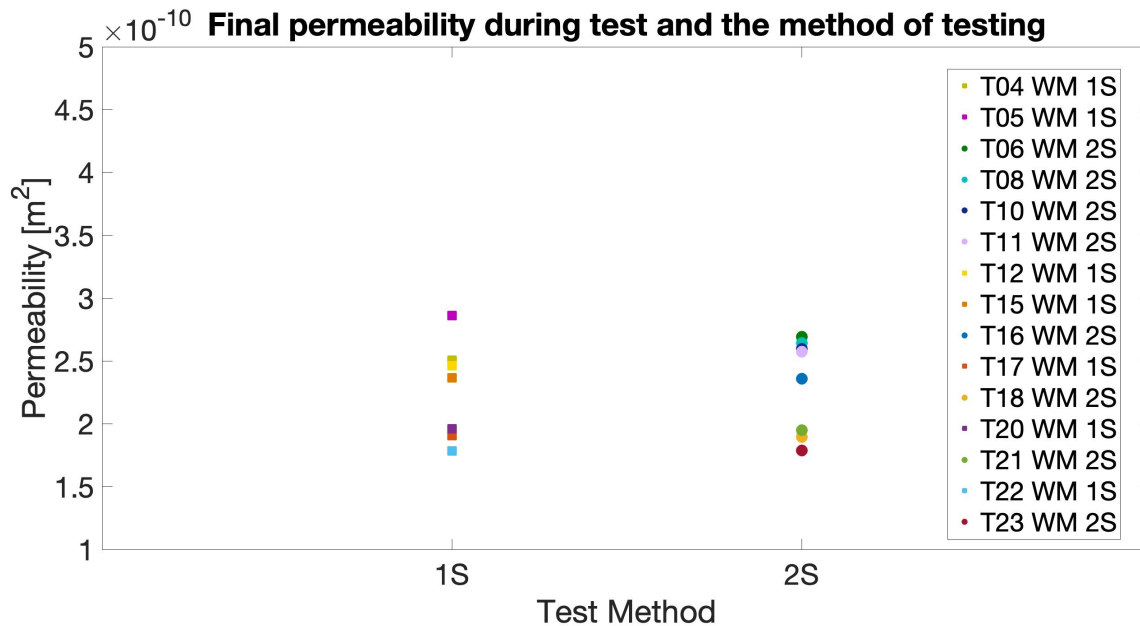


Figure 3.16: Method Analysis of the Final Permeability Values across Module 4 Filter Media during the Clean Water Experiments. 1S is 1 Stage, 2S is 2 Stage and WM is Whole Module.

permeability results was the same with the Module 4 Top Bag and Bottom Bag permeability results.

Additionally, it was found that across the Whole Module the flow rate did not have a clear impact on the permeability result (Figure 3.17). Which indicates the calculation of the Reynolds Number being between 1 and 10 (Section 3.5.2) was correct. Which means the flow rate remained laminar throughout the tested flow rates, resulting in Darcy's Law being applicable.

A key result from the Clean Water Experiments found that the final permeability reading had decreased throughout the experimental period, as shown in Figure 3.18. The figure shows that the final permeability value decreased over time, from a peak of $2.86 \times 10^{-10} m^2 \pm 0.06 \times 10^{-10} m^2$ for T05 to $1.79 \times 10^{-10} m^2 \pm 0.04 \times 10^{-10} m^2$ for T23 over 67 days. It appears that this is due to rearrangement of the filter media itself, as during periods of time where there was no experiments the drop in permeability was small or similar to

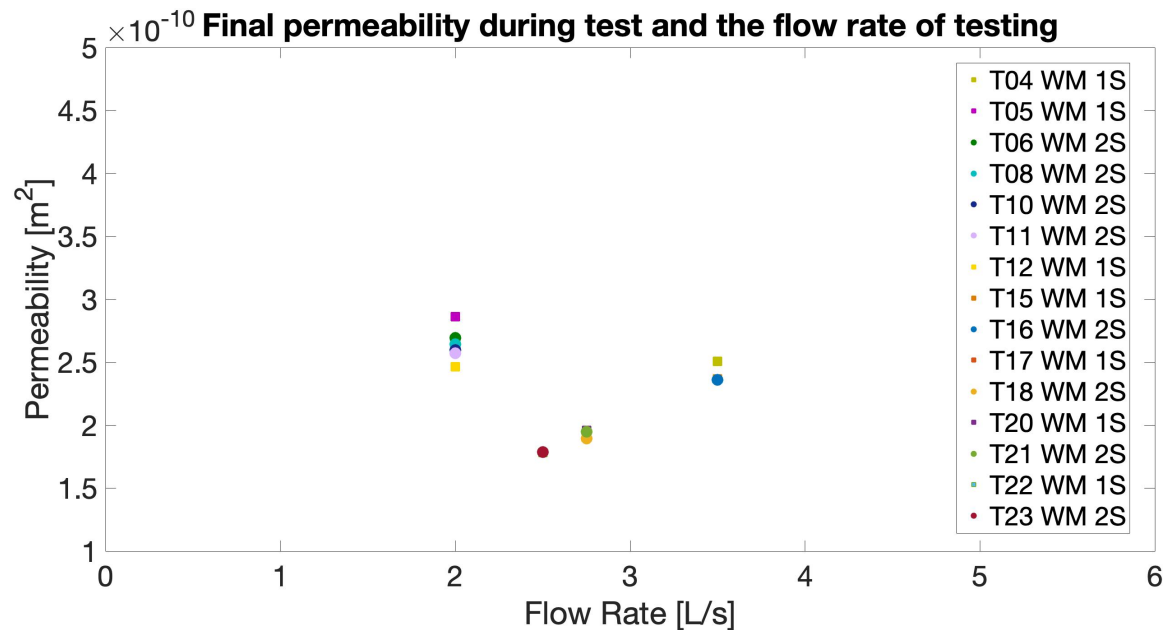


Figure 3.17: Final permeability values against experiment flow rate. 1S is 1 Stage, 2S is 2 Stage and WM is Whole Module.

that between experiments. Which leads to the assumption that the water was chlorinated enough to impede biological growth, as during periods of no flow passing through the media the largest drops in permeability would be expected. The effect of the decreasing permeability was seen visually, as shown by Figures 3.19a and 3.19b, where the water level had risen over the experimental period.

The decline seen in permeability appears to be diminishing, suggesting that the permeability was approaching a long term stable value. However, at the end of the Clean Water Experiments it may not have reached a stable value.

Plotting the final permeability value of the whole of Module 4 against test number provides Figure 3.20. This shows that the final permeability values decreased slowly as flows were passed through the filter bed for individual experiments. The average final permeability reading drop between each experiment from T05 to T23 was $0.06 \times 10^{-10} \text{ m}^2$ which was a average percentage drop of 2.1%.

The valve training exercises, described in Section 3.1, at T07, T09, T13, T14 and T19

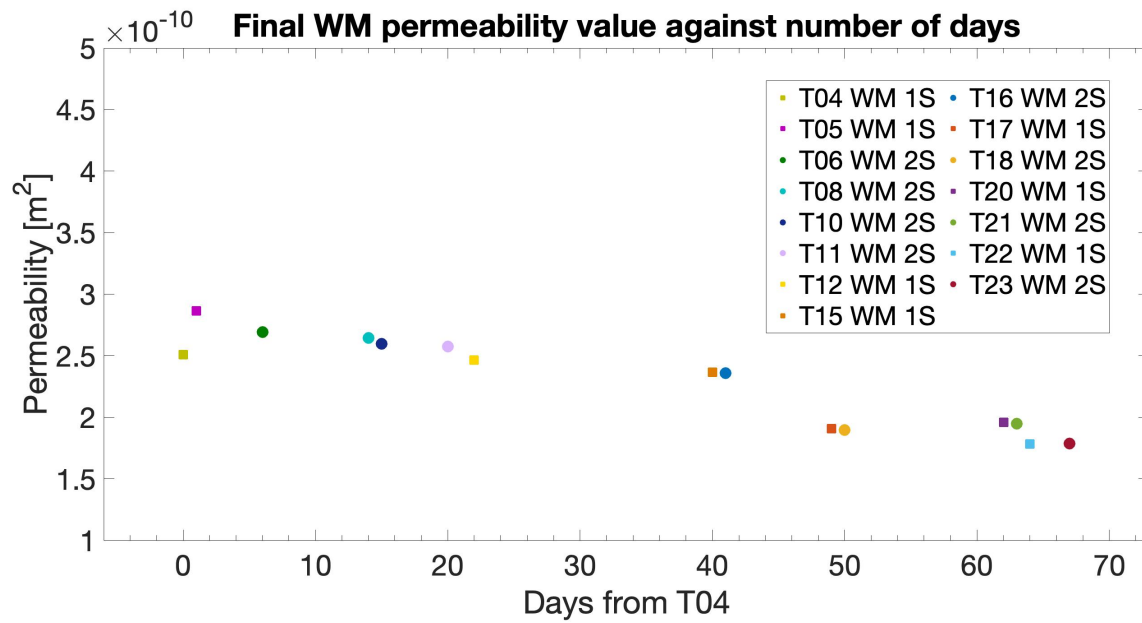
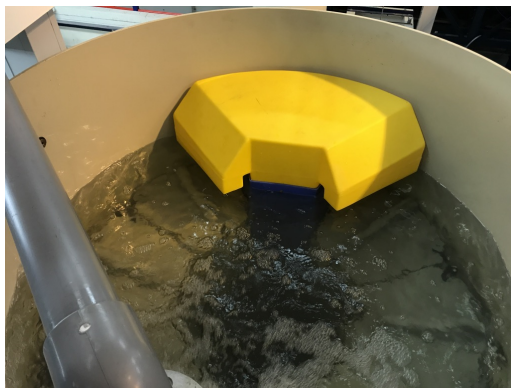


Figure 3.18: Permeability against number of days from T04. 1S is 1 Stage, 2S is 2 Stage and WM is Whole Module.



(a) Photo of Up-Flo® rig water level at 60 mins for T04, 3.5 Ls^{-1} flow rate. (b) Photo of Up-Flo® rig water level at 30 mins for T16, 3.5 Ls^{-1} flow rate.

Figure 3.19: T04 and T16 images of water level in the rig, demonstrating the rise in water level through the experimental program indicating a long term decrease in permeability.

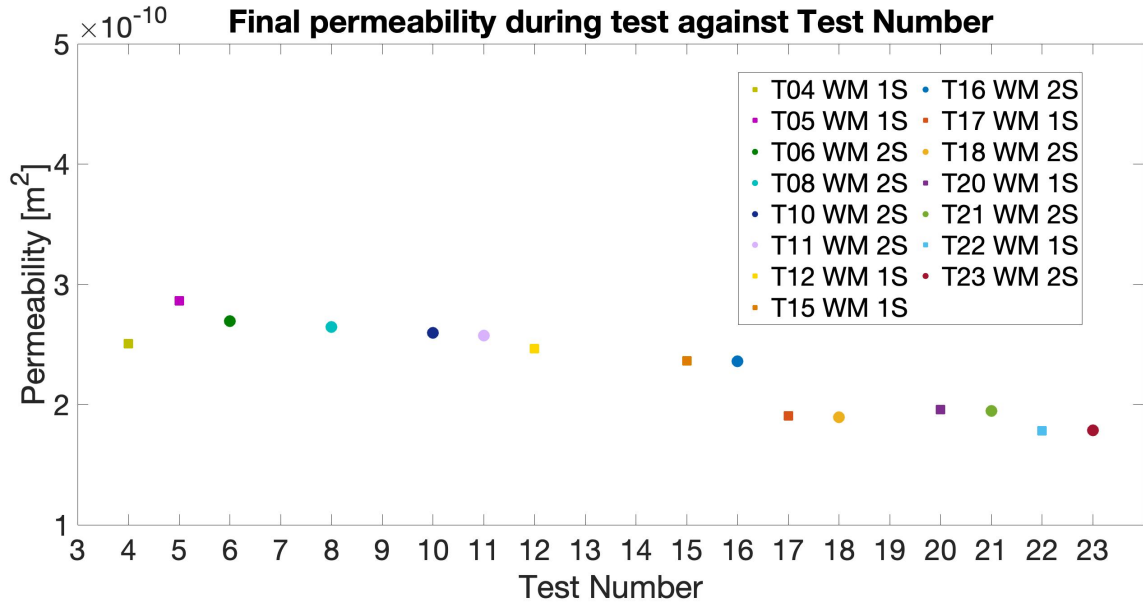


Figure 3.20: Final permeability readings across the Whole Module for M4 Clean Water Experiments against Test Number. 1S is 1 Stage, 2S is 2 Stage and WM is Whole Module.

does not appear to have impacted the long term decline. Which suggests the higher flow rate, max 8 L s^{-1} , caused relatively low disruption and the decline was due to the number of experiments.

A noticeable drop in permeability is shown between T16 and T17, with the permeability dropping from $2.36 \times 10^{-10} \text{ m}^2 \pm 0.05 \times 10^{-10} \text{ m}^2$ to $1.91 \times 10^{-10} \text{ m}^2 \pm 0.04 \times 10^{-10} \text{ m}^2$, a 19% drop in Whole Module permeability. The time between T16 and T17 was 8 days, resulting it being a longer wait than some other experimental intervals. However the difference between T15 and T16 was 13 days, and the permeability value for T16 was $2.36 \times 10^{-10} \text{ m}^2 \pm 0.05 \times 10^{-10} \text{ m}^2$ which is only a 4% drop in permeability from the previous permeability readings at T12, $2.46 \times 10^{-10} \text{ m}^2 \pm 0.05 \times 10^{-10} \text{ m}^2$. This, again, indicates that the drop in permeability was not resultant from biological growth.

The drop between each value of final permeability reading seemed to be reaching zero as the number of experiments increased (Figure 3.21). This implies that the media was

reaching a stable value. The change from Experiments T05, T17 and T22 are not shown in this figure, due to them providing outlier results which masked the observed trend seen.

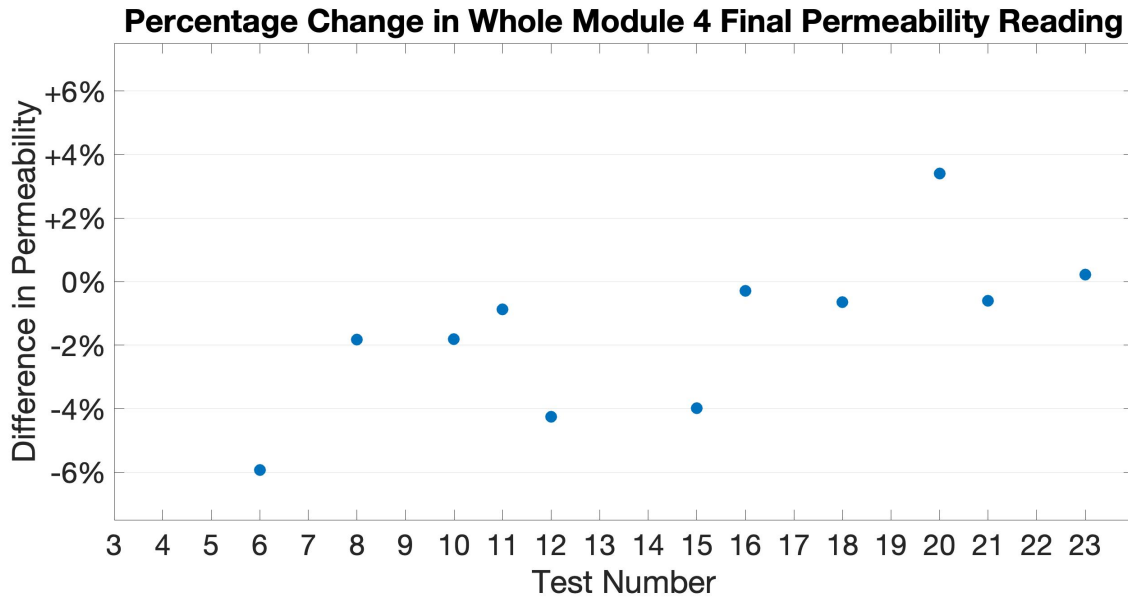


Figure 3.21: Percentage changes in Whole Module 4 Final Permeability Value from last recorded experiment Final Permeability Value with outliers removed.(T05, T17 and T22).

The results for the Bottom Bag and Top Bag of Module 4 showed a similar pattern as shown in Figures 3.22 and 3.23. The figures show the permeability in each Module 4 filter bag decreased throughout the experimental period, as with the Whole Module result. The Top Bag permeability value dropped from a peak value of $4.82 \times 10^{-10} \text{ m}^2 \pm 0.12 \times 10^{-10} \text{ m}^2$ for T05 to $2.82 \times 10^{-10} \text{ m}^2 \pm 0.06 \times 10^{-10} \text{ m}^2$ for T23. Whilst the Bottom Bag permeability dropped from a peak value of $2.04 \times 10^{-10} \text{ m}^2 \pm 0.04 \times 10^{-10} \text{ m}^2$ for T05 to $1.29 \times 10^{-10} \text{ m}^2 \pm 0.03 \times 10^{-10} \text{ m}^2$ for T22. This suggests that the drop in permeability in Clean Water Experiments is driven primarily by the changes in the Top Bag.

Also shown is that the final permeability value in the Top Bag was higher than that of the Bottom Bag. Throughout the Clean Water Experiments the permeability of the Top Bag was on average 230% higher than that of the Bottom Bag. This higher permeability

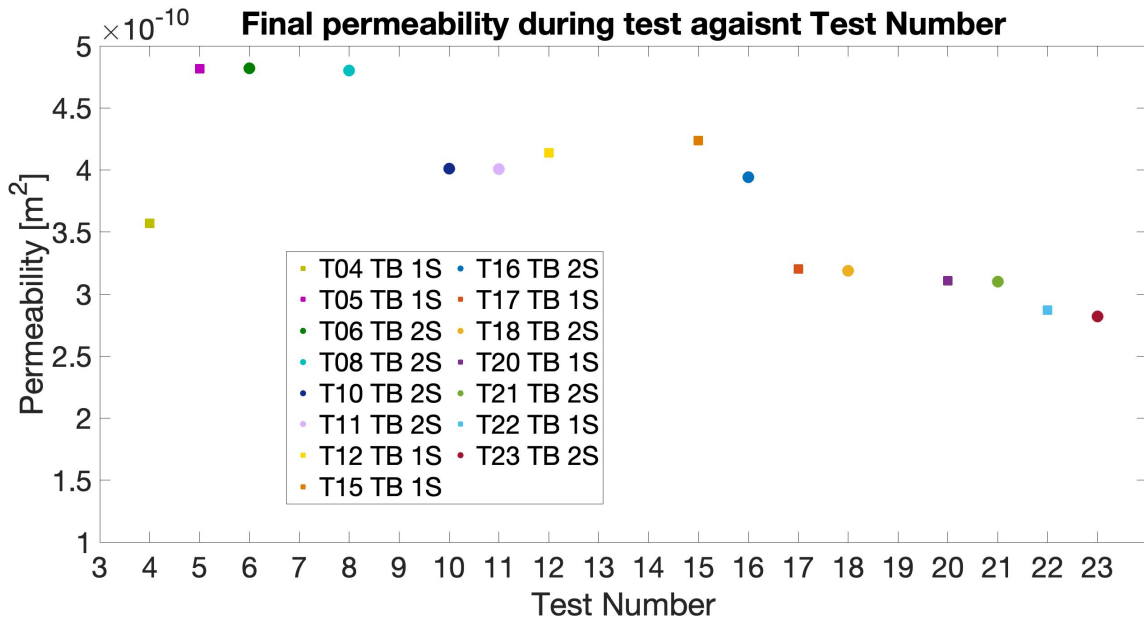


Figure 3.22: Final permeability readings across the Top Bag for Module 4 Clean Water Experiments against Test Number. 1S is 1 Stage, 2S is 2 Stage and TB is Top Bag.

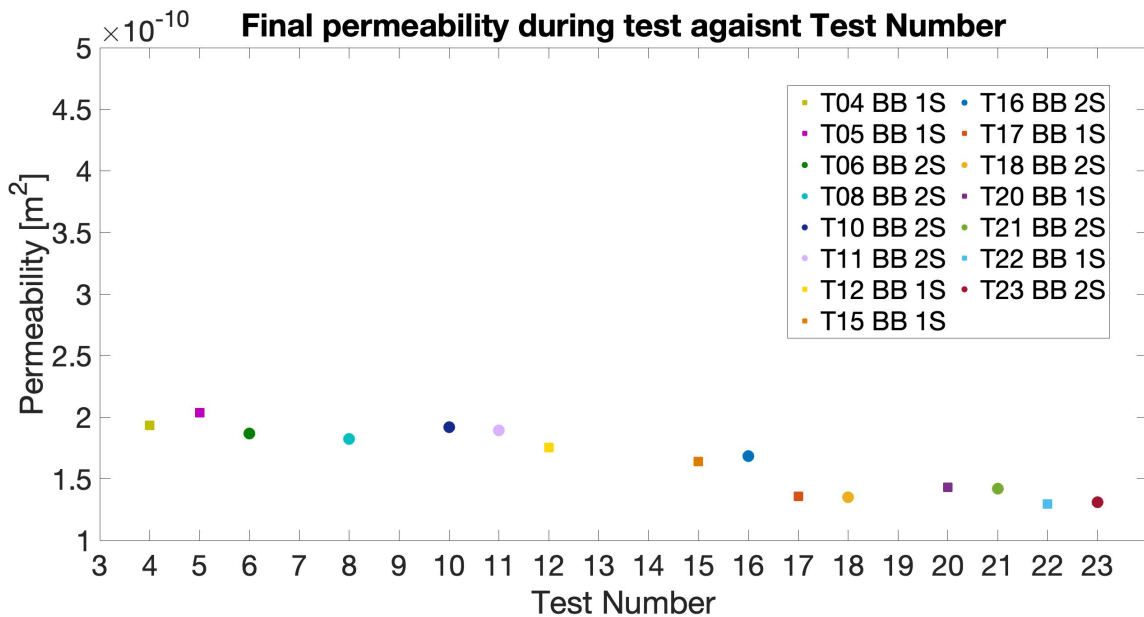


Figure 3.23: Final permeability readings across the Bottom Bag for Module 4 Clean Water Experiments against Test Number. 1S is 1 Stage, 2S is 2 Stage and BB is Bottom Bag.

is to be expected as the Bottom Bag is constrained by the Top Bags weight, resulting in higher consolidation. With the less constrained nature of the Top Bag, the larger drop seen in the permeability is to be expected. As being less constrained would lead to more rearrangement than in the Bottom Bag.

As shown in Figure 3.15, the permeability decreased throughout the T11 experiment. This was seen in all experiments conducted, the exponential line of best fit allows for the decline through the experiment to be quantified. Similarly to the final permeability percentage drop showing a decline, the slope of the exponential line decreased between T04 and T23.

The MatLAB program (Appendix B.7) created an exponential line of best fit for the permeability results. The constant representing the slope of the exponential line of best fit for each experiment is shown in Figure 3.24. This figure shows that as the number of experiments increased the slope decreased in value and approached 0, which would result in a stable permeability value. This indicates that the drop in permeability was due to the flow being passed through it, and as the rate of decline in permeability decreases in later experiments this indicates the decline was a feature of media rearrangement. A large increase is seen between T12 and T15, this is resultant from the 5 Ls^{-1} experiments in T13 and T14. These experiments resulted in overflow events, meaning the results can not be presented. The 5 Ls^{-1} would result in a continued permeability decline.

Due to the continued decrease of the permeability of the filter media, and that at 3.5 Ls^{-1} the flow was touching the overflow, 2 Ls^{-1} was chosen as the experimental flow rate for the ST01, ST02 and ST03. This allowed suitable head room in the tank for an in-depth sediment study.

The slow decrease in permeability in Module 4 appears to be resultant from the repeated experiments. With little decrease seen during long periods between experiments. The impact of other flow rates on permeability seems to be minimal, as Figure 3.17 shows. This further is evidenced by the insignificant effect on the permeability caused by the valve training.

This would impact the operation and maintenance of the Up-Flo® Filter, as the declining

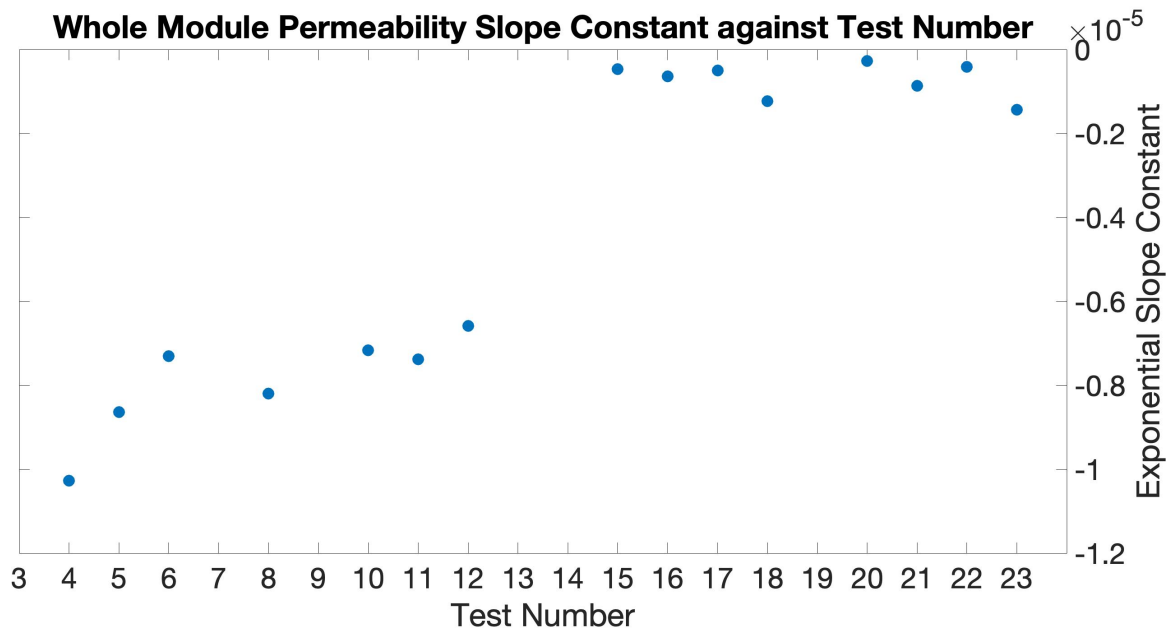


Figure 3.24: Exponential constant against test number from Whole Module 4 permeability results.

permeability with no sediment loading reduces the max flow rate possible through the Up-Flo[®] Filter System. This was seen in the experiments, this is significant as the reduced flow rate would allow untreated flow to bypass the filter.

To maintain the Up-Flo[®] Filter System removal capabilities, the filter media would need to be changed or somehow sufficiently disturbed to restore its capability to pass flow.

As the permeability decreased with each experiment, this was taken into account into the sediment experimental methodologies. By measuring the permeability drop over a series of clean water flows, the background drop in permeability could be estimated. Which allowed the drop in permeability caused by sediment capture to be estimated.

3.8 ST01 Permeability Results

The permeability results for ST01 are shown in Figure 3.25. During the sediment dosing experiment of T28 the Filter Socks became blocked at 152 mins, resulting in the experiment being stopped and final results collected.

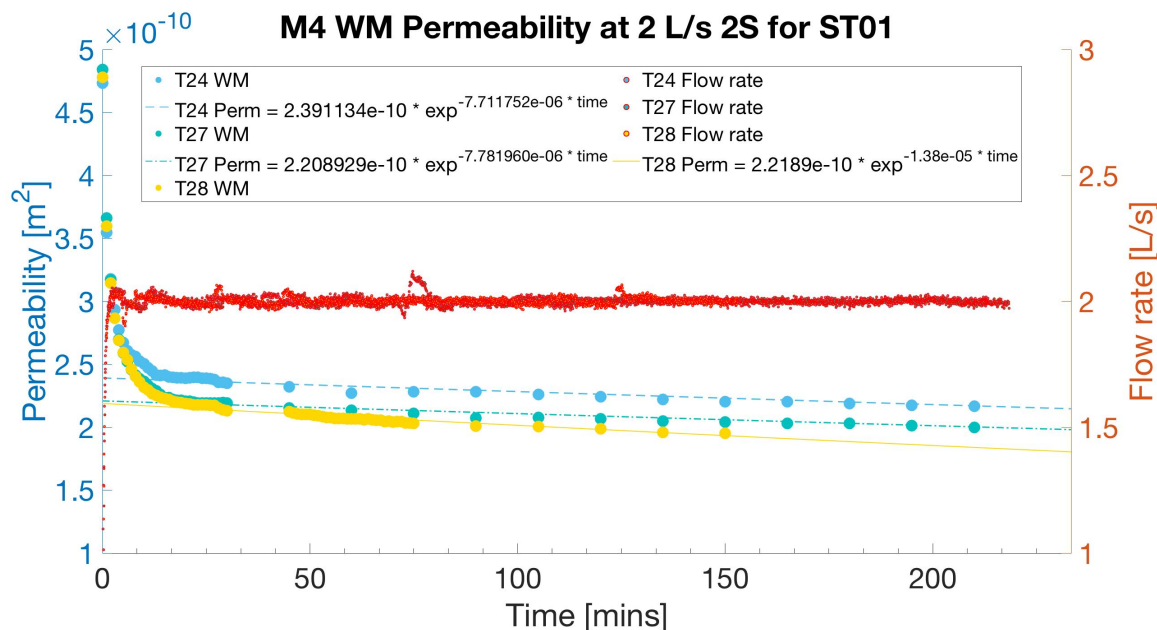


Figure 3.25: Permeability results for ST01 for Module 4 across the Whole Module (WM).

Figure 3.25 shows a continued decrease in permeability between the experiments. The first Clean Water Cycle experiment, T24, showed a final permeability value of $2.17 \times 10^{-10} \text{ m}^2 \pm 0.05 \times 10^{-10} \text{ m}^2$. Between T24 and T27 the final permeability value dropped to $2.00 \times 10^{-10} \text{ m}^2 \pm 0.04 \times 10^{-10} \text{ m}^2$. This was a 7.8% drop in permeability over 4 days of clean water being passed through the media, the average drop per day was approximately 2.0% or $0.04 \times 10^{-10} \text{ m}^2$. This average drop over the Clean Water Cycle experiments is similar to the average drop of $0.05 \times 10^{-10} \text{ m}^2$ seen in the Clean Water Experiments.

The final permeability, T28, value dropped to $1.95 \times 10^{-10} \text{ m}^2 \pm 0.04 \times 10^{-10} \text{ m}^2$, which was a 2.5% drop in permeability. Assuming the 7.8% drop in permeability was equal between each experiment, the 2.5% drop in permeability is slightly larger than expected which

allows the conclusion the impact of sediment was measurable by observation of permeability changes.

Further, as mentioned in Section 3.6, the experiment T28 ended early due to the Filter Socks blocking. As the decline in permeability of the filter media occurs as flow is passed through it. This suggests if the experiment was continued to 210 mins, the final permeability value would be even lower. This would lead to a better distinction between the background drop caused by the flow and that caused by sediment capture. The rate of decline can also be seen in the exponent best fit constant, the clean water exponent constant was around -7.7×10^{-6} however in the sediment experiment the constant increased by 181.8% to -1.4×10^{-5} . This again shows the sediment had a measurable impact on the permeability, with the decline in permeability increasing.

The Top Bag and Bottom Bag saw similar declines in final permeability values between T24 and T27, with a 7.43% and 7.94% drop respectively. Between T27 and T28 the Top Bag dropped by 6.55% and the Bottom Bag dropped 0.63%. The drop in permeability within the Top Bag is much larger than the background, suggesting sediment was being caught primarily in the Top Bag.

3.9 ST02 Permeability Results

The results from ST01 lead to an adapted method for ST02, which Section 3.4 describes. As mentioned in Section 3.6 due to an issue with the equipment, the second sediment dosing experiment day, T34, had 5 mins of additional lower dosed flow at a higher flow rate at the beginning of the experiment. The experiment was stopped and testing restarted once the issue was corrected. T34 also ended 5 mins early at 205 mins due to the mixer being empty, by ending early the mixer did not need refilling and a more accurate mass balance was conducted.

Part of the adapted method was the monitoring of the permeability in an extra two modules. This was to ensure that the assumption that the flow rate in each module being the same was correct. Figure 3.26 shows the permeability over Modules 1, 2 and 4 for T29, the first Clean Water Experiment part of ST02.

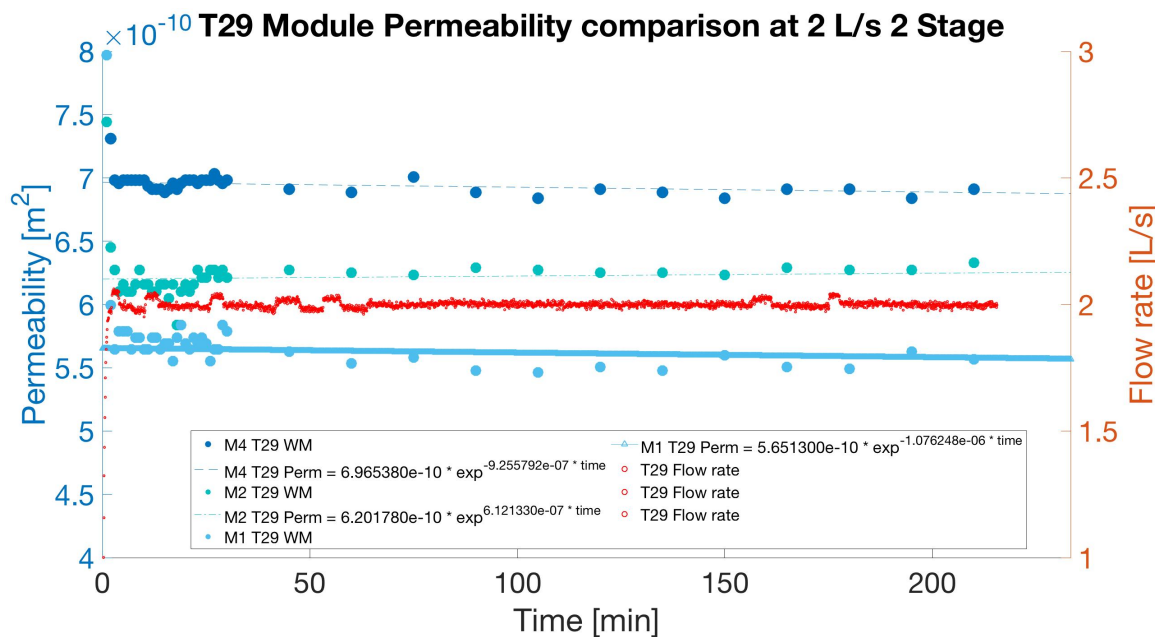


Figure 3.26: Permeability across Modules 4 (M4), 2 (M2) and 1 (M1) during ST02 T29.

Figure 3.26 shows that the permeability in each module is different, with Modules 4, 2 and 1 having the respective final permeability values $6.91 \times 10^{-10} m^2 \pm 0.16 \times 10^{-10} m^2$,

$6.32 \times 10^{-10} \text{ m}^2 \pm 0.14 \times 10^{-10} \text{ m}^2$ and $5.57 \times 10^{-10} \text{ m}^2 \pm 0.12 \times 10^{-10} \text{ m}^2$. It shows the closer to the Up-Flo[®] exit chamber the lower the permeability, however since the same filter media was used in each filter bag and each was measured to the same weight it is unlikely to be a difference in permeability. The difference could be resultant from either the flow being different in each module, with a faster flow rate closer to the exit module, or a changing head to drive water across the modules.

Looking at the head change in each module in Figure 3.27, the head change in Module 1 is larger than Module 2 which is also larger than Module 4. This is expected due to the fact that to drive water to the exit module, Module 4 requires a larger water head than Module 2 and Module 1. This larger head on top of the media would result in a smaller head change across the module. This increased head on top of the module would result in additional downward force, which would lower water velocity within the filter media.

Assuming that each filter media bag had the same permeability, then the average permeability can be used to calculate what the flow rate in each module was. For Modules 4, 2 and 1, respectively, the flow through each module was 0.31 L s^{-1} , 0.34 L s^{-1} and 0.38 L s^{-1} , this shows that closer to the outlet the flow through the module increased. This increased velocity in modules closer to outlet would be expected, as the water head over the module would be reduced resulting in less downward force.

When analysing the M4 permeability results for T29 in Figure 3.26, it is noticeable that the permeability was much greater than ST01 and the Clean Water Experiments. This would be resultant from the larger particle sizes seen in Figure 3.11 for this new filter media. The larger particle size would result in a larger pore size, and a larger permeability.

Figure 3.28 shows the permeability over the Whole Module 4 in each experiment of ST02. Similarly to ST01, the permeability is shown to have decreased between each experiment. The final permeability value dropped to $6.59 \times 10^{-10} \text{ m}^2 \pm 0.15 \times 10^{-10} \text{ m}^2$ in T32, which was a drop of 4.6% over the 4 days of clean water pass through from T29. This is equivalent to a drop per day of 1.15%, the drop over the 4 days is smaller than the drop seen in ST01. Considering the larger particle size of the Garside Sand, this smaller drop is

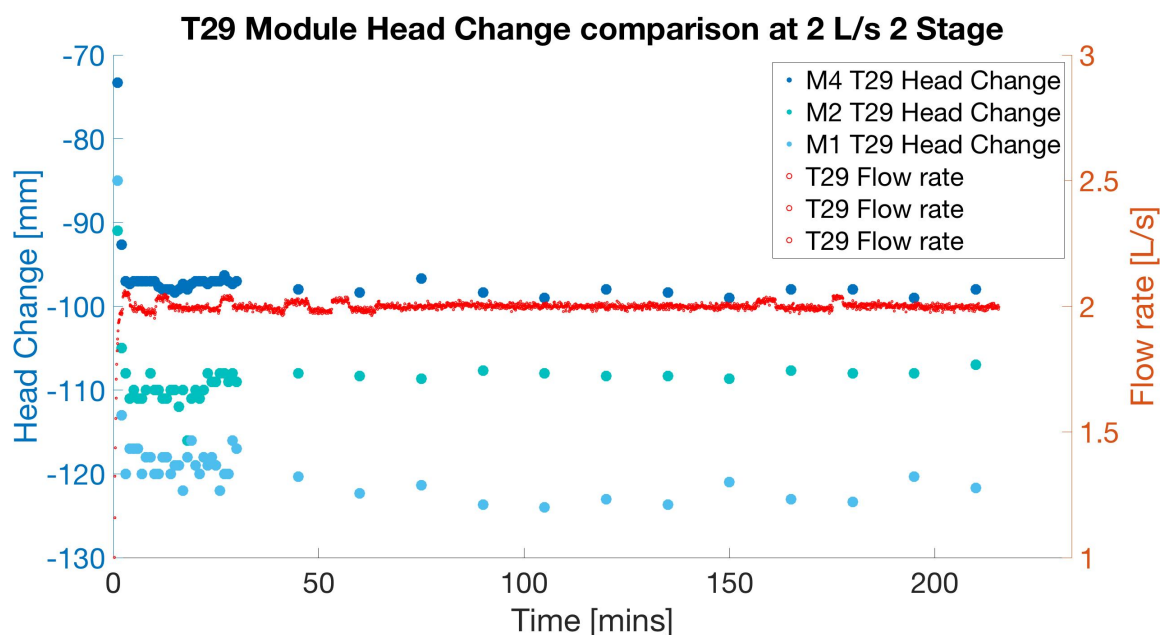


Figure 3.27: Water head comparison in each module during T29. M4 is Module 4, M2 is Module 2 and M1 is Module 1.

to be expected as larger sized particles would rearrange less.

The permeability dropped again to $6.37 \times 10^{-10} \text{ m}^2 \pm 0.14 \times 10^{-10} \text{ m}^2$ in the first sediment dosing day T33, it then dropped to $6.34 \times 10^{-10} \text{ m}^2 \pm 0.14 \times 10^{-10} \text{ m}^2$. Over both sediment days the drop in permeability was 3.79%, with an average drop of 1.90% which was a larger rate of decrease than over the 4 days of clean water. This suggests the sediment capture within the media was detectable.

The top and bottom bag showed a change in permeability between T29 and T32 of +23.1% and -11.2%, respectively. This shows that the decrease in Whole Module permeability over the Clean Water Experiments is driven primarily by changes in the bottom bag. Surprisingly, the permeability seems to have increased in the top bag during the Clean Water Experiments. This could be resultant from rearrangement in the top bag and influenced by the less constrained nature of the top bag.

Over T33 and T34 the top and bottom bag showed a change of +16.9% and -7.6%, respectively. As with the permeability changes between T29 and T32, there is a surprising

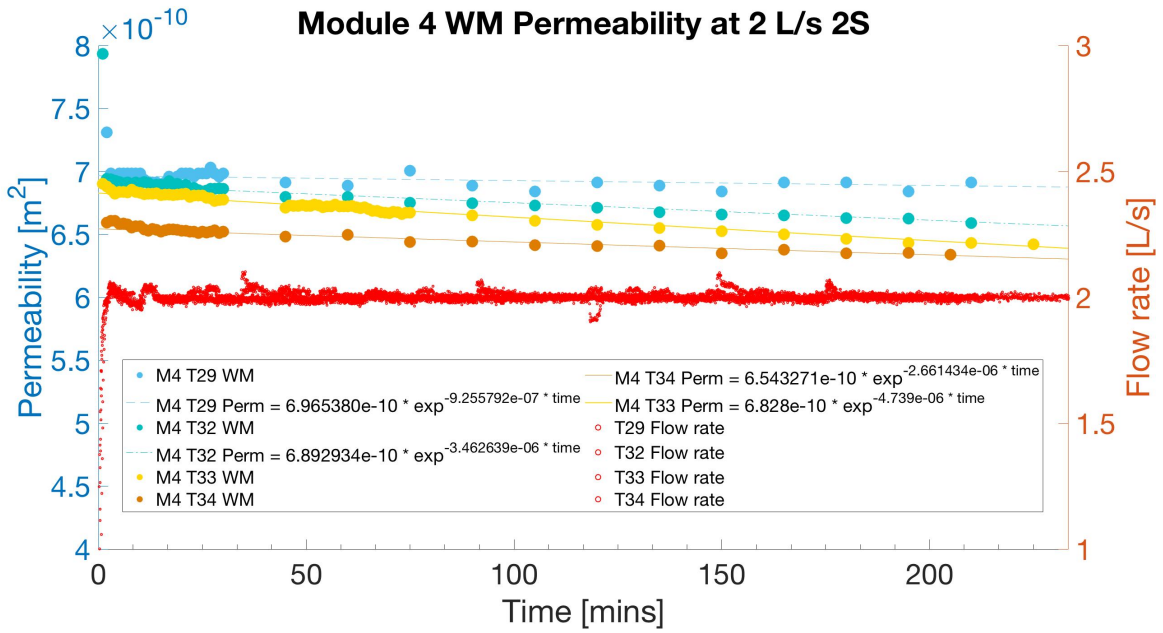


Figure 3.28: Permeability across Module 4 (M4) over ST02 at 2 L s^{-1} 2 Stage.

increase in permeability for the top bag. The bottom bag is shown, again, to be responsible for the permeability drop over the Whole Module observed. The drop in permeability in the bottom bag is approximately 3.8% drop a day, whilst over the Clean Water Experiments the drop was 2.8%. This suggests an extra 1.0% drop in permeability is seen over the bottom bag due to sediment loading.

3.10 ST03 Permeability Results

Due to camera calibration issues in ST03, again, only Module 4 permeability results have been presented. The permeability results are shown in Figure 3.29. As discussed in Section 3.6 at the start of ST03 T34, the sediment inlet pipe became blocked. This resulted in approx 10 mins of clean water flow at 2 L s^{-1} , the flow was turned off and the experiment stopped. Once the pipe was fixed the experiment restarted, the results from ST03 T34 suggest little impact due to the event.

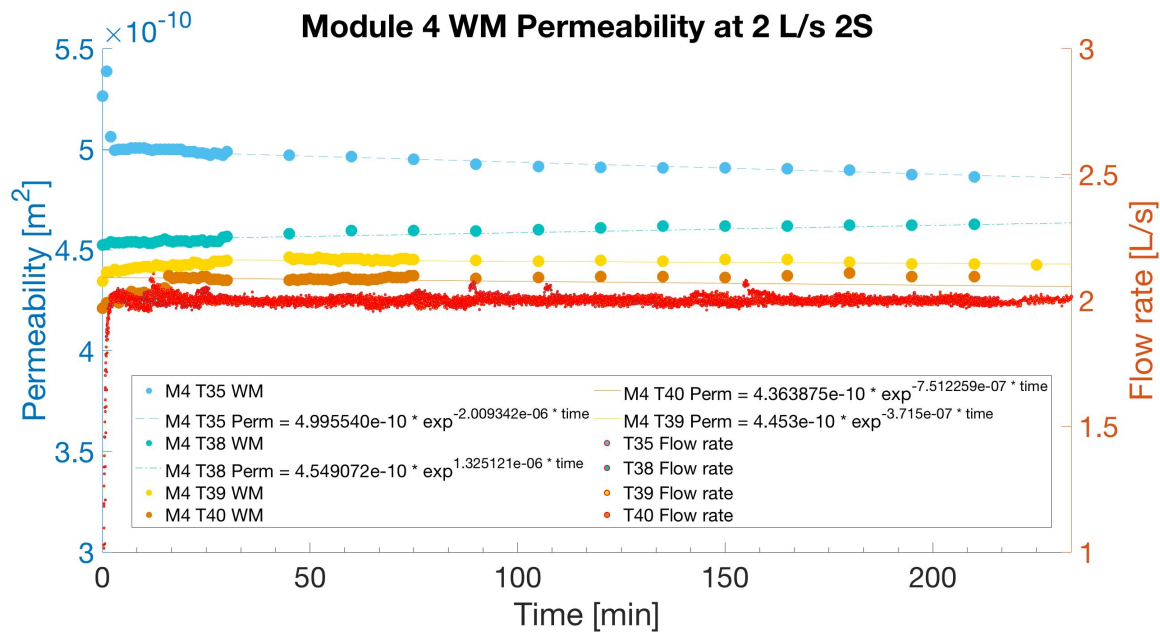


Figure 3.29: Permeability across Module 4 over ST03. WM is Whole Module.

The Whole Module 4 filter media permeability in ST03 consistently decreased between each experiment. The final permeability value for the first Clean Water Experiment, T35, was $4.86 \times 10^{-10} \text{ m}^2 \pm 0.11 \times 10^{-10} \text{ m}^2$. The permeability then decreased between the 4 days of clean water to $4.63 \times 10^{-10} \text{ m}^2 \pm 0.10 \times 10^{-10} \text{ m}^2$ for T38. This was a decrease of 4.7% from the end of T35 to the end of T38, which was a similar decrease in filter media permeability seen for Module 4 between ST02 T29 and T32. This provided an average decrease of 1.18%, similar to ST02.

The final permeability value then decreased to $4.43 \times 10^{-10} \text{ m}^2 \pm 0.10 \times 10^{-10} \text{ m}^2$ in T39 a drop of 4.32% from T38. The final permeability value then decreased to $4.37 \times 10^{-10} \text{ m}^2 \pm 0.09 \times 10^{-10} \text{ m}^2$ for T40, a drop of 1.35% from T39.

Over both of these sediment experiments, T39 and T40, the permeability dropped 5.6% from the end of the last Clean Water Experiment, T38. This drop in permeability was higher than that shown in ST02, suggesting additional sediment was caught during ST03. The average drop was 2.8%, higher than ST02.

Between the clean water flows, T34 and T38, the top and bottom bag permeabilities changed +2.0% and -7.3%, respectively. This shows again the top bag has an increasing permeability during initial clean water flow in the media, and the bottom bag is responsible for the drop in permeability seen over the Whole Module. The reduced changes seen, could be resultant from variances in packing and installation.

Over the sediment experiments, T39 and T40, the top and bottom bag permeabilities changed -4.8% and -5.9%, respectively. This is a drop of 2.4% and 3.0% per day in the top and bottom bag, respectively. Again, the drop in permeability is higher than the 1.8% drop per day seen in the bottom bag during the clean water flows.

3.11 Permeability Results Comparison

The results outlined in Sections 3.7 to 3.10 have provided in-depth information into the filter media used in the Up-Flo® Filter System Modules.

The Clean Water Experiment results have shown that the permeability declines with each experiment, however the rate of decline also reduces. The reducing rate of decline and the data showing small changes in final permeability values in later experiments indicate that the changes are resultant from rearrangement within the filter media. This reducing permeability is also seen in the Clean Water Experiment phase of ST01, ST02 and ST03. This, again, indicates that the filter media rearrangement occurs as flow passes through it.

In each sediment dosed experiment, the permeability had an additional decline to that measured in the Clean Water Cycle experiments. Suggesting the filter media was capturing some sediment, however, the difference in declines was small with 0.5%, 0.7% and 1.6% for ST01, ST02 and ST03. This results in difficulty in measuring the impact of sediment on permeability, however it is clear the larger sized sediment Fraction E results in an increased permeability drop. This is to be expected as larger sized sediment captured would result in reduced pore spacing.

Comparing ST01 and ST02 permeability differences is difficult due to the ST01 ending early. By dividing total percentage drop by experimental time, the average drop per minute can be estimated which allows for a better comparison. The average percentage drop per minute in the Clean Water Cycle experiments was $9.3 \times 10^{-3}\%$, $5.5 \times 10^{-3}\%$ and $5.6 \times 10^{-3}\%$. In the sediment dosed experiments the average percentage drop per minute was $16.7 \times 10^{-3}\%$, $8.6 \times 10^{-3}\%$ and $12.4 \times 10^{-3}\%$. This results in an additional permeability drop from sediment in ST01, ST02 and ST03 of $7.4 \times 10^{-3}\%$, $3.1 \times 10^{-3}\%$ and $6.8 \times 10^{-3}\%$. This shows that the the sediment caused a higher drop per minute in ST01 than in ST02, this is likely resultant from the lower permeability of Fraction B, and the fact it had reached peak rearrangement. This suggests having a well conditioned filter media, where peak stratification has been reached, would help to remove more sediment and allow the effect of sediment to be more easily distinguished from background changes.

Results from the Clean Water Experiments, ST01, ST02 and ST03 all show that the bottom bag permeability is lower than the top bag permeability, this is to be anticipated due to the more constrained nature of the bottom bag. The changes in bottom bag permeability are also shown to dominate the changes in permeability across the Whole Module.

The switch in filter media from Fraction B Sand to Garside Sand caused an increase in permeability from $2.86 \times 10^{-10} \text{ m}^2 \pm 0.06 \times 10^{-10} \text{ m}^2$ to $6.91 \times 10^{-10} \text{ m}^2 \pm 0.16 \times 10^{-10} \text{ m}^2$. This increased permeability was expected due to the slightly larger filter media size, which would cause an increased porosity and permeability.

3.12 Up-Flo® Filter Total Suspended Solids Results

This section presents the results from the Total Suspended Solids (TSS) and Particle Size Analysis (PSA), then using the TSS results an analysis of the Up-Flo® Filter System removal efficiency in ST01, ST02 and ST03 is made. Combining the TSS and removal data with the PSA data, allows for analysis of the Up-Flo® Filter System removal efficiency against particle sizes to be presented.

3.12.1 ST01 TSS

The TSS results for ST01 are provided in Figure 3.30. It is shown that as the sediment was introduced at 45 mins the Up-Flo® Rig Effluent TSS increases until it appeared to reach a maximum TSS of around $132.5 \text{ mgL}^{-1} \pm 0.6 \text{ mgL}^{-1}$ at around 80 mins. The sump of the Up-Flo® also showed a sharp increase in TSS once the sediment was introduced, with the TSS ranging between $130.5 \text{ mg/} \pm 0.6 \text{ mgL}^{-1}$ to $171.2 \text{ mgL}^{-1} \pm 0.7 \text{ mgL}^{-1}$, however due to the lack of samples for ST01 there is insufficient data to form an in depth understanding. The Pre-Influent TSS showed little change throughout ST01, the average TSS value was $3.5 \text{ mgL}^{-1} \pm 0.6 \text{ mgL}^{-1}$, indicating that the sediment had not contaminated the laboratory sump.

The Influent TSS results are not plotted due to the wide variance, this is believed to be due to the difficulty in obtaining a good sample as the sediment inlet pipe was too close to the opening of the Up-Flo® inlet pipe, it was only 390 mm. Resulting in influent not being well mixed before entering the sump. The British Water Standard released in 2017 (Chapter 2 discusses) utilises a static mixer so the sediment within the influent flow would be well mixed before entering the rig, allowing more accurate sampling. This project experimental methodology was designed before the publication, however in future work this should be integrated into methodologies as it would solve the problem described.

Using Equation 3.12 presented in Section 3.5.7 the average influent TSS for ST01 was estimated as $501 \text{ mgL}^{-1} \pm 0.6 \text{ mgL}^{-1}$, designated as $\text{TSS}_{\text{ST01IA}}$. This used the total

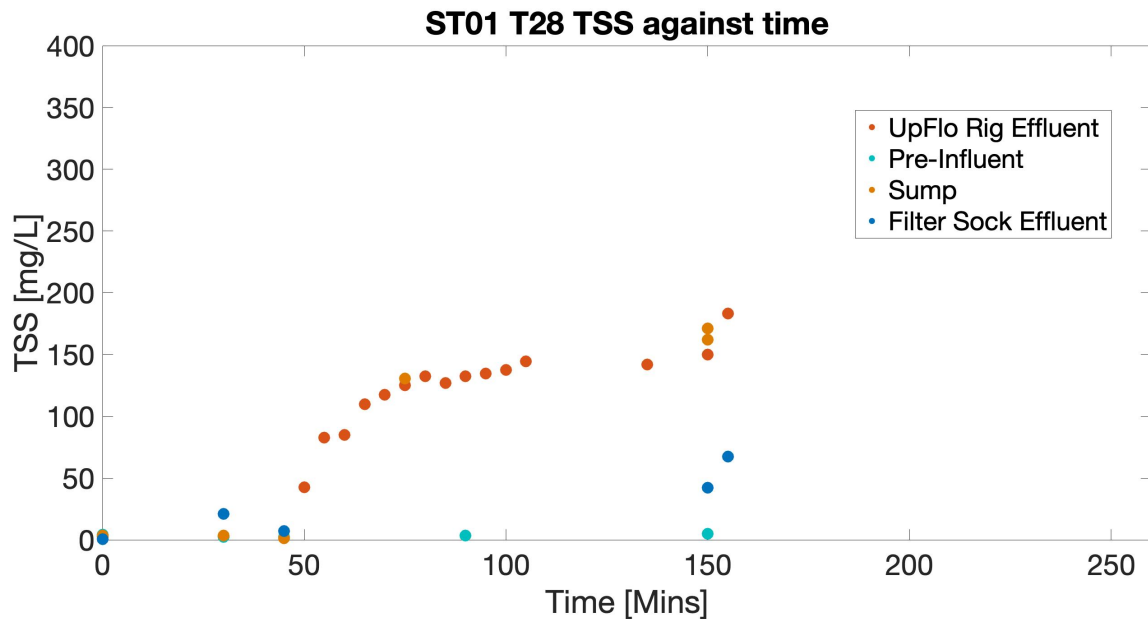


Figure 3.30: TSS values during ST01 T28 against time with Influent being $501 \text{ mgL}^{-1} \pm 2.8 \text{ mgL}^{-1}$. T28 Sediment start time at 45 mins, experiment ended at 152 mins due to Filter Sock clogging.

mass of sediment introduced to the Up-Flo® Filter System and the total flow passed through the system.

3.12.2 ST02 TSS

Figure 3.31 shows the TSS values obtained for both sediment experiment days, T33 and T34, in ST02. As with ST01, the individual influent TSS results were not plotted, due to the wide variance, resultant from the difficulty in acquiring a good sample. Using Equation 3.12, ST02 influent TSS was estimated as $569.6 \text{ mgL}^{-1} \pm 3.1 \text{ mgL}^{-1}$, known as $\text{TSS}_{\text{ST02IA}}$.

Figure 3.31 shows that the Up-Flo® Filter System Rig Effluent increased throughout T33, reaching a peak of $160.8 \text{ mgL}^{-1} \pm 0.7 \text{ mgL}^{-1}$ at 195 mins. During T34 the Rig Effluent TSS also increased throughout the experiment, reaching a maximum value of $168.8 \text{ mgL}^{-1} \pm 0.7 \text{ mgL}^{-1}$ at 150 mins. This means that on both sediment days the

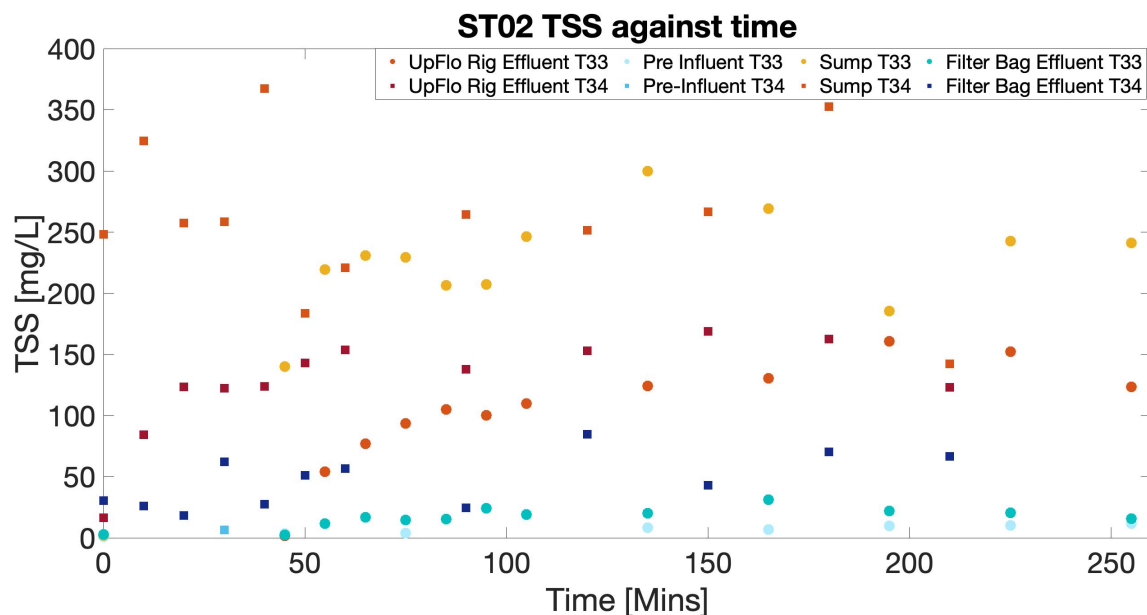


Figure 3.31: TSS values during ST02 T33 & T34 against time with influent being $569.6 \text{ mgL}^{-1} \pm 3.1 \text{ mgL}^{-1}$. T33 sediment dosing start time 45 mins. T34 sediment dosing start time 0 mins.

maximum TSS value for the Up-Flo® Rig Effluent was at 150 mins of sediment dosing. The Rig Effluent TSS value for both sediment dosed experiments was higher than the ST01 Rig Effluent value, +21.4% and +27.4% for T33 and T34 respectively. This increased Rig Effluent TSS could be resultant from the increased Influent TSS value or greater loss through the media. However, as the Influent TSS value was only approximately +13.6% greater than ST01, the increased TSS value is likely resultant from increased loss through the media.

Changes to the experimental method in ST02 allowed for more sampling of the sump, this allowed for a more complete picture of sump TSS. Figure 3.31 shows that for T33 the Up-Flo® sump increased once the sediment was introduced at 45 mins, it appears at 65 mins the T33 sump TSS reached a more steady value. T34 sump TSS data shows that the TSS increased similarly when the sediment was introduced at 0 mins. The maximum TSS value for T33 was 300 mgL^{-1} at 135 mins and 367 mgL^{-1} for T34 at 40 mins.

The Filter Sock Effluent TSS results show that the maximum value was $31.2 \text{ mgL}^{-1} \pm 0.4 \text{ mgL}^{-1}$ at 165 mins for T33 and $84.9 \text{ mgL}^{-1} \pm 0.5 \text{ mgL}^{-1}$ at 120 mins for T34. The Filter Sock Effluent TSS results from T34 were higher than T33. This would be resultant from the change in method in T34, which Section 3.6 discusses, of only having the last row of Filter Socks installed instead of two rows. This was to extend the life of the Filter Socks due to a significant amount of Filter Socks being utilised for T33. It was not expected to impact the results significantly, as the internal experiments previously showed little removal after first bag. The increased loss is expected to be resultant from less flow restriction resulting in less settlement within the Filter Sock area. By using the TSS results, the loss through the Filter Socks was estimated and taken into account in the mass balance equations later on.

The Pre-Influent TSS samples showed no significant change throughout T33 with a maximum value of $11.7 \text{ mgL}^{-1} \pm 0.4 \text{ mgL}^{-1}$. The maximum measured value for T34 was $6.3 \text{ mgL}^{-1} \pm 0.4 \text{ mgL}^{-1}$.

3.12.3 ST03 TSS Results

Figure 3.32 shows the TSS values obtained for both T39 and T40 for ST03. Once again the influent TSS was too varied to provide reliable data, this appears due to the difficulty in acquiring a well mixed accurate sample. Using the total mass of sediment introduced to the Up-Flo® Filter System and the total flow passed through the system, the influent TSS was averaged out as $561.21 \text{ mgL}^{-1} \pm 3.1 \text{ mgL}^{-1}$ known as $\text{TSS}_{\text{ST03IA}}$.

Figure 3.32 shows that the Up-Flo® Filter System Rig Effluent TSS values are significantly reduced compared to ST01 and ST02. With a maximum of $21.4 \text{ mgL}^{-1} \pm 0.4 \text{ mgL}^{-1}$ throughout both T39 and T40. This suggests the Up-Flo® Filter System removal of the larger particle sized Fraction E was greater than that of the silica flour. The Pre-Influent and Filter Sock Effluent TSS results showed little variance throughout ST03.

The sump TSS values for T39 and T40 are very varied, this is believed to be resultant

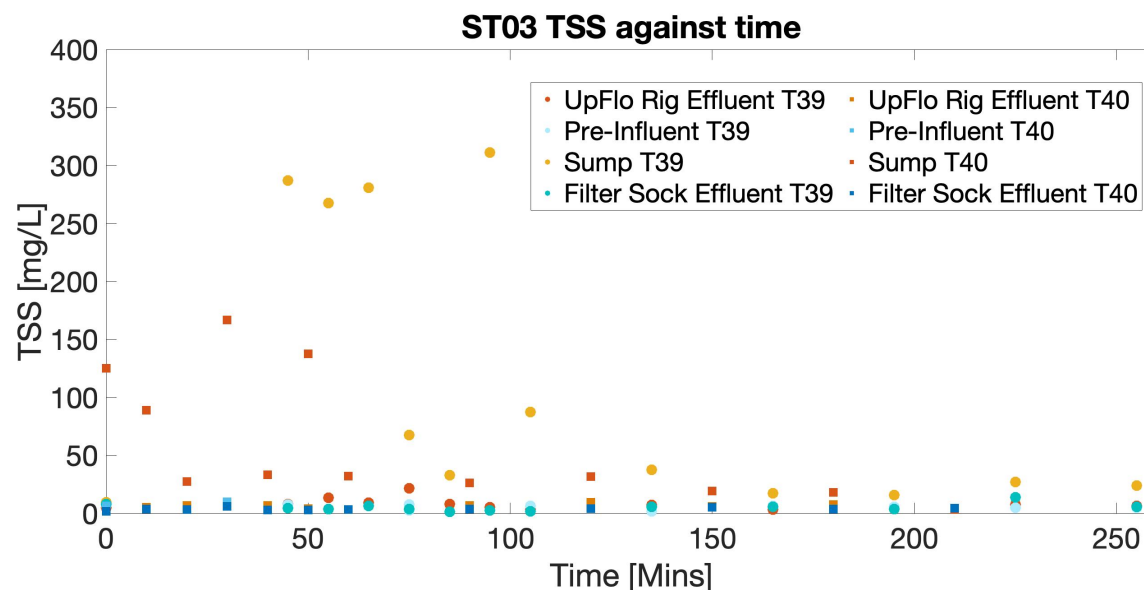


Figure 3.32: TSS Values during ST03 T39 & T40 against time. Influent TSS estimated to be $561.21 \text{ mgL}^{-1} \pm 3.1 \text{ mgL}^{-1}$. Sediment dosing began at 45 mins in T39 and 0 mins in T40.

from the increased settlement of the Fraction E. As Section 3.13 discusses, 84% of Fraction E was caught by the sump.

3.12.4 TSS Removal Efficiencies

Using Equation 3.11, the removal efficiencies against time for ST01, ST02 and ST03 were calculated. The calculated average Influent TSS values given previously was used for TSS_{STXXIA} , however instead of the average Rig Effluent TSS value, TSS_{STXXRA} , the Rig Effluent TSS value at the specific time was used. Figure 3.33 shows the Up-Flo® Filter Systems removal efficiency against time for all sediment experiments. Firstly, the impact of a larger particle size is apparent with ST03 having been close to 100% sediment removal. ST01 and ST02 showed similar removal efficiencies, both also showed the removal efficiency decreased over the experiments until it reached an equilibrium around 20 mins after sediment dosing start.

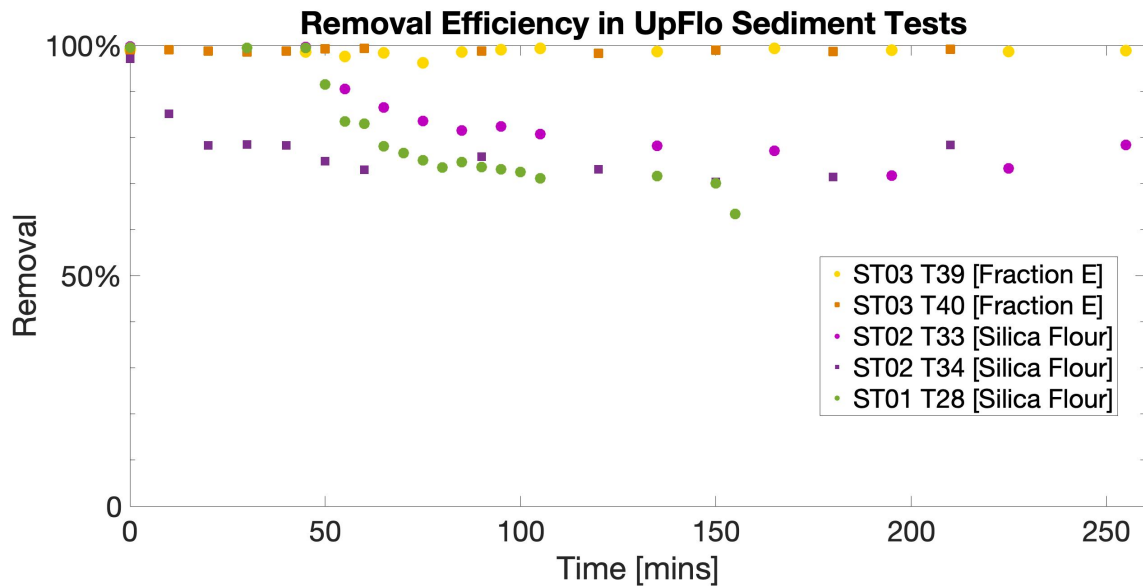


Figure 3.33: Sediment Experiment Up-Flo® Filter System overall removal efficiencies against time. Sediment start time; T28, T33 and T39 was 45 mins, T34 and T40 was 0 mins.

Using the average Rig Effluent TSS, the average removal efficiency of the Up-Flo® Filter System over the entire experiment for ST01, ST02 and ST03 was calculated to be $75.1\% \pm 0.2\%$, $78.3\% \pm 0.2\%$ and $98.7\% \pm 0.1\%$, respectively. When comparing ST01 and ST02 removal efficiency with the NJCAT verification study of the Up-Flo® Filter System [11] which used sil-co-sil 106 over various flow rates, the removal efficiency was worse. For $1.89 Ls^{-1}$ the average removal was 84%, with the relationship derived forecasting a 83.7% for the $2 Ls^{-1}$ flow. However, the NJCAT study had a lower sediment loading, which may impact the results. Additionally of note was that the filter media used was different from that utilised in this work and the drain-down ports were restricted but not sealed.

A key difference in results would be resultant from the significantly reduced duration of sediment dosed flow, as the longest dosed duration was 9 mins. The results from ST01 and ST02 show the removal efficiency drops over time, so the shorter duration would result in a higher removal efficiency as the system would not have reached an equilibrium. This is because it takes time for sediment particles time to fall below the modules. Where

either, they continue to fall, if upward water velocity is less than particles settling velocity, or the particles are carried with the upward flow through the granular media. As Chapter 2 discusses, as particle size increases so does the settling velocity. Hence, as particles most likely to go through the media have a smaller settling velocity, it takes a longer time for the particles to fall below the modules and reach a removal efficiency equilibrium.

3.12.5 Particle Size Removal

Particle Size Analysis (PSA) was conducted on Up-Flo® Rig Effluent samples from ST01 and ST02. The Total Suspended Solids (TSS) results for ST03 was too low for PSA to be conducted accurately. The PSA showed a decrease of the d_{50} size between the Rig Effluent samples and the silica flour PSA, presented in Section 3.4. Using Equation 3.15, the PSA results and the samples matching TSS value a Up-Flo® Filter System removal efficiency against particle size was plotted, r_{PSA} , shown in Figures 3.34 to 3.36.

$$r_{PSA} = \left[1 - \frac{TSS_{STXXREYY} \times PSA_{STXXREYY}}{TSS_{STXXIA} \times Influent_{PSA}} \right] \times 100 \quad (3.15)$$

Where; $TSS_{STXXREYY}$ is the Rig Effluent sample TSS in mgL^{-1} , $PSA_{STXXREYY}$ is the PSA of the sample in μm , TSS_{STXXIA} is the previously defined average Influent TSS value and $Influent_{PSA}$ is the PSA of the experimental sediment. XX denotes sediment test number and YY denotes sample number.

Figure 3.34 shows the removal efficiency of the particle sizes by the Up-Flo® Filter System for ST01 T28 at 150 mins. Only 150 mins was analysed due to ST01 primarily being focused on TSS, the ST01 PSA results led to an adapted method in ST02. It shows that at larger particle sizes the Up-Flo® Filter System was better at removing the silica flour. Particles above $48.62 \mu m$ had greater than 80% removal, which is the designed removal rate of the Up-Flo® Filter System.

However, Figure 3.34 also shows that at the lowest particle sizes the removal efficiency slightly increased. At $1.6 \mu m$ the removal efficiency was 55.6% but then dropped until $3.784 \mu m$ when the removal efficiency was 48.1%. These sizes typically represent fine silts

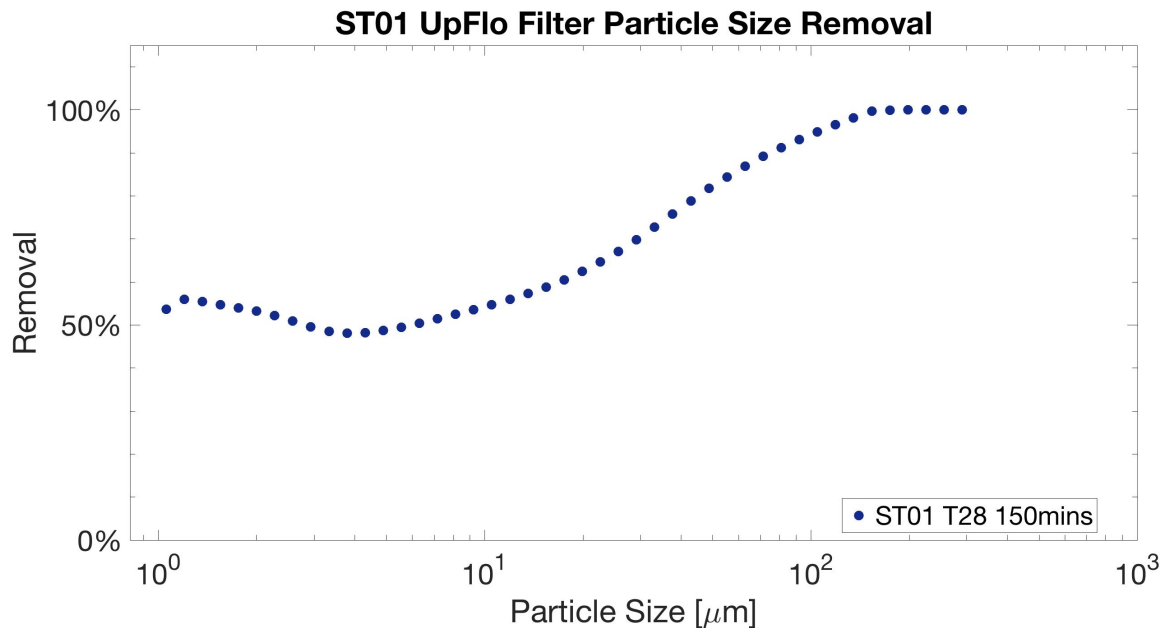


Figure 3.34: ST01 T28 Up-Flo® Filter System removal efficiency of particle sizes.

and clays [103], which, as Chapter 2 outlines, carry a significant amount of pollution. There are only three possible removal processes that describe this increased particle removal at this size range; increased particle adhesion in the filter media, flocculation resulting in settlement in the Up-Flo® sump, or the settling velocity being so small it takes significant time for particles to go below the modules. Later sections look at the individual removal processes involved, which will allow for the removal technique of the particles in this size range to be explored.

Figure 3.35 shows that for ST02 T33 the larger particle size resulted in better removal, as with ST01. It appears that the experimental time had little impact on the Up-Flo® Filter Systems removal efficiency of particles with sizes greater than 104.6 μm , however below this size the experimental time had a significant impact on the removal efficiency. As the experimental time increased the removal efficiency decreased, until 195 mins when it increased at 225 mins and 255 mins. The minimum particle size for greater than 80% removal was 55.24 μm , however the minimum particle size reduced the earlier the sample taken in the experiment with 75 mins the minimum particle size was 29.18 μm .

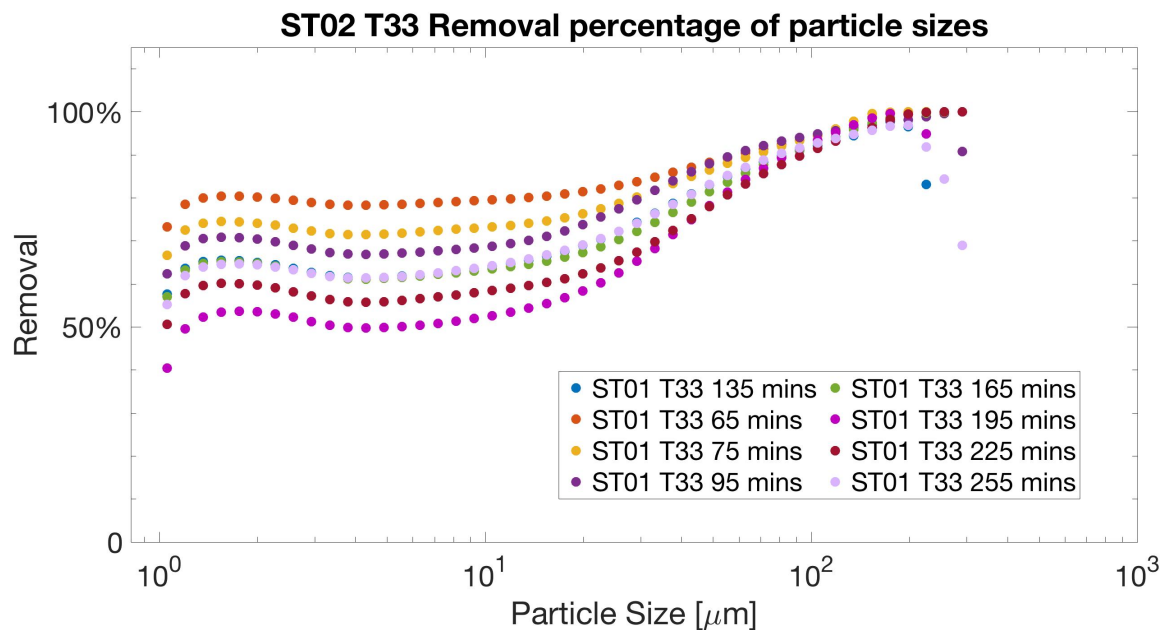


Figure 3.35: ST02 T33 Up-Flo® Filter System removal efficiency of particle sizes.

As with ST01 T28 particles below $3.784 \mu\text{m}$ had a slight increased removal efficiency. The additional PSA of the samples has provided the data to analyse what happens as experimental time increases. Figure 3.35 shows as experimental time increased the removal efficiency decreased until 195 mins where it increased at 225 mins and 255 mins, as with particles above this range. However the difference in removal efficiency between particles in the fine silt and clay range and the particles over $3.784 \mu\text{m}$ increases with experimental time. This aids with analysis of removal techniques in later sections.

Additionally, as the figure shows, 65 mins resulted in close to or above 80% removal for all particle sizes. This was only 20 mins after sediment influent had begun, as the experimental time increased the removal efficiency of the Up-Flo® Filter System dropped significantly for particles with sizes below $42.79 \mu\text{m}$. This is likely due to the time for these particles to settle to a point where they can be taken through the filter media. Suggesting, the maximum 8 min experimental time used in NJCAT is not sufficient to capture what happens at the lower particle size range.

ST02 T34 particle size removal by the Up-Flo® Filter System is shown in Figure 3.36, as

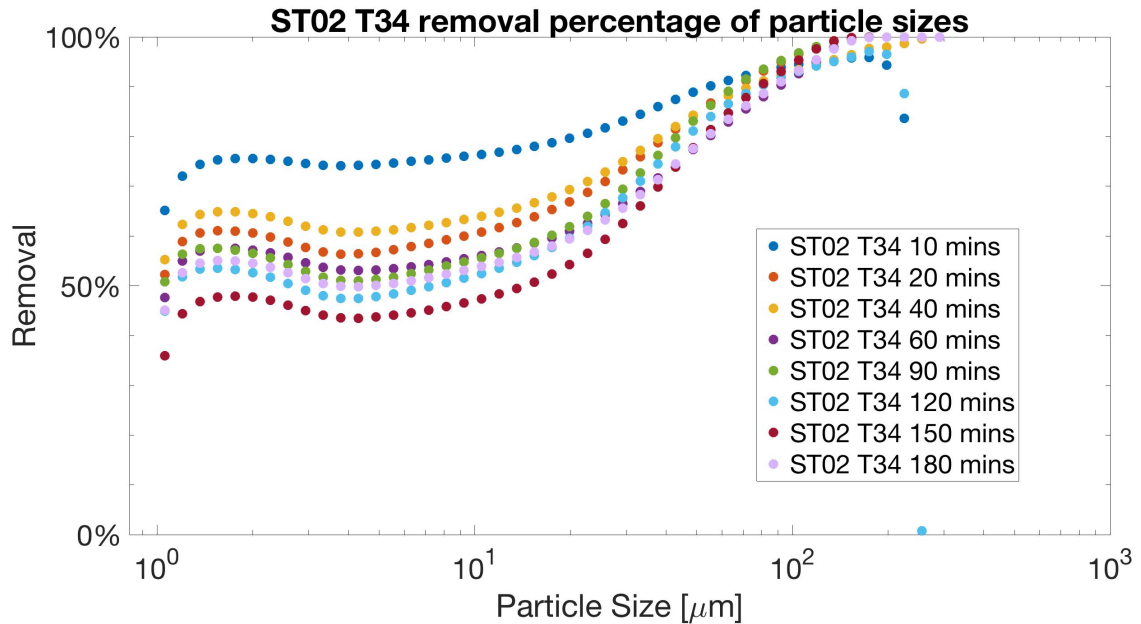


Figure 3.36: ST02 T34 Up-Flo® Filter System removal efficiency of particle sizes.

with ST01 T28 and ST02 T33 the removal efficiency increased with particle size. The time of sample being taken seems to have had an effect on the sediment removal, with later sample times showing a decreased efficiency. As with ST02 T33 removal efficiency of particle sizes greater than $104.6 \mu\text{m}$ was not impacted as much by the experimental time. The minimum particle size for greater than 80% removal was $55.24 \mu\text{m}$, however the minimum particle size reduced the earlier the sample taken in the experiment, with 40 mins the minimum particle size was $42.79 \mu\text{m}$.

As with ST01 T28 and ST02 T33 sediment particles below $3.784 \mu\text{m}$ have a better removal efficiency than anticipated. Additionally, the gap between the removal efficiency for fine silts and clays, and larger sized particles widens with increased experimental time.

Similarly to ST02 T33, removal of particles below $42.79 \mu\text{m}$ takes time to drop significantly. Again, suggesting the NJCAT experimental time of 8 mins is insufficient, as particles below $42.79 \mu\text{m}$, which make up over 70% of the NJCAT experimental sediment, Sil-Co-Sil 106, would not have sufficient time to pass through the system providing an artificially high removal efficiency.

The results from ST01 and ST02 show that as particle size increases the removal efficiency also increases. This could be a result of straining in the filter media or settlement within the sump. However, the permeability results in the previous section had no significant decrease across these two sediment dosed experiments. This suggests the increased removal at larger particle sizes is largely resultant from increased settlement within the sump, the next section investigates this.

The higher number of PSA measurements conducted in ST02 shows that removal efficiency declined as experimental time increased, as seen in the TSS removal efficiency results in Figure 3.33. However, the PSA data shows this is not consistent across all particle sizes. The decline is seen primarily in particles with sizes below $42.79 \mu m$, this is anticipated as particle size impacts settling velocity. So, at smaller particle sizes additional time is needed for the particles to go fully through the system. This also shows that the low experimental time for NJCAT verification is insufficient, as over 70% of Sil-Co-Sil 106 is below this size.

ST01 and ST02 have both shown that the particles in the fine silt to clay range have a slightly increased removal efficiency compared to other small particles. This increased removal will be resultant from one of, or a combination of, three processes. Either; flocculation resulting in settlement in the Up-Flo® sump, increased particle adhesion within the filter media or a significantly high settling velocity resulting insufficient time for the particles to pass fully through the filter media. The following sections covering mass balance and filter media PSA will investigate this further and determine which processes can be eliminated from consideration and define the most likely process.

3.13 Mass Balance Results

To develop the knowledge of the Up-Flo[®] Filter Systems sediment removal mechanisms further a full mass balance was conducted, using the method outlined in Sub-section 3.5.6. This enabled for increased knowledge of where the sediment was captured, as well as verifying results collected in the TSS analysis. To allow for an accurate mass balance the Rig Effluent and Filtersock Effluent TSS data was used, to estimate the losses through the Filter Socks, using Equations 3.13 and 3.14 in Sub-section 3.5.7.

Mass Balance of ST01 with 6473.55g sediment influent with losses through SigaFiltration Filter Socks factored in

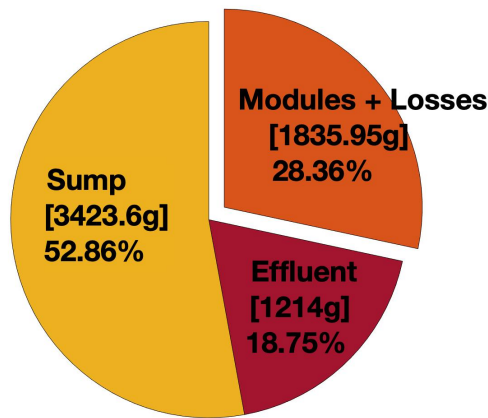


Figure 3.37: ST01 Mass Balance.

The mass balance for ST01 shows that the removal efficiency of the Up-Flo[®] Filter System was $81.2\% \pm 0.0\%$. This was higher than the removal efficiency calculated through TSS and closer to that seen in the NJCAT verification study. The difference would be resultant from the reduced TSS sampling used to estimate the removal efficiency. Difference between the mass balance removal efficiency result and NJCAT, is again assumed to be resultant from the reduced experimental time in NJCAT. Resulting, in it not achieving equilibrium as explained in the previous section.

**Mass Balance of ST02 with 28336g sediment influent
with losses through SigaFiltration Filter Socks factored in**

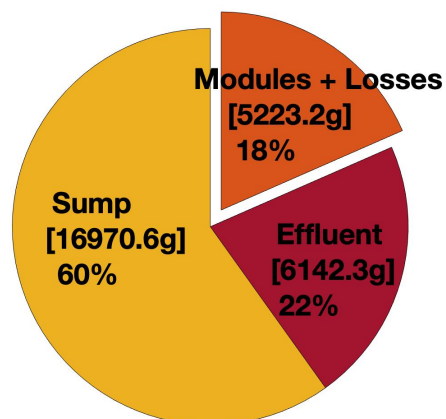


Figure 3.38: ST02 Mass Balance.

The ST01 mass balance shows that the sump was responsible for most of the silica flour removal, with 65.1% of the sediment removed by the Up-Flo® Filter System being retained by the sump and the filter media only catching 34.9%. Silica flour that did not settle in the sump passed through the filter media in the Up-Flo® Filter Modules, an estimate for the filter media removal efficiency is calculated to be 60.2% of the total sediment passed through these modules.

ST02 mass balance shown in Figure 3.38, provided the removal efficiency of the Up-Flo® Filter System as $78.0\% \pm 0.3\%$. This value is similar to the calculated average TSS removal efficiency of 78.3%. The reduced removal efficiency is likely due to the initial increased permeability, due to the slightly larger grain size and the fact no long term Clean Water Experiments were conducted, which would have reduced permeability. The mass balance shows that once again that the sump was responsible for the majority of the sediment removal, with 76.9% of the total sediment captured by the Up-Flo® Filter System having been retained in the sump. An estimate for the filter media removal efficiency is also calculated to be 46.0% of the total sediment passed through the filter modules. This lower filter media efficiency is expected, when considering the slightly

**Mass Balance of ST03 with 28285g sediment influent
with losses through SigaFiltration Filter Socks factored in**

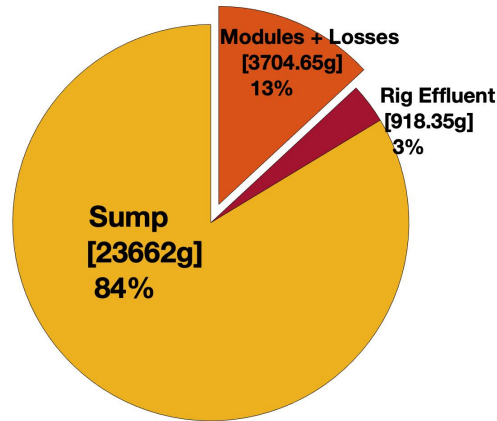


Figure 3.39: ST03 Mass Balance.

coarser grain size of the Garside Sand, and the reduced drop seen in filter media permeability when compared with ST01.

Figure 3.39 shows the mass balance of ST03, the Up-Flo[®] Filter System removal efficiency provided by this was $96.8\% \pm 0.3\%$. This value again is similar to the calculated TSS average removal of 98.7%. Settlement in the sump had been the major source of total removal, as with ST01 and ST02, however with ST03 the effect had been greater with 86.5% of total sediment captured having been caught in the Up-Flo[®] sump. This increase of settlement in the sump is anticipated, as the d_{10} of Fraction E was 107 μm which is similar to the d_{90} of silica flour, 105 μm . As particle size increases the settling velocity of the particle also increases, so, as the Fraction E is larger than the silica flour capture by the sump would be higher.

An estimate for the filter media removal efficiency was also calculated from this as 80.1% of sediment passing through the media. Which is expected, as the larger sediment size would be strained more by the pores of filter media, this was also seen in the larger drop in permeability in ST03. Additionally, the increased settling velocity would result in a

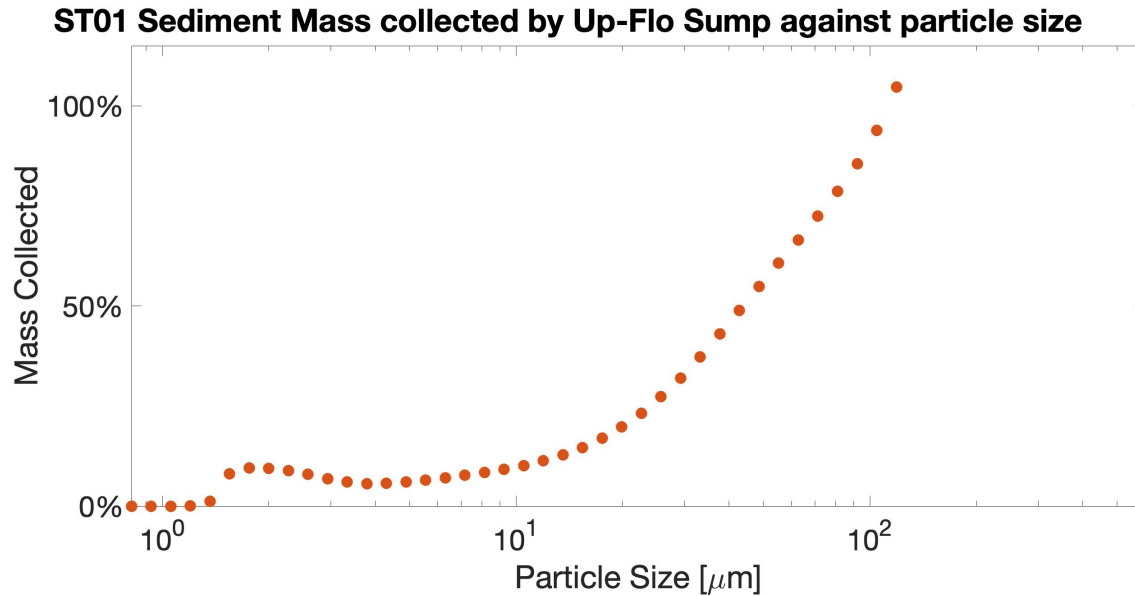


Figure 3.40: ST01 Sediment Mass collected by the Up-Flo® sump.

reduced velocity passing through the filter media, increasing residency time and more potential for particle collisions and adhesion.

As shown in Figures 3.37 to 3.39 the sump was responsible for the majority of the removal in the Up-Flo® Filter System. Using mass balance data and PSA analysis on the samples taken from the mass balance in ST01, ST02 and ST03, an analysis of the sizes caught by the sump is presented in Figures 3.40 to 3.42. Equation 3.16 provides the equation used to create the plots, the MB_{Sump} and MB_{Inf} is the mass of the sediment caught in the sump and the mass introduced to the system, respectively. $Sump_{PSA}$ and $Influent_{PSA}$ are the measured particle sizes of the sump and the silica flour introduced to the system.

$$Sump_{PSD_{caught}} = \frac{MB_{Sump} \times Sump_{PSA}}{MB_{Inf} \times Influent_{PSA}} \quad (3.16)$$

As Figure 3.40 shows the sump was better at capturing larger sized sediment particles in ST01. Between particle sizes $1.2 \mu\text{m}$ and $3.331 \mu\text{m}$ the sump has a larger capture percentage than anticipated. However when comparing it to the removal efficiencies of the Up-Flo® Filter System in Figure 3.34, where this occurs is also where there was a slight

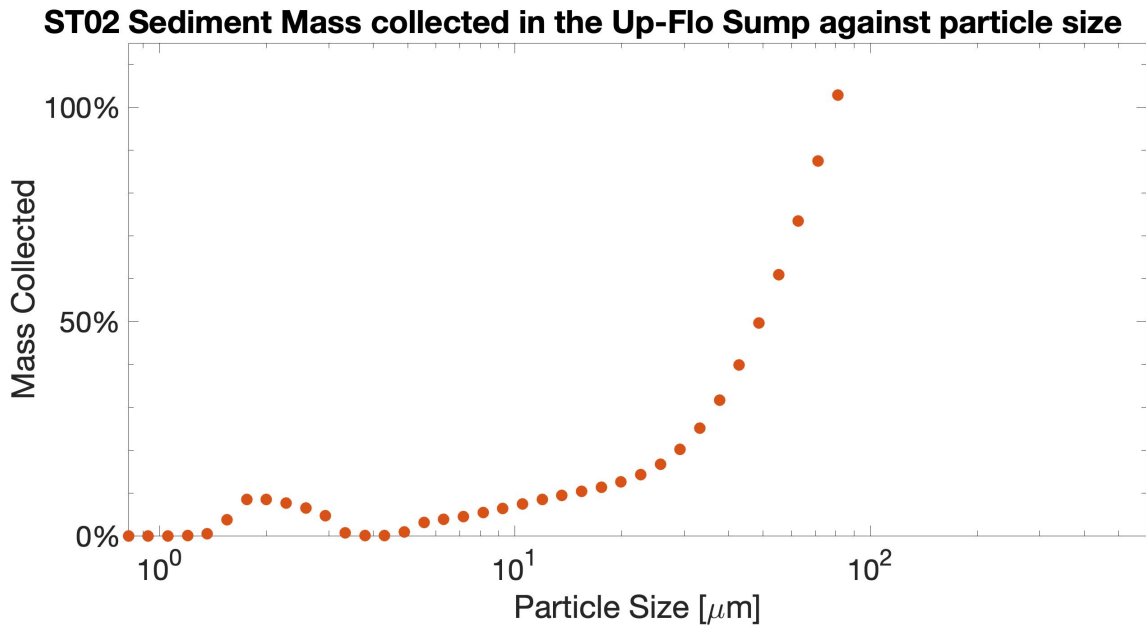


Figure 3.41: ST02 Sediment Mass collected by the Up-Flo[®] sump.

increase in total removal efficiency. This suggests that particles in fine silt to clay size range were not passing entirely through the filter media and instead settled in the Up-Flo[®] sump. Which rules out adhesion and particle straining within the filter media, leaving only flocculation or significantly small settling velocity.

The ST02 sediment mass collected in the Up-Flo[®] sump shown in Figure 3.41, shows a similar effect to ST01. The larger particle sizes was captured by the Up-Flo[®] sump with 100% of particles over 81.02 μm being collected by the sump, however between 1.363 μm and 3.331 μm the sump collected more than anticipated once again. This again matched with what was seen in the total Up-Flo[®] Filter System removal efficiency in Figures 3.35 and 3.36. This also corroborated the data seen in ST01. This further indicates the increased is resultant from either flocculation or low settling velocity, Section 3.15 discusses this in more detail.

Figure 3.42 shows the Fraction E sediment collected by the Up-Flo[®] sump. The sump collected 100% of media at 81.02 μm , however this dropped until 153.4 μm with 80.6% removal. As the particle size increased above this the sump retention of Fraction E

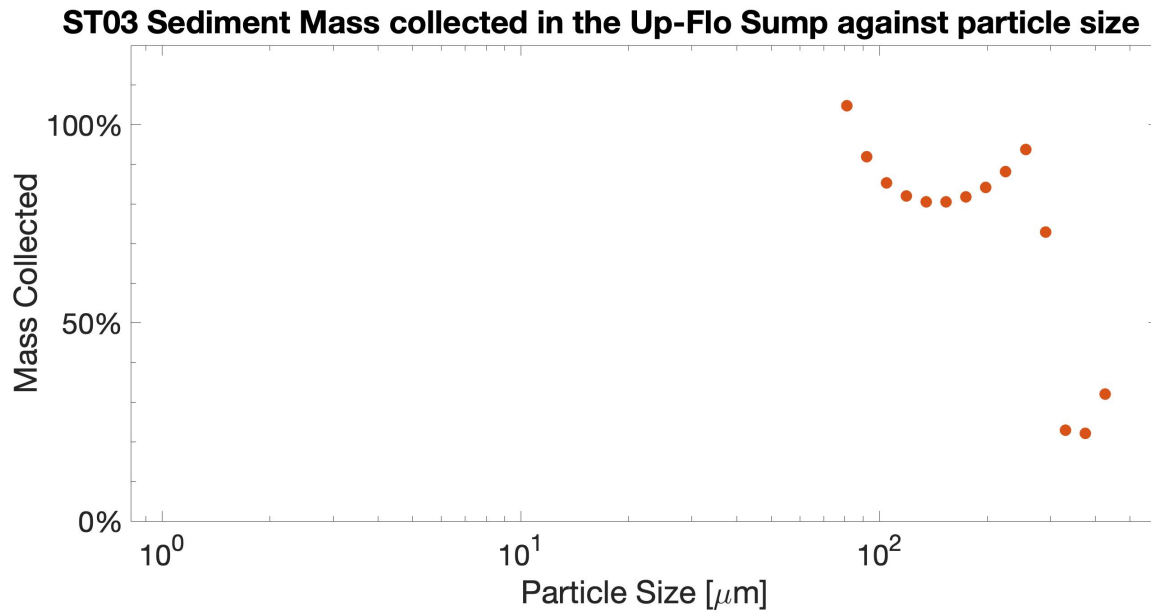


Figure 3.42: ST03 Sediment Mass collected by the Up-Flo® sump.

increased to 93.7% at 255.6 μm . Outlier results appeared at 290 μm and above, this would be resultant from the narrow size range of Fraction E, at 290 μm the volume of particles at this size was just 0.45%. This data shows that Fraction E met the Up-Flo® removal target of 80% for all particle sizes in its range through settlement alone. Whilst the plot is a slightly weird shape, this is due to the very narrow size range for Fraction E. Figure 3.43 shows the PSA of Fraction E and the sump sample, the size distribution is very similar with some slight variance at the peak.

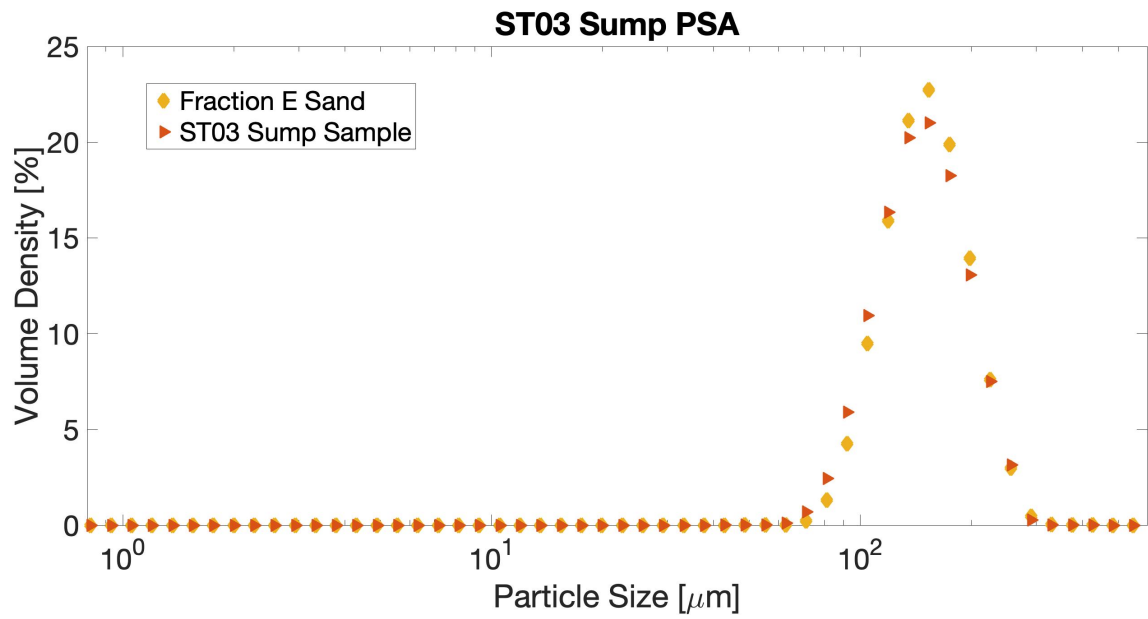


Figure 3.43: PSA using the Malvern Mastersizer 3000 of Fraction E and a sample from the Up-Flo[®] sump.

3.14 Filter Media Efficiency Results

To develop the understanding of the removal processes within the filter media from what was seen in the permeability results, particle size analysis was conducted on filter media bags from ST02 and ST03. ST01 filter media particle size analysis was not conducted, as previously sieve experiments were conducted. They found no significant increase which resulted in particle size analysis being conducted instead in ST02 and ST03.

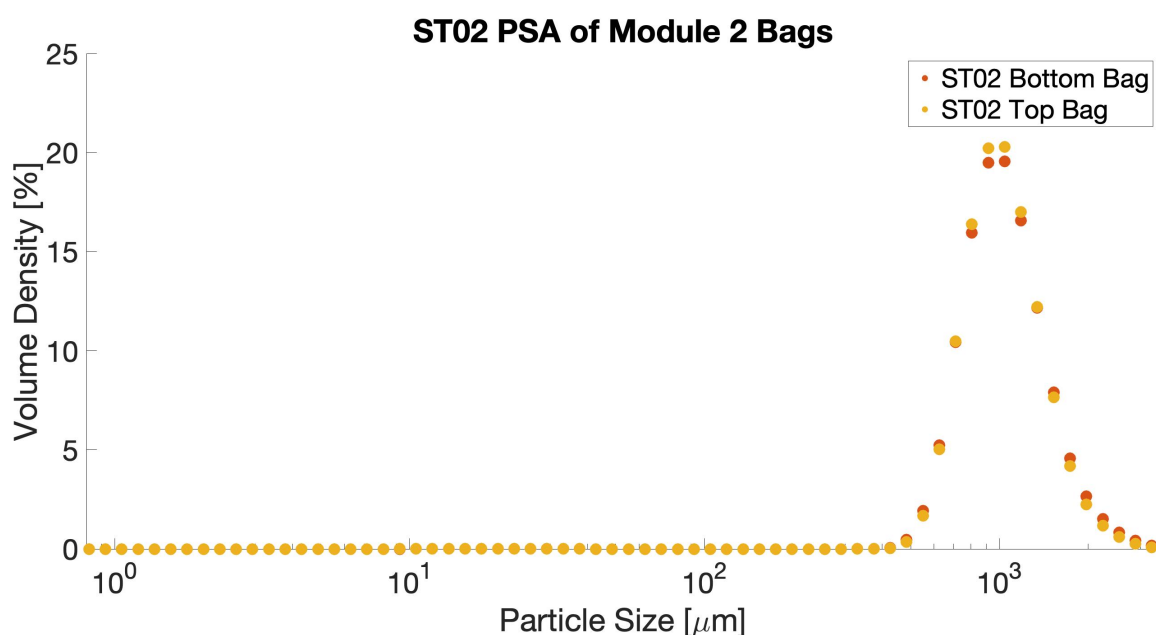


Figure 3.44: ST02 Core Sample Particle Size Analysis of Module 2 Top Bag and Bottom Bags.

Figure 3.44 shows the PSA of both the Top and Bottom Bags of the filter media from Module 2 of the Up-Flo® Filter System. In ST02, assuming sediment caught was equally distributed between modules and bags, the maximum amount caught in each filter media bag is estimated to be 435.3 g, which is an increase of 2.52% mass. Figure 3.44 shows no increase between 10⁰ to 10² μm where the particle size distribution of the silica flour is prominent. Significantly, between 10⁰ and 10¹ μm where the Up-Flo® sump was not effective in sediment removal, but Rig Effluent samples showed a minimum reduction of

48.1% between these sizes there is no increase. There are many potential reasons for this, it could be due to the low quantity of estimated sediment caught and the 5 core samples used in the PSA not being sufficient. Also of note is that the 435.3 g, was the total collected in the Whole Module and not just the filter media. During the removal of the filter bags it was clear some media was caught in the curves of the modules, in the matalla and on top of the filter bags, as demonstrated in Figure 3.45.

Also of note is that the top bag d_{10} , d_{50} and d_{90} was $711.6 \mu m \pm 2.5 \mu m$, $1015.1 \mu m \pm 7.3 \mu m$ and $1532.8 \mu m \pm 29.5 \mu m$. This represented a change of -4.9%, +1.8% and +12.7% respectively from the clean Garside Sand seen in Figure 3.11. For the bottom bag the d_{10} , d_{50} and d_{90} was $706.2 \mu m \pm 2.7 \mu m$, $1022.7 \mu m \pm 8.0 \mu m$ and $1582.0 \mu m \pm 33.2 \mu m$. This represented a change of -5.7%, +2.6% and +16.3% respectively from the Garside Sand. The broader particle size distribution seen compared to clean Garside Sand could be resultant from the silica flour bonding to the filter media. Whilst mixing and ultrasound was used to break up the particle bonds, it may not have been sufficient to break the particle bonds.

In ST03, again assuming each module caught the same amount of media equally, each filter bag would have caught a maximum of 308.7 g of Fraction E. This would be an increase of 1.8% of the filter bag weight. The PSA for ST03 Module 2 filter bags is given in Figure 3.46, this shows a peak around $10^3 \mu m$, similar to Garside Sand and ST02 filter bags. There is no peak around $10^2 \mu m$ size where Fraction E size distribution was prominent. As with ST02 the particle size distribution is broader than for clean Garside Sand, with the top bag d_{10} , d_{50} and d_{90} being $698.0 \mu m \pm 2.3 \mu m$, $1035.7 \mu m \pm 9.3 \mu m$ and $1650.7 \mu m \pm 37.3 \mu m$, respectively. This represented a change in the measured clean Garside Sand d_{10} , d_{50} and d_{90} values of -6.8%, +3.9% and +21.4%. The reduced d_{10} value could be resultant from measurement of Fraction E, but not sufficient amounts for a peak to be shown in the figure. The increased d_{90} could be resultant from particle bonding between the Fraction E and the filter media.

The bottom bag in Module 2 d_{10} , d_{50} and d_{90} was $713.3 \mu m \pm 2.0 \mu m$, $997.8 \mu m \pm 4.6 \mu m$ and $1454.8 \mu m \pm 18.7 \mu m$, respectively. This represented a change in the measured clean Garside Sand d_{10} , d_{50} and d_{90} values of -4.8%, +0.1% and +7.0%. Again, the

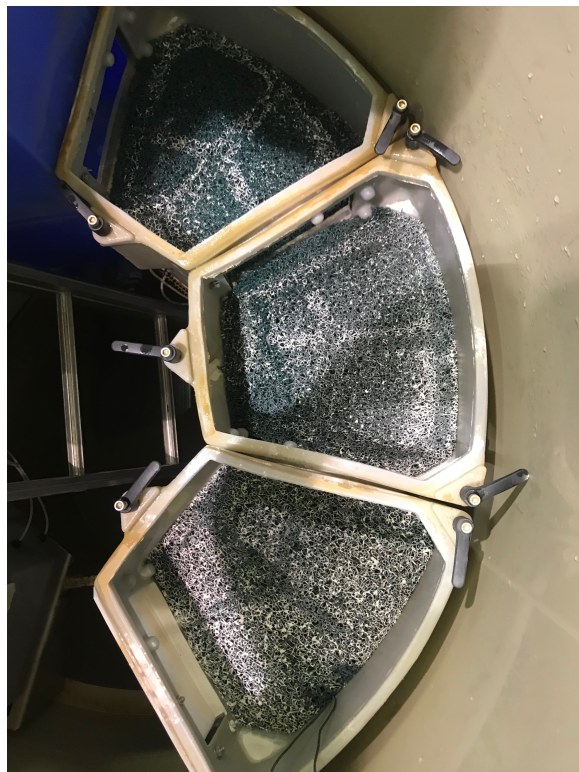


Figure 3.45: Flow distributing top matallas after ST02.

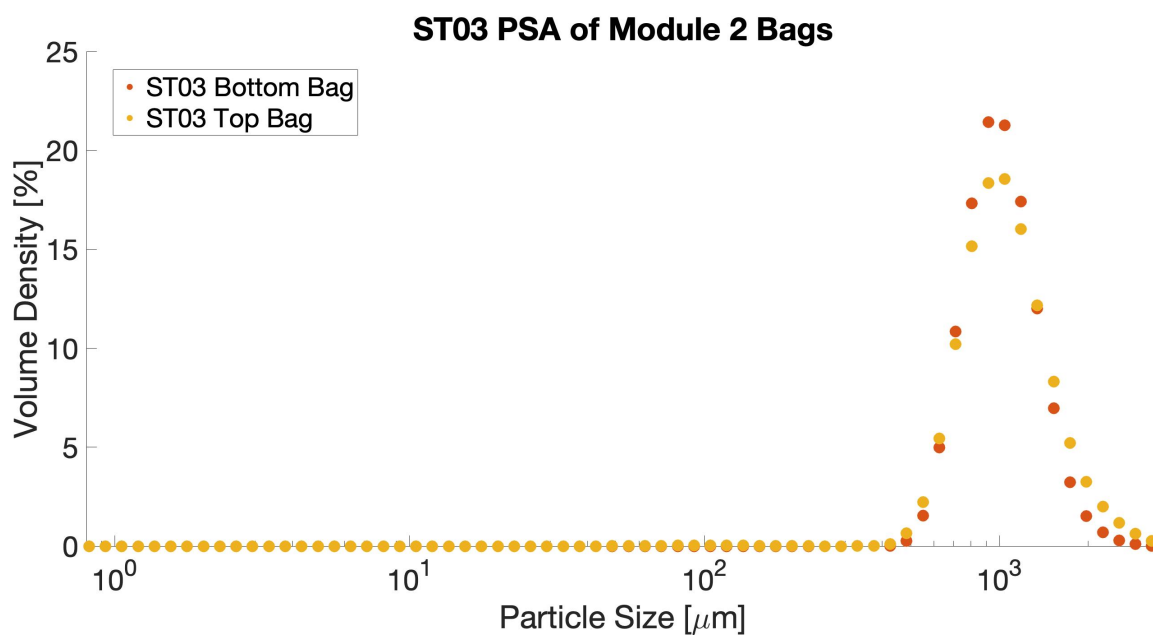


Figure 3.46: ST03 Core Sample Particle Size Analysis of Module 2 Top and Bottom Bags.

reduced d_{10} could be resultant from measurement of Fraction E, but not enough was measured for a peak to form. The increased d_{90} could also be resultant from some particle bonding, that did not break apart under the mixing and ultrasound.

The difficulty in measuring the sediment within the filter media in both ST02 and ST03, is likely to be resultant from the small amounts estimated to be captured. As discussed earlier, ST02 and ST03 had a maximum of 2.5% and 1.8% mass increase, respectively. This increase is small, and is the very maximum, but observations from filter media bag removal found sediment captured in the module curves, matalla and on top of the bags. This reduces the amount of media actually captured within the media, making it more difficult to measure sediment capture within the media.

Data from the PSA and mass balance allowed for an estimation of sediment capture within the filter media against particle sizes for ST02. This was not conducted for ST01 and ST03, due to insufficient PSA data of the effluent exiting the Up-Flo[®] rig. Equation 3.17 was used to estimate the silica flour caught within the filter media. The equation works out the total silica flour captured by the Up-Flo[®] Filter System against average particle size and the total silica flour captured by the sump against its particle size is then calculated. Once calculated these are subtracted from one another, to estimate what was caught within the filter media against particle size. This is under assumption that the only sources of capture is the sump or the filter media.

$$FM_{Mass \times PSA} = \left[1 - \frac{RE_{PSA} \times MB_{Eff2}}{Influent_{PSA} \times MB_{Inf}} \right] - \left[\frac{Sump_{PSA} \times MB_{sump}}{Influent_{PSA} \times MB_{Inf}} \right] \quad (3.17)$$

Where; RE_{PSA} is the average PSA of the Rig Effluent samples, MB_{Eff2} is the mass of the effluent captured within the Filter Socks (with losses factored in), $Influent_{PSA}$ is the PSA of silica flour, MB_{Inf} is the mass of silica flour introduced to the system, $Sump_{PSA}$ is the PSA of the sump material and MB_{sump} is the mass captured in the sump.

Section 3.13 found the filter media removal efficiency of silica flour in ST02 was 46%, however as with the system as a whole the removal efficiency was dependent on the sediment particle size.

Figure 3.47 shows that at smaller particle sizes the filter media was primarily responsible

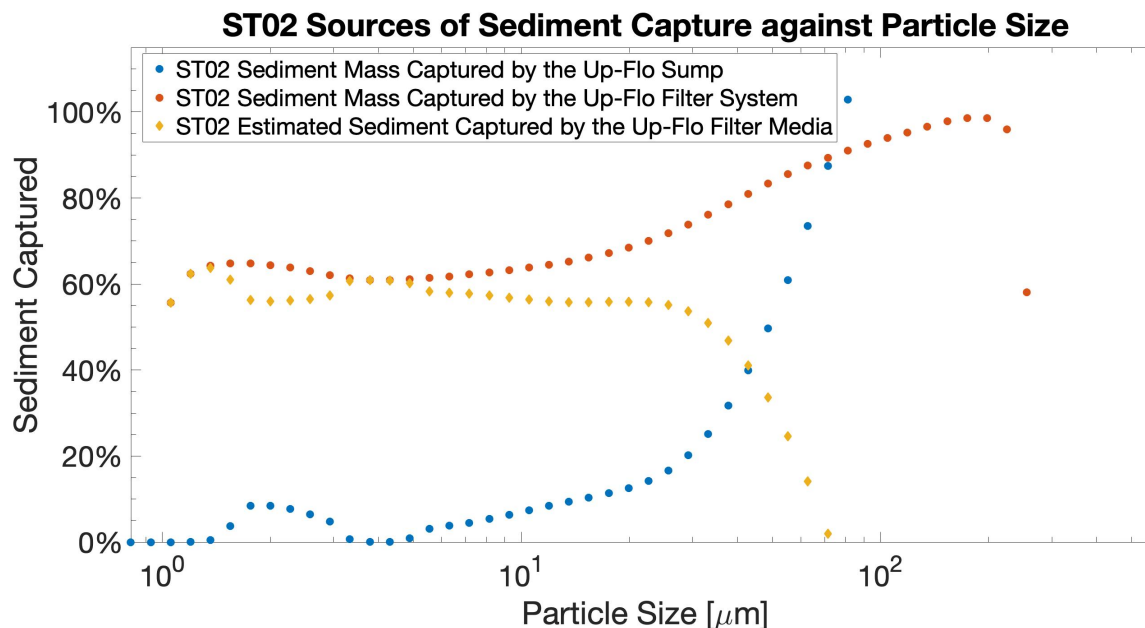


Figure 3.47: ST02 filter media capture estimate against particle size.

for the removal of sediment particles. Above particle sizes of $25.68 \mu\text{m}$ the filter media removal efficiency rapidly drops from 55.1% to 2.0% at a particle size of $71.31 \mu\text{m}$.

During this drop the sump retention of the silica flour increases significantly, resultant from the increased settling velocity in this size range.

Before $25.68 \mu\text{m}$ the removal efficiency of the silica flour was fairly stable, the maximum removal efficiency was 63.8% and the minimum was 55.1%. In the clay to fine silt size range, $1.363 \mu\text{m}$ to $3.331 \mu\text{m}$, the filter media removal efficiency dropped slightly and the sump retained more media, before increasing again and the sump retained very little until $4.885 \mu\text{m}$. This increased settlement within the sump will be resultant from either flocculation or a very low settling velocity, Section 3.15 discusses this.

One interesting aspect of the figure is that the filter media removal efficiency doesn't appear to have increased as the particle size increased, as expected. Instead the capture by the sump became the dominant effect in the Up-Flo® filtration.

Clearly, sites where the lower particle sizes are expected in a significant loading then an alternate filter media with a lower pore size would need to be considered instead. The

research data from Hydro International Ltd [9], presented in Chapter 2, shows that construction sites, urban roads and park and rides contain a large amount of particles below $30 \mu m$. The construction site would be temporary, which means if the Up-Flo[®] Filter System is used then a lower pore sized media can initially be utilised but then switched to typical media when construction has finished. Urban roads and park and rides would require a lower pore sized media permanently.

3.15 Chapter Discussion

The results presented within this chapter allows for an increased understanding of the Up-Flo® Filter System sediment removal mechanisms and the design and maintenance considerations that need to be made.

The Clean Water Experiments initially conducted on the Up-Flo® Filter System provides in-depth information on the filter media permeability. Results from Section 3.7 showed that in the absence of sediment the filter media within the Up-Flo® Filter System experiences declining permeability. Between T05 and T23 the final recorded permeability value dropped from $2.86 \times 10^{-10} \text{ m}^2 \pm 0.06 \times 10^{-10} \text{ m}^2$ to $1.79 \times 10^{-10} \text{ m}^2 \pm 0.04 \times 10^{-10} \text{ m}^2$, which was a 37.4% drop. Filter media permeability decline was additionally seen in the Clean Water Cycle of ST01, ST02 and ST03. When comparing the permeability values to typical values for intrinsic permeability presented by Bear [49] they were within the range of well sorted clean sands.

The drop in filter media permeability during clean water flow could be resultant from three possible sources; biological growth within the media, unknown sediment capture or rearrangement of filter media grains.

As the water was chlorinated, biological growth is unlikely and Figure 3.18 shows no significant drops in permeability where there was long gaps between experiments, where significant drops would be expected. As for sediment capture from unknown sources, the sediment experiments Total Suspended Solids (TSS) show that Pre-Influent samples had a maximum TSS of $11.7 \mu\text{m} \pm 0.4 \text{ mgL}^{-1}$. This TSS is very small and considering the permeability changes in ST01 and ST02, where the influent water contained over 500 mgL^{-1} of silica flour, was not much more than the clean water permeability changes it is unlikely that $11.7 \mu\text{m} \pm 0.4 \text{ mgL}^{-1}$ caused the clean water permeability drop.

As the biological growth and sediment capture is ruled out, only filter media grain rearrangement is left as the source of declining permeability. This would happen due to the difference in filter media grain sizes, Stokes Law which was outlined by Equation 2.1 in Chapter 2 shows that the settling velocity of particles in water is dependent on particle

size, with a higher settling velocity with increasing particle size. The filter media used in the Clean Water Experiment had a range of different sizes, resulting in different settling velocities. As water flows through the media, the particles will start stratify with larger sized particles at the bottom and smaller sized particles at the top. This rearrangement would result in the decreased permeability seen, as the top of the filter media would have reduced porosity.

This filter media grain rearrangement would have two characteristics; (i) the permeability would decline during each experiment as the filter media slowly stratifies and (ii) the decline in permeability would slow and eventually stop, as more experiments were conducted due to finite rearrangement possibilities. Figure 3.15 shows that during T11 the filter media permeability declines during a Clean Water Experiment, Figure 3.24 plots the exponential constant that represents the decline for the exponential best fit against test number. This figure finds that in each Clean Water Experiment the best fit of the permeability showed a decline, fulfilling the characteristic (i). This was also seen in the sediment experiment results where the permeability declined during the Clean Water Cycle experiments.

Figure 3.24 also shows that the exponent decreased in value with increasing number of experiments, which indicates the (ii) characteristic was also met. This was also seen in the drops in final permeability values between the Clean Water Experiments, Figure 3.21 shows that the final permeability percentage change approached 0.0% the more experiments were conducted. This again, indicates again that (ii) characteristic has been met. Both figures suggest that by T15 the filter media had reached, or was close to reaching, peak stratification as the changes in permeability between experiments was close to 0.0% and the exponential constant was close to zero. This indicates it takes a minimum of 27 hours of flow being passed through the media to reach peak stratification. Rearranging the Darcy equation and the T14 pressure data, where the overflow operated, provides Figure 3.48. This shows that at this peak stratification, the maximum treatable flow rate would be 2.9 Ls^{-1} , down from 4.4 Ls^{-1} for T05. If the new filter media, Garside Sand, experiences a similar long term decline the maximum treatable flow rate will reduce from 10.4 Ls^{-1} to 6.5 Ls^{-1} .

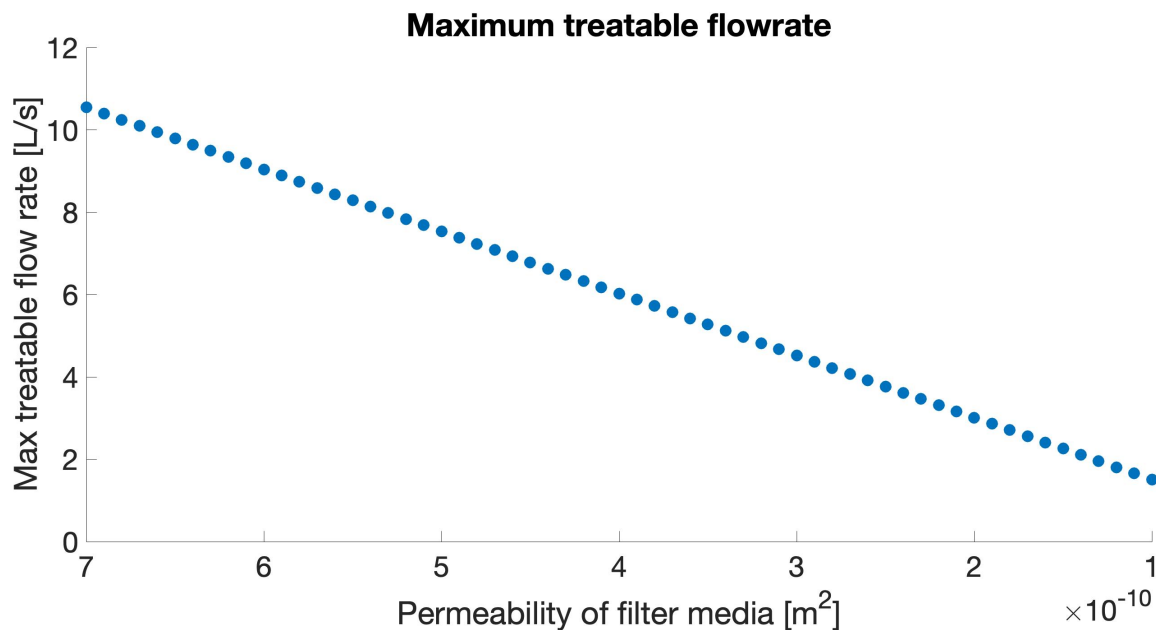


Figure 3.48: Max treatment capacity against permeability. Using T14 pressure data where overflow was used.

This falling filter media permeability has repercussions for both the maintenance and installation of the Up-Flo® Filter System. The reduced permeability lowers the maximum treatable flow rate of the Up-Flo® Filter System which would need to be taken into account in its installation, with possible alternate filter medias used. Further research is required, to investigate whether disturbing the media significantly, through mixing, would result in the original permeability being restored. If it can be, it can be integrated into the maintenance procedure to ensure the targeted max treated flow rate is retained, if it can't then the filter media would need replacement during maintenance even if no sediment was caught.

If filter media replacement is the only option to restore the permeability, this leads to environmental and resource waste. Alternate filter medias should be investigated, a more mono-sized granular media would significantly reduce the problem. However, this would likely increase the cost of the filter media significantly making it uneconomical. A slightly larger filter media may be beneficial, as the slightly coarser Garside Sand replacement in ST02 and ST03 showed a lower decrease in permeability during clean water flow.

However, this might increase the sediment loss through the filter media. Once further research has been conducted, an assessment can be made on the most economical and sustainable route to maintain filter media permeability and treatment capacity.

Results from the Clean Water Experiments also found that the Bottom Bag dominated the permeability of the Whole Module and always had a lower permeability, average 56.9% lower than Top Bag. This was also seen in ST01 and with the new filter media in ST02 and ST03. The lower permeability seen in the Bottom Bag, is to be anticipated as the Top Bag is on top of it resulting in it being more constrained. As the Bottom Bag permeability impacts the Whole Module permeability the most, changes in the Bottom Bag permeability tend to impact the Whole Module more.

Figure 3.26 in Section 3.9 shows the permeability results from Modules 1, 2 and 4 during the clean water experiment T29, it shows that the permeability in each module was different. However, this is deemed unlikely due to the filter bags containing the same media weighed to the same level. Figure 3.27 shows the head change in each module, it shows that the head on top of the filter media in Module 4 was larger than Module 2 which was larger than Module 1. This shows the further away from the exit module the larger the head of water above the filter media, this explains the different permeabilities calculated. The larger head further away from the exit module, will drive the water across the top of the filter medias in different modules towards the exit module.

The different water levels within the modules will result in different flow rates through individual modules, due to the different downward forces in each module. The larger head would result in a reduced flow rate, this explains why in internal experiments Hydro International Ltd found increasing the number of filter modules reduced the total max flow rate per module. This would be resultant from the longer module chain requiring a higher head to drive the water across the modules, reducing the flow rate in each module further away from the exit module. Up-Flo[®] Filter System maintenance will need to be adapted to take this into account, as the different flow rates would subject different modules to different levels of sediment loading causing different levels of failure.

The sediment experiments in ST01, ST02 and ST03 allowed for in-depth knowledge to be

developed regarding the Up-Flo® Filter System removal processes and how sediment impacts its filter media. Results from the TSS and mass balance show that the Up-Flo® Filter System was capable of removing between 75.5% and 98.7% of the sediment dosed into the system. However, the removal efficiency is dependent on the sediment particle size, the filter media grain size and it takes time to reach an equilibrium.

Figures 3.34 to 3.36 showed that the larger the sediment particle size the better removal by the Up-Flo® Filter System. This was also shown by the increased removal in ST03 of between 96.8% to 98.7% for Fraction E sediment, this was a large increase from the removal of the smaller sized silica flour used in ST01 and ST02.

The change of filter media used in the Up-Flo® Filter System between ST01 and ST02 showed that the larger grain size had a slight impact on the total removal of silica flour, with a drop of approximately 3.0% of removal efficiency in ST02. When compared to the increased initial permeability seen in ST02 and ST03 for the Garside Sand filter media, this is expected as the increased permeability would result in a larger pore size, resulting in less particles being retained by the filter media. This was further seen by the increase in the minimum particle size value to achieve the 80% or greater removal in ST02, and the filter media removal efficiency dropping from 60.2% to 46.0% for ST01 and ST02, respectively.

The mass balance showed that the sump of the Up-Flo® Filter System was responsible for the majority of the sediment removal in ST01, ST02 and ST03. Using the PSA data on the drain-downed sump sediment, the capture of sediment was dependent on the particle size of the sediment. An increased sediment particle size resulted in increased capture by the sump.

This increased settlement with larger particles is expected when considering Stokes Law, Equation 2.1 in Chapter 2, as the larger size results in a higher settling velocity. As the flow rate was 2 L s^{-1} , the upward fluid velocity through the filter media was 3.3 mm s^{-1} , Stokes Law can be rearranged to provide the minimum particle size for settlement. Using the information in Section 3.1, the minimum particle size where the settling velocity is equal to the upward velocity is estimated to be greater than $60.6 \text{ }\mu\text{m}$. Figures 3.40 and

3.41 show that the sump captured 66.5% and 73.5% of silica flour in ST01 and ST02 around this size, above this size settlement increases sharply.

As noted earlier, each module has a different water head in it so the effluent water could be driven across the top of the filter medias to the exit module. This results in different minimum particle sizes, dependent on where the sediment particles location within the Up-Flo[®] Filter System. Modules 4, 2 and 1 in ST02 had the estimated flow rates per module 0.31 Ls^{-1} , 0.34 Ls^{-1} and 0.38 Ls^{-1} , respectively. This results in the minimum particle size, where the sediment would begin to settle, being $58.0 \mu\text{m}$, $60.7 \mu\text{m}$ and $64.2 \mu\text{m}$ for Modules 4, 2 and 1 respectively.

A surprising aspect from ST01 and ST02 PSA results was a slight increase in silica flour removal by the Up-Flo[®] Filter System for particle sizes between $1.2 \mu\text{m}$ and $3.331 \mu\text{m}$, which represent fine silts and clays and typically contain significant pollution, shown in Figures 3.34 to 3.36. This increased removal was found not to be resultant from increased adhesion or straining within the filter media, but from increased settlement within the sump as seen in Figures 3.40 and 3.41.

The increased settlement will be resultant from either flocculation, where particles bond together to form larger particles which then have an increased settling velocity.

Alternatively the settling velocity could be so large that particles in this range do not have time to fully pass below the filter modules to be taken through the filter media.

If it was resultant from the low settling velocity, the effect would be larger than the 8.4% extra settlement within the sump, this leaves flocculation as the reason for the increased settlement. With flocculation, the effect would result in smaller settlement as it takes time and a number of successful collisions for the flocs to form. As these fine silts and clay sized particles typically contain a lot of pollutants, more removal will protect the environment more. As the surface charge which prevents the flocculation of particles is thermodynamically unstable[37], a number of techniques can be used to boost the formation of flocs. Temperature and PH are both important for succesful flocculation, however in installations of the Up-Flo[®] Filter System it will be difficult to optimise these. Additionally increased time or particle concentration would result in more collisions and

increasing the chance of floc formation.

Using the mass balance, TSS, PSA data and the permeability results, an in depth understanding of the filter media and its effects on the Up-Flo® Filter System could be explored. The mass balance shows that the filter media was capable of removing 60.2%, 46.0% and 80.1% of sediment that passed through it, for ST01, ST02 and ST03. This shows that the change in filter media resulted in a 14.2% drop in filter media silica flour retention, this drop is likely resultant from the larger Garside Sand and the fact the media had not reached peak stratification. The larger sized Fraction E sediment in ST03 resulted in a significantly higher removal efficiency, this will be resultant from either increased straining or the settling velocity being higher resulting in more residency time allowing more successful filter media adhesion.

There is also the possibility that the additional removal in ST03 could be resultant from the removal by the filter media bag itself, however this is seen as unlikely. This is due to the little changes in permeability observed and settlement in the sump being the primary removal technique. Only sediment particles with sizes close to and above the d_{90} could be caught by the bag, but these will also have the highest settling velocities. This results in the higher likelihood of being captured in the sump.

By using Equation 2.4, in Chapter 2, the filtration coefficient can be estimated for the filter media as $3.0 m^{-1}$, $2.3 m^{-1}$ and $4.0 m^{-1}$ for ST01, ST02 and ST03. This shows that the lower sized filter media, Fraction B, had a higher filtration coefficient. The larger sized sediment, Fraction E, also meant the filter media had a higher filtration coefficient.

As outlined in Chapter 2, filter media capture utilises two types of processes. Either; straining, where the sediment particles are larger than the filter media pore size which results in capture, or adhesion, where sediment particles passing through the filter media attach to the grains under similar methods to flocculation.

The PSA of the drain-downed ST02 sump sediment, the silica flour influent and the average ST02 Rig Effluent provided an estimation of the filter media removal efficiency against particle size, shown in Figure 3.47. This showed that the removal efficiency of the filter media was fairly stable, 55.1% to 63.8%, for smaller sized silica flour particles in

ST02, until settling in the sump became a greater effect in particles with sizes greater than $25.68 \mu\text{m}$. Larger sized particles did not result in increased capture within the filter media, this suggests the sediment removal process within the filter media was sediment particle adhesion, not straining. As if straining was responsible, then larger particles would have increased removal. Additionally the permeability results from ST02, shown in Figure 3.28, showed only an additional 0.7% average drop per day in final permeability over the sediment days compared to the Clean Water Cycle experiments. If straining was the main mechanism of removal, the permeability would expect to have a higher drop as straining would block flow path ways.

Permeability results from ST01, ST02 and ST03 show that the capture of the sediment can be detected by measuring the changes in the permeability. The average per day percentage drop in Whole Module 4 filter media permeability for Clean Water Cycle was 2.0%, 1.2% and 1.2% in ST01, ST02 and ST03. During sediment dosing experiments this increased to 2.5%, 1.9% and 2.8%, whilst small, the rise in the decrease of permeability was detectable from the background drop. ST01 had only 107 mins of sediment flow compared to 420 mins in ST02 and ST03, this means the change in sediment experiment permeability was more difficult to compare. If the average percentage drops per minute is studied, the effect of sediment capture in ST01 can be more easily compared.

The average percentage drop per minute in the Clean Water Cycle experiments was $9.3 \times 10^{-3}\%$, $5.5 \times 10^{-3}\%$ and $5.6 \times 10^{-3}\%$. In the sediment dosed experiments the average percentage drop per minute was $16.7 \times 10^{-3}\%$, $8.6 \times 10^{-3}\%$ and $12.4 \times 10^{-3}\%$. This shows that the drop per minute was much larger in ST01 than in ST02 and ST03, also by looking at the difference between the Clean Water Cycle experiment drop and the sediment experiment drop, it is clear the ST01 drop caused by sediment was larger than ST02. This is due to the ST01 having a well conditioned media where peak stratification was reached, resulting in the difference being more measurable. Otherwise it could be resultant from the increased sediment capture rate in the ST01 filter media.

The maintenance of the Up-Flo[®] Filter System is described in-depth in Chapter 5, a key part of the maintenance is that the filter bag is replaced when the wet weight is 9 kg heavier than the wet weight of the clean filter bag. This increase in weight is substantial,

using the ST02 results this suggests that to achieve this extra weight a minimum total of 600 *kg* of silica flour for each filter bag to capture 9 *kg*. If the typical TSS presented by Ellis [18] is used, then the influent TSS is 190 mgL^{-1} , this means that 3,157,894.7 *x* of urban stormwater to reach this. If an average 2 Ls^{-1} flow rate is used, then the Up-Flo® Filter System would last for 438 hours and 36 minutes of stormwater flow before the filter bags reached the replacement mass.

However, as the number of particles caught within the media increases, the removal efficiency of the filter media would also increase. This would result in a lower amount of sediment needed and shorter replacement interval. Additionally, as mentioned earlier the permeability has a natural decline due to stratification within the filter media. This will impact the filter media efficiency as well, to acquire a more accurate lifespan of the filter media long term experiments are required after the media has reached peak stratification. If the method presented in this chapter is used, and the removal rate of the Garside Sand stayed similar, then over 125 sediment dosed experiments would be required.

A more important consideration to be made is that the max treatable flow rate would decrease as sediment was caught, and due to the stratification. Using the extra drop in permeability per kilogram of sediment captured, the expected permeability drop with 9 *kg* of sediment caught would be a drop of 28.8%. This drop would be significant and would cause a significant drop in maximum treatable flow rate through the device. If the Garside Sand experiences a 37.4% drop in permeability, till it reaches peak stratification as Fraction B did, and then experiences an additional 28.8% decline due to 9 *kg* of sediment, the max flow rate through the Up-Flo® Filter System would reduce from 10.4 Ls^{-1} to 3.5 Ls^{-1} . This reduction would lead to more bypass events resulting in untreated stormwater contaminating the environment.

From these results a number of considerations need to be made during the installation and the maintenance plan of the Up-Flo® Filter System. Firstly the expected sediment size and flow characteristics of the site would need to be taken into account. In sites where larger sized sediment is expected, particularly where sizes are above 55.24 μm , the Up-Flo® Filter System would be suitable as it is with the Garside Sand filter media. Whilst sites with these higher size range are not typical, some residential sites in the

outlined Hydro International Ltd report in Chapter 2 have size ranges where less than 50% of particles are smaller than $50\mu m$.

If a site does have this size range, it raises questions on the role of the filter media, as the sump is responsible for the majority of sediment removal. It appears from the results at this size range (greater than $55\mu m$) the filter media slows down the flow enough to aid in the settlement of the sediment in the sump. Which could be achieved through the use of an artificial flow control device, such as a large redesigned flow restrictor commonly found in showers and taps, allowing the Up-Flo[®] Filter System to be more sustainable and to reduce the maintenance costs associated.

If the Garside Sand was used for this purpose, the maintenance routines would need to be adapted, the filter media would not need to be replaced as often but would require possible disturbance to maintain the max flow rate of the Up-Flo[®] Filter System. As the permeability of the Clean Water Experiments, ST01, ST02 and ST03 showed repeated flow through the filter media reduces the medias permeability, reducing the max flow rate which raises the risk of sediment bypassing the Up-Flo[®] Filter System through its overflow chamber. Whilst valve training exercises subjected the filter media to larger flows, this flow rate appears to not have impacted the media with only a max of $8 Ls^{-1}$ being passed through the media. A experiment will be required in future to measure the permeability after removing the filter bags and subjecting them to varying levels of disturbance (such as shaking) and mixing to see whether the filter medias permeability can be restored to previous levels recorded.

However, sites where a smaller particle range is expected, where the sump retains very little, the filter media becomes more important. Currently the Garside filter media captures between 55.1% to 63.8% of the sediment particles less than $25.68\mu m$ in size which passes through the filter media. These removal efficiencies for this size range are below the targeted 80% of the Up-Flo[®] Filter System, to improve this an alternate filter media with a smaller particle size would need to be considered. However, this results in numerous issues in the operation of the Up-Flo[®] Filter System. Due to the smaller pore size needed the permeability would reduce further, resulting in a lower treatment capacity for the Up-Flo[®] Filter System. In sites with less intense storm events this could be the

ideal solution, however sites with more intense storm events the storm effluent would pass through the overflow chamber resulting in contamination of the environment.

Additionally, to ensure the best removal from the installation the filter media would need significant conditioning to boost removal rates, by ensuring maximum stratification. As adhesion is the filtration method in the filter media, choosing medias that are more likely to form the particle bonds would aid in boosting the removal rate further.

The maintenance of the Up-Flo® Filter Systems filter media would need to be adapted for sites with a lower particle size. As the filter media captures more the sump would not need to be emptied as often but the media would need more frequent replacement, especially coupled with the effect of reducing permeability through repeated flows.

However to improve the sustainability of the Up-Flo® Filter System, not all filter media in each module would need to be replaced. The ST02 Clean Water Cycle result show each module had different head to drive water to the exit chamber, this results in different flow rates and possible different capture efficiencies. By studying this further, the maintenance could be optimised by concentrating on the more likely modules to acquire sediment.

3.16 Chapter Summary

This chapter has presented the work conducted to; improve the Up-Flo[®] Filter Systems performance, how to optimise the maintenance protocols, increasing physical knowledge of granular media and stormwater treatment techniques. Which were part of the academic and industrial aims of this project.

Section 3.4 outlined the experimental methodology, first with clean water experiments and then followed by sediment experiments, as set out in the strategy in Section 3.3. This allowed for information on how the filter medias properties change with clean water flow to be developed. Then the sediment experiments developed knowledge regarding the Up-Flo[®] Filter Systems removal processes and the impact of sediment on the filter media.

The Clean Water Experiments, Section 3.7, showed that the permeability of the filter media was within the expected range for a well sorted sand. However the permeability was shown to decline, dropping 37.4% over 23 experiments, even in the absence of sediment. This is due to rearrangement within the filter media, causing stratification, as the change declines as more experiments were conducted. This has implications on the maximum treatable flow rate, as this decreases as the permeability decreases. The flow rate is estimated to have dropped from 4.4 L s^{-1} to 2.9 L s^{-1} over the Clean Water Experiments.

Sediment experiments, results in Sections 3.8 - 3.14, conducted on the Up-Flo[®] Filter System showed that the systems removal efficiency ranged from 75.5% to 98.7%. However, this was dependent on sediment particle size as an increased particle size lead to greater removal of sediment, as the larger sized Fraction E sediment ($d_{50} = 150.0 \mu\text{m}$) resulted in close to 98.7% removal but silica flour ($d_{50} = 38.8 \mu\text{m}$) had between 75.5% to 78.3% removal.

Additionally, changing the filter media from Fraction B ($d_{50} = 961.0 \mu\text{m}$) to Garside Sand ($d_{50} = 997.0 \mu\text{m}$) resulted in an increased permeability and a reduced sediment removal through filter media, dropping from 60.2% to 46.0% removal.

The size of the sediment influenced its treatment mechanism. The larger sized particles in the silica flour sediment showed increased removal, this was shown to be resultant from settlement with the Up-Flo® sump. Lower sized particles, typically below 25.68 μm , treatment was due to adhesion in the filter media. The removal efficiency of the filter media ranged between 55.1% and 63.8% for silica flour particles below 25.68 μm .

In the fine silt and clay size particle range, the Up-Flo® Filter System showed a slight increase in removal efficiency. These particles were detected in the Particle Size Analysis of the silica flour collected in the sump. This is likely due to flocculation resulting in increased settlement, due to the low amount collected in this size range.

The permeability results throughout all sediment experiments, showed an increased permeability drop to that observed in the Clean Water Cycle experiments. With an additional 0.5%, 0.7% and 1.6% permeability drop per day when sediment was introduced to the system. This suggests that by measuring permeability changes the sediment capture could be detected.

Finally, Section 3.15 took the results from the experiments outlined in this chapter and presented a discussion on them. This included the impacts on the installation, maintenance and product design of the Up-Flo® Filter System. This discussion estimated that to achieve the 9 *kg* of captured silica, as set by Hydro International Ltd in maintenance procedure, then 600 *kg* of silica flour sediment must pass through the system.

Chapter 4

FILTER MEDIA MONITORING EXPERIMENTS

A number of experiments were conducted in order to assess the viability of an effective sensor system for filter media monitoring, as outlined by the projects aims and objectives in Chapter 1 Section 1.3. This chapter summarises the experimental work and outlines the effectiveness of acoustic and conductance techniques in filter media monitoring.

Section 4.1 reports the acoustic experiments. In Section 4.2 the acoustic experimental strategy is detailed. The experimental methodology is then presented in Section 4.3.

Section 4.4 details the method used to prepare the clogged media samples that are used in the method outlined in Section 4.3. In Section 4.5 the acoustic experimental data analysis techniques are presented. Section 4.6 presents the results collected by the author throughout the acoustic experiments, and analyses these results.

Section 4.7 discusses the experimental work conducted by MSc Student Feng Xu who made use of the experiments developed by this author. This work studies the impact of distance on the acoustic signal in various sized sands.

Sections 4.8 and 4.9 outline the experimental method and the data analysis techniques used for the conductance probe experimental work. Section 4.10 discusses the results collected by the author using the conductance probe.

A discussion is presented in Section 4.11 on the viability of these techniques in relation to their use in a filter media monitoring system. The future work required to develop this authors work into a fully functioning sensor system is outlined. Section 4.12 highlights key results and the main conclusions from this chapter.

4.1 Acoustic Experiment Identification Table

Table 4.1 presents the summary of the acoustics experiments conducted throughout the EngD project for the readers information. A less condensed table is shown in Table C.1 in Appendix C.

Experiments AT42 to AT53 were on various deaired media. Experiments progressed in AT54 to AT61, which consisted of further experiments without the vacuuming stage. Experiments AT62 to AT82 consisted of testing of various media samples using a smaller sample size in plastic bags. Further experiments, AT83 to AT92, were then conducted at lower frequencies using hydrophones on various bagged media samples. Experiments AT93 to AT99 consisted of in-situ experiments within the Up-Flo[®] Filter System, during experiments ST02 and ST03 described in Chapter 3. The experimental method is discussed in Sections 4.3 and 4.8.

Table 4.1: Acoustic Experiment Number Identification Table.

Experiment Number	Date	Media	Set-up	Transducer or Hydrophone
AT42 - AT53	06/03/17 - 11/05/17	Water, Saturated Fraction B Sand, 50%, 5%, 10%, 20% Clogged Media, Dirty Water	Vacuumed Experiment	Transducer
AT54 - AT61	15/05/17 - 31/05/17	Saturated Fraction B Sand, 20% Clogged Media, Dry Fraction B Sand	Non-Vacuumed Experiment	Transducer
AT62 - AT82	01/06/17 - 28/06/17	Dry Fraction B Sand, Saturated Fraction B Sand, 5%, 10%, 15%, 20% Clogged Media, Water	Bagged Experiment	Transducer

Continuation of Table 4.1				
Experiment Number	Date	Media	Set Up	Transducer or Hydrophone
AT83 - AT92	29/06/17 - 05/10/17	Water, Saturated Fraction B Sand, 20% Clogged Media	Hydrophone Experiment	Hydrophone
AT93 (T29) - AT99 (T40)	03/04/18 - 02/05/18	Up-Flo [®] Filter Media	ST02 & ST03 Clean Water and Sediment Experiments	Transducer
End of Table 4.1				

4.2 *Acoustic Experimental Strategy*

An acoustic sensor system had many potential benefits, which Chapter 2 outlines. For it to work effectively, the interaction of the acoustic signal and the Up-Flo[®] filter media needed to be studied in detail. A experimental strategy was formed to identify the key research areas that required further development to form an effective sensor system that was able to work in a large range of locations. To accomplish this, research was divided into three stages. It started with idealistic scenarios (stage 1), then in stages 2 and 3 complexity was to be added gradually to form a more real-life scenario.

Firstly, an in-depth understanding of the acoustic response of clean filter media was required using a broad range of frequencies. That would have allowed for the signal going through clean media in the Up-Flo[®] in ideal conditions to be better explained, with variations of the signal being better understood. Key aims were to understand the frequency range, type of signal to use and the transducers. In order to accomplish that, testing was necessary in clear deaired water so to exclude the influence of bubbles on the acoustic signal. These experiments would have provided the necessary data required for calculation of the sound attenuation caused by clean filter media. The next step in experimentation was to study sound propagation in fully-saturated and deaired clean filter media. This would have enabled the measurement of attenuation of the acoustic signal and its relationship to the porosity and grain size.

Secondly, an in-depth understanding of the effect of distance on the acoustic signal in clean filter media was required. This work would have informed the development of a sensor system that could be easily retrofitted to different sized Up-Flo[®] modules.

Finally, stage 3 would study sound propagation in artificially ‘clogged’ media samples, by undertaking various measurements of the attenuation of sound in media samples with varying clogging percentages. Initially the work would be carried out in deaired samples so as to limit abnormalities related to air bubbles. The effect of bubbles on the acoustic sound attenuation would then be studied to provide a better representation of more realistic samples. This would have aided the development of an effective acoustic sensor system which could cope with change.

This strategy outlined the approach and the key experimental areas that needed development to create an effective acoustic sensor system. Due to the complexity of the interaction between an acoustic signal and filter media the initial measurements were to be conducted in close to ideal conditions. This formed a basis for the future work. Then, through increasing the complexity of the problem, an in-depth understanding of the filter media and clogging effects could be developed. Resulting in a comprehensive sensor system that would have been able to discern clogging from other effects.

4.3 Acoustic Experimental Method

Three pairs of Acoustic Immersion Ultrasound Transducers, 0.5 MHz , 1 MHz and 2.25 MHz , were initially acquired from Olympus IMS. See Appendix D.1 for the key information, including frequency response, of these transducers. These three pairs of transducers covered a relatively large frequency range for experimentation. Experiments AT01 to AT41 found that acoustic attenuation for signals with frequencies above 600 kHz in saturated Fraction B media was too large. This discovery led to the adoption of the 0.5 MHz Transducer for the rest of the the experiments.

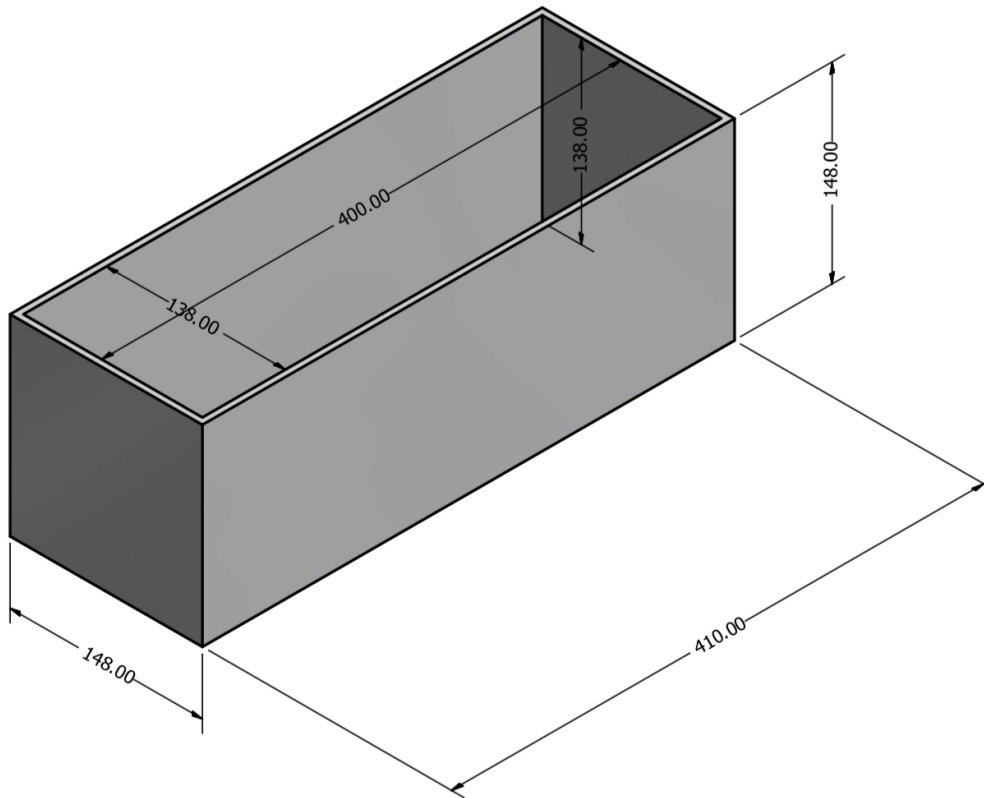


Figure 4.1: Aluminium Acoustic Test Vessel, measurements in mm .

A special testing vessel was constructed out of aluminium to contain various types of filter media and transducers (see Figures 4.1 and 4.2). Aluminium was chosen to allow

the media to be deaired by applying a vacuum. The aluminium vessel was strong and rigid enough not to flex which resulted in little or no change in the packing of the media. The high directionality of the acoustic transducers ensured that there were no reflections from the side walls of the vessel that would have impacted the acoustic results. For this purpose the width and height of the test box was over three times the diameter of the acoustic transducers, this allowed for a suitable distance from the walls.

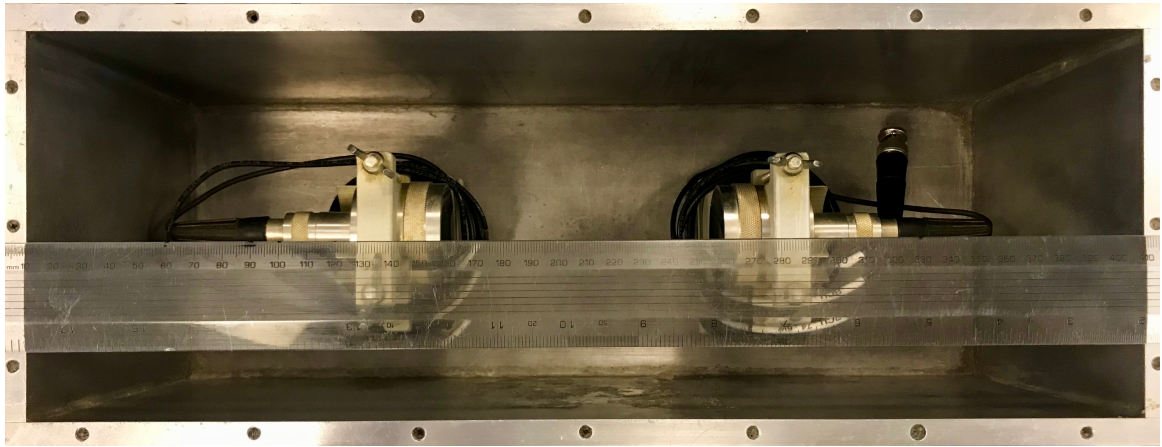


Figure 4.2: Aluminium Test Vessel.

Olympus' Equation 4.1 below provides the signal divergence for flat faced transducers, such as the ones used in this experiment. θ provides the angle of divergence, c_p provides the speed of sound in the medium, f is the frequency of the signal and x is the length of media the signal is passing through. For a 350 kHz signal, the divergence would be 7.9 mm for the experimental conditions outlined below. This ensures there would be no side wall reflections. While end wall reflections could still impact the results, only the first received pulse was analysed. This ensured no end wall effects impacted the data, the extra pulses recorded was only used to estimate the pulse velocity.

$$\text{Sin}\left(\frac{\theta}{2}\right) = 0.514c_p/fx \quad (4.1)$$

Experiments AT01 to AT41 led to the development of the transducer holders, designed for the 0.5 MHz transducers. Shown in Figures 4.3 and 4.4, they were 3D printed out of a

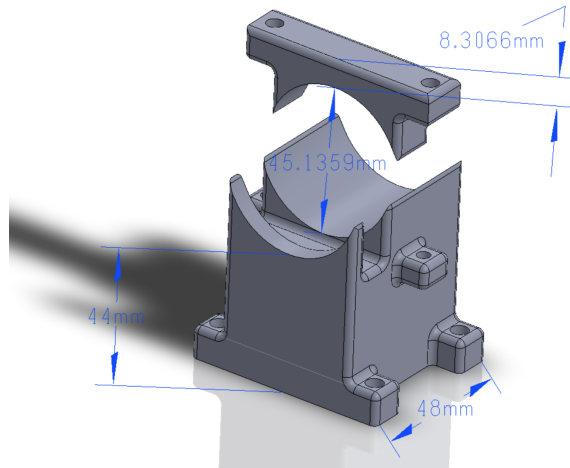


Figure 4.3: The final transducer holder made using a 3D printer.

plastic resin which prevented the signal from conducting through the aluminium testing vessel. It was also designed to enclose the transducers in place which removed directionality problems and prevented the transducers from moving, which had the additional benefit of improved repeatability. The acoustic transducers were set in the optimal orientation in the holder and tightened in place.

The box was adapted for the holders to be at a fixed distance of 120 *mm*. An additional experiment was designed and carried out by an MSc student to study the effect of distance on the acoustic attenuation. Section 4.7 details this work.

4.3.1 Deaired Saturated Media Experiments

Experiments AT42 to AT53 were carried out with deaired deionised water, deaired Fraction B sand saturated with water (Chapter 3 discusses the properties of Fraction B), media samples with various clogging (5%, 10%, 20% and 50% of pore space filled with silica flour) and dirty water containing 6453.3 mgL^{-1} of silica flour. Section 4.4 details the methodology for the preparation of clogged media samples. The set-up used throughout the experimentation is shown in Figure 4.5.



Figure 4.4: Photo of Acoustic Transducer in 3D printed holder.

During the experiments on deaired water saturated media samples (AT42 to AT52), 6.5 volumetric litres (approx 10.6 *kg*) of media was deposited in the aluminium vessel through a funnel at a height of 100 *mm*. This was then filled with deaired water until a thin layer of water sat on top of the media sample. To fully saturate the media sample the testing vessel was sealed and a vacuum applied for a minimum of 4 hours to ensure entrapped air was removed from the media sample.

After the media was fully saturated and deaired, a partition was made in the media sample, as shown in Figure 4.6, to free space for the transducer holders whilst limiting disturbance to the central part of the media sample through which the acoustic signal was broadcast. Once installed the media sample was deposited back and the partition removed. The transducers were then connected to an Tektronix AFG3021C single channel arbitrary function generator and an Tektronix TDS 2004C four channel digital oscilloscope. The function generator was connected to channel 1 (CH1) of the oscilloscope through the use of a two way adaptor and the receiving transducer was connected to channel 3 (CH3). The oscilloscope was also connected to a windows laptop running OpenChoiceDesktop by Tektronix. The settings used by the oscilloscope was uploaded from a 'set' file, shown in Appendix D.2, the key settings used were; CH1 Scale 50 V,

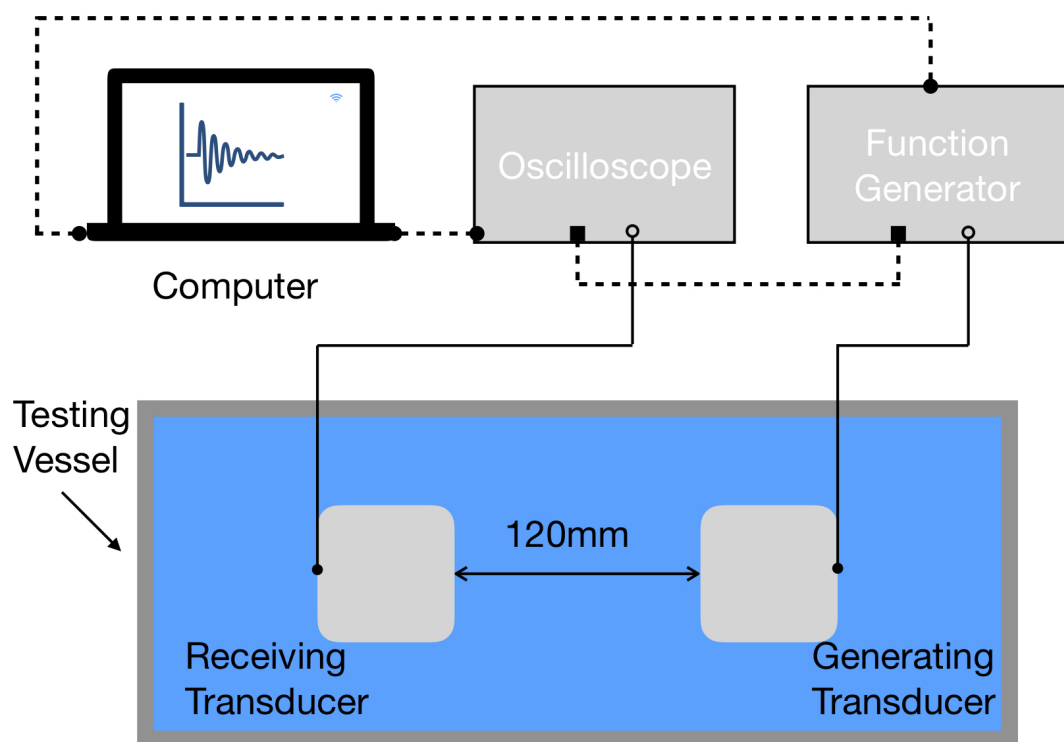


Figure 4.5: Experimental set-up used for experiments AT42 to AT53 [Not to scale].

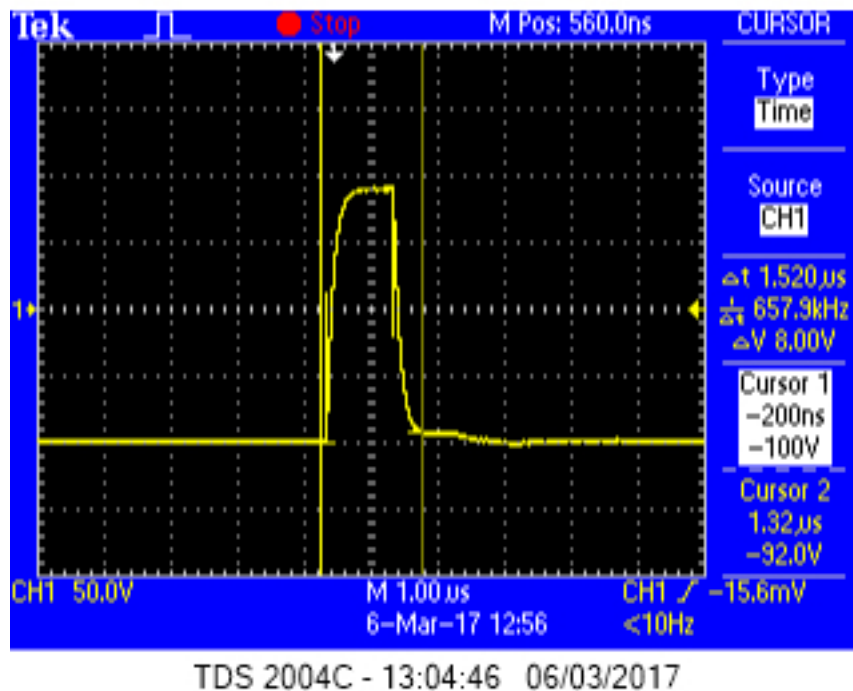
CH3 Scale 2 V, a horizontal scale 100 μs , sampling frequency 25 MHz, trigger on CH1 when slope of signal is detected and averaging 64 signals. CH1 was set to 50 V scale due to the internal resistance resulting in the 10 V peak to peak signal being read as 200 V.

The amplitude of the function generator was set to 10 V peak to peak, square wave pulse with an interval time of 1 s. The frequency was set initially to 200 kHz and the averaged signal were recorded after a minimum of 2 minutes, the oscilloscope was then stopped and OpenChoiceDesktop was used to import the data from CH1 and CH3. This was then repeated with frequencies 250 kHz to 500 kHz in steps of 50 kHz. Figure 4.7 shows an example of the sent 10 V square pulse, this had a duration of approximately 1.52 μs .

After the pulse data had been obtained, the experiment was repeated with a continuous sine wave. The generating transducer was then disconnected from CH1 and the receiver transducer was transferred to CH1. A LabVIEW programme, shown in Appendix D.3,



Figure 4.6: Partition in the media.

Figure 4.7: Image of experiment AT42 500 kHz sent pulse, with a duration of 1.52 μs .

was utilised to control the function generator to apply a continuous sine wave at various frequencies between 20 kHz and 600 kHz , in steps of 20 kHz , with an amplitude of 10 V peak to peak. The received signal was recorded as a text file, the LabVIEW software also recorded the received peak to peak voltage of the signal, which allowed for the peak to peak voltage to be plotted against frequency. At the end of the experiment, temperature was measured and recorded using a glass thermometer.

4.3.2 Non-deaired saturated media experiments

The results from Sub-section 4.3.1 led to further experiments with an adapted method. Experiments AT53 to AT61 were to study sound propagation in deaired deionised water, saturated non-deaired Fraction B media and saturated non-deaired 20% clogged media. The non-deaired saturated media testing followed the method outlined by Sub-section 4.3.1. This method was adapted so that the media sample was not deaired, which allowed for the transducers to be placed into the testing vessel before the media sample was deposited. This reduced disturbance on the media sample. The media sample was then saturated with deaired deionised water as described earlier. The testing vessel was filled until a small layer of water covered the top of the media sample. Once saturated, an experiment was carried out following the method outlined in Sub-section 4.3.1.

4.3.3 Bagged Media Experiments

Problems with low signal-to-noise ratio encountered in the experiments on non-deaired saturated media samples, required further study in greater detail on the effect of air in the media sample on the measured acoustic attenuation (experiments AT64 to AT82). In these experiments the media sample was deposited in plastic sample bags. The testing vessel was filled half way with deaired deionised water, a plastic sample bag was then placed between the transducers with the media sample within it. The pulse testing described in Sub-section 4.3.1 was then carried out using the same method at 500 kHz only. The continuous sine wave testing was not conducted on these samples. These experiments were carried out on clean dry sand, clean saturated sand at varying deairing,

various clogged mixtures (5%, 10%, 15%, 20%) with varying deairing and deionised deaired water. The plastic sample bags contained 1.5 volumetric litres of the media, approximately 2.5 *kg*, and saturated media bags contained an additional 1.5 *L* of deaired deionised water. Deaired samples used in these experiments, were deaired by placing into a chamber connected to the vacuum pump which was then deaired between 1 and 16 hours.

4.3.4 *Hydrophone Media Experiments*

Low signal-to-noise ratio problems were encountered in the experiments on the bag media. These were related to the air trapped in the media samples pores. These problems led to a switch to lower frequencies of sound and to the use of hydrophones which were able to operate at the frequency of sound well below 100 *kHz* (AT83 to AT92), where attenuation of sound is less. A new testing vessel was adopted for these experiments. It was a large plastic rectangular box filled with water. In this vessel the transducers were suspended 180 *mm* below the surface of the water using chemical clamp stands. The separation between the transducers was 210 *mm* for experiments AT83 and AT84. It was reduced to 120 *mm* for experiments AT85 to AT91. The new set-up is shown in Figure 4.8. AT83 to AT92 consisted of testing on water, filled slowly sand (sand filled using a funnel to restrict flow), clean deaired saturated sand, clean non deaired sand, 20% mix with varying degrees of deairing.

Pulse experiments, at 20 *kHz* and 50 *kHz*, were conducted using the same function generator and oscilloscope. A B&K Nexus Conditioning Amplifier Type 2693-0S4 connected to the receiving hydrophone and a B&K Nexus Power Amplifier Type 2713 was connected to the generating hydrophone. As the hydrophones were omnidirectional the hydrophones were placed close to the bagged media, and the window of the oscilloscope was tiny. Coupled with the large vessel, this allowed for only the first received pulse to be analysed. The function generator was set to 1 *V* peak to peak square burst, with a 2 second interval. This fed into oscilloscope CH1 and the power amplifier, set to a gain of 5 and 20 *dB* with a 75 *V* limit. The Power Amplifier was connected to the suspended hydrophone, which broadcast the signal. The receiving hydrophone was connected to the

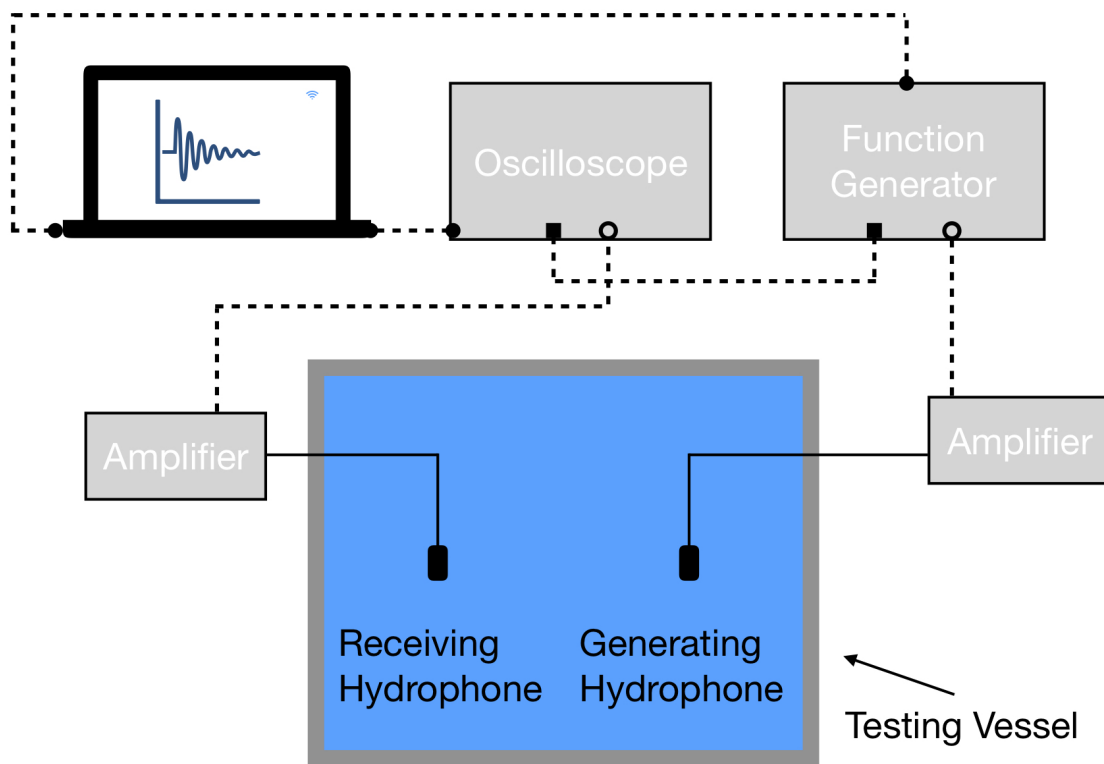


Figure 4.8: Hydrophone experimental set-up [Not to scale].

conditioning amplifier which sensitivity was set to 10 mV/unit . This hydrophone was connected to the oscilloscope channel CH3. The oscilloscope used the same trigger and average settings as described previously. However, the horizontal scale was reduced to $25 \mu\text{s}$, with a sampling rate of 100 MHz . CH1 and CH3 was set to a 5 V scale for the deaired samples. The scale on CH3 was reduced to 1 V and the gain on the conditioning amplifier was set to 100 mV/unit , so as to overcome signal-to-noise ratio problem.

In order to overcome problems with a low signal-to-noise ratio in the experiments with bagged media in various states (deaired, non-deaired and filled slowly) a sinusoidal sweep was applied. The distance between the hydrophones was reduced to 100 mm for this purpose. The sinusoidal sweep was generated in the frequency range of 1 Hz to 50 kHz . The amplitude was set to 1 V peak to peak, sweep of 4 s and a return of 1 ms . The function generator was connected to the same amplifier as previously, with the same settings. The receiving hydrophone was connected to the conditioning amplifier as previous, however it was set to 1 mV Pa^{-1} . The conditioning amplifier was then connected to a National Instrument computer which sampled the signal at a frequency of 250000 Hz .

4.3.5 Up-Flo[®] Filter System Experiments

Experiments AT93 to AT100 were carried out to study the influence of sediment in filter media on the acoustic signal at a real scale Up-Flo[®] Filter System installed in the Water Lab. The Olympus transducers in their holders were utilised in the Up-Flo[®] Filter System experiments ST02 and ST03 (which are described in Chapter 3 Section 3.4). The bottom bag of Module 3, (Figure 3.4), was adapted to house the transducers at a separation of 125 mm . The transducers were connected to a rail ensuring that they remained facing each other as in the previous experiments. The connected transducers were placed in the bottom bag, with an opening made at the top of the bottom bag. This was then filled with the filter media Garside Sand, using a funnel, described in Chapter 3. Once the transducers were surrounded by the filter media and the bag was full, the opening was closed and the top bag of module 3 was placed on top.

The transducers were connected to the function generator and oscilloscope used previously. The settings of the function generator were as described in Sub-section 4.3.1 with a frequency of sound set to 350 kHz . The oscilloscope was set to a horizontal scale of $25\ \mu\text{s}$, the maximum amplitude of CH1 was set to 50 V scale, CH2 was set to 100 mV scale and it acquired a signal when detecting the sent signal of the function generator. The received signal was averaged 64 times.

As outlined in Chapter 3 Section 3.4, ST02 and ST03 both consisted of 4 experiments with clean water flow and 2 sediment dosed experiments. In the clean water flow experiments, only during the first and last experiments measurements were taken, which the acoustic experiments followed. Acoustic measurements were taken over both sediment dosed experiments in both ST02 and ST03. The acoustic signal was recorded approximately every 15 mins throughout each experiment. The signal was recorded onto a USB for later processing.



Figure 4.9: Acoustic transducers in bottom bag of Module 3 for experiments ST02 and ST03.

4.4 Clogged Media Preparation

To prepare clogged media samples the volume of the Fraction B sand was measured, this volume was then multiplied by the porosity, 26.05% (average porosity measured internally using packing technique in testing vessel). This provided the total pore volume within the media, which was then multiplied by the targeted clogging percentage. This clogged volume was then multiplied by the particle density of silica flour, 2650 kgm^{-3} [101], to provide the total weight of the sediment needed.

Using the Fraction B sand and the weighed silica flour, the clogged media sample was combined and mixed together under a dust extraction system. Once combined the mixing vessel was sealed until the mixture was deposited within the testing vessel, using the same method as previously described.

4.5 Acoustic Data Analysis Techniques

To analyse the acoustic measurements from the outlined experiments, a number of techniques were used. To analyse the pulse data collected in experiments AT42 to AT92 a Fast Fourier Transform (FFT) was used. This related linearly to the sound pressure in the wave incident on the sensor. The code used to acquire the FFT is attached in Appendices D.4 and D.5. The code selected an appropriate time window to capture the first received pulse, then applied the FFT over this window. No filtering was necessary before the FFT was applied, as the signal was the average of 64 readings which provided a clear signal. The absolute value of the FFT was then taken, averaged (where needed), and plotted. When averaged the standard deviation of the results were estimated and plotted as the results error.

Experiments AT93 to AT99 used the code attached in Appendix D.6. This code calculated the energy of the pulse by taking the selected signal over an appropriate time window, squaring it and then integrating it. This was then plotted against the pulses experimental time.

4.6 Acoustic Results

This section presents the key acoustic results collected throughout the experimental work. Sub-sections 4.6.1 to 4.6.4 present the data in the form of a FFT. The continuous wave experimental data is not presented in this chapter as the pulse data provided more useful information. The results presented in Sub-section 4.6.5 are pulse energy against the experimental time.

4.6.1 Vacuumed Vessel Experimental Results

The FFT results for the vacuumed vessel experiments, using a 350 kHz sent pulse, of various media samples are shown in Figure 4.10. The results for deaired water were repeatable. The peak recorded energy was around 400 kHz, a higher frequency than the signal which was sent. This would be resultant from the transducers resonance frequency being 500 kHz.

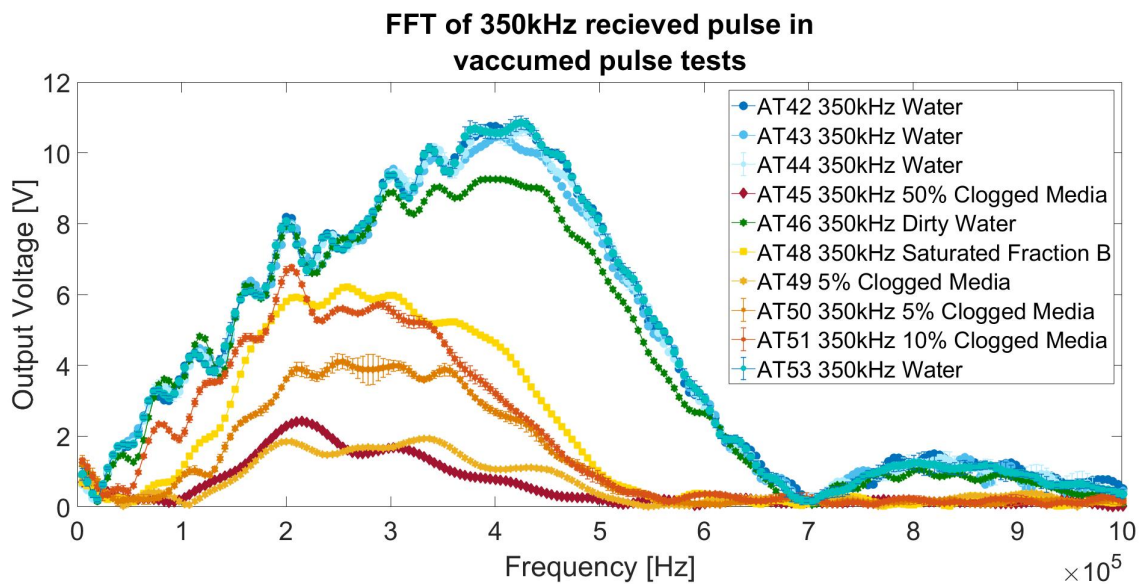


Figure 4.10: FFT results of the received 350 kHz pulse in various vacuumed media samples.

The presence of Fraction B Sand and the clogged media samples resulted in increased attenuation of the acoustic pulse. Where the frequency of the pulse was over 500 kHz , the attenuation was significant as the pulse became fully attenuated. Results of the clogged media samples experiments were variable, with the two 5% clogged samples showing a large difference. Experiment AT51, 10% clogged media sample, provided a stronger signal than experiments AT49 and AT50 5% mixes and the experiment AT45 50% mix. Experiment AT51 also showed a similar FFT result to the Saturated Fraction B below 350 kHz . Above 350 kHz the AT51 10% and AT50 5% mixes attenuated faster than the Saturated Fraction B Sand.

Experiment AT46 shows that dirty water had minimal impact on signals below 300 kHz . However, above 300 kHz the signal became more attenuated than that for the clean water experiments. Results for experiment AT52, 20% clogged media, could not be shown due to the low signal-to-noise problems.

Whilst no clear relationship can be made between clogged percentage and attenuation, the presence of silica flour is shown to further increase attenuation of the acoustic pulse than in clean Fraction B sand. The variability of the clogged media samples is believed to result from the experimental method, as the removal of media to place the transducers within the vessel disturbed the media sample.

4.6.2 Non-Vacuumed Vessel Experimental Results

The variability in the clogged media results for the vacuumed vessel experiments, and the low signal-to-noise problems, led to the adapted experimental method outlined in Sub-section 4.3.2. Figure 4.11 shows the results for non-vacuumed media samples within the test vessel. As with the vacuumed media experiments, frequencies above 500 kHz were fully attenuated when either Fraction B sand or the clogged media sample was present.

The saturated Fraction B media experiments (AT54-58) showed a repeatable result with little variance. At lower frequencies below 350 kHz the signal was not attenuated, instead

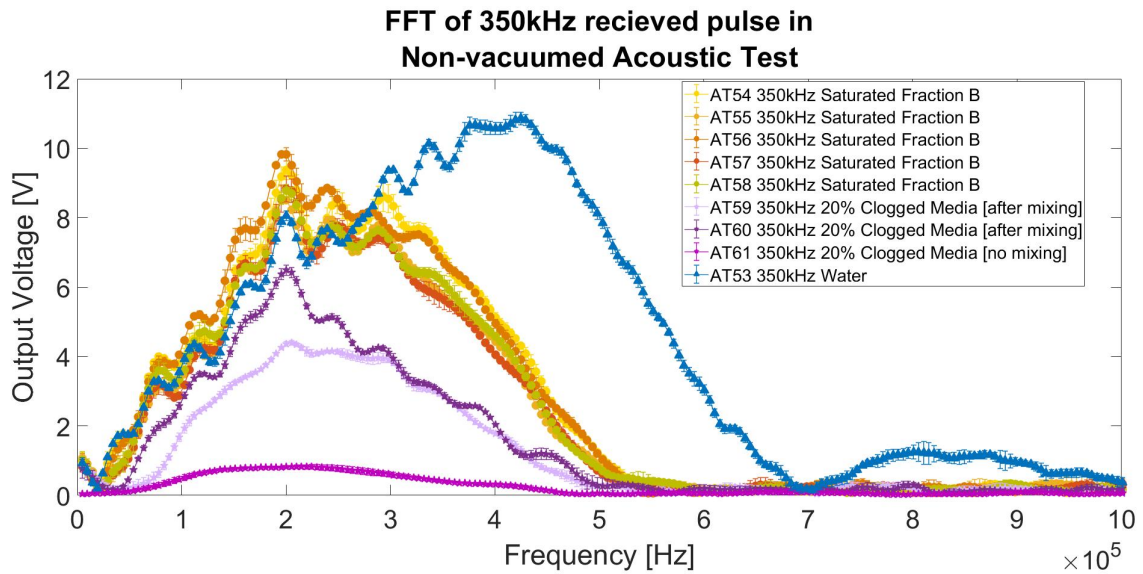


Figure 4.11: FFT results of the received 350 kHz pulse in various non-vacuumed media.

the signal amplitude was greater than the pulse in deaired water.

The removal of the vacuuming stage resulted in issues getting a reliable signal, due to the low signal-to-noise problems. In experiments AT59 and AT60 the pulse travelling through the 20% clogged media was fully attenuated, and required mixing the media in between the transducers to acquire a reading. The result from the mixing, as seen in Figure 4.11, provided a variable result. However, the presence of silica flour resulted in a more attenuated pulse. In experiment AT61 a pulse was acquired from 20% clogged media, without the mixing step. Figure 4.11 shows that this received pulse was highly attenuated compared to the mixing and the Fraction B results.

The variability in the 20% clogged media samples could result from the possible air entrapment within the samples. Mixing of the sample within the vessel would remove air entrapment within the media, allowing the signal to be measured. As with the vacuumed experimental results, the clogged media sample resulted in more acoustic attenuation than the Fraction B sand.

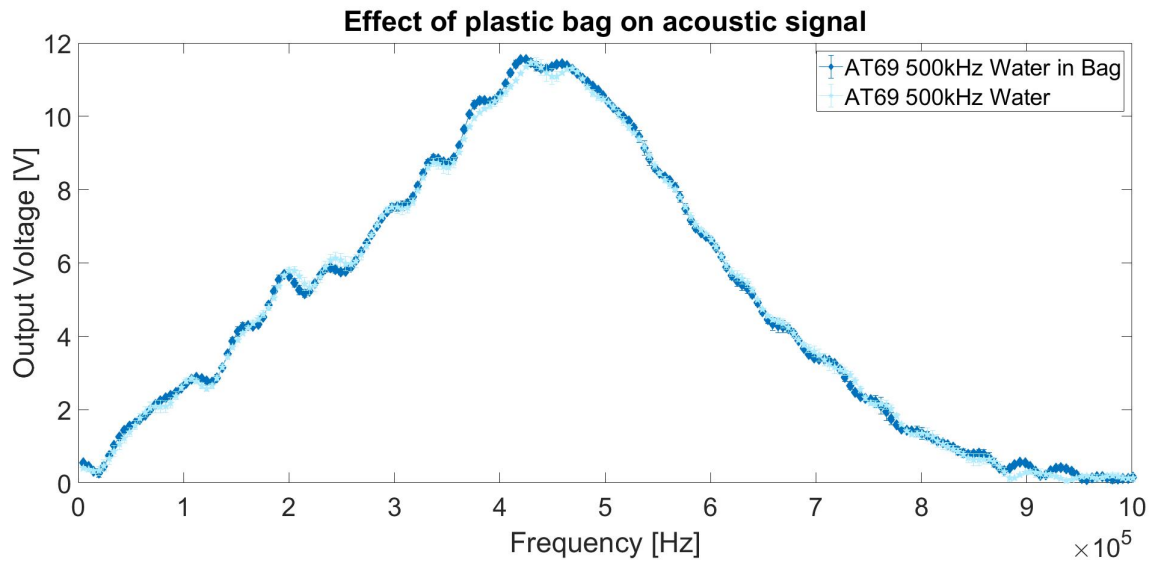


Figure 4.12: FFT analysis of 500 kHz pulse in water and water in bag.

4.6.3 Bagged Media Experimental Results

The variability in the results in the vacuumed and non-vacuumed vessel experiments, led to the adapted experimental method outlined in Sub-section 4.3.3, using a 500 kHz pulse. Experiment AT69 was conducted to ensure the plastic bag used in the bagged media sample experiments was acoustically transparent. Figure 4.12 shows that the impact of the bag was negligible.

Experiments AT62 to AT67 tested various clogged percentages of media. Experiment AT62 was an unsaturated Fraction B Sand sample, this resulted in full attenuation of the pulse. Experiments AT63 to AT67 are shown in Figure 4.13, all samples were saturated with deaired water and samples were not vacuumed. Figure 4.13 shows that frequencies above 550 kHz were fully attenuated.

Similarly to the non-vacuumed experimental results, clogged media samples provided variable results in the bagged media experiments. No clear relationship between attenuation and clogged media percentage could be determined. However there appears to be a shift, where the pulses peak amplitude was in terms of frequency. Higher clogging

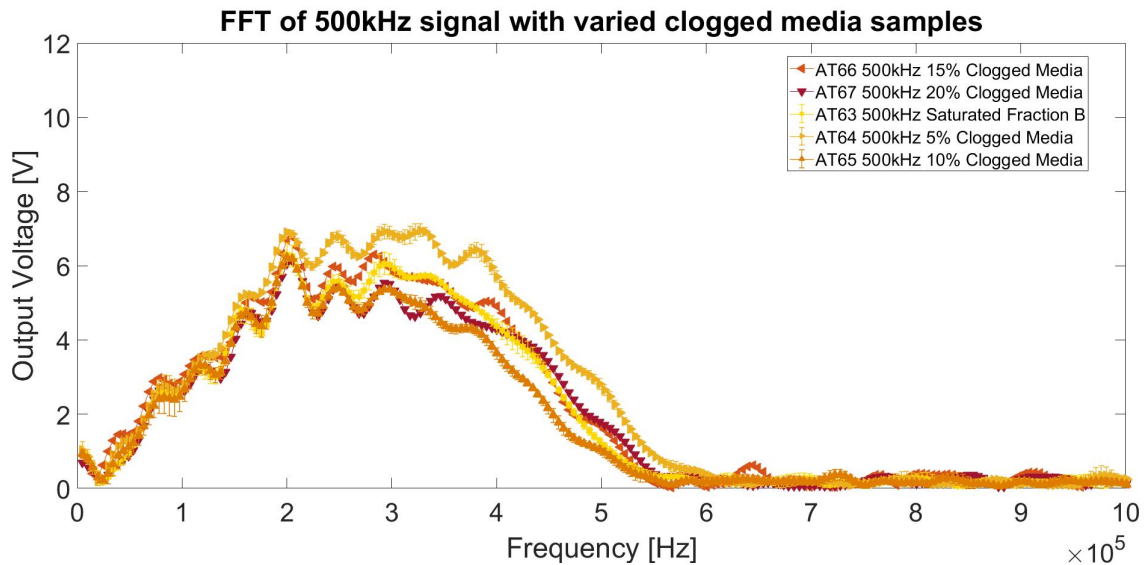


Figure 4.13: FFT results of the received 500 kHz pulse in various clogged media in bag.

appears to result in a peak value at a lower frequency.

Experiment AT68 and experiments AT70 to AT72 investigated the impact of mixing type, and level of deairing. Experiment AT68 was a 5% clogged sample where the mixing method was adapted, 10% of the deaired water required to saturate the sample was added during the mixing phase, then the sample was saturated with the other 90%. This resulted in low signal-to-noise problems, experiment AT70 was the same mix but remixed after saturation, this overcame the low signal-to-noise problem and provided the FFT result shown in Figure 4.14. Experiment AT71 was a 5% mix and experiment AT72 was a 20% mix, both deaired for a minimum of an hour.

Figure 4.14 shows that deairing is important to gain a stronger signal. No significant difference was noted between the experiments AT71 and AT72, however the increased proportion of silica flour in experiment AT72 seemed to result in the pulse attenuating rapidly at a lower frequency of approx 300 kHz , compared to experiment AT71's approx 400 kHz . Which is consistent with the non-vacuumed results shown in Figure 4.11, where the 20% mix decreased from a frequency of 300 kHz . This suggests the low signal-to-noise problems caused by air bubbles prevents a relationship between the peak

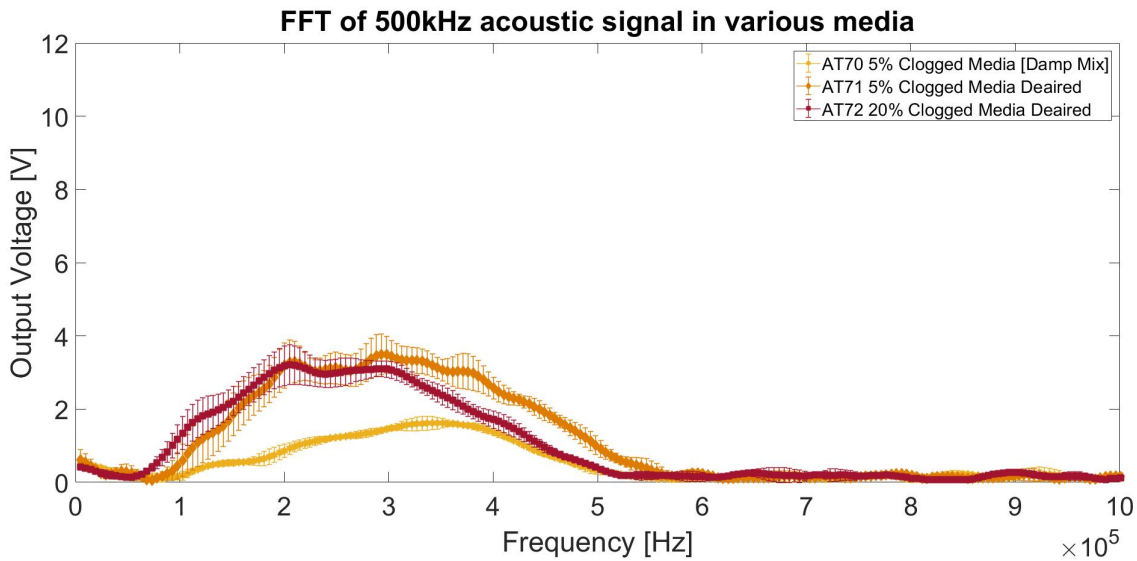


Figure 4.14: FFT results of the received 500 kHz pulse in various deaired clogged media.

values and clogged pore percentage being developed, but it could be possible to detect increased sediment by the change in frequency where attenuation increases rapidly. Additionally, studying the peak amplitude in relation to the frequency; the 20% media sample had a peak value around 200 kHz whilst 5% media sample had a peak value around 300 kHz , suggesting that by detecting a reduction in peak frequency the clogged media could be detected.

To investigate the impact of deairing on the media sample and the position of the bag, bagged media experiments were conducted with Fraction B Sand with varying timings of deairing, and positions. Figure 4.15 shows that with a longer duration of deairing the received pulse has a higher amplitude. Position was also an important effect on the received pulse amplitude, Figure 4.15 shows the signal was dependent on placement between the two transducers, with a higher standard deviation than seen previously.

Bagged media experiments of 10% clogged media were then investigated, to estimate the effect of position and duration of deairing on sound. Additionally, the longer duration of deairing resulted in less variability from different positions, shown by the lower standard deviation.

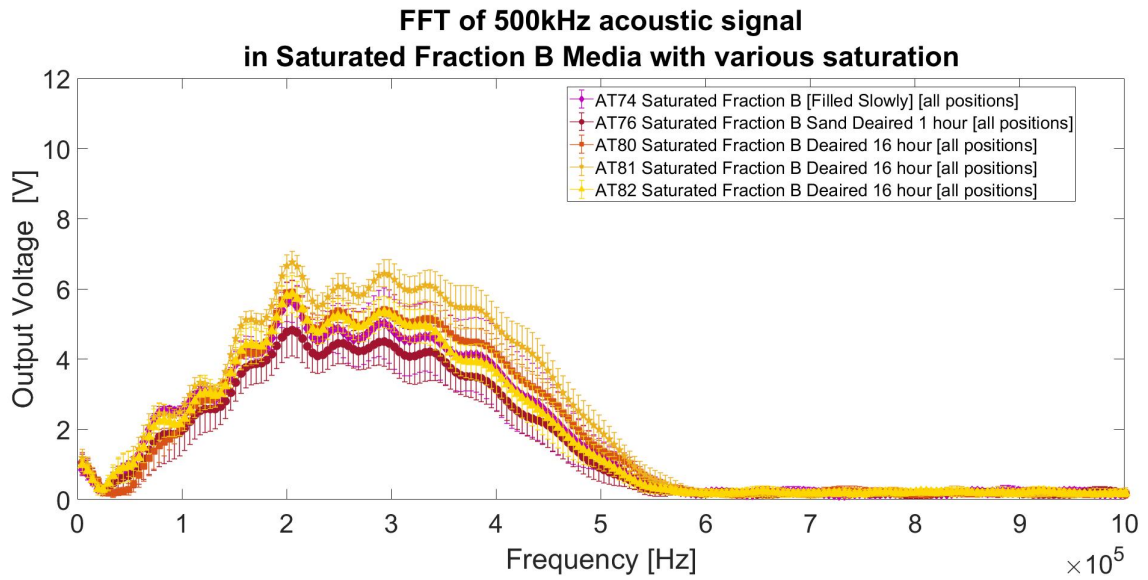


Figure 4.15: FFT results of the received 500 kHz pulse in various deaired Fraction B media.

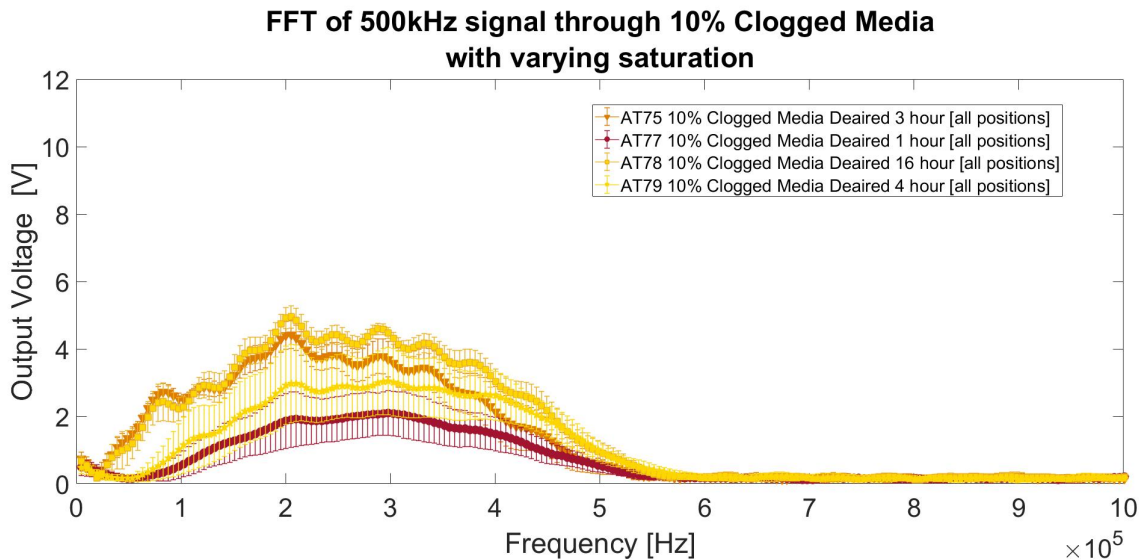


Figure 4.16: FFT results of the received 500 kHz pulse in various deaired 10% clogged media.

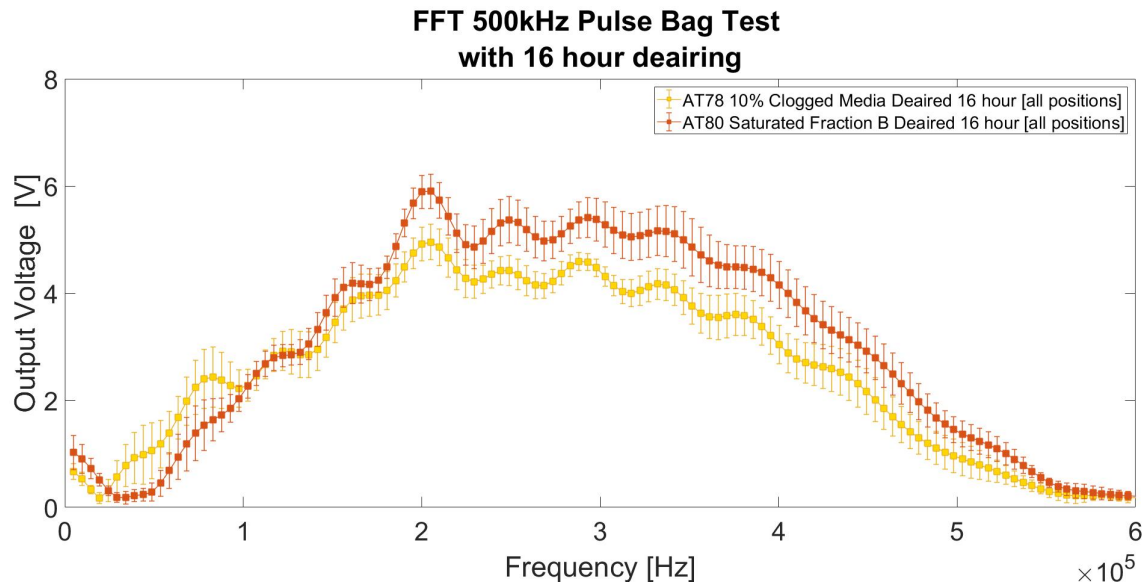


Figure 4.17: FFT results of the received 500 kHz pulse in various 16 hour deaired media.

Due to the 16 hour vacuuming providing more repeatable results, experiments were conducted on a 16 hour saturated Fraction B sand sample (AT80) and a 16 hour 10% clogged media sample (AT78). Figure 4.17 shows that the addition of silica flour resulted in a lower signal than in the 16 hour saturated deaired Fraction B. The decline in signal for experiment AT78 was also seen at a lower frequency compared to experiment AT80.

$$\alpha_p = \frac{20 \log_{10} \left(\frac{V}{V_0} \right)}{x} \quad (4.2)$$

Where: V and V_0 are the recorded signal of the media samples and water respectively, and x is the distance between the transducers.

The attenuation, α_p calculated by Equation 4.2, in experiments AT80 and AT78 is shown in Figure 4.18. Figure 4.18 shows that as frequency increases the attenuation caused by the media sample increased, additionally the presence of silica flour resulted in a greater attenuation. By plotting the lines of best fit where the attenuation would scale with either $f^{1/2}$ and f^1 , allows the assessment of whether Biot-Stoll or Hamilton frequency dependence was seen.

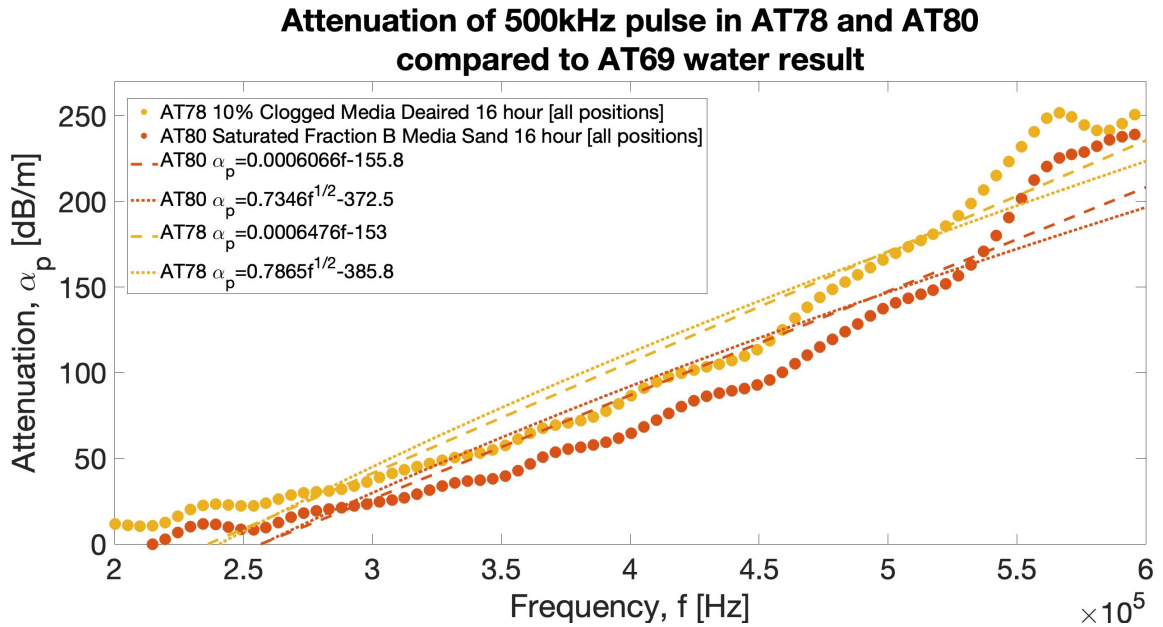


Figure 4.18: Attenuation of 500 kHz pulse in various media.

As described in Chapter 2, there are two types of frequency dependence for Biot-Stoll; low and high. With low frequencies the attenuation scales by f^2 , but in high frequencies it scales by $f^{1/2}$. Equation 2.14 defines the Biot-Stoll characteristic frequency, which then determines whether low or high frequency dependence is observed. Using Equation 2.14 the characteristic frequency was estimated to be 220 Hz for 30% porosity. As the frequencies used in this project's experiments were much larger than the characteristic frequency, high frequency dependence ($f^{1/2}$) would be observed.

Figure 4.18 shows that whilst both lines of best fit were similar, the Hamilton (f^1) showed a better match with measured data. The range of values for attenuation between these frequencies show close agreement with values presented by Williams, et al. [108], where attenuation at 400 kHz was around $10^2 dBm^{-1}$. In this paper the authors also found the Biot-Stoll $f^{1/2}$ relationship did not model the attenuation at large frequencies well, although it did better at lower frequencies. As the data suggests, there is indeed an f^1 relationship. This means the Hamilton attenuation coefficient, K_p , in Equation 2.16 is $6.48 \times 10^{-4} dBm^{-1}Hz^{-1}$ for T78 and $6.07 \times 10^{-4} dBm^{-1}Hz^{-1}$ for T80. As the attenuation coefficient is related to the medias properties, including porosity, the change can provide

information on sediment capture. The coefficient increased 6.8% with silica flour present, which was 10% of pore spacing within the media sample, suggesting silica flour impacted the attenuation of the sound wave.

Figure 4.18 also shows that at higher frequencies the difference in attenuation of the media samples increased, which suggests that using higher frequency sound waves would result in greater sensitivity to sediment capture. As frequencies above 500 kHz were fully attenuated, as shown in past figures, it is recommended to conduct experiments between 300 and 400 kHz . This frequency range would provide a sufficiently strong signal for detection and be highly sensitive to the presence of sediment.

4.6.4 Hydrophone Experimental Results

Due to the various problems encountered in the previous experiments, a number of experiments were conducted using hydrophones. AT83 and AT84 helped to develop the method outlined in Sub-section 4.3.4. The key results are shown in Figure 4.19, results for AT90 to AT92 are not presented. The time window length was set to 250 μs . This was sufficient to achieve 50 kHz resolution.

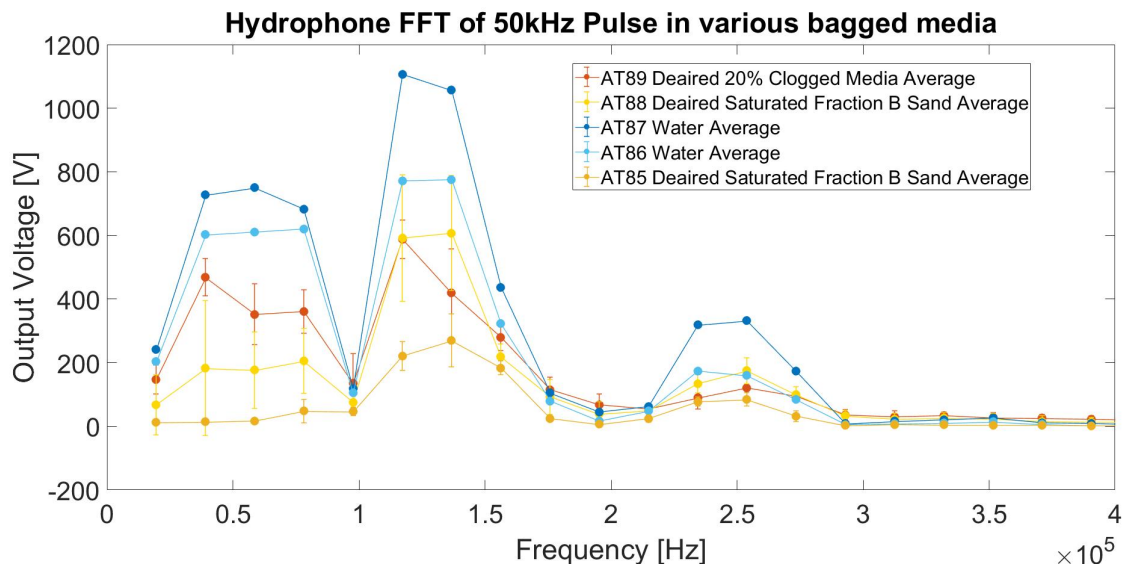


Figure 4.19: FFT of Hydrophone Data.

Figure 4.19 shows that the results are varied, more considerably than seen in the other experiments. This could be resultant from the experimental set-up, further experiments with a better designed set-up could provide usable information.

4.6.5 ST02 and ST03 Experimental Results

The acoustic data collected in the permeability experiments outlined in Chapter 3 are shown in Figures 4.20 and 4.21 below. Section 4.5 outlines how the pulse energy was calculated. These results allow the assessment of whether acoustics can be used within a filter media monitoring sensor system.

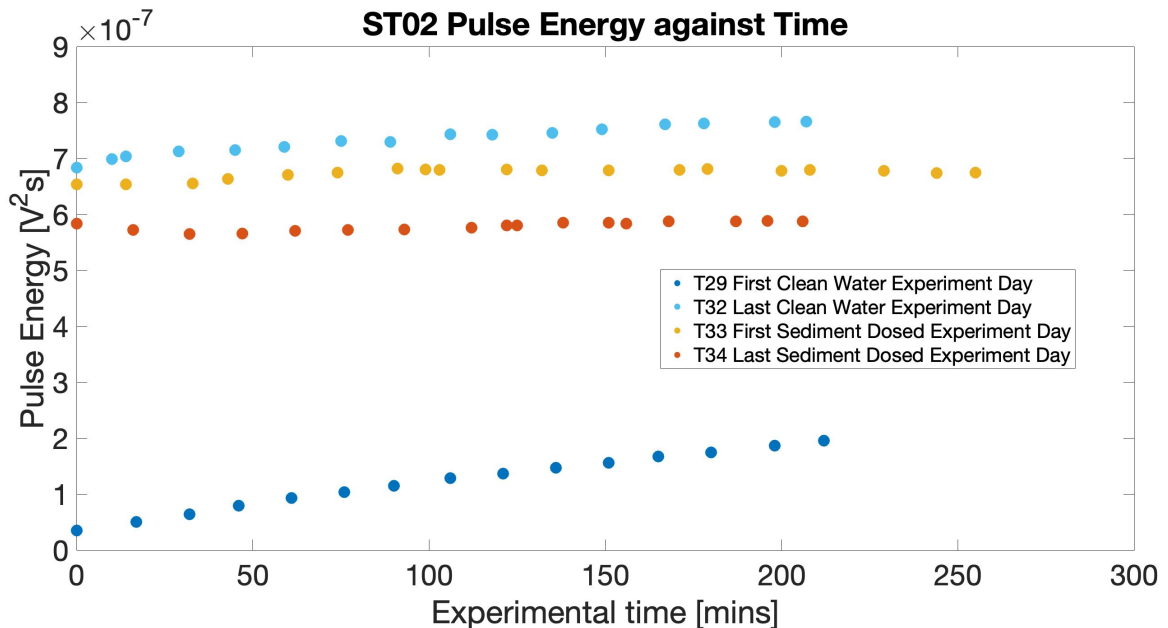


Figure 4.20: Pulse energy against experimental time for ST02.

Figure 4.20 shows the received pulse energy throughout ST02 experiments T29, T32, T33, and T34. For reference; experiments T29 and T32 consisted of clean water experiments for 210 mins at 2 Ls^{-1} . Experiment T33 had 45 mins of clean water flow, followed by 210 mins of sediment dosed flow. As described in Chapter 3 experiment T33 was longer to acquire background permeability readings before sediment was introduced to the system.

Experiment T34 consisted of 210 mins of sediment dosed flow.

Results from experiment T29 show that as flow passed through the newly installed filter media, the energy of the received pulse increased. This appears to suggest that increased saturation, with a possible reduction of air bubbles within the media, results in lower attenuation of the acoustic pulse. Results from experiment T32 show a much stronger pulse energy, with the final recording being approximately $3.9 \times$ the final pulse energy reading for T29.

The increased pulse energy is expected to be resultant from the increased saturation in T32 from T29. Experiment T29 was a freshly installed dry media, by experiment T32 12 hours of clean water flow had been passed through the media. The results also show that the rate of increase, of the acoustic pulse energy, slowed when compared to T29 suggesting that the filter media was reaching full saturation.

However, this could also be resultant from media rearrangement throughout the flow. The permeability results showed a continued decrease with repeated flows. As the media grains rearrange, stratification occurs where the smaller grains are at the top of the bag and larger grains at the bottom. This causes a larger pore size at the bottom of the bag, where the transducers were located.

Experiment T33 showed a similar pulse energy at the start of the experiment to T32. For the first 45 mins of clean water flow, and the first 45 mins of sediment flow the pulse energy increased. However, after 45 mins sediment flow the received pulse energy decreased, which resulted in a widening divergence with T32. Indicating that as sediment is retained by the filter media the acoustic pulse became more attenuated.

The final recorded pulse energy was 12.0% lower than the final pulse energy in experiment T32. Indicating that the acoustic pulse was impacted by the capture of sediment. However, the large decrease raises the question of whether it may be too sensitive to the sediment capture as the impact on permeability was very small.

Experiment T34 had a lower initial pulse energy than that of experiments T33 and T32. This indicates that the collected sediment from T33, impacted the signal for T34. The

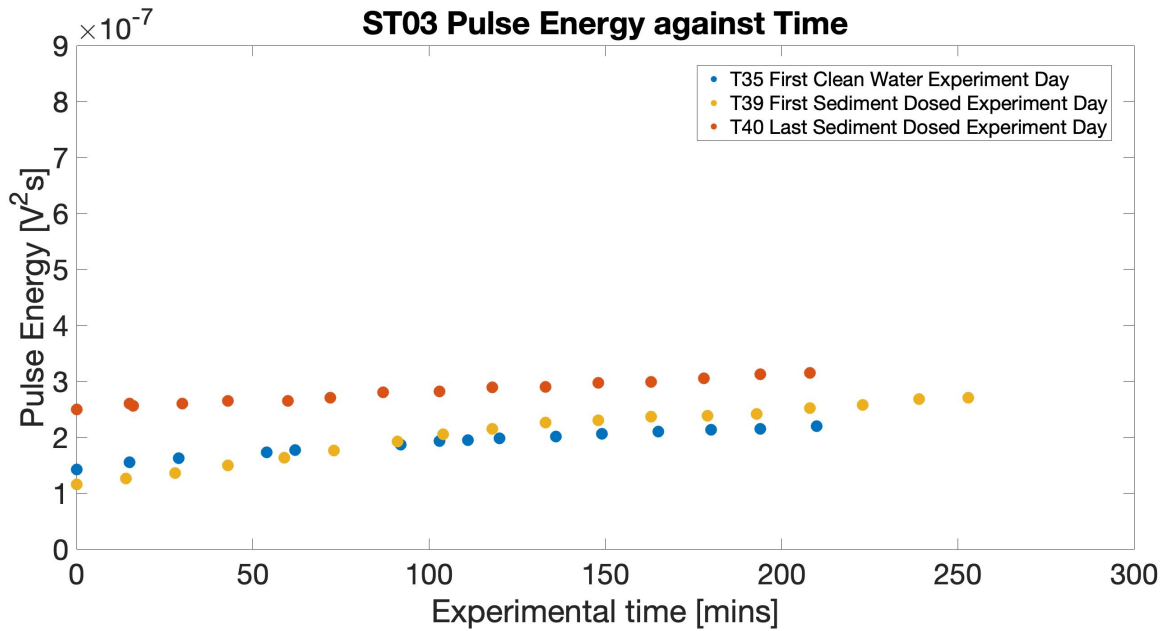


Figure 4.21: Pulse energy against experimental time for ST03.

initial pulse energy of experiment T34, was approximately 13.5% lower than the final T33 pulse energy. Which is similar to the 14.6% drop seen in the initial T33 pulse energy, when compared to the final T32. This indicates when the flow stops the media loses some saturation, impacting the initial readings the next day.

Throughout experiment T34 there was no increase in signal, unlike experiments T32 and T33. This indicates the increasing sediment impacted the level of attenuation of the pulse. The drop in final recorded pulse energy for experiment T34 compared with T33 was 12.8%, a similar drop seen in the T33 results. As the silica flour was dosed for the same duration and feed rate on both T33 and T34, this indicates silica flour has a direct impact on the acoustic pulse energy.

Figure 4.21 contains the pulse energy received against experimental time for experiment ST03. For reference experiment T35 was a clean water experiment, and experiments T39 and T40 were sediment dosed experiments. As with ST02, the first sediment dosed experiment had 45 mins of clean water flow. Due to an equipment malfunction, no acoustic data was recorded for the last clean water experiment T38.

The first clean water experiment, T35, showed a similar measured pulse energy to T29 in ST02. The slight variations in the measured pulse energy and rate of increase, could be resultant from variations in installation. The ST03 results showed a lower permeability than ST02, this will impact the saturation as it is more difficult for water to pass through the filter media.

The pulse energy for experiment T39 shows a similar initial pulse energy to that of T35. As mentioned in Chapter 3, the drain-down ports became slightly unsealed in ST03, resulting in the water level draining below the filter media over the weekend break. This would result in the lower signal measured in experiment T39, as the media would be less saturated and air possibly entered the filter media.

As Figure 4.21 shows, the pulse energy for experiment T40 was higher than T39, likely due to the increased saturation of the media from the previous days experiment. Experiment T40 shows a smaller increase in energy over the experiment compared to T39, indicating the effect of increased saturation was offset by Fraction E capture.

This is further evidenced by experiment T39, the first 45 minutes of clean water flow and the first 75 mins of dosed flow the increasing saturation resulted in increased pulse energy. However, after the 75 mins of dosed flow the rate of increase dropped. The drop in the rate of increase suggests that capture of sediment reduces the impact of increased saturation.

4.7 Acoustic Distance Experimental Results

MSc student Feng Xu [109] used Sub-section 4.3.1's methodology to conduct research on the impact of distance and different medias on sound transmission. Feng Xu used a larger aluminium vessel, which allowed multiple distances to be studied. The experiments were designed to allow for the results to be relatable to work outlined in this chapter, with the same transducers, holders, media, frequencies and signal type used.

The main findings from the research were that; attenuation was greater in smaller grain sized media, higher frequency results in greater attenuation, and as the distance increased so did the signal loss. Feng Xu presented Equation 4.3 that relates the signal amplitude to distance.

$$A = A_{in} \times e^{-0.073x_{acoustic}} \quad (4.3)$$

where; A is the received signal amplitude, A_{in} is the amplitude of input signal, and $x_{acoustic}$ is the distance between the transducers.

Additionally, the researcher had signal-to-noise issues with non-vacuumed media samples. Further suggesting that the impact of air within the media sample is an important consideration when developing filter media monitoring systems. This work fulfilled the distance work set out in the strategy.

4.8 Conductance Probe Experimental Method

In the Up-Flo[®] Filter System experiments ST02 and ST03 (methodology in Chapter 3) the multi-probe conductance device described in Chapter 2 was installed into Module 4, location shown in Figure 3.4. A bespoke multi-probe conductance device was designed, with a length of 380 mm and width of 90.74 mm (design in Appendix D.7), so that once attached to the interior wall of Module 4 it covered both filter media bags, the matallas and the conveyance channel within the Up-Flo[®] Filter System module. Figure 4.22 shows the installed multi-probe conductance device.

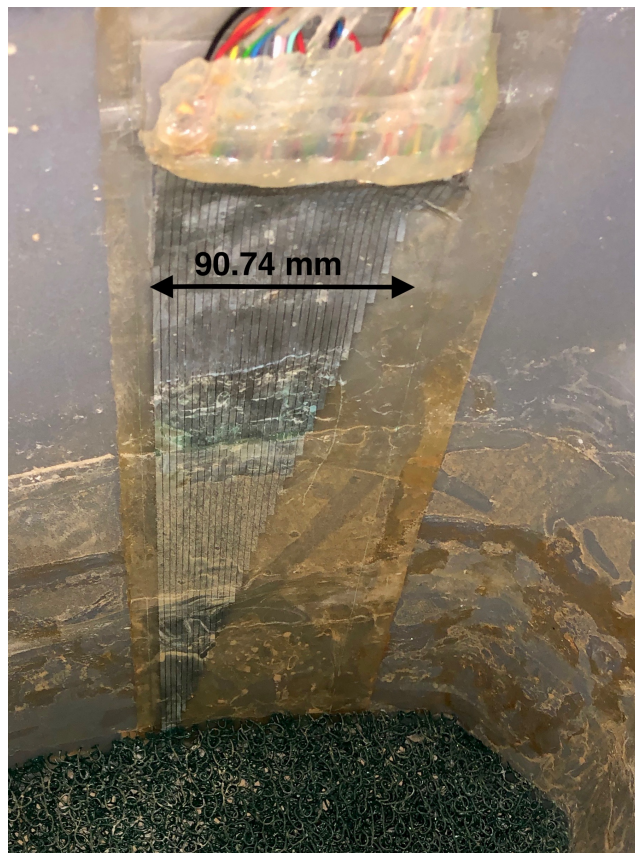


Figure 4.22: Multi-probe conductance device after ST03.

Throughout ST02 and ST03 experiments the multi-probe conductance device measured the conductance within the module. A LabVIEW programme controlled the device by

applying a 8 kHz , 1 V peak to peak square wave centred on 0 V on each probe sequentially, and measuring the conductance reading between that and the neighbouring probe. It takes a reading across the whole array of probes approximately every 1.5 seconds. The LabVIEW programme recorded the conductance results onto a text file specified by the user, this LabVIEW programme is attached in Appendix D.8.

4.9 Conductance Probe Data Analysis Techniques

The conductance probe data was analysed using the MATLAB programme in Appendix D.9, designed by the author of this Thesis and Andrew Nichols. The programme plotted the data as a contour plot (example shown in Figure 4.23), and then the user selected periods of time for further analysis. Using the x-axis locations of the period of time, the voltage was plotted against distance from the bottom of the probe. Then the code plotted an additional figure of the voltage gradient across both filter media bags (probe numbers = 3 to 20, left to right) against experimental time, this allowed for analysis of how sediment impacted the conductance.

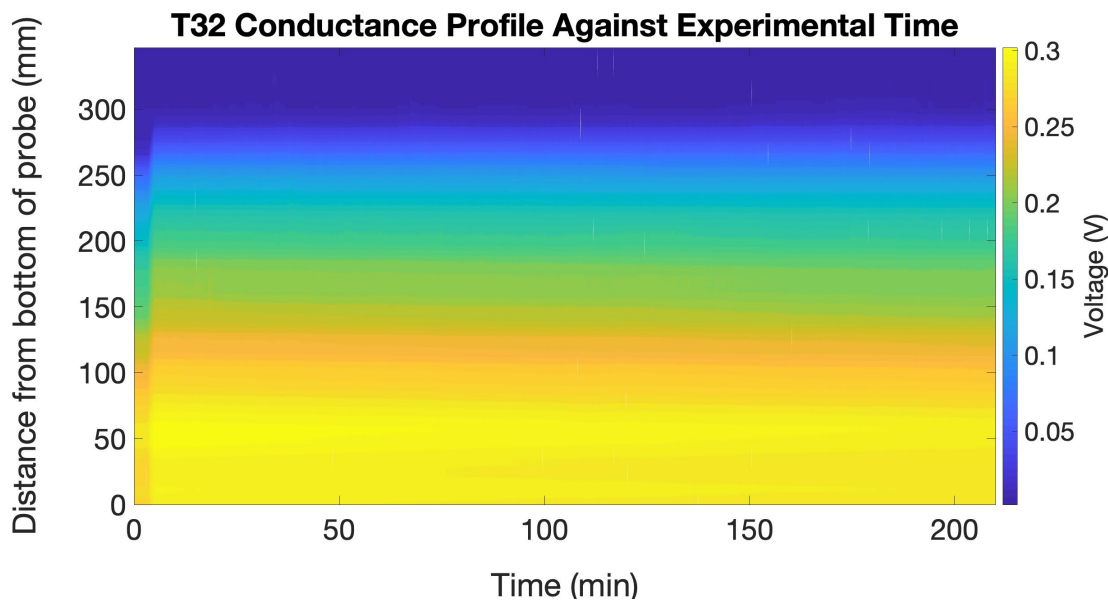


Figure 4.23: Conductance profile recorded in Module 4 during ST02 T32 clean water experiment.

Figure 4.23 shows an example of a contour plot obtained from one of the experiments within ST02. This figure shows that the further away from the bottom of the multi-probe conductance device the lower the voltage recorded. The top of the conductance device showing little to no conductance, which is to be anticipated as the top of the device would

be within the air phase of the conveyance channel.

4.10 Conductance Probe Experimental Results

The results from the multi-probe conductance device experiments showed a number of interesting results. Firstly, the flow rate had an impact on the voltage recorded across the probes. Figure 4.24 shows the effect of different flow rates on the conductance profile in Module 4. It shows that at higher flow rates the recorded voltage increased, with 0 and 0.3 Ls^{-1} providing the lowest recorded voltages, and 7 Ls^{-1} providing the highest.

Additionally, the distance where the air phase was met was higher for higher flow rates. This is anticipated as at higher flow rates the water level within the module would be higher to drive water to the outlet module. The 7 Ls^{-1} flows provided a water head of 184.4 mm above the filter media bags, compared to 150.2 mm for 0 Ls^{-1} .

As there is a larger voltage measured within the filter media during higher flow rates, this suggests there is bed expansion which increases pore spacing, which then increases conductance. This bed expansion allows for filter bed rearrangement, causing the drop in permeability seen in the Up-Flo[®] Filter System clean water experiments. The ability of the device to detect changes in flow rate and also the level of head above the filter media is particularly useful for a filter media monitoring system. Both of these would allow for changes in filter media condition to be monitored, if the water level in the Up-Flo[®] Filter System is known then the permeability could also be estimated.

The result from experiment T40 0 Ls^{-1} appears to be an outlier result, which would be resultant from the draining down of the rig between experiments during ST03. The desaturation would cause a reduction in the conductivity, resulting in the lower voltage seen. Due to the extra flow before the dosed sediment started, an extra 0 Ls^{-1} reading is shown (noted as after incident). The extra result shows that the additional flow caused the conductance to return to a similar pattern as seen in experiment T34 0 Ls^{-1} readings and all 0.3 Ls^{-1} readings. Further suggesting the outlying T40 0 Ls^{-1} reading was due to the drain down between experiments. The issues in T40 suggest that saturation levels of the filter media could be monitored, further experiments with varying moisture content levels would develop a useful conductance curve to monitor media saturation.

The changes in conductance between the 2 Ls^{-1} ST02 experiments were minimal, as was

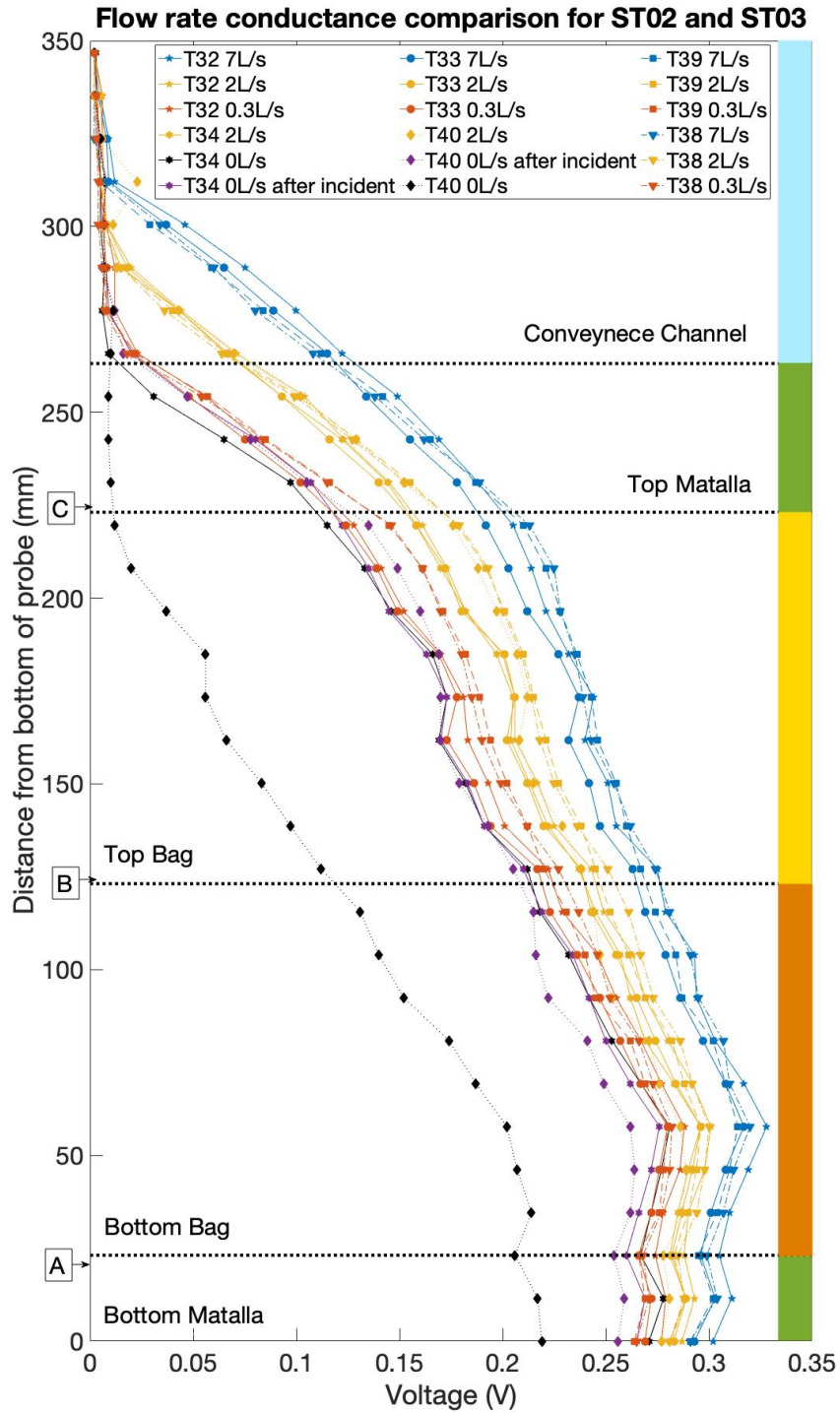


Figure 4.24: Conductance profiles in Module 4 of Up-Flo[®] Filter System at various flow rates, with the modules regions highlighted. Points A, B and C denote the approximate locations of the pressure tappings.

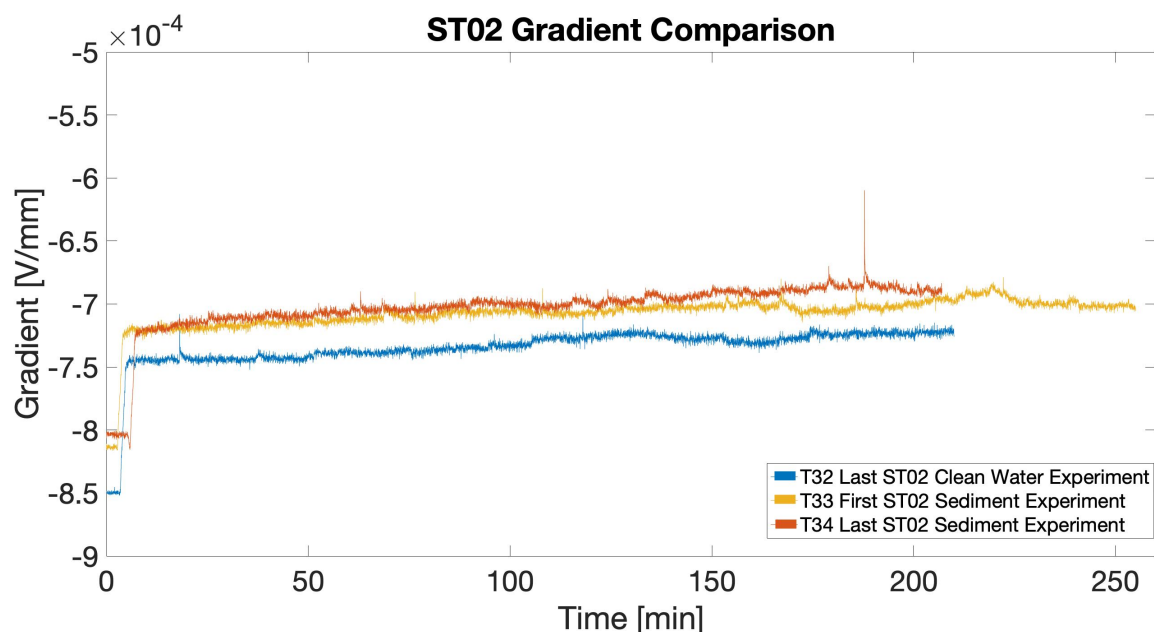


Figure 4.25: ST02 Gradient Comparison. (Sediment start times: T33 45 mins, T34 0 mins).

the changes between 2 Ls^{-1} ST03 experiments. There is a slight difference between the conductance results between ST02 and ST03, however, this could be resultant from the different permeabilities recorded. As the changes between each experiment within ST02 and ST03 were minimal, the impact of sediment was studied by plotting the gradient of the voltage over both filter media bags against experimental time.

Figure 4.25 shows the conductance gradient over both filter media bags during ST02. The clean water experiment T32 shows the steepest gradient indicating the greatest conductance change over the filter media bags, which is expected as the permeability was larger in T32 than in T33 and T34. Additionally the magnitude of the gradient changed over T32 decreasing from $-7.5 \times 10^{-4} \text{ Vmm}^{-1}$ to $-7.2 \times 10^{-4} \text{ Vmm}^{-1}$, this change shows that the conductance measured across the bag decreased over the experiment. This is to be anticipated as the permeability of the filter media in T32 decreased throughout the experiment, this decrease would also decrease the measured conductance due to a lower amount of pore spacing.

The conductance gradient at the start of T33 was $-7.2 \times 10^{-4} \text{ Vmm}^{-1}$, this is the conductance gradient value seen at the end of experiment T32. Over the experiment the conductance gradient decreased to $-7.0 \times 10^{-4} \text{ Vmm}^{-1}$, which suggests that the changes in permeability and sediment capture can be detected using the multi-probe conductance device. However there does not appear to be a significant extra impact by the sediment, as no significant change is seen after 45 mins when it was dosed into the system.

Considering that the amount of sediment caught within the filter media bags was small, and that the impact on permeability was small, no significant impact on conductance is to be anticipated. However in the long term, as stratification within the filter media reaches peak rearrangement, and more sediment is caught, larger drops in permeability caused by sediment is to be anticipated. Suggesting the multi-probe conductance device could be used for detection of sediment capture.

The change in conductance gradient over the experiment was also seen in T34, with the final conductance gradient value dropping to $-6.9 \times 10^{-4} \text{ Vmm}^{-1}$. However the conductance gradient at the start of T34 was $-7.2 \times 10^{-4} \text{ Vmm}^{-1}$, this is the same as the start of T33. This suggests the loss in conductance in T33 was regained at the start of T34, which could be explained by the extra flow applied before the start of T34 due to a procedural error (explained in Section 3.6). As this flow was higher (max 9.1 Ls^{-1}) this would cause an increased saturation of the filter media, resulting in a higher conductance value at the start of the experiment. As the conductance gradient appears to be impacted by permeability changes and saturation levels, this could be a potential way to monitor sediment capture within filter media.

Figure 4.26 shows the gradient comparison over ST03. Comparing the gradient profile for the clean water experiment T38 to ST02 T32, the gradient has decreased resulting in lower conductance. This lower gradient can be explained by the lower permeability recorded in ST03 during T38, which is anticipated to be resultant from the installation process causing a different packing arrangement when installed within the system. This means to use conductance to monitor the filter bed condition the changes must be relative to the clean state rather than comparing it to absolute values, as with monitoring permeability. Similarly to ST02 the conductance gradient decreased throughout the clean

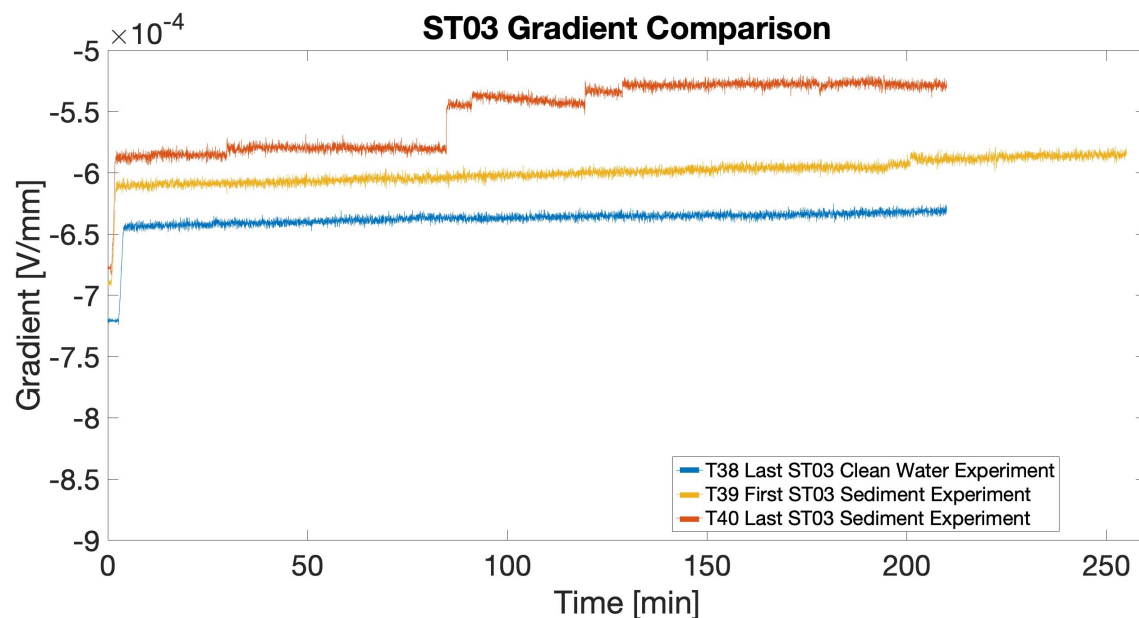


Figure 4.26: ST03 Gradient Comparison. (Sediment start times: T39 45 mins, T40 0 mins).

water experiment T38, falling from $-6.5 \times 10^{-4} \text{ Vmm}^{-1}$ to $-6.3 \times 10^{-4} \text{ Vmm}^{-1}$.

In T39 the conductance gradient starts at a lower value of $-6.1 \times 10^{-4} \text{ Vmm}^{-1}$, this is lower than that recorded at the end of T38. The lower conductance gradient can be explained by the drain down port seal failing in ST03 (described in Section 3.6), which resulted in the rig draining down very slowly between experiments. The drain down would result in a lower saturation, which would result in the lower conductance gradient seen. During T39 the conductance gradient decreased to $-5.9 \times 10^{-4} \text{ Vmm}^{-1}$, suggesting the changes in permeability was still detected by the multi-probe conductance device despite the saturation effect. As with ST02 T33, no significant impact from the sediment loading is seen after sediment dosing started at 45 mins. The lack of effect of sediment is to be expected as even less sediment was retained within the filter media in ST03.

In T40 the conductance gradient again starts off at a lower value than the last value of the previous experiment, starting at $-5.8 \times 10^{-4} \text{ Vmm}^{-1}$, suggesting that saturation did again impact the conductance. As with all other experiments, the conductance gradient

decreased throughout the experiment but at approximately 85 mins there was a large decrease in conductance. As Figure 3.29 shows, at 85 mins there was no significant decrease in Module 4 permeability. This could be resultant from a number of possible reasons, including; equipment malfunction, or something touching the probes directly at this time. Further investigation is required to determine the possible reasons behind it, with multiple devices tested over long term experiments.

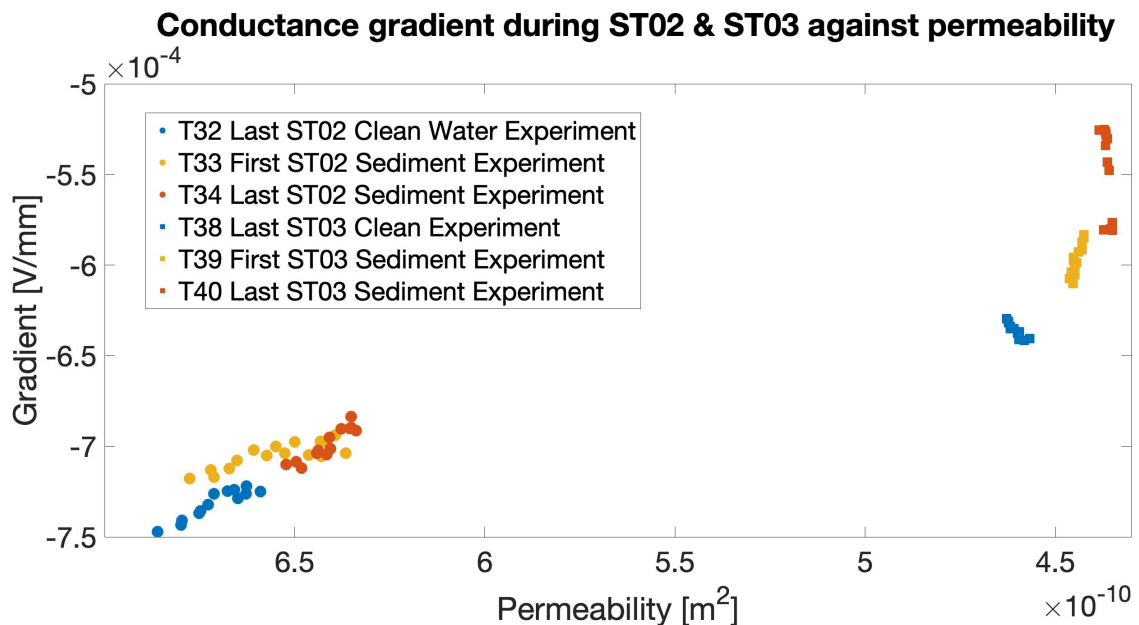


Figure 4.27: Conductance gradient across both filter media bags against recorded permeability during experiments ST02 and ST03 at $2 Ls^{-1}$. Experimental times taken: 30 mins then every 15 mins until end of experiment.

As there appears to be a link to conductance gradient over the filter media bags and the measured permeability, the conductance gradient values against their time matched permeability values were plotted in Figure 4.27. This figure shows a relationship between permeability and the conductance gradient, with the gradient magnitude falling as permeability decreases, which is particularly useful in filter media monitoring. This relationship would potentially allow this device to monitor the health of the filter media, and the treatment capacity of the Up-Flo[®] Filter System. More experiments are needed to better define the relationship, with the conductance for filter medias with

permeabilities between 5.0 and $6.0 \times 10^{-10} \text{ m}^2$ in particular needing to be measured.

Additionally, measuring conductance gradient with a range of flow rates and moisture content will be required to fully develop the device into a functioning monitoring system.

4.11 Chapter Discussion

The experimental results presented in this chapter allows for a discussion on the potential use of acoustic and conductance techniques in a filter media monitoring system.

One effect seen throughout the vessel experiments was the difference in the peak received signal and the pulse frequency applied. This was most observable in 350 kHz water results. Whilst the transducers are capable of supporting frequencies between 100 kHz and 1 MHz , the peak resonant frequency is 500 kHz . This results in a shift in the signal peak from 350 kHz to closer to 500 kHz .

Whilst the results from the acoustic experimental work was varied and no firm relationship could be made, the impact of sediment in filter media on the acoustic signal can be seen. As shown in Figure 4.18 the deaired clogged media caused the signal to experience greater attenuation than in the deaired clean filter media, with the attenuation coefficient of the clogged media sample being larger than the clean media sample. Whilst repeatability issues remained with non-deaired media samples, it seems that one possible way to detect sediment would be to look at what sound frequency had the peak amplitude.

Figure 4.18 also shows a frequency dependence on the attenuation. This frequency dependence is seen in all the Sound Propagation models outlined in Chapter 2, including Biot-Stoll, Hamilton, Buckingham, and Williams. However the level of dependence varied contingent on the model used. Biot-Stoll predicted, at high frequencies, the attenuation scales with the square root of the frequency [70]. While Hamilton predicted a first power dependence [73]. Figure 4.18 shows that the data better fits a first power dependence, suggesting that the Hamilton empirical based model is more accurate than the physical based model of Biot-Stoll. The values of attenuation also matched values presented by Williams et al. [108], the researchers also found that at these high frequencies the first power dependence is also a better fit, as found during these experiments.

Whilst the problems in the vessel experiments resulted in difficulty establishing a clear relationship, results from the in-situ experiments showed that acoustics was a possible

technique for filter media monitoring. The results from the in-situ ST02 experiments show that silica flour had a significant impact on the energy of the sound pulse passing through the filter media. However ST03 results showed that when the drain-down ports were not fully sealed off, the impact of air reentering the media made the impact of Fraction E sediment harder to detect. It appears that the introduced sediment in ST03 did, however, reduce the rate of increase in pulse energy caused by the increasing saturation. This suggests even with the drain-down ports in operation it may be possible to detect sediment capture within the filter media. The main limitation of an acoustic based monitoring system would be that the Up-Flo[®] Filter System drain-down ports would not be sealed in realistic operation, resulting in the sediment capture being more difficult to detect.

Results from the conductance probe experiments show that it is capable of providing useful segments of information. Firstly, it was capable of monitoring the changes in saturation of the media, the water level over the filter media, and flow rate through the media. This alone opens up the potential use to monitor the state of the media, if the rig water level and flow rate are known the measured head over the media could potentially allow for the monitoring of filter media permeability.

The conductance probe gradient over the filter media bags showed that during the experiments the gradient decreased, when considering that permeability declined in these experiments it appears to suggest the device is capable of monitoring changes. This was also seen when comparing the clean water experiment results from ST02 and ST03, the lower permeability showed a significant decrease in the magnitude of the gradient. Figure 4.27 showed the conductance gradient results against the respective permeability measurements, this showed that as the permeability decreased the gradient also decreased. Further experiments could develop this relationship further, including the effects of flow and saturation, which then could present a useful monitoring system. The permeability ultimately dictates the treatment capacity of the Up-Flo[®] Filter System, this could allow for the device to measure when the treatment capacity has significantly dropped requiring maintenance.

Limitations of the multi-probe conductance device include that it only monitors the

outside of the filter media bags, resulting in no monitoring of what is happening within the filter media. Additionally, whilst it can monitor the water level within the module, which is incredibly useful, it is limited by the accuracy. The difference between probe lengths is 11.6 *mm* which is quite large, this can be fixed by the addition of more conductance probes allowing a smaller difference in probe lengths for a more accurate water level measurement. Finally, the other limitation is the fragility of the probes, which raises issues in installation and maintenance routines of the Up-Flo[®] Filter System.

Whilst both the conductance probe and acoustical set-up show individual potential for a filter monitoring system, combined they may form a more comprehensive system. Whilst problems arise with the acoustics, with low saturation levels providing variable results, the conductance probe could be used to monitor the saturation level of the filter media. Then, by monitoring the pulse energy at a set saturation level the filter media could be monitored more easily. By combining this with the gradient changes monitored by the conductance probe, the health of the media could be quantified and monitored. Potential limitations with this approach would be the extra costs involved and the power requirements for two devices.

To develop this into a functioning system, further experimental research and product development is required. More in-situ experiments would be required to validate its use and to form key background information for data comparison. Further experiments would be required to test different cheaper transducers, as the Olympus Transducers used for experimental work would be too expensive for commercial use. Finally, further work would be needed in product development with Hydro International Ltd to develop installation techniques.

Once developed into a fully functioning system the choice of module would be important. Results from Chapter 3, and discussed in Section 3.15, show that the modules further from the outlet have a smaller flow rate. The different flow rates in the modules may result in different levels of capture. Individual requirements of the site would need to be taken into account when deciding which module the system would be installed within. Furthermore, once developed, the sensor system could in future be adapted to other sand based filter medias.

4.12 Chapter Summary

This chapter has outlined the work undertaken to develop a filter media monitoring system, as part of the aims and objectives of this project to improve the sustainability of the Up-Flo[®] Filter System.

Section 4.3 outlined the acoustic experimental methodology, first with clean filter media samples and then with artificially clogged samples, as set out in the acoustic experimental strategy in Section 4.2. This provided information on sound propagation within both clean and artificially clogged media samples. The methodology developed to include in-situ measurements within Module 4 of the Up-Flo[®] Filter System during ST02 and ST03, described in Chapter 3. This allowed an assessment of acoustic techniques in a filter media monitoring system.

The results from the sound experiments, Section 4.6, were unable to develop a relationship between the percentage of clogging of the media and the attenuation of the sound wave traversing it. This appeared to depend on the amount of air trapped within the media samples and issues surrounding the experimental method. Whilst these issues were present, a greater reduction of signal amplitude was seen when sediment was within the media sample. Figure 4.18 shows the measured attenuation of media samples, these were within the range previously published by Williams et al. [108], it also shows that the attenuation was frequency dependent. The frequency dependence seemed to fit the first power dependence proposed by Hamilton, Buckingham and others. Results from the in-situ experiments suggest that it is possible for an acoustic based system to be used, problems were encountered when air was within the system but the effect of sediment could still be observed.

Section 4.8 outlined the in-situ experiments conducted with the multi-probe conductance device experiments, as part of the Up-Flo[®] Filter System sediment removal experiments. A multi-probe conductance device was bespoke made to fit a interior wall of Module 4, it covered both matallas and filter media bags and part of the conveyance channel.

The results of the multi-probe conductance device experiments, Section 4.10, show that

the device could be used to detect flow rate, saturation, water level, and permeability. Figure 4.24 shows the conductance value measured across the module at different flow rates, it found that higher flow rates resulted in increased conductance indicating bed expansion. The device was able to measure the difference between water and air, allowing the estimation of water level above the filter media to be made. Figure 4.27 presents the measured conductance gradient over both filter media bags against its respective permeability measurement. This shows as permeability decreases the magnitude of the conductance gradient also decreases, indicating the multi-probe conductance device is capable of measuring changes in permeability.

In Section 4.11 a discussion is presented on using these techniques as a filter media monitoring system and the work required to develop it. The author argues that whilst each technique has individual potential, using both techniques in conjunction would present a basis for an effective sensor system. Using both techniques in conjunction would allow for the individual limitations to be overcome, however this also raised cost and power requirements.

Whilst the work outlined in this chapter has not fully met the objectives of developing a fully functioning sensor system, its research presents a basis to develop one with future work. It also outlines the challenges a sensor system entails in use within the Up-Flo[®] Filter System.

Chapter 5

REGULATORY COMPLIANCE & MAINTENANCE

Chapter 2 presents the UK approach to urban stormwater treatment. However, other countries take a different regulatory approaches to manage the problem of urban stormwater pollution. These different approaches present a challenge on whether the Up-Flo[®] Filter System can meet the various approaches. The results from the Up-Flo[®] Filter System experimental work allows for an assessment of the systems use in various regulatory frameworks. Section 5.1 of this chapter presents these assessments, which are then analysed in Section 5.2.

To ensure the Up-Flo[®] Filter System remains compliant with the regulations it must be maintained, and the best maintenance practices must be used. Section 5.3 presents the current maintenance protocols of the Up-Flo[®] Filter System and recommendations on improving them.

These discussions and assessments are then summarised in Section 5.4, where the main highlights are presented for the readers information.

5.1 The Up-Flo® and Treatment Regulations

The experimental results in Chapter 3 describes the hydraulic and sediment retention performance of the Up-Flo® Filter System. Understanding the performance allows for the Up-Flo® Filter System's use in various regulatory environments to be assessed fully.

Sub-sections 5.1.1 to 5.1.4 outline the key regulatory requirements in four countries across four continents. Using the regulatory frameworks of these countries, the Up-Flo® Filter System is assessed on whether the system can meet the standards.

Sub-section 5.1.1 presents an analysis of the regulatory frameworks in North America. The United States of America is chosen for the analysis, as the Up-Flo® Filter System is currently sold there and due to its geographic size.

The regulatory frameworks in Europe are then analysed in Sub-section 5.1.2, due to its size and geopolitical role within the region Germany is chosen for analysis.

Sub-section 5.1.3 then presents the analysis of regulatory frameworks in the Oceania region, New Zealand is chosen as the Up-Flo® Filter System is currently sold there under exclusive license by Hynds [110]. As of 2012 the Up-Flo® Filter System was also the only up-flow treatment device available in New Zealand.

Finally, the regulatory frameworks for stormwater treatment in Asia is analysed in Sub-section 5.1.4. The Peoples Republic of China is chosen for this analysis, due to China's geographic and population size and its economic growth in the region.

5.1.1 *United States of America*

In the USA the regulation of manufactured stormwater treatment devices is state dependent, which results in difficulty in the assessment of the suitability of the Up-Flo[®] Filter System country wide. Because of this, the focus of this analysis is based on the regulations of the State of New Jersey. As New Jersey currently provides certification for the Up-Flo[®] Filter System and has a Technology Acceptance Reciprocity Partnership (TARP), which reduces subsequent review and approval time in partner states [111]. The TARP partner states are California, Massachusetts, Maryland, Pennsylvania, and Virginia.

In the State of New Jersey, the New Jersey Corporation for Advance Technology (NJCAT) and the New Jersey Department of Environmental Protection (NJDEP) work jointly under a Performance Partnership Agreement (PPA) to regulate stormwater treatment. NJCAT is responsible for performing the technology verification reviews, whilst NJDEP uses the technological verification reviews to certify the technologies meet regulatory intent and that the technology has net environmental beneficial effects. The PPA also requires that NJDEP enters into reciprocal environmental technology agreements with the USA EPA, which allows for the potential use of certified technologies in other states [112].

Part of the NJCAT verification testing is that the manufactured treatment devices must have a removal efficiency of more than 80.0% [113] of Sil-Co-Sil 106. In 2017 the Up-Flo[®] received NJCAT and NJDEP certification [114], which was conditional on a number of circumstances related to the installation and maximum treatable flow rates. The site run-off must be less than the maximum treatable flow rate of the system, this dictated what configuration and size of Up-Flo[®] Filter System could be used.

Due to the similarity between Sil-Co-Sil 106 and silica flour, an analysis of whether the Up-Flo[®] Filter meets the NJDEP and NJCAT requirements can be made. ST01 had the following removal efficiencies 75.5% and 81.2% for average TSS and mass balance calculations respectively. For ST02 the removal efficiencies calculated through average TSS and mass balance was 78.3% and 78.0%, respectively.

ST01 shows that the Up-Flo® Filter meets the 80.0% target when calculated using the full mass balance method. Using the TSS method results in the Up-Flo® failing to meet the standard. Whilst the TSS method of calculation results in the Up-Flo® failing the standard, this is likely resultant from the lower number of samples it was based on and the mass balance would be more accurate.

The results for ST02, using both methods of calculation, were below the 80.0% target set by NJCAT and NJDEP. However, the results showed a decreased removal efficiency with increased experimental time. The NJCAT and NJDEP only required a experimental time of around 9 mins dosed flow for the 6 module set-up, and as the removal efficiencies are close to 80.0% it appears that with a reduced experimental time the Up-Flo® would meet the regulatory target. As Figure 3.33 shows the TSS removal efficiency at 10 mins after sediment dosing started for ST02 T33 and ST02 T34 was 90.5% and 85.2%. Further suggesting the Up-Flo® does meet the regulatory target.

The lower removal efficiency as experimental time increased and the lower removal efficiency seen on ST02 T34 raises questions on the method of experimentation the NJCAT verification utilises. As during any reasonable storm the flow is longer than 9 min, and media will not be replaced after each storm event. Typical rainfall duration in the North East of the USA is around 3 hours in summer and seven hours in winter [115]. This results in the 80.0% target not being met in realistic operation, however the NJCAT verification also uses Sil-Co-Sil 106. This has a median size of 38.8 μm , whilst a US geological study found the median particle size of suspended solids in urban run-off ranged from 42 μm to 200 μm , dependent on site use [116]. Results from ST03 showed that with the longer experimental period and a larger median particle size of 150 μm , the removal efficiency was 98.7% which implies that the Up-Flo® would meet the 80.0% removal of suspended solids in realistic operations.

5.1.2 Federal Republic of Germany

Similarly to the USA, the responsibility of the management of urban stormwater in Germany is delegated to municipalities. However, as with the UK it is bound by the European Union's Water Framework Directive, described in Chapter 2, which was implemented into German domestic legislation with the German Federal Water Act 2009 [117]. This set the legal frameworks nationally for stormwater management. The German Association for Water, Wastewater and Waste (DWA) also has responsibility in the standardisation of stormwater treatment [118].

Whilst German guidance documents are based on load reduction targets as with US NJCAT, in implementation an indicator based system has been adopted [119]. In the DWA's guidelines on stormwater treatment dimensionless values are used to quantify air quality, $A_{quality}$, and surface contamination, $S_{contamination}$. These two values are used to provide an emission value, $T_{emission}$ ($T_{emission} = A_{quality} + S_{contamination}$). This emission value is then compared to the receiving waters sensitivity, represented by an admissible value $T_{admissible}$. If the emission value is higher than the admissible value then treatment is required. The removal efficiency, $T_{removal}$, of the treatment device must bring reduce the total emission below the admissible value, as shown below [119].

$$(A_{quality} + S_{contamination}) \times T_{removal} < T_{admissible} \quad (5.1)$$

Due to the more complicated treatment guidelines, forming an analysis of whether the Up-Flo[®] Filter System would work in this regulatory environment is difficult. However, the treatment guidelines fit well with the findings of the Up-Flo[®] Filter System experiments in Chapter 3. As discussed in Section 3.15, to fully optimise the operation of the Up-Flo[®] Filter System in-depth information about the installation environment must be known. This treatment standard requires a unique design for each location, which would allow the Up-Flo[®] Filter System to be optimised to the installed locations.

However, whilst this standard may be appropriate for the optimisation of the Up-Flo[®] Filter System, it does cause issues with marketing and sales. As it cannot be sold as a certified technology it provides difficulty in marketing it as an effective treatment device. A way to solve this would be the development of a calculator, which takes the basic

information the standard requires, and then it can either approve or disapprove the Up-Flo® Filter System according to the site characteristics. This would be a more indirect sales model, and would require more of a site design approach where all Hydro International Ltd technologies would be assessed. The technological set-up that meets the standard could then be recommended.

5.1.3 New Zealand

New Zealand stormwater management is a devolved issue, where the devolved institutions are responsible for regulation. Auckland Council is chosen for this analysis as the Up-Flo[®] Filter System was originally approved for use by Auckland Council. It was approved as it met a TSS removal target of 75% outlined in the TP10 guidance [110]. However this approval excluded locations where concentrations of heavy metals were anticipated to be above average, such as roads with more than 20,000 vehicles a day [110].

However, TP10 has been superseded by GDD1 and the target of 75% removal of TSS has been removed and replaced with a design performance based approach [120]. The solution to stormwater management outlined by GDD1 is to deal with it in three stages [120].

1. Stormwater is first treated with hydraulic and physical processes. Which includes sedimentation and screening.
2. Stormwater is then to be filtered, so as to remove fine particles and sediment.
3. The final stage requires that the stormwater is treated using biological, chemical and thermal processes.

A key requirement introduced in the GDD1 for sediment removal is that whilst there is no longer a targeted percentage removal of TSS, TSS of treated effluent must be below 20 mgL^{-1} . Which represented typical effluent from most TP10 certified devices [121].

Using urban stormwater data from the Auckland region allows for the estimation on whether the Up-Flo[®] Filter meets the stricter standard. The d_{50} for urban run-off in Pakuranga Auckland is approximately $45 \mu\text{m}$ [122] and the mean TSS in urban run-off is 130 mgL^{-1} in the Auckland region [123]. Approximately 81.0% removal was seen for this particle size range during ST02, this removal would result in the treated water containing 24.7 mgL^{-1} of TSS. This results in the Up-Flo[®] Filter not being usable in this scenario. This also demonstrates how the current New Zealand standard is much stricter than that

of the USA standard, as it meets the 80% removal target of New Jersey but fails to reduce the TSS to below the New Zealand requirements.

Whilst the Up-Flo® Filter System fails in the outlined scenario, it can still be used in other areas of Auckland as long as the TSS of the urban run-off no more than approximately 104 mgL^{-1} . For use under the current New Zealand regulatory environment, in-depth information of the installation is required before the Up-Flo® Filter System can be utilised.

A way to solve this might be to place two Up-Flo® Filter Systems in series, this would significantly raise the installation and maintenance costs. A cheaper way to solve this could be to change the filter media, to one with a lower grain size. This would increase the retention of sediment within the filter media, however this would result in a reduced treatment capacity.

5.1.4 Peoples Republic of China

On January 1st 2018 the revised ‘Water Pollution Prevention and Control Law’ was brought into effect. This law strengthened the governmental responsibility and supervision of stormwater treatment [124]. The law previously established the national stormwater treatment standards known as the ‘Environmental Quality Standards for Surface Water GB 3838-2002’, which were formed to implement the fore-mentioned law and the ‘Environmental Protection Law’, and to control pollution and to protect water resources [125], [126]. These standards classified water bodies, according to the utilisation and protection objectives, and set the requirements for the surface water body.

The fundamental requirements outlined by the standard is that all water bodies should not contain the following substances which result from artificial causes:

1. “substances that can precipitate and become disgusting sediments”
2. “floating matter, such as fragment, floating slag, oil and other matter that leads to unpleasant perception”
3. “substances that produce disgusting colour, smell and turbidity”
4. “substances that are harmful, toxic to or has negative physical effects on human beings, animals and plants”
5. “substances that benefits the disgusting aquatic organism”

The Up-Flo[®] Filter System would aid in fulfilling the fundamental requirements of 1 and 2, and may aid in the other requirements. However, unlike the previous case studies TSS has no specific requirements. Instead other stormwater pollutants are targeted, meaning analysis of the Up-Flo[®] Filter System potential to meet the standards is difficult.

However, as discussed in Chapter 2, sediment is a source of other pollutants due to its adsorption capabilities. As heavy metals are one pollutant typically associated with sediment particles[127], and the numerous amounts of pollutant targets within the

Table 5.1: China case study heavy metal concentrations in Beijing road run-off and the limits of receiving water bodies.

Source and targets	Copper, Cu [mgL ⁻¹]	Lead, Pb [mgL ⁻¹]	Cadmium, Cd [mgL ⁻¹]	Zinc, Zn [mgL ⁻¹]
Class I [125][126]	<0.01	0.01	0.001	0.05
Class II [125][126]	1.0	0.01	0.005	1.0
Class III [125][126]	1.0	0.05	0.005	1.0
Class IV [125][126]	1.0	0.05	0.005	2.0
Class V [125][126]	1.0	0.1	0.01	2.0
Beijing [128]	0.053 - 0.987	0.056 - 0.774	0.020 - 0.162	1.421 - 59.855

standards, this case study will assess the Up-Flo® Filter System suitability in meeting the heavy metal surface water targets.

To assess the Up-Flo® Filter System, Beijing road run-off heavy metal concentrations are used as it is an urbanised area. The regulatory limits for each class of water body and typical stormwater run-off heavy metal concentrations are shown in Table 5.1. The full regulatory limits from the previous GB 3838-88 in English are shown in Appendix E.1, the full list in English could not be sourced for GB 3838-2002.

Table 5.1 shows that Pb, Cd and Zn all fail the regulatory targets for the receiving water body that have been set, and Cu fails for Class I water bodies and is close to the limits for the other classes. The receiving water will have a dilution effect on the polluted stormwater. But as the receiving water won't be pure clean water, and so will have background pollution, to reduce the risk of the water body exceeding the regulatory limits it is best to treat the run-off to below or close to the regulatory limits.

Table 5.2: Heavy metal size ranges with the average removal efficiency of Up-Flo[®] Filter from ST02. (Range of metal TSS using distribution and Beijing case study [mgL^{-1}]) * down to $1.056\mu m$.

Size Range [μm]	Copper, Cu [%]	Lead, Pb [%]	Cadmium, Cd [%]	Zinc, Zn [%]	ST02 Up-Flo [®] Mean Capture [%]
>100	7 (0.0037 - 0.0691)	4 (0.0022 - 0.0310)	18 (0.0036 - 0.0292)	5 (0.0711 - 2.9928)	96.7
50-100	8 (0.0042 - 0.0790)	4 (0.0022 - 0.0310)	11 (0.0022 - 0.0178)	6 (0.0853 - 6.5841)	89.2
40-50	3 (0.0016 - 0.0296)	2 (0.0011 - 0.0155)	6 (0.0012 - 0.0097)	3 (0.0426 - 1.7957)	82.1
32-40	4 (0.0021 - 0.0395)	4 (0.0022 - 0.0310)	5 (0.0010 - 0.0081)	5 (0.0711 - 2.9928)	77.3
20-32	4 (0.0021 - 0.0395)	5 (0.0028 - 0.0387)	5 (0.0010 - 0.0081)	5 (0.0711 - 2.9928)	71.9
10-20	11 (0.0058 - 0.1086)	8 (0.0045 - 0.0619)	9 (0.0018 0.0146)	16 (0.2274 - 9.5768)	65.87
<10	63 (0.0333 - 0.6218)	73 (0.0409 - 0.5650)	46 (0.0092 - 0.0745)	60 (0.8526 - 35.9130)	62.3*

By comparing the heavy metal particle sizes and the average Up-Flo[®] Filter System removal efficiency for that size range allows for an estimation of the heavy metal removal by the Up-Flo[®] Filter System. Vignoles and Herremans [129] conducted research into the distribution of heavy metals in various sediment size ranges. The distribution of metal sizes is shown in Table 5.2.

Using Vignoles and Herremans weighting and the average Up-Flo[®] Filter System removal efficiency for the corresponding particle size range, the treated Beijing stormwater would have the characteristics shown in Table 5.3.

Table 5.3: Estimate of treated Beijing run-off using the weightings and removal efficiencies in Table 5.2. With the regulatory targets for reference.

Source and targets	Copper, Cu [mg L ⁻¹]	Lead, Pb [mg L ⁻¹]	Cadmium, Cd [mg L ⁻¹]	Zinc, Zn [mg L ⁻¹]
Class I [125][126]	<0.01	0.01	0.001	0.05
Class II [125][126]	1.0	0.01	0.005	1.0
Class III [125][126]	1.0	0.05	0.005	1.0
Class IV [125][126]	1.0	0.05	0.005	2.0
Class V [125][126]	1.0	0.1	0.01	2.0
Treated Beijing	0.0165 - 0.3077	0.0187 - 0.2592	0.0052 - 0.0418	0.4543 - 19.4594

The treated flow shows that the Up-Flo[®] Filter System would produce a treated effluent that was above the majority of the heavy metal limits imposed in China. This is resultant from the less than 10 μm particles making up significant sources of the heavy metals, which is where the Up-Flo[®] Filter System has poor removal efficiencies. The Up-Flo[®] Filter System could be adapted to reach the standards presented by a change of filter media, a lower pore sized media would allow more capture of heavy metals. Also, using a different material for a filter media would allow for potential chemical treatment to remove the heavy metals.

However, the treated effluent is much closer to the standards. As long as the receiving body had sufficient volume and are sufficiently below the heavy metal limits, the dilution effect should result in the receiving body remaining below the limits. If however the receiving water body was very close to the heavy metal limits, then the stormwater would need further treatment.

As with the treatment standards in Germany and New Zealand, the Up-Flo[®] Filter System needs in-depth information on the surrounding environment to establish whether it is a viable option for stormwater treatment.

5.2 Regulation Discussion

Analysing the role of the Up-Flo[®] Filter System within various regulatory frameworks, has outlined the different approaches countries take to stormwater management and regulation. The analysis shows that the Up-Flo[®] Filter System struggles with some types of regulatory frameworks. Whilst the Up-Flo[®] Filter System meets the USA New Jersey standards, it faces problems with some of the more modern standards developed in Germany, New Zealand and China. All the standards have positive and negative aspects to them, which are discussed below.

The USA standard allows for independent certification of the treatment devices, meaning its performance has been verified. This allows for the Up-Flo[®] Filter System to be sold more easily as it will have approval by the state, this also leads to easier product development as the key requirements are clear. However, drawbacks to the standard are that the Sil-Co-Sil 106 is a smaller size range than what is to be expected leading to over design of manufactured treatment devices. Problems are also encountered with its experimental verification, the length of experimental time is shorter than typically seen in a storm event. Which results in a unrealistic removal efficiency.

Additionally, the USA standard doesn't take into account the receiving water bodies sensitivity to pollution. In this scenario a manufactured treatment device could reach the 80% removal, but the treated effluent may still negatively impact the receiving water body.

The German standard appears to be a more developed standard than that of the USA. By taking into account the pollution and the receiving water bodies characteristics, the standard is much more related to what is more beneficial at each site. However, the lack of certification and verification causes issues with developing a market for the Up-Flo[®] Filter System. With a new method to develop the market needed. The requirement for such detail as well, adds further time and cost to stormwater treatment. Potentially causing problems in the development of manufactured stormwater treatment devices in the longer term, as companies have less clear objectives to complete.

The New Zealand standard presents almost a hybrid of the USA and German standard. The standard is stricter than that of the USA standard, but does present more clear objectives in the stormwater treatment than the German standard. Problems associated with the New Zealand standard is that the 20 mgL^{-1} effluent target appears to be too strict for the Up-Flo[®] Filter System to meet. Which could be fixed with a smaller pore sized media, however this may lead to over design where the media becomes clogged too quickly and run-off bypasses the Up-Flo[®] Filter System. The standard would also require in-depth information about each sites run-off characteristics, which adds time and cost to the installation processes. However, this was recommended to optimise the Up-Flo[®] Filter System processes anyway. As with the German standard, certification is not utilised which will result in difficulties in marketing and product development. Further, as with the USA standard this standard doesn't take into account the sensitivity of the receiving water body.

The China standard is the most difficult standard for the Up-Flo[®] Filter, as it does not target suspended solids themselves but related pollutants using a similar method to New Zealand. The case study shows that the Up-Flo[®] Filter System could be used to treat Beijing urban stormwater run-off, if the dilution effect of the receiving body is sufficient. The exclusion of specific TSS standards results in difficulty in product development, and the targets set for heavy metals will result in over design. Which would cause the filter to clog more quickly, and potential bypassing.

The four standards presented show a wide range of approaches to the issue of stormwater management. The newer standards are stricter than the more traditional standards, which is more beneficial to the environment. However, there is a potential with the newer standards to over design which in the long term would be worse for the environment and longevity of the devices manufactured.

A combination of the standards may be more appropriate, building in a certification and verification process as with the USA would allow for more product development. This process would require a more realistic experimental sediment than that of Sil-Co-Sil 106. Additionally, the 80.0% target of the USA standard would not be good enough. A target of a max TSS of treated effluent as with the New Zealand standard would be more

appropriate and would allow for the most appropriate device to be used at each site. However, the 20 mgL^{-1} target may be too strict leading to the over design of treatment devices. Research is needed to determine the most appropriate level for this TSS value. The German technique that takes into account the receiving water bodies susceptibility to pollution, may be a more appropriate method. However, this adds complexity to the treatment process.

Alternatively, a class based system could be designed, where the receiving water characteristics are classified, and a max effluent TSS target could be set for each class. This would combine the benefits of both the German and New Zealand standards.

As newer standards move towards the more strict models, the Up-Flo[®] Filter System will require further in-depth experiments to ensure that it remains usable. Additionally, the method used by Hydro International Ltd to sell the Up-Flo[®] Filter System would need to adapt. In the USA as long as it passes the certification process, the system could be sold off the shelf. However this type of business model has a high level of risk, as there is a high probability that countries will move away from this type of regulation. This is seen in the newer standards, the removal of certification in New Zealand, and the fact that the USA is moving towards more strict regulations. There is a limit to how strict a standard can be, so it could be that a change in regulatory approach will be seen in future.

In regulatory environments like Germany and New Zealand a more bespoke a consultative sales approach is required. In this approach the treatment plan would be designed by Hydro International Ltd, which allows for the Up-Flo[®] Filter System to be optimised to the installation site. With this approach Hydro International Ltd would need to employ more consultants, increasing the cost of the Up-Flo[®] Filter System. This obviously raises the risk of the system not selling, however competitors would be in the same position. If Hydro International Ltd takes on a more consultancy based sales approach in these countries now, then as more countries adopt this style of regulation Hydro International Ltd would have the knowledge and expertise available to adapt and ensure the continued sales of the Up-Flo[®] Filter System. Additionally, it would mean they have an advantage over the competition, who might have to build their consultative based approach from scratch.

Hydro International Ltd typically works with a local business partner in other countries to sell the Up-Flo[®] Filter System, such as Hynds Environmental in New Zealand or Rocla in Australia. It would be important to pick a partner that has a consultative sales based approach to ensure the long term sellability of the system. China will be a key potential future market for the Up-Flo[®] Filter System, so it is important to ensure the system can be easily sold there. Whilst there are no specific treatment standards for sediment in stormwater run-off at this moment in time, if these are brought in then it is likely to follow a similar method to Germany or New Zealand. This is because at the moment their standards are very specific to the receiving water body. This means that any sediment stormwater treatment standards introduced would likely follow the existing approach rather than adopting a USA type method.

Development of a stormwater treatment calculator, that takes into account the installation sites and receiving water specifications, would aid in the consultative sales model. Having a calculator that can highlight the estimated pollutant removal could aid the consultants treatment design. Additionally, making this available to businesses partnered with Hydro International Ltd may aid in the Up-Flo[®] Filter System being chosen for treatment.

Through ensuring the sale method is prepared for the changing regulatory approaches, and by conducting more in-depth research, the risk of the Up-Flo[®] being unsellable reduces.

5.3 Maintenance Guidelines

The research presented in this thesis allows for the maintenance routine of the Up-Flo[®] Filter System to be analysed and recommendations made.

As part of the NJDEP certification, the Up-Flo[®] Filter System must be maintained using the maintenance document provided by Hydro International Ltd. This maintenance document requires that during the first year installation, the Up-Flo[®] Filter System is inspected and maintained every 6 months. From this the inspection frequency is determined, with a minimum frequency of one year.

During the maintenance cycle, the sump is emptied and the filter bags are weighed. If the wet weight is 9 *kg* heavier than the wet weight of a clean filter media bag then the filter media bags are to be replaced [130].

However, the results from the permeability experiments indicate that even with a clean water flow the permeability drops. This results in a reduced max flow rate over time and leads to more stormwater bypassing the system.

Unless the system is inspected during a storm event, it would be difficult to acquire this knowledge. In order to return the media back to optimum working condition the media would need to either be replenished or potentially severely disturbed. This is recommended during each maintenance routine, as weighing the bag to determine bag exhaustion would not be enough to maintain the Up-Flo[®] Filter System and its filter media performance.

As discussed earlier, the changing regulatory landscape requires that the site environment is taken into account further. With these new approaches, the maintenance plan can be adapted further to the needs of the environment. For example, sites which have a particle size range closer to that of Fraction E would capture less within the filter media and more within the sump. This would require the sump to be emptied more frequently, and the filter media would need to be changed or disturbed more regularly than present to maintain the treatment capacity.

A final recommendation would be to impose an additional inspection each year where the Up-Flo[®] Filter System is checked during a storm event, where the water height in the Up-Flo[®] Filter System would be checked. Additionally, then storm and catchment data would be used to estimate the flow rate into the Up-Flo[®] Filter System. Then by comparing the estimate flow rate to the water height the max flow rate changes could be estimated. Once the max flow rate had reduced significantly then the filter media would need to be replenished or severely disturbed.

These recommendations would allow the Up-Flo[®] Filter System operation to be maximised and the environment protected further, by preventing storm overflow operating. If the filter media could be brought back to the designed permeability through severe disturbance, this would allow for Hydro International Ltd to reduce maintenance costs by not changing the media when the media has not been exhausted.

5.4 Chapter Summary

This chapter has highlighted the regulatory and maintenance issues that surround the Up-Flo[®] Filter System and possible solutions around them.

The four regulatory frameworks presented has shown the wide variance in stormwater management. The Up-Flo[®] Filter System struggles to pass some of the more modern and stricter standards, such as by New Zealand. The more modern standards are more site specific, requiring more information on the characteristics of the stormwater and the receiving water body to ensure the treatment reaches the standard. This is better for the environment but may lead to more over development of treatment device designs. Which may result in longer term problems of the treatment devices. As the stormwater treatment standards are developed further, and the more stricter approaches used, further research will be needed on the Up-Flo[®] Filter System to ensure its viability in the more modern frameworks. This would also require the business model of selling to adapt, with a more bespoke method of selling required.

The protocols currently used to maintain the Up-Flo[®] Filter System require that the site characteristics are taken into account further, as with the modern regulatory frameworks. Additionally, the results from the permeability experiments show that even when there is no sediment capture the permeability decreases. This decrease in permeability would increase removal efficiency, as shown in ST01, but this also results in a drop in treatment capacity. As the max flow rate through the device drops, leading to more bypass events. So to ensure the Up-Flo[®] Filter System remains in peak operational condition, a further inspection is required each year where a storm event is taking place. If the flow rate through the media has dropped significantly then the bags will need either significantly disturbing or replacing.

Chapter 6

DISCUSSION

Chapters 1 and 2 both outline the effect of diffuse urban pollution within stormwater on surface water bodies. The effects can be devastating to both aquatic flora and fauna, and can limit the economic use of surface water bodies. As the UK utilises more separate drainage systems, where stormwater and sewage are drained separately to prevent combined sewage overflow events, the need to treat stormwater before it damages the environment becomes more important than ever. The Up-Flo[®] Filter System is one device that is designed to treat stormwater pollution and is sold in various countries. This project was formed to address some of the system's maintenance issues, and to enhance understanding of its performance so as to optimise it, further protecting the environment. To accomplish this, the project was conducted with both industrial and academic support. This formed two aims and was measured against a number of objectives. This chapter discusses how these aims and objectives were met, and outlines what future work is required.

Section 6.1 brings together the main discussion points from the previous chapters and discusses how the aims to optimise the Up-Flo[®] Filter System's performance and maintenance, and increase knowledge of granular media, were achieved. Including an analysis of the objectives completed, and details future work required. Additionally, the experimental method used in this project is compared to the NJCAT experimental method used by Hydro International Ltd. Recommendations are also made to improve Hydro International Ltd product development in the future.

One way to complete the aim to optimise the Up-Flo[®] maintenance protocols was through the assessment of a filter media monitoring system. Section 6.2 discusses how this was done, what was found, and what further work may be required.

Section 6.3 summarises the discussion for the reader, with a summary of how the aims and objectives were achieved.

6.1 Up-Flo® Filter System Experiments

To complete the aims of optimising the Up-Flo® Filter System's performance and maintenance, and increase knowledge of granular media, various work was undertaken which was measured against a number of objectives.

Objective 1 was to research the background theories and to form a review of the current literature. This objective was fully completed. Chapter 2 presents the literature review covering the theory behind the sediment removal processes of the Up-Flo® Filter System. Two processes are key to the Up-Flo® Filter System's stormwater treatment; sedimentation and separation, and filter media capture. These are governed by a number of physical laws, including Stoke's Law and Darcy's Law.

Objective 2 was to design and build the experimental set-up and equipment for the project. To complete this objective a rig was designed to house the Up-Flo® Filter System. The bespoke constructed rig allowed for the Up-Flo® Filter System to be installed in a similar fashion to standard manhole installations of the system, while allowing for in-depth measurements to be carried out. The rig sat within the experimental set-up shown in Figure 3.2, and later within the adapted set-up shown in Figure 3.6. This set-up allowed for the system to be tested with; a constant pressure head allowing a stable flow rate, and mass balances for an in-depth sediment removal mechanism investigation.

Objective 3 was to conduct experiments measuring variables such as permeability and sediment removal efficiency. Chapter 3 outlines the work undertaken to complete Objective 3. Experiments were first conducted with clean water to provide a better understanding on the permeability of the filter media and its background changes without sediment loading. Experiments then progressed to examine the impact of sediment loading on the Up-Flo® Filter System, including removal efficiencies and mechanisms.

Objective 4 was to interpret the collected data. The discussion presented in Chapter 3 interpreted this data, developed recommendations in regards to system and maintenance optimisation, and developed knowledge of granular media permeabilities and removal

techniques.

Objective 5 was to form an analysis of different legal frameworks the Up-Flo® Filter System may operate in, and how its use can be optimised. Using the results and discussion presented in Chapter 3 allowed for analysis of whether the Up-Flo® currently meets the standards presented in Chapter 5. Additionally it allowed for the system viability to be assessed against developing regulations and standards.

Objective 6 was to form an EngD thesis, presenting the results and analysis of the work conducted, this thesis completes this objective.

Through completing Objectives 1 to 6, knowledge has been developed that can be used to optimise the performance and maintenance of the Up-Flo® Filter System, enhancing environmental protection. Additionally, it has developed knowledge in regards to granular media permeability and sediment removal techniques.

By first undertaking clean water experiments, key information regarding the Up-Flo® Filter System treatment capacity, system longevity, and permeability changes in granular media were found. The clean water experiments found that the filter media permeability declined as flow was passed through it, falling 37.4% between experiments T05 and T23. This decline was also seen in the clean water cycle experiments before the sediment dosed experiments in ST01, ST02 and ST03. Section 3.15 analysed the reasons behind this fall in permeability and three possible reasons were highlighted; biological growth within the media, sediment capture from the background TSS of the influent water, or rearrangement of filter media grains. Through a process of elimination it was found that filter media grain rearrangement was the only reasonable cause behind the filter media permeability decline, as the data matched the two characteristics anticipated from filter media grain rearrangement.

Firstly, the permeability would decline as flow is passed through the media. Figure 3.24 showed that the exponential line of best fit had a negative constant, indicating the permeability declined as flow was passed through the filter bed. Secondly, the decline in permeability would slow and eventually stop when it reached a peak rearrangement. This second condition was also met, as Figure 3.24 and 3.21 showed that the permeability

decline between each test and during each test declined until they reached very small value by experiment T15.

This filter media grain rearrangement occurs due to Stoke's Law. As water flows through the filter media, stratification occurs as smaller sized particles rise to the top of the bag and larger sized arrange at the bottom of the bags. This is resultant as the settling velocities are different, with the larger sized particles having a larger settling velocity, whilst smaller particles have a smaller velocity. This results in smaller particles being carried up by the water velocity faster than the larger particles. As the grains are restrained in the bag, this eventually results in stratification where the larger particles are at the bottom, and the smaller particles are at the top.

This permeability drop impacts the total treatment capacity of the Up-Flo[®] Filter System as a lower permeability requires larger water level in the rig to pass the same flow rate through. This causes the maximum treatable flow rate to fall, as the water level approaches the overflow device. This is significant as this can cause untreated stormwater to bypass the system, resulting in pollution in surface water bodies. Figure 3.48 was developed using recorded water level readings when the Up-Flo[®] Filter System's overflow operated, this shows the maximum treatable flow rate against filter media permeability. This figure shows that as the permeability decreases the maximum treatable flow rate also falls, the maximum treatable flow rate specified by Hydro International Ltd for the 6 module system is 9.5 Ls^{-1} . This treatment capacity corresponds to a permeability of $6.6 \times 10^{-10} \text{ m}^2$, which is similar to the clean water measured result in ST02. By measuring the permeability, the treatment capacity of the Up-Flo[®] Filter System can be monitored. This presents an interesting route to maintenance optimisation. If the system experiences a similar decline in permeability to that seen in the clean water experiments, then the maximum treatable flow rate will reduce to 6.2 Ls^{-1} without any sediment capture. This has repercussions on the environment, as it will cause untreated stormwater to enter surface water bodies.

This clearly impacts the performance of the Up-Flo[®] Filter System, as any increased filter media capture caused by the lower permeability is negated by the potential of untreated effluent mixing in with the treated water. For example, if we consider a TSS of

200 mgL^{-1} (with a similar profile to Silica Flour) influent at 8 Ls^{-1} , after the decline due to stratification this would result in the effluent containing 79.1 mgL^{-1} rather than the 44 mgL^{-1} expected if all the flow was treated.

In order to optimise the performance of the Up-Flo® Filter System it is important to take the stratification effect into account. If the installation sites have a typical influent of less than 6.2 Ls^{-1} , then the system is usable with no optimisation required. This is because even after the stratification related permeability drop, the capacity of the device is large enough to treat the influent without the overflow being used. In sites where the flow rate is above 6.2 Ls^{-1} then it is necessary to redesign the system to ensure that the flow is less likely to pass through the overflow device. There are a number of ways to do this; firstly increasing the height of the Up-Flo® Filter System's overflow chamber would allow an increase in maximum treatable flow rate. However, this would be restricted by the installation site characteristics and would increase manufacturing cost. A second route to mitigate the falling permeability would be to use a more mono-sized media, resulting in less changes in permeability due to stratification. This would result in an increased cost in the operation of the Up-Flo® Filter System, as a more mono-sized media would be more expensive. Thirdly, using a larger sized filter media could help as it will result in a larger treatment capacity from the beginning, mitigating the effect of the falling permeability. However this would result in a lower treatment efficiency by the filter media. When filter media filtration is not as important to the treatment of the influent, then this could be an ideal solution. Sites with a lower sized sediment would result in the filter media being more important. Fourthly, at sites where the influent sediment is above 55 μm , filtration by the filter media is not a key process. This results in a flow control device being a suitable alternative as sediment will be settled in the sump and treatment capacity is maintained.

As the sump is the main source of capture, and the estimated extra decrease in permeability caused by silica flour is small. The 9 kg per filter bag required for necessary replacement causes an estimated 28.8% drop in permeability. This shows the changes due to filter media grain rearrangement has more of an impact on maximum treatable flow rate than sediment capture will have. This raises questions whether sediment capture

within filter media should be the key concern in the maintenance of the Up-Flo[®] Filter System. As outlined in Chapter 5 the maintenance routine involves weighing the bags. If the bags are 9 kg heavier than the clean weight, then they are changed. To ensure the Up-Flo[®] Filter System remains in optimal operation, the maintenance will need to be adapted. The filter media will either need severe disturbance or replacement during maintenance, even if the 9 kg is not met. Further work is needed to investigate whether severe disturbance could restore the designed permeability, and hence the designed treatment capacity.

The discovery of the stratification effects allows the optimisation of the Up-Flo[®] Filter System performance and maintenance routines, a key aim of this project. Additionally, the discovery shows that stratification is an important effect in granular medias contained in an up-flow filter design. This is resultant from the different settling velocities.

The work in Chapter 3 showed that the measured permeabilities in different modules were different. The discussion of these results show that this is due to the extra head required to drive the treated effluent across the conveyance channel to the outlet module. Which results in a lower flow rate the further away the module is from the outlet module (Modules 4, 2 and 1 having an estimated flow rates of 0.31 Ls^{-1} , 0.34 Ls^{-1} and 0.38 Ls^{-1}). As the flow rate lowers when further away from the outlet, numerous considerations need to be made. Firstly, the maximum flow rate per module of approximately 1.0 Ls^{-1} given by Hydro International Ltd is wrong. When more modules are added, the increase in total max treatment capacity would not be as high as estimated by Hydro International Ltd. The extra flow rate capacity caused by the addition of modules would decrease as more modules are added. This is significant as it means that the treatment capacity is lower than anticipated, to ensure this does not happen this effect will need to be taken into consideration during the stormwater treatment design and installation. By taking this into account the Up-Flo[®] Filter System performance can be optimised, a key aim in this project. Further work is needed to fully establish this relationship, with different flow rates tested across various numbers of installed modules.

Additionally, the maintenance of the Up-Flo[®] Filter System will be impacted by this. As

modules have different levels of flow passing through them, then there will be different levels of sediment capture and stratification. This will result in filter bags in different modules requiring replacement at different time intervals. However as the difference in flow rates is relatively small this may not have a massive impact on sediment capture. If we assume that after settlement there was 100 mgL^{-1} passing through the filter media in a three hour storm, Module 4 would be exposed to 334.8 g of sediment whilst Module 1 would be exposed to 410.4 g . Whilst the modules furthest away would have the lowest amount of sediment exposed to them, these modules may capture more as the removal mechanism is adhesion not straining. The reduced flow rate results in a longer residency time within the filter media, resulting in more successful adhesion. Further work is needed in regards to the effect of increasing modules and filter media capture, to determine which modules would capture more sediment.

This knowledge of different flow mechanisms allows for the better optimisation of the Up-Flo® Filter System performance. With further work, the maintenance routines could be better optimised, fulfilling key aims of the project.

When the filter media was switched due to supply issues, there was a noted increase in permeability which was expected due to its slightly coarser profile. Additionally, the decline due to stratification was lower than that seen in the clean water experiments and ST01. This requires further work to investigate the long term decline in permeability caused by stratification, and to investigate whether there is still a total 37.4% drop in permeability. This is incredibly important as it determines the max treatment capacity.

The sediment dosed experiments outlined in Chapter 3, found a number of results that can optimise the Up-Flo® Filter System performance and maintenance routines. Firstly, the system was found to be capable of removing between 75.5% and 98.7% of dosed sediment at 2 Ls^{-1} . This was dependent on sediment particle size, filter media grain size, and it took time to reach equilibrium. Secondly, it was found that the sump of the system was responsible for the majority of sediment capture with an increased particle size resulting in increased settlement. Thirdly, at the fine silts and clay size range there was a slight increase in sediment removal caused by increased settlement.

Figure 3.47 shows that as sediment size increases, the removal efficiency also increases. This is also apparent by ST03 data which showed the larger sized sediment managed 98.7% removal. Whilst influent sediment size is difficult to control, having in-depth knowledge in regards to the removal efficiency and particle size relationship, will allow for the optimisation of the Up-Flo[®] Filter System during the stormwater treatment design by changing either the type or size of the filter media. In sites with a large particle size range ($>55 \mu m$) the sump is responsible for the majority of sediment removal, and the filter media is responsible for restricting the flow enough to increase settlement. The maintenance routine would need to be adapted, as the filter media would not need replacement due to sediment capture as often, but would require replacement or possible disturbance to overcome the stratification issue reducing the maximum treatable flow rate.

However in sites where the particle size is typically less than $25.68 \mu m$ in size, the capture of sediment by the filter media is more important. The results from the experiments in Chapter 3 showed that the filter media sediment removal technique in the Up-Flo[®] Filter System is resultant from adhesion and not straining. The analysis shows that the Garside Sand filter media is capable of removing between 55.1% to 63.8% of silica flour below this size range. To ensure optimal stormwater treatment, a smaller grade of filter media is required to remove 80.0% of the sediment. Maintenance of the system would also need to be adapted. The sump would not need to be emptied as often but the media would need more frequent replacement. This filter media replacement would also be required more often to mitigate the effects of the stratification. As the sump doesn't capture much at this particle size range, the amount of flow required to reach 9 kg of sediment in each bag reduces from 600 kg to between 169.3 kg and 196.0 kg. This significantly reduces the system's longevity, reducing the total amount of stormwater that can pass through the system until filter media replacement is required. Dropping from 3,157,894.7 L to between 891,050 L and 1,032,000 L. This is a significant decrease in the maximum stormwater treatable, assuming an average of $2 Ls^{-1}$ then the Up-Flo[®] Filter System would last between 123 and 143 hours, significantly less than the approximate 438 hours for a sediment particle size range of silica flour. Many sites are unlikely to have such a small sediment particle size range, however construction sites could, and to optimise the

Up-Flo® Filter System this would need to be taken into account.

As mentioned previously, there was additional removal by settlement in the clay to fine silt size range. This size range typically contains a significant amount of particulate bound pollutants, so optimising the Up-Flo® Filter System to remove these is important. The analysis showed the extra removal by settlement is caused by flocculation. To increase the removal of these pollutants it is important to ensure there is optimal conditions for flocculation to occur. As mentioned in Chapter 2 a number of parameters affect flocculation, such as temperature, pH, concentration, and time. All these are difficult to control within installations of the Up-Flo® Filter System, but additional time could be given by the use of a smaller sized filter media and a larger overflow height. This combination would give further time for the particles to collide and form flocs, while additionally increasing removal by the filter media.

These results and analyses allow for the optimisation of the Up-Flo® Filter System performance and maintenance, by allowing the system to be optimised, if the installation sites environment is taken into account. Additionally, the analysis has enhanced understanding of the Up-Flo® filter media by showing its sediment removal technique is due to adhesion. This helps to complete the aims of this research project.

Chapter 5 explored the regulatory frameworks of stormwater treatment in various countries. It shows that more modern regulatory guidance requires a more bespoke treatment arrangement for stormwater management. This was especially seen in the German standards, which require information on both the influent stormwater and the receiving water body. Further, in the New Zealand standards, instead of percentile removal targets of sediment, treated effluent limits are utilised. These approaches suit the Up-Flo® Filter System as the analysis of the results has shown more information is required on the site characteristics to fully optimise treatment and maintenance routines. The different types of regulatory approaches will require different sales model. To ensure the continued sellability of the Up-Flo® Filter System within the more modern regulatory frameworks, Hydro International Ltd should prepare for a consultative selling approach. This approach would require Hydro International Ltd consultants to take into account the requirements and design the treatment approach.

The Up-Flo[®] Filter System experiments conducted in this project differ from the methods utilised by Hydro International Ltd for NJCAT verification and product development. A key difference was the long term permeability measurements of the filter media with clean water flow. This discovered the permeability long term decline with repeated flow events even without sediment loading. This is a recommended measurement for future experiments and product development, due to its importance in estimating the permeability changes to fully understand the lifespan of the product and its treatment capacity. If this recommendation is followed, experiments on alternate filter medias could allow for the adoption of an alternate filter media with a reduced permeability drop between flow events, maximising long-term treatment capacity.

Another difference between the experimental methods was timing. The NJCAT maximum experimental time was 9 mins and this projects minimum was 210 mins. As shown in the Chapter 3 experimental results, the removal efficiency dropped with a longer experimental time as it took time to reach an equilibrium. This means the NJCAT provides an artificially high removal efficiency, and as typical rainfall duration in the North East of the USA is around 3 hours in summer and seven hours in winter [115]. This means the NJCAT method doesn't produce realistic results. Whilst a longer experimental time is not required for Up-Flo[®] Filter certification, it is recommended so as to study the removal under a more realistic rainfall event, and would allow for more robust data to ensure the product is compliant with the changing regulatory frameworks.

Another difference was the undertaking of a full mass balance. This allowed for more in-depth information on the removal mechanisms to be developed. This brought the knowledge that the Up-Flo[®] sump is the primary source of sediment removal. It is recommended to conduct full mass balances in future experiments. Whilst time consuming, the extra knowledge allows for better product development and a better understanding of the impact on product design changes.

This projects experimental method also differed in that two artificial sediment sizes were utilised and particle size analysis was conducted, which showed that the Up-Flo[®] Filter is better at removing larger sized particles. This is recommended for all future experiments, so that the impact of particle size on removal efficiency can be estimated when changes to

product design are made. Additionally, it would also provide better estimates of removal efficiencies in realistic conditions, as the silica flour is finer than sediment typically expected in stormwater run-off.

One aspect where the NJCAT experimental verification method is successful is the different flow rates that are investigated. This previously found that the larger the flow rate, the lower the removal efficiency. Due to the time constraints of this research project, multiple flow rates with dosed water were not investigated. The recommendation is to continue testing multiple flow rates to provide a more detailed picture of sediment removal processes. While the NJCAT experiments provided a useful relationship between removal efficiency and flow rate, the experimental time was too short which provided an artificially high removal efficiency.

If the experimental methodology recommendations are adopted, the detailed information provided would allow the Up-Flo® Filter to be more easily adapted to future stormwater regulations. Whilst more time consuming and resource intensive, it would save the requirement to do further experiments with each regulatory update, potentially saving time and resources in the long term.

6.2 *Filter Media Monitoring*

At the start of the project, it was originally envisaged that to complete the aims, designing a filter media monitoring system would be the most appropriate route. This led to the aim to assess a filter monitoring system and Objectives 1 to 4, this section discusses how these objectives were completed.

Chapter 2 presents the background theory to acoustic and conductance techniques. This includes different models of sound propagation in granular medias with Hamilton and Biot-Stoll theories highlighted. This completed Objective 1 to research the background and form a review of literature.

Chapter 4 presents the experimental set-up and methodology for both the acoustics and conductance technique assessments. This completes Objectives 2 and 3 to design, build and conduct experiments.

Objective 4 was to interpret and analyse the data, this objective was completed. Chapter 4 presents an analysis of the data and develops recommendations on a filter media monitoring system.

Completing objectives 1 to 4 allows for an assessment of a filter monitoring system. Due to the time limit of the project and low signal-to-noise issues surrounding the acoustic techniques the assessment could not be developed further into a working solution. However the work has outlined its viability and a good basis for a filter media monitoring system has been outlined and with further work, a functioning system could be developed.

Experimental work began with bench scale experiments where acoustic transducers were tested. The experiments suffered from low signal-to-noise issues due to air within the media samples which resulted in difficulty in establishing a relationship with filter media clogging and attenuation of sound. However, the analysis of the experiments found key information regarding granular media and acoustic response as shown in Figure 4.18. Firstly, it was found that the optimum frequency range to conduct measurements was

between 300 and 400 kHz . Above 500 kHz , the attenuation was too high causing significant low signal-to-noise problems. Below 300 kHz , the difference between the measured signal of a clean filter media sample and a 10% artificially clogged media sample was very small. By conducting measurements between the frequency range of 300 and 400 kHz , it would allow a measurable signal while also showing a noticeable difference between the samples, as clogged media showed greater attenuation.

Secondly, it was found the measured attenuation in the frequency range specified matched well with previously published data by Williams et al. [108]. Thirdly, the attenuation matched a first power dependence on frequency, as proposed by the Hamilton model and others. This suggests that the predictions made by the Biot-Stoll model, that in the high frequency range attenuation scales with square root of the frequency, is incorrect.

These results aid in the development of an acoustic based filter media monitoring system, and also help fulfil the aim of increasing knowledge of granular media.

The vessel experiments led to further in-situ testing during ST02 and ST03 of the Chapter 3 experiments. The results from ST02 showed that the 350 kHz pulse that was sent through a bottom filter media bag attenuated, as sediment was caught within the media. The recorded pulse energy declined by approximately 12% during each sediment dosed experiment. In ST03 the seal on the drain down port failed, resulting in the rig slowly draining below the modules over a weekend. As in realistic operation, the drain down port would not be sealed. The results from ST03 mimic what would happen realistically. The failure of the seal resulted in additional attenuation due to air entering the sample. This made it difficult to obtain a similar relationship seen in ST02. However, there appears to be a decline in the rate of increase of pulse energy caused by the increasing saturation, suggesting that the effect of sediment could still be observed. This will need further work to estimate the extent of the sediment impact on the sound wave traversing the filter media.

Whilst the problems with attenuation due to air remain, the in-situ experiments suggest that acoustics could still be a viable basis for filter media monitoring. Additionally, it confirms that the effect of air within filter media is important to take into account when

understanding the response in granular media.

During ST02 and ST03 experiments, the multi-probe conductance device was also tested to assess its potential as a filter media monitoring technique. The testing of the multi-probe conductance device found that the device provided numerous useful measurements such as saturation, flow rate, and water level within the module (Figure 4.24). All these measurements are particularly useful and can be useful in monitoring of filter media health, as these factors either effect or are affected by sediment capture.

Additionally, the conductance gradient over both filter media bags was found to be related to the measured permeability over both bags. As the permeability of the filter media declines, the magnitude of the conductance gradient also decreases. This suggests the multi-probe conductance device could be an effective filter media monitoring device. This relationship is shown in Figure 4.27. Further experiments are required to develop these relationships further, with different permeability conductance measurements.

Whilst the multi-probe conductance device shows promising results, and an effective route to filter media monitoring, there remains limitations. For example, it only monitors the outside of the filter media bags, resulting in the device missing changes occurring within the centre of the media. Additionally, the devices ability of measuring water level above the filter media is limited by its accuracy, with the difference in probe lengths being 11.6 *mm*. This could be mitigated by additional probes allowing for a smaller difference in probe lengths. Finally, the probes were found to be quite fragile but could be fixed by printing the probes on a less fragile board.

The analysis in Chapter 4 proposed that to overcome the individual limitations, both techniques should be used together. The acoustics would provide information regarding the filter media in the central part of the bag, overcoming the limitation of the conductance device. By using the conductance device, the limitation regarding the acoustic technique attenuation issues could be overcome. The conductance device could detect a set saturation point, at which an acoustic pulse measurement could be taken. This would allow for the limitations of both techniques to be overcome, combined with the conductance gradient and permeability relationship, the health of the filter media

could be monitored.

The analysis of the results from Chapter 3 showed that the permeability declines as flow passes through the filter bed due to stratification. This had a larger effect than the estimated effect from capturing 9 *kg* of sediment. As permeability dictates the maximum treatment capacity of the Up-Flo[®] Filter System, this decline can cause untreated stormwater to bypass treatment. This suggests that the monitoring system would need to be primarily concentrated on permeability changes caused by stratification. The conductance device has shown that it is capable of monitoring this, resulting in the proposed sensor system arrangement providing key treatment capacity information.

Whilst the project has unable to develop a fully functioning filter media monitoring system prototype, the aims of the project have still been met and a basis for a future monitoring system has been laid out. To develop the system into a fully usable prototype further work is required, and whilst much of that further work has already been outlined in this section, other work is required to make it feasible.

A full cost-benefit analysis will be needed to determine the ideal cost of the completed sensor system. Hydro International Ltd have estimated that a realistic and acceptable market value would be approximately £1000, which would represent 10%-15% of the capital cost of the Up-Flo[®] Filter System. This may be difficult as whilst the multi-probe conductance device is low cost, the acoustic transducers can become expensive. Choosing an appropriate acoustic transducer, with a frequency within the range of 300 to 400 *kHz*, will be important in final development. If an appropriate transducer, that is capable of providing reliable data at a cost that is economical, can not be chosen, then the filter monitoring system could be based solely on the multi-probe conductance device. As the device was capable of measuring changes in permeability due to stratification, and as this impacts the systems treatment capacity more than sediment capture would, this could be a reasonable compromise.

Additionally, the full cost-benefit analysis would have to take into account the ideal measurement frequency and data communication option. Higher frequency of measurements would provide more data of the health of the system, but would result in

greater power usage and processing. The permeability change due to stratification would also result in the need to take into account the installation site conditions. Sites with increased storm events would require an increased measurement frequency. This could be set through the use of trials in installed Up-Flo[®] Filter Systems. Data communication would also be an important consideration, due to the remote locations of the Up-Flo[®] Filter System. Long range radio, such as 3G or 4G, may be more appropriate, however these can cost more than short range methods such as bluetooth or wireless fidelity.

Chapter 3 shows that the flow rate per module is different, which would result in different rates of sediment capture. If only one module is used for monitoring, so as to reduce costs, then the module choice will be important. Choosing the modules with the highest rate of capture, may result in the replacement of media before the total Up-Flo[®] removal capacity is reached. However if the module with the lowest rate of capture is chosen, it may result in stormwater bypassing the filter modules.

Once a sensor system is fully developed, the maintenance routine in Chapter 5 could be optimised to reduce resource and cost waste. Care would be needed to ensure that the maintenance routine takes into account that the sump is responsible for the majority of sediment removal. Either this will require continued visual inspections, or the installation of a secondary monitoring system for the sump. The conductance work presented in Chapter 4, shows that the conductance probe (developed by Nichols) can detect differences in media. Developing a long conductance probe to go along the side of the sump would allow for sediment level and water level to be measured.

6.3 Conclusion

The completion of the aims and objectives of this project has been assessed in this chapter. It was found that the aims and objectives of the project; to optimise the performance and maintenance of the Up-Flo[®] Filter System and to increase knowledge about granular media, were achieved.

Section 6.1 brought together the key discussion points from the thesis, and key recommendations regarding optimising the Up-Flo[®] Filter Systems performance and maintenance were made. Recommendations to deal with the stratification of the filter media included; increasing the height of the overflow device, a more mono-sized filter media, a larger sized filter media, or replacement with a flow control device. To optimise the maintenance, the filter media should be replaced or severely disturbed even when the 9 kg sediment capture hasn't been met. Recommendations were also made to optimise the system due to the different flow rates in different modules, flocculation of clay to fine silt sized particles, and sump being the primary removal mechanism.

Additionally, the section explored recommendations on experimental methodology for product development by Hydro International Ltd. Whilst these recommendations would increase the time and resource costs, it is argued that with the changing regulatory frameworks, (shown in Chapter 5) more in-depth information would result in easier adaptations to these regulatory changes. It may also save long term cost and resources as less experiments would need to be conducted in future, if the initial experiments provided significant amounts of data.

Chapter 4 showed that a filter media monitoring system has potential, but requires further development. Section 6.2 brought together the discussion on a filter media monitoring system from the findings in the previous chapters. A number of recommendations were made to what is required to develop this monitoring system further into a fully functioning prototype. Key recommendations include further work studying the impact of air, as real life operation the Up-Flo[®] Filter would have the drain-down ports installed. Another recommendation is to study the impact of declining permeability with clean water flow, to distinguish between sediment capture and the

background decline. Once fully developed, a number of considerations that need to be taken into account have been highlighted, including module location, data communication and the impact on maintenance routines.

Chapter 7

THESIS SUMMARY

This research project was formed to improve the treatment of stormwater, by improving the performance and maintenance protocols of the Up-Flo[®] Filter System.

Chapter 1 outlined the background to the project, the background to the Up-Flo[®] Filter System, the projects aims and objectives, and the formation of this Thesis. Chapter 2 then expanded the background of the project, explored the systems sediment removal mechanisms, and the physical laws that govern them. It was envisaged that to complete the aims and objectives, a filter media monitoring system would be key. This chapter outlined the requirements of a filter media monitoring system, and then explored two techniques that could potentially meet the requirements. Acoustic and conductance techniques were highlighted of interest, the chapter explored the laws that govern these techniques and their limitations.

To complete the aims of this project, full scale experiments on a six-module Up-Flo[®] Filter System were designed and conducted. Chapter 3 outlines these experiments, including their set-up, method, results and analysis. Initially 23 clean water experiments were conducted over a 4 month period. The experiments ran for 210 mins after a conditioning cycle, this allowed in depth knowledge regarding the change in filter media permeability. It was found that the permeability of the filter media suffers from a long term decline due to filter media grain rearrangement. This rearrangement occurs due to Stoke's Law, where the smaller particles end up at the top of the bag and the larger particles at the bottom of the bag. The results from the clean water experiments helped to develop the methodology for the sediment dosed experiments, which consisted of 2 Ls^{-1} flow rate and clean water experiments conducted before the dosing. The experiments provided a range of results covering removal efficiencies, mass balances,

permeability impacts, and detailed particle size analysis. The key results found that the removal efficiency ranged from 75.5% to 98.7%, dependent on the sediment and filter media sizes. The removal was also shown to be primarily resultant from the sump, with between 52.9% and 84% of sediment passing through the system captured by the sump. This again was dependent on particle size, with the larger sized sediment ($d_{50} = 150 \mu m$) Fraction E sand showing much greater retention within the sump (84.0%). Figure 3.47 shows the removal efficiency of silica flour in ST02, it shows at lower sized particles the filter media is responsible for removal but at larger sizes the settlement dominates. It was also found that filter media used adhesion for sediment removal. Additionally, at lower particle sizes there is additional settlement caused by flocculation. This additional removal is important, as at these clay to fine silt sizes significant particulate bound pollutants are found. Using these results a discussion is presented at the end of the chapter, covering the effects of the long term permeability changes on the treatment capacity of the system (max flow rate decreasing from 4.4 to 2.9 Ls^{-1} over 18 clean water experiments). Additionally the impact on the performance and maintenance is discussed, with recommendations made.

A key area of this project was to assess the viability of a filter media monitoring system, in an attempt to complete the projects aim of optimising the Up-Flo[®] Filter System's performance and maintenance. Chapter 4 sets out the work undertaken to do this. Initially bench scale experiments were conducted to assess acoustic techniques. This then progressed into in-situ experiments within a module of the system, during the sediment experiments in Chapter 3 where both acoustics and conductance was assessed. In the initial bench scale experiments it was found that low signal-to-noise problems, due to air within the sample, caused issues in developing a relationship between attenuation of the sound wave and clogging of filter media. However in deaired samples, attenuation values were similar to that provided in literature. The attenuation is seen in Figure 4.18, which also showed that with additional sediment further attenuation of the signal occurs. The attenuation of the signal was found to have a first power relationship with frequency. Suggesting that the empirical model of Hamilton is more accurate at high frequencies, as observed by others. Once testing began in-situ it was found that the energy of the pulse attenuated further as more sediment was captured. Increased attenuation due to air

remained however, when the drain down port seal failed in ST03. The effect of sediment could still be seen though, by the reduction in rate of increase of pulse energy caused by the increasing saturation. The multi-probe conductance device measurements found that the device was capable of providing a number of key measurements regarding saturation, water level, and flow rate through the filter media. Additionally, looking at the conductance gradient over the filter media bags there was a relationship between measured permeability and the conductance gradient, as Figure 4.27 shows. The discussion of this chapter discussed both techniques, their limitations and proposed that a suitable monitoring device should use both techniques to provide in-depth information on filter media health.

Chapter 5 used the knowledge developed from the work presented in the previous chapters, to present a review of the Up-Flo[®] Filter System's regulatory compliance and how to optimise the maintenance routines. Four regulatory frameworks across four continents were assessed, which showed different approaches to stormwater management. It was found that the Up-Flo[®] Filter System struggles to pass some of the more modern and stricter standards, but the more modern standards are more site specific. The requirement to take into account information regarding the stormwater and receiving surface water characteristics allows for the Up-Flo[®] Filter System and its maintenance practices to be optimised for the situation, and is recommended in the results analysis. Some standards have been shown very difficult to achieve, and may result in long term problems as treatment devices may be designed to pass the standard but realistically clog very quickly. Resulting in untreated effluent going into the environment. To ensure the Up-Flo[®] remains compliant with regulations the device must be maintained, this chapter also presents recommendations to optimise this. The work in this chapter has helped to complete the aims of this project of optimising the Up-Flo[®] Filter System's performance and maintenance.

Chapter 6 then brings together the key discussion analyses from the previous chapters, discusses whether the project has met the aims and objectives, and outlines any future work that is necessary. It was found that the aims of the project have been met, with recommendations on optimising performance and maintenance routines presented.

Additionally, knowledge of granular media has been expanded with the relationship with sound explored more, finding that Hamilton model is better suited at the frequency range used, and stratification in an up-flow design being an important effect. The knowledge gained from the filter media monitoring work, allows for a monitoring system to be developed with future work. It is proposed that using conductance and acoustics jointly together can reduce the individual limitations.

REFERENCES

- [1] The World Bank, *Urban Population (% of total) — Data — Table*, Date accessed 31 March 2015, 2013. [Online]. Available: http://data.worldbank.org/indicator/SP.URB.TOTL.IN.ZS?order=wbapi_data_value_2013%20wbapi_data_value%20wbapi_data_value-last&sort=desc.
- [2] Department for Environment Food & Rural Affairs, “Water Quality and Agriculture: Basic Measures IA No: Defra1819,” Tech. Rep., 2014. [Online]. Available: https://consult.defra.gov.uk/water/rules-for-diffuse-water-pollution-from-agriculture/supporting_documents/New%20basic%20rules%20Consultation%20Impact%20Assessment.pdf.
- [3] ———, “The government’s strategic review of diffuse water pollution from agriculture in England: Agriculture and Water: A Diffuse Pollution Overview,” Tech. Rep. June, 2002. [Online]. Available: <http://webarchive.nationalarchives.gov.uk/20130123162956/http://www.defra.gov.uk/environment/water/dwpa/reports/pdf/dwpa01-b.pdf>.
- [4] BBC Panorama, *Britain’s Dirty Beaches*, Date accessed 22 June 2016, 2009. [Online]. Available: http://www.bbc.co.uk/panorama/hi/front_page/newsid_8236000/8236957.stm.
- [5] I. White and J. Howe, “The mismanagement of surface water,” *Applied Geography*, vol. 24, no. 4, pp. 261–280, 2004, ISSN: 01436228. DOI: 10.1016/j.apgeog.2004.07.004.
- [6] C. Huhne and J. Slingo, “Climate: Observations, projections and impacts,” Tech. Rep., 2011, pp. 1–149.
- [7] Department for Environment Food & Rural Affairs, *Tackling water pollution from the urban environment: Consultation on a strategy to address diffuse water pollution from the built environment*, 2012. [Online]. Available: <https://www.gov.uk/>

- government/uploads/system/uploads/attachment_data/file/82602/consult-udwp-doc-20121120.pdf.
- [8] D. Drapper, R. Tomlinson, and P. Williams, “An investigation of the quality of the stormwater runoff from road pavements; a south-east queensland case study,” in *Proceedings of the International Conference On Urban Storm Drainage*, 1999, pp. 1225–1232.
- [9] M. G. Faram, K. O. Iwugo, and R. Y. G. Andoh, “Characteristics of urban run-off derived sediments captured by proprietary flow-through stormwater interceptors,” *Water Science & Technology*, vol. 56, no. 12, pp. 21–27, 2007, ISSN: 02731223. DOI: 10.2166/wst.2007.747.
- [10] S. R. Greb, R. T. Bannerman, S. R. Corsi, and R. E. Pitt, “Evaluation of the Multichambered Treatment Train, a Retrofit Water-Quality Management Practice,” *Water Environment Research*, vol. 72, no. 2, pp. 207–216, 2000, ISSN: 10614303. [Online]. Available: <http://www.jstor.org/stable/25045360>.
- [11] Hydro International Ltd, “NJCAT Technology Verification: Up-Flo Filter,” Tech. Rep., 2008. [Online]. Available: <http://www.njcat.org/uploads/newDocs/UpFloFilterNJCATLaboratoryVerification1108.pdf>.
- [12] —, *Up-Flo Filter*, Date accessed 20 April 2016, 2013. [Online]. Available: <http://www.hydro-int.com/uk/products/flo-filter>.
- [13] —, *Design Data: Up-Flo Filter; Fluidised Bed Up Flow Filtration System*, Date accessed 23 June 2016. [Online]. Available: https://www.hydro-int.com/sites/default/files/up-flo_filter_design_data_d0117.pdf.
- [14] R. C. Ferrier and J. B. Ellis, *Diffuse Pollution Impacts: The Environmental Impacts of Diffuse Pollution in the U.K.* B. J. D’Arcy, J. B. Ellis, R. C. Ferrier, A. Jenkins, and R. Dils, Eds. Lavenham: Terence Dalton Publishers, 2000, pp. 33–40, ISBN: 1 870752 46 5.
- [15] A. J. Erickson, P. T. Weiss, and J. S. Gulliver, *Optimizing Stormwater Treatment Practices*. New York, NY: Springer New York, 2013, ch. 2, pp. 1–337, ISBN: 978-1-4614-4623-1. DOI: 10.1007/978-1-4614-4624-8. [Online]. Available: <http://link.springer.com/10.1007/978-1-4614-4624-8>.

- [16] H. Taylor, "Surface waters," *Handbook of Water and Wastewater Microbiology*, pp. 611–626, Jan. 2003. DOI: 10.1016/B978-012470100-7/50037-6. [Online]. Available: <https://www.sciencedirect.com/science/article/pii/B9780124701007500376>.
- [17] W. Selbig, M. Fienen, J. Horwath, and R. Bannerman, "The Effect of Particle Size Distribution on the Design of Urban Stormwater Control Measures," *Water*, vol. 8, no. 1, p. 17, 2016, ISSN: 2073-4441. DOI: 10.3390/w8010017. [Online]. Available: <http://www.mdpi.com/2073-4441/8/1/17>.
- [18] B. Ellis, "Urban runoff quality in the UK: problems, prospects and procedures," *Applied Geography*, vol. 11, no. 3, pp. 187–200, 1991, ISSN: 01436228. DOI: 10.1016/0143-6228(91)90029-9.
- [19] J. B. Ellis, "Sediment yield and BMP control strategies in urban catchments," in *Erosion and Sediment Yield: Global and Regional Perspectives*, IAHS Pubi, 1996. [Online]. Available: https://iahs.info/uploads/dms/iahs_236_0555.pdf.
- [20] T. H. Goodwin, A. R. Young, M. G. R. Holmes, G. H. Old, N. Hewitt, G. J. L. Leeks, J. C. Packman, and B. P. G. Smith, "The temporal and spatial variability of sediment transport and yields within the Bradford Beck catchment, West Yorkshire," *The Science of the Total Environment*, pp. 475–494, 2003. DOI: 10.1016/S0048-9697(03)00069-X. [Online]. Available: https://ac.els-cdn.com/S004896970300069X/1-s2.0-S004896970300069X-main.pdf?_tid=681c6328-39aa-4af5-b250-d186a00262f0&acdnat=1537351886_91506ebe2d955917476dc0966b37a541.
- [21] D. Butler and J. Davies, *Urban Drainage*, ser. Spon Text. CRC Press, 2010, ISBN: 9780203849057. [Online]. Available: <https://books.google.co.uk/books?id=8Y0Mj1ZV6rsC>.
- [22] R. L. Wilby, H. G. Orr, M. Hedger, D. Forrow, and M. Blackmore, "Risks posed by climate change to the delivery of Water Framework Directive objectives in the UK," *Environment International*, vol. 32, no. 8, pp. 1043–1055, 2006, ISSN: 01604120. DOI: 10.1016/j.envint.2006.06.017.

- [23] J. B. Ellis and G. Mitchell, “Urban diffuse pollution: key data information approaches for the Water Framework Directive,” *Water and Environment Journal*, vol. 20, no. 1, pp. 19–26, Mar. 2006, ISSN: 1747-6585. DOI: 10.1111/j.1747-6593.2006.00025.x. [Online]. Available: <http://doi.wiley.com/10.1111/j.1747-6593.2006.00025.x>.
- [24] Parliamentary Office of Science and Technology, *postnote: RIVER BASIN MANAGEMENT PLANS*, 2008. [Online]. Available: <https://www.parliament.uk/documents/post/postpn320.pdf>.
- [25] A. Kirby, “SuDS - innovation or a tried and tested practice?” *Proceedings of the Institution of Civil Engineers*, no. ME01, pp. 1–8, 2005.
- [26] B. Woods Ballard, S. Wilson, H. Udale-Clarke, S. Illman, T. Scott, R. Ashley, and R. Kellagher, *The SUDS manual*, 5th ed. CIRIA, 2015, ISBN: 9780860176978. DOI: LondonC697. [Online]. Available: https://www.ciria.org/Resources/Free_publications/SuDS_manual_C753.aspx.
- [27] New Civil Engineer, *Hard vs Soft SuDS - weighing up the pros and cons*, Date accessed 08 November 2018, 2008. [Online]. Available: <https://www.newcivilengineer.com/hard-vs-soft-suds-weighing-up-the-pros-and-cons/1326348.article>.
- [28] M. Pitt and HM Government, “Floods Review,” Tech. Rep., 2008. [Online]. Available: http://webarchive.nationalarchives.gov.uk/20100812084907/http://archive.cabinetoffice.gov.uk/pittreview/_/media/assets/www.cabinetoffice.gov.uk/flooding_review/pitt_review_full%20pdf.pdf.
- [29] J. M. Goodson, “Briefing : Keeping up with the Suds revolution and legislative evolution,” vol. 164, pp. 67–70, 2011. DOI: 10.1680/muen.2011.164.2.67.
- [30] Parliament of the United Kingdom, *Flood and Water Management Act 2010 Chapter 29*, 2010. [Online]. Available: https://www.legislation.gov.uk/ukpga/2010/29/pdfs/ukpga_20100029_en.pdf.
- [31] Department for Environment Food & Rural Affairs, “National Standards for sustainable drainage systems Designing, constructing, operating and maintaining drainage for surface runoff,” Tech. Rep., 2011.

- [32] Department for Environment Food & Rural Affairs and Department for Communities & Local Government, “Consultation on delivering Sustainable Drainage Systems A summary of responses to the consultation and the government response,” Tech. Rep., 2014. [Online]. Available: https://assets.publishing.service.gov.uk/government/uploads/system/uploads/attachment_data/file/388941/suds-consult-sum-resp-201412.pdf.
- [33] Department for Communities & Local Government, *House of Commons: Written Statement (HCWS161)*, 2014. [Online]. Available: <https://www.parliament.uk/documents/commons-vote-office/December%202014/18%20December/6.%20DCLG-sustainable-drainage-systems.pdf>.
- [34] Secretary of State for Ministry of Housing Communities and Local Government, *National Planning Policy Framework*. 2018, ISBN: 978-1-5286-0745-2. [Online]. Available: <http://forms.communities.gov.uk/>.
- [35] New Civil Engineer, *First UK SuDS technology code of practice*, Date accessed 12 September 2018, Mar. 2017. [Online]. Available: <https://www.newcivilengineer.com/business-culture/first-uk-suds-technology-code-of-practice/10018283.article>.
- [36] British Water, *Code of Practice for the Assessment of Manufactured Treatment Devices Designed to Treat Surface Water Runoff*, 2017. [Online]. Available: <https://www.britishwater.co.uk/Publications/manufactured-treatment-devices.aspx>.
- [37] J. C. Crittenden, R. R. Trussell, D. W. Hand, K. J. Howe, and G. Tchobanoglous, *MWH’s Water Treatment: Principles and Design*, 3rd ed., ser. EngineeringPro collection. Wiley, 2012, ISBN: 9781118103777. [Online]. Available: <https://books.google.co.uk/books?id=1S1HAAAAQBAJ>.
- [38] suez, *water treatment different types of sedimentation : settling*, Date accessed 20 September 2018. [Online]. Available: <https://www.suezwaterhandbook.com/water-and-generalities/fundamental-physical-chemical-engineering-processes-applicable-to-water-treatment/sedimentation/different-types-of-sedimentation>.

- [39] S. Judd, *Watermaths: Process Fundamentals for the Design and Operation of Water and Wastewater Treatment Technologies*, ser. Maths for water and wastewater technologies. Judd and Judd Limited, 2013, ISBN: 9780957557802. [Online]. Available: <https://books.google.co.uk/books?id=SYICnwEACAAJ>.
- [40] M. M. Benjamin and D. F. Lawler, *Water Quality Engineering: Physical / Chemical Treatment Processes*. Wiley, 2013, ISBN: 9781118632277. [Online]. Available: <https://books.google.co.uk/books?id=vRovU0TD8s0C>.
- [41] N. C. H. R. Program, N. R. C. (T. R. Board, A. A. of State Highway, T. Officials, of Civil Construction, E. Engineering, U. of Florida. Department of Environmental Engineering Sciences, G. Consultants, and I. Low Impact Development Center, *Evaluation of Best Management Practices for Highway Runoff Control*, ser. NCHRP report. Transportation Research Board, 2006, ISBN: 9780309098694. [Online]. Available: <https://books.google.co.uk/books?id=jKR-CF7PG6AC>.
- [42] S. Yang and J. Evans, “Metering and dispensing of powder; the quest for new solid freeforming techniques,” *Powder Technology*, vol. 178, no. 1, pp. 56–72, Sep. 2007, ISSN: 0032-5910. DOI: 10.1016/J.POWTEC.2007.04.004. [Online]. Available: <https://www.sciencedirect.com/science/article/pii/S0032591007002094>.
- [43] E. W. Schmidt, J. A. Gieseke, P. Gelfand, T. W. Lugar, and D. A. Furlong, “Filtration Theory for Granular Beds,” *Journal of the Air Pollution Control Association*, vol. 28, no. 2, pp. 143–146, 1978, ISSN: 0002-2470. DOI: 10.1080/00022470.1978.10470582. [Online]. Available: <http://www.tandfonline.com/action/journalInformation?journalCode=uawm16>.
- [44] J. R. Nimmo, “POROSITY AND PORE-SIZE DISTRIBUTION,” in *Encyclopedia of Soils in the Environment*, D. Hillel, Ed., 2005, pp. 295–303, ISBN: 9780123485304. DOI: Elsevier. [Online]. Available: https://ac.els-cdn.com/B0123485304004045/3-s2.0-B0123485304004045-main.pdf?_tid=7fb97653-7c41-4b27-972e-dff124d71dc6&acdnat=1537524247_2c7c5b4edf4993b36cdea63f635f8773.
- [45] H. S. Kandra, D. McCarthy, T. D. Fletcher, and A. Deletic, “Assessment of clogging phenomena in granular filter media used for stormwater treatment,” *Journal*

- of Hydrology*, vol. 512, pp. 518–527, May 2014, ISSN: 00221694. DOI: 10.1016/j.jhydrol.2014.03.009. [Online]. Available: <http://www.sciencedirect.com/science/article/pii/S0022169414001838>.
- [46] M. F. Hamoda, I. Al-Ghusain, and D. M. Al-Jasem, “Application of granular media filtration in wastewater reclamation and reuse,” *Journal of environmental science and health. Part A, Toxic/hazardous substances & environmental engineering*, vol. 39, no. 2, pp. 385–95, 2004, ISSN: 1093-4529. [Online]. Available: <http://www.ncbi.nlm.nih.gov/pubmed/15027822>.
- [47] L. P. Dake, *Fundamentals of Reservoir Engineering*, 1st. Elsevier, 1983, ISBN: 9780080568980.
- [48] D. H. F. Liu and B. G. Liptak, *Groundwater and Surface Water Pollution*. CRC Press, 1999, ISBN: 9781566705110.
- [49] J. Bear, *Dynamics of Fluids in Porous Media*. Dover Publications, Inc, 2011, ISBN: 9780486656755.
- [50] C. W. Fetter, *Applied Hydrogeology*, 4th. Pearson Education Limited, 2000, ISBN: 978-0130882394.
- [51] E. Lindquist, “On the flow of water through porous soil,” in *Premier Congres des grands barrages*, Stockholm, 1933, pp. 81–101.
- [52] H. E. Rose, “An Investigation into the Laws of Flow of Fluids through Beds of Granular Materials,” *Proceedings of the Institution of Mechanical Engineers*, vol. 153, no. 1, pp. 141–148, 1945. DOI: 10.1243/PIME{_}PROC{_}1945{_}153{_}018{_}02. [Online]. Available: https://doi.org/10.1243/PIME_PROC_1945_153_018_02.
- [53] —, “On the Resistance Coefficient-Reynolds Number Relationship for Fluid Flow through a Bed of Granular Material,” *Proceedings of the Institution of Mechanical Engineers*, vol. 153, no. 1, pp. 154–168, 1945. DOI: 10.1243/PIME{_}PROC{_}1945{_}153{_}020{_}02. [Online]. Available: https://doi.org/10.1243/PIME_PROC_1945_153_020_02.

- [54] G. Schneebeli, “EXPÉRIENCES SUR LA LIMITE DE VALIDITÉ DE LA LOI DE DARCY ET L’APPARITION DE LA TURBULENCE DANS UN ÉCOULEMENT DE FILTRATION,” *La Houille Blanche*, no. 2, pp. 141–149, 1955. DOI: 10.1051/lhb/1955030. [Online]. Available: <https://doi.org/10.1051/lhb/1955030>.
- [55] M. K. Hubbert, “DARCY’S LAW AND THE FIELD EQUATIONS OF THE FLOW OF UNDERGROUND FLUIDS,” *International Association of Scientific Hydrology. Bulletin*, vol. 2, no. 1, pp. 23–59, 1957. DOI: 10.1080/02626665709493062. [Online]. Available: <https://doi.org/10.1080/02626665709493062>.
- [56] N. Dukhan, Ö. Bağci, and M. Özdemir, “Experimental flow in various porous media and reconciliation of Forchheimer and Ergun relations,” *Experimental Thermal and Fluid Science*, vol. 57, pp. 425–433, 2014, ISSN: 08941777. DOI: 10.1016/j.expthermflusci.2014.06.011.
- [57] R. M. Fand, B. Y. K. Kim, A. C. C. Lam, and R. T. Phan, “Resistance to the Flow of Fluids Through Simple and Complex Porous Media Whose Matrices Are Composed of Randomly Packed Spheres,” *Journal of Fluids Engineering*, vol. 109, no. 3, pp. 268–273, Sep. 1987, ISSN: 0098-2202. [Online]. Available: <http://dx.doi.org/10.1115/1.3242658>.
- [58] S. S. Hsiau, J. Smid, C. Y. Wang, J. T. Kuo, and C. S. Chou, “Velocity profiles of granules in moving bed filters,” *Chemical Engineering Science*, vol. 54, no. 3, pp. 293–301, 1998, ISSN: 00092509. DOI: 10.1016/S0009-2509(98)00257-7.
- [59] L. Henke, *Principles of Filtration: How do Filters Filter Anyway? - WCP Online*, Date accessed 21 September 2018, 2015. [Online]. Available: <http://www.wcponline.com/2015/02/10/principles-of-filtration-how-do-filters-filter-anyway/>.
- [60] M. A. Biot, “Theory of Propagation of Elastic Waves in a Fluid-Saturated Porous Solid. I. Low-Frequency Range,” *The Journal of the Acoustical Society of America*, vol. 28, no. 2, pp. 168–178, 1956, ISSN: 0001-4966. DOI: 10.1121/1.1908239. [Online]. Available: <http://asa.scitation.org/doi/10.1121/1.1908239>.

- [61] ———, “Theory of Propagation of Elastic Waves in a Fluid Saturated Porous Solid. II. Higher Frequency Range,” *J. Acoust. Soc. Am.*, vol. 28, no. 2, pp. 179–191, 1956, ISSN: 00014966. DOI: 10.1121/1.1908241.
- [62] R. D. Stoll, “Acoustic Waves in Saturated Sediments,” in *Physics of Sound in Marine Sediments*, L. Hampton, Ed., Boston, MA: Springer US, 1974, pp. 19–39, ISBN: 978-1-4684-0838-6. DOI: 10.1007/978-1-4684-0838-6_2. [Online]. Available: https://doi.org/10.1007/978-1-4684-0838-6_2.
- [63] R. D. Stoll, “Acoustic waves in ocean sediments,” *Geophysics*, vol. 42, no. 4, p. 715, 1977. DOI: 10.1190/1.1440741. [Online]. Available: <http://dx.doi.org/10.1190/1.1440741>.
- [64] R. D. Stoll, “Theoretical aspects of sound transmission in sediments,” *The Journal of the Acoustical Society of America*, vol. 68, no. 5, pp. 1341–1350, 1980, ISSN: 0001-4966. DOI: 10.1121/1.385101. [Online]. Available: <http://asa.scitation.org/doi/10.1121/1.385101>.
- [65] R. D. Stoll and T. K. Kan, “Reflection of acoustic waves at a water-sediment interface,” *The Journal of the Acoustical Society of America*, vol. 70, no. 1, pp. 149–156, 1981, ISSN: 0001-4966. DOI: 10.1121/1.386692. [Online]. Available: <http://asa.scitation.org/doi/10.1121/1.386692>.
- [66] R. D. Stoll, *Sediment Acoustics*, ser. Lecture Notes in Earth Sciences. Springer New York, 1989, ISBN: 9783540971917. [Online]. Available: <https://books.google.co.uk/books?id=e8sQAQAIAAJ>.
- [67] P. C. Etter, *Underwater Acoustic Modeling and Simulation*, 4th. Taylor & Francis, 2013, ISBN: 9781466564930. [Online]. Available: <https://books.google.co.uk/books?id=0zVTzHi0QXYC>.
- [68] J. H. Steele, S. A. Thorpe, and K. K. Turekian, *Elements of Physical Oceanography: A derivative of the Encyclopedia of Ocean Sciences*, ser. Encyclopedia of ocean sciences. Elsevier Science, 2009, ISBN: 9780123757258. [Online]. Available: <https://books.google.co.uk/books?id=ISrnKDMyNTMC>.

- [69] C. W. Holland and B. A. Brunson, "The Biot-Stoll sediment model: An experimental assessment," *The Journal of the Acoustical Society of America*, vol. 84, no. 4, pp. 1437–1443, 1988, ISSN: 0001-4966. DOI: 10.1121/1.396590.
- [70] M. Buckingham, "Theory of acoustic attenuation, dispersion, and pulse propagation in unconsolidated granular materials including marine sediments," *The Journal of the Acoustical Society of America*, vol. 102, no. 5, pp. 2579–2596, 1997. DOI: 10.1121/1.420313. [Online]. Available: <https://asa.scitation.org/doi/10.1121/1.420313>.
- [71] J. L. Buchanan, "An Assessment of the Biot-Stoll Model of a Poroelastic Seabed," 2005. [Online]. Available: <http://www.dtic.mil/dtic/tr/fulltext/u2/a437036.pdf>.
- [72] E. L. Hamilton, "Sound velocity-density relations in sea-floor sediments and rocks," *The Journal of the Acoustical Society of America*, vol. 63, no. 2, pp. 366–377, 1978, ISSN: 00014966. DOI: 10.1121/1.381747.
- [73] E. L. Hamilton, "Geoacoustic modeling of the sea floor," *The Journal of the Acoustical Society of America*, vol. 68, no. 5, pp. 1313–1340, 1980, ISSN: 00014966. DOI: 10.1121/1.385100.
- [74] E. L. Hamilton and R. T. Bachman, "Sound velocity and related properties of marine sediments paper," vol. 52, no. 6, pp. 1891–1904, 1982.
- [75] A. C. Kibblewhite, "Attenuation of sound in marine sediments: A review with emphasis on new low-frequency data," *The Journal of the Acoustical Society of America*, vol. 86, no. 2, pp. 716–738, 1989, ISSN: 00014966. DOI: 10.1121/1.398195.
- [76] K. L. Williams, "An effective density fluid model for acoustic propagation in sediments derived from Biot theory," *The Journal of the Acoustical Society of America*, vol. 110, no. 5, pp. 2276–2281, 2001, ISSN: 0001-4966. DOI: 10.1121/1.1412449. [Online]. Available: <http://asa.scitation.org/doi/10.1121/1.1412449>.
- [77] R. Stretitzki, J. A. Evans, and A. J. Clarke, "The Influence of Porosity and Pore Size on the Ultrasonic Properties of Bone Investigated Using a Phantom Material," *Osteoporos Int*, vol. 7, no. 4, pp. 370–375, 1997. DOI: 10.1007/BF01623780.

- [Online]. Available: <https://link.springer.com/content/pdf/10.1007%2F01623780.pdf>.
- [78] M. Goueygou, Z. Lafhaj, and M. Kaczmarek, "Relationship between porosity, permeability and ultrasonic parameters in sound and damaged mortar," in *Non-Destructive Testing in Civil Engineering 2003*. [Online]. Available: <https://www.ndt.net/article/ndtce03/papers/v005/v005.htm>.
- [79] J.-P. Sessarego, A. Ivakin, and D. Ferrand, "Frequency Dependence of Phase Speed, Group Speed, and Attenuation in Water-Saturated Sand: Laboratory Experiments," *IEEE Journal of Oceanic Engineering*, vol. 33, no. 4, pp. 359–366, Oct. 2008, ISSN: 0364-9059. DOI: 10.1109/JOE.2008.927584. [Online]. Available: http://www.researchgate.net/publication/224370794_Frequency_Dependence_of_Phase_Speed_Group_Speed_and_Attenuation_in_Water-Saturated_Sand_Laboratory_Experiments.
- [80] A. N. Ivakin and J.-P. Sessarego, "High frequency broad band scattering from water-saturated granular sediments: Scaling effects.," *The Journal of the Acoustical Society of America*, vol. 122, no. 5, pp. 165–171, Nov. 2007, ISSN: 1520-8524. DOI: 10.1121/1.2784534. [Online]. Available: <http://www.ncbi.nlm.nih.gov/pubmed/18189451>.
- [81] J.-P. Sessarego, R. Guillermin, and A. N. Ivakin, "High-Frequency Sound Reflection by Water-Saturated Sediment Interfaces," English, *IEEE Journal of Oceanic Engineering*, vol. 33, no. 4, pp. 375–385, Oct. 2008, ISSN: 0364-9059. DOI: 10.1109/JOE.2008.2002457. [Online]. Available: <http://ieeexplore.ieee.org/articleDetails.jsp?arnumber=4769691>.
- [82] C. J. Hickey and J. M. Sabatier, "Choosing Biot parameters for modeling water-saturated sand," *The Journal of the Acoustical Society of America*, vol. 102, no. 3, pp. 1480–1484, Sep. 1997, ISSN: 00014966. DOI: 10.1121/1.421037. [Online]. Available: <http://adsabs.harvard.edu/abs/1997ASAJ..102.1480H>.
- [83] J. Sabatier and C. McNeill, "The Biot Type II wave in the fluid and matrix of soils," *The Journal of the Acoustical Society of America*, vol. 123, no. 5, p. 3035, 2008. DOI: 10.1121/1.2932695.

- [84] N. Chotiros and M. Isakson, "A Poro-Elastic Model for Underwater Sand and Silt," in *Poromechanics V*, Vienna, Austria: American Society of Civil Engineers, Jun. 2013, pp. 352–358, ISBN: 978-0-7844-1299-2. DOI: 10.1061/9780784412992.041. [Online]. Available: <http://dx.doi.org/10.1061/9780784412992.041>.
- [85] F. Shields, J. Sabatier, and M. Wang, "The effect of moisture on compressional and shear wave speeds in unconsolidated granular material," *The Journal of the Acoustical Society of America*, vol. 108, no. 5 Pt 1, pp. 1998–2004, Nov. 2000, ISSN: 1520-8524. DOI: 10.1121/1.1314317. [Online]. Available: <http://www.ncbi.nlm.nih.gov/pubmed/11108338>.
- [86] Z. Lu and J. M. Sabatier, "Effects of Soil Water Potential and Moisture Content on Sound Speed," *Soil Science Society of America Journal*, vol. 73, no. 5, pp. 1614–1625, May 2009, ISSN: 1435-0661. DOI: 10.2136/sssaj2008.0073. [Online]. Available: http://www.researchgate.net/publication/24264876_Effects_of_Soil_Water_Potential_and_Moisture_Content_on_Sound_Speed.
- [87] A. L. Anderson and L. D. Hampton, "Acoustics of gas-bearing sediments I. Background," *The Journal of the Acoustical Society of America*, vol. 67, no. 6, pp. 1865–1889, Jun. 1980, ISSN: 0001-4966. DOI: 10.1121/1.384453. [Online]. Available: <http://asa.scitation.org/doi/10.1121/1.384453>.
- [88] —, "Acoustics of gas-bearing sediments. II. Measurements and models," *The Journal of the Acoustical Society of America*, vol. 67, no. 6, pp. 1890–1903, 1980, ISSN: 0001-4966. DOI: 10.1121/1.384454. [Online]. Available: <http://asa.scitation.org/doi/10.1121/1.384454>.
- [89] M. Herskowitz, S. Levitsky, and I. Shreiber, "Attenuation of ultrasound in porous media with dispersed microbubbles," *Ultrasonics*, vol. 38, no. 1, pp. 767–769, 2000, ISSN: 0041624X. DOI: 10.1016/S0041-624X(99)00156-0.
- [90] T. Leighton, *The Acoustic Bubble*. Academic Press, 1994, ISBN: 0124419208.
- [91] T. G. Leighton, "Theory for acoustic propagation in marine sediment containing gas bubbles which may pulsate in a non-stationary nonlinear manner," *Geophysical Research Letters*, vol. 34, no. 17, 2007, ISSN: 00948276. DOI: 10.1029/2007GL030803.

- [92] T. G. Leighton and G. B. N. Robb, "Preliminary mapping of void fractions and sound speeds in gassy marine sediments from subbottom profiles," *Journal of the Acoustical Society of America*, vol. 124, no. 5, EL313–EL320, 2008, ISSN: 1520-8524. DOI: Doi10.1121/1.2993744. [Online]. Available: <http://dx.doi.org/10.1121/1.2993744>.
- [93] A. Mantouka, H. Dogan, P. R. White, and T. G. Leighton, "Modelling acoustic scattering, sound speed, and attenuation in gassy soft marine sediments," *The Journal of the Acoustical Society of America*, vol. 140, no. 1, pp. 274–282, 2016, ISSN: 0001-4966. DOI: 10.1121/1.4954753. [Online]. Available: <http://asa.scitation.org/doi/10.1121/1.4954753>.
- [94] H. Dogan, P. R. White, and T. G. Leighton, "Acoustic wave propagation in gassy porous marine sediments: The rheological and the elastic effects," *J. Acoust. Soc. Am.*, vol. 141, no. 3, pp. 2277–2288, 2017, ISSN: 00014966. DOI: 10.1121/1.4978926.
- [95] Network solution LLC, *Electrical Resistivity Tomography*, Date accessed 03 September 2015, 2013. [Online]. Available: <http://surfacesearch.com/page11/page3/page4/page4.html>.
- [96] V. Damasceno and D. Fratta, "Monitoring Chemical Diffusion in a Porous Media using Electrical Resistivity Tomography," in *Site and Geomaterial Characterization*, Shanghai, China: American Society of Civil Engineers, May 2006, pp. 174–181, ISBN: 978-0-7844-0861-2. DOI: doi:10.1061/40861(193)22. [Online]. Available: [http://dx.doi.org/10.1061/40861\(193\)22](http://dx.doi.org/10.1061/40861(193)22).
- [97] D. Zumr, M. Sněhota, and M. Císlerová, "Observation of water movement in soil with electric resistivity tomography," *Natural Hazards (optimisation of protection, interaction with structures)*, Prague, Tech. Rep., 2011, pp. 195–200.
- [98] G. Lekmine, M. Pessel, and H. Auradou, "2D Electrical Resistivity Tomography surveys optimisation of the solutes transport in porous media.," *ArcheoSciences. Revue d'archéométrie*, vol. 33, no. (suppl.) Pp. 309–312, 2009. DOI: 10.4000/archeosciences.1756.

- [99] A. Nichols, "Quantifying the depth and composition of flow and sediment," Tech. Rep.
- [100] ———, *Device and method for measuring the depth of media*, 2014.
- [101] A. Revil, A. Jardani, P. Sava, and A. Haas, *The Seismoelectric Method: Theory and Applications*, ser. Analytical Methods in Earth and Environmental Science Series. Wiley, 2015, ISBN: 9781118660263. [Online]. Available: <https://books.google.co.uk/books?id=44pxBgAAQBAJ>.
- [102] *FILTRO URGARBI UPFLO*, Date accessed 23 May 2018. [Online]. Available: <http://www.urgarbi.eu/aguas-pluviales-tratamiento-filtro-upflo.html/#?playlistId=0&videoId=0>.
- [103] British Standards Institution, *BS EN ISO 14688-1:2018 Geotechnical investigation and testing. Identification and classification of soil. Identification and description*. BSI Standards Limited 2018, 2018, ISBN: 978 0 580 87598 4.
- [104] Harvard University, *Summary of Rules for Error Propagation*, Date accessed 05 September 2018. [Online]. Available: https://sites.fas.harvard.edu/~scphys/nsta/error_propagation.pdf.
- [105] T. Al-Shemmeri, *Engineering Fluid Mechanics*. Al-Shemmeri & Ventus Publishing ApS, 2012, ISBN: 978-87-403-0114-4. [Online]. Available: [http://eprints.staffs.ac.uk/222/1/engineering-fluid-mechanics\[1\].pdf](http://eprints.staffs.ac.uk/222/1/engineering-fluid-mechanics[1].pdf).
- [106] R. E. Collins, *Flow of Fluids Through Porous Materials*. New York: Reinhold, 1961. DOI: 10.1002/aic.690080102.
- [107] J. C. Ward, "Turbulent flow in porous media," *Journal of Hydraulics Division*, vol. 90, no. 5, pp. 1–12, 1964.
- [108] K. L. Williams, D. R. Jackson, E. I. Thorsos, D. Tang, and S. G. Schock, "Comparison of sound speed and attenuation measured in a sandy sediment to predictions based on the Biot theory of porous media," *IEEE Journal of Oceanic Engineering*, vol. 27, no. 3, pp. 413–428, 2002, ISSN: 03649059. DOI: 10.1109/JOE.2002.1040928.
- [109] F. Xu and A. Krynkin, *Acoustic Communication System [MSc Thesis]*. 2017.

- [110] J. Moores, J. Gadd, P. Pattinson, and C. Hyde, “Field evaluation of media filtration stormwater treatment devices,” Tech. Rep., 2012. [Online]. Available: www.nzta.govt.nz.
- [111] Commonwealth of Massachusetts, “The Technology Acceptance Reciprocity Partnership Protocol for Stormwater Best Management Practice Demonstrations,” Tech. Rep., 2016. [Online]. Available: <https://www.mass.gov/files/documents/2016/08/rd/swprotoc.pdf>.
- [112] Hydro International Ltd, “NJCAT Technology Verification,” Tech. Rep., 2015. [Online]. Available: <http://www.njcat.org/uploads/newDocs/NJCATTECHNOLOGYVERIFICATIONUFF.pdf>.
- [113] The State of New Jersey, “Procedure for MTD Verification Procedure for Obtaining Verification of a Stormwater Manufactured Treatment Device from New Jersey Corporation for Advanced Technology For use in accordance with the Stormwater Management Rules,” Tech. Rep., 2013. [Online]. Available: www.njstormwater.org.
- [114] J. J. Murphy and State of New Jersey Department of Environmental Protection, “N.J.D.E.P MTD Laboratory Certification Up-Flo Filter,” Tech. Rep., 2017. [Online]. Available: http://www.state.nj.us/dep/dwq/bnpc_home.htm.
- [115] J. M. Thorp and B. C. Scott, “Preliminary calculations of average storm duration and seasonal precipitation rates for the northeast sector of the united states,” *Atmospheric Environment (1967)*, vol. 16, no. 7, pp. 1763–1774, Jan. 1982, ISSN: 0004-6981. DOI: 10.1016/0004-6981(82)90269-4. [Online]. Available: <https://www.sciencedirect.com/science/article/pii/0004698182902694>.
- [116] W. R. Selbig and R. T. Bannerman, “Characterizing the Size Distribution of Particles in Urban Stormwater by Use of Fixed-Point Sample-Collection Methods: U.S. Geological Survey Open-File Report 2011-1052,” Tech. Rep., 2011. [Online]. Available: <http://www.usgs.gov/pubprod>.
- [117] D. Nickel, W. Schoenfelder, D. Medearis, D. P. Dolowitz, M. Keeley, and W. Shuster, “German experience in managing stormwater with green infrastructure,” *Journal of Environmental Planning and Management*, vol. 57, no. 3, pp. 403–423, Mar.

- 2014, ISSN: 0964-0568. DOI: 10.1080/09640568.2012.748652. [Online]. Available: <https://doi.org/10.1080/09640568.2012.748652>.
- [118] H. Zum and U. Mit Regenwasser, *Advisory Leaflet DWA-M 153E Recommended Actions for Dealing with Stormwater*. Hennef: DWA German Association for Water, Wastewater and Waste, 2007, ISBN: 978-3-941089-97-6. [Online]. Available: www.dwa.de.
- [119] J. Sage, E. Berthier, and M.-C. Gromaire, "Pollution Control: A Comparative Assessment of International Practices," *Environmental Management*, vol. 56, no. 1, pp. 66–80, 2015. DOI: 10.1007/s00267-015-0485-1. [Online]. Available: <https://hal.archives-ouvertes.fr/hal-01145865>.
- [120] A. Cunningham, A. Colibaba, B. Hellberg, G. Silyn Roberts, R. Symcock, N. Vigar, and W. Woortman, *Stormwater Management Devices in the Auckland Region. Auckland Council guideline document, GD2017/001*. Auckland, 2017, ISBN: 978-1-98-852977-6. [Online]. Available: http://content.aucklanddesignmanual.co.nz/project-type/infrastructure/technical-guidance/stormwatermanagement/Documents/GD01_SWMD.pdf.
- [121] Auckland Council, *Auckland Unitary Plan stormwater management provisions: Technical basis of contaminant and volume management requirements. TR2013/035*. 2013, ISBN: 978-1-927266-11-3. [Online]. Available: <http://www.knowledgeauckland.org.nz/assets/publications/TR2013-035-Auckland-Unitary-Plan-stormwater-management-provisions-no-appendices.pdf>.
- [122] Auckland Regional Council, *Particle size and settling velocity distributions for the design of stormwater treatment devices in the Auckland region. Technical Report No. 2010/006*. 2010, ISBN: 978-1-877540-53-0. [Online]. Available: <http://knowledgeauckland.org.nz/assets/publications/TR2010-006-Particle-size-and-settling-velocity-distributions-stormwater-treatment-devices-Auckland.pdf>.
- [123] Auckland Council, *Urban Runoff Quality Information System*, Date accessed 21 August 2018. [Online]. Available: <https://urqis.niwa.co.nz/#/report/a4e5eb9e730eb48f70fed294f1da463fe4568cf5>.

- [124] China Water Risk, *Revised 'Water Pollution Prevention and Control Law' Approved* — *China Water Risk*, 2017. [Online]. Available: <http://chinawaterrisk.org/notices/revised-water-pollution-prevention-and-control-law-approved/>.
- [125] Peoples Republic of China Ministry of Ecology and Environment, *The National Standards of the People's Republic of China*, Date accessed 16 August 2018. [Online]. Available: <http://english.mep.gov.cn/SOE/soechina1997/water/standard.htm>.
- [126] S. K. Sharma, *Heavy Metals In Water: Presence, Removal and Safety*. Royal Society of Chemistry, 2014, ISBN: 9781849738859. [Online]. Available: https://books.google.co.uk/books?id=BF_YBAAAQBAJ.
- [127] H. Rügner, M. Schwientek, R. Milačić, T. Zuliani, J. Vidmar, M. Paunović, S. Laschou, E. Kalogianni, N. T. Skoulikidis, E. Diamantini, B. Majone, A. Bellin, G. Chiogna, E. Martinez, M. López de Alda, M. S. Díaz-Cruz, and P. Grathwohl, “Particle bound pollutants in rivers: Results from suspended sediment sampling in Globaqua River Basins,” *Science of The Total Environment*, vol. 647, pp. 645–652, Jan. 2019, ISSN: 00489697. DOI: 10.1016/j.scitotenv.2018.08.027. [Online]. Available: <https://linkinghub.elsevier.com/retrieve/pii/S0048969718329966>.
- [128] J. Wang, Y. Zhao, L. Yang, N. Tu, G. Xi, and X. Fang, “Removal of Heavy Metals from Urban Stormwater Runoff Using Bioretention Media Mix,” *Water*, vol. 9, no. 11, p. 854, 2017, ISSN: 2073-4441. DOI: 10.3390/w9110854. [Online]. Available: <http://www.mdpi.com/2073-4441/9/11/854>.
- [129] R. Field and D. Sullivan, *Wet-Weather Flow in the Urban Watershed: Technology and Management*. CRC Press, 2002, p. 229, ISBN: 9781420012774. [Online]. Available: <https://books.google.co.uk/books?id=EmuDk3G4vVOC>.
- [130] Hydro International Ltd, “Up-Flo Filter Operation and Maintenance Manual,” Tech. Rep. [Online]. Available: www.hydro-int.com.

Appendix A

PERMEABILITY EXPERIMENT IDENTIFICATION TABLE

Table A.1: Permeability Experiment Number Identification Table. (Long)

Experiment Number	Date	Flow Rate [L/s]	Flow Condition	Notes	Reynolds Number
T01	23/05/17	Max 10	Valve Training [VT]	NT	-
T02	23/05/17	4	One Stage	NP	6.94
T03	20/07/17	Max 10	VT	NT	-
T04	20/07/17	3.5	One Stage	-	6.07
T05	21/07/17	2	One Stage	-	3.47
T06	26/07/17	2	Two Stage	-	3.47
T07	26/07/17	Max 10	VT	NT	-
T08	03/08/17	2	Two Stage	-	3.47
T09	03/08/17	Max 10	VT	NT	-
T10	04/08/17	2	Two Stage	-	3.47
T11	09/08/17	2	Two Stage	-	3.47
T12	11/08/17	2	One Stage	-	3.47
T13	15/08/17	5	One Stage	-	8.67
T14	16/08/17	5	Two Stage	-	8.67
T15	29/08/17	3.5	One Stage	-	6.07
T16	30/08/17	3.5	Two Stage	-	6.07
T17	07/09/17	2.75	One Stage	-	4.77

Continuation of Table A.1					
Experiment Number	Date	Flow Rate [L/s]	Flow Condition	Notes	Reynolds Number
T18	08/09/17	2.75	Two Stage	-	4.77
T19	14/09/17	Max 10	VT	NT	-
T20	20/09/17	2.75	One Stage	-	4.77
T21	21/09/17	2.75	Two Stage	-	4.77
T22	22/09/17	2.5	One Stage	-	4.34
T23	25/09/17	2.5	Two Stage	-	4.34
T24	23/11/17	2	Two Stage	ST01 CWC	3.47
T25	24/11/17	2	Two Stage	ST01 CWC NT	3.47
T26	27/11/17	2	Two Stage	ST01 CWC NT	3.47
T27	28/11/17	2	Two Stage	ST01 CWC	3.47
T28	29/11/17	2	Two Stage	ST01	3.47
T29	03/04/18	2	Two Stage	ST02 CWC MC	3.47
T30	04/04/18	2	Two Stage	ST02 CWC NT	3.47
T31	05/04/18	2	Two Stage	ST02 CWC NT	3.47

Continuation of Table A.1					
Experiment Number	Date	Flow Rate [L/s]	Flow Condition	Notes	Reynolds Number
T32	06/04/18	2	Two Stage	ST02 CWC	3.47
T33	09/04/18	2	Two Stage	ST02	3.47
T34	10/04/18	2	Two Stage	ST02	3.47
T35	25/04/18	2	Two Stage	ST03 CWC MC UW	3.47
T36	26/04/18	2	Two Stage	ST03 CWC NT UW	3.47
T37	27/04/18	2	Two Stage	ST03 CWC NT UW	3.47
T38	30/04/18	2	Two Stage	ST03 CWC UW	3.47
T39	01/05/18	2	Two Stage	ST03 UW	3.47
T40	02/05/18	2	Two Stage	ST03 UW	3.47
End of Table A.1					

Appendix B

PERMEABILITY CHAPTER APPENDIX

The following files are available at the following link: <https://goo.gl/9qNv6e>

B.1 VT.jpg

B.2 Hydro UpFlo Installation Blueprint.pdf

B.3 Flow control.vi

B.4 Error propagation.pdf

B.5 ST02 M4 Camera Calibration.pdf

B.6 ST03 M4 Calibration.pdf

B.7 PERMCOMPLETE v2.m

B.8 PSA Settings.pdf

B.9 Sand.pdf

Appendix C

ACOUSTIC EXPERIMENT IDENTIFICATION

TABLE

Table C.1: Acoustic Experiment Number Identification Table. (Long)

Experiment Number	Date	Media	Set Up	Transducer or Hydrophone
AT42	06/03/17	Water	Vacuumed Test	Transducer
AT43	07/03/17	Water	Vacuumed Test	Transducer
AT44	08/03/17	Water	Vacuumed Test	Transducer
AT45	14/03/17	50% Clogged Media	Vacuumed Test	Transducer
AT46	15/03/17	Dirty Water	Vacuumed Test	Transducer
AT47	15/03/17	Water (for reference)	Vacuumed Test	Transducer
AT48	16/03/17	Saturated Fraction B Sand	Vacuumed Test	Transducer
AT49	04/04/17	5% Clogged Media	Vacuumed Test	Transducer
AT50	05/04/17	5% Clogged Media	Vacuumed Test	Transducer
AT51	20/04/17	10% Clogged Media	Vacuumed Test	Transducer
AT52	28/04/17	20% Clogged Media	Vacuumed Test	Transducer
AT53	11/05/17	Water	Vacuumed Test	Transducer
AT54	15/05/17	Saturated Fraction B Sand	Non-Vacuumed Test	Transducer
AT55	15/05/17	Saturated Fraction B Sand	Non-Vacuumed Test	Transducer
AT56	17/05/17	Saturated Fraction B Sand	Non-Vacuumed Test	Transducer

Continuation of Table C.1				
Experiment Number	Date	Media	Set Up	Transducer or Hydrophone
AT57	19/05/17	Saturated Fraction B Sand	Non-Vacuumed Test	Transducer
AT58	22/05/17	Saturated Fraction B Sand	Non-Vacuumed Test	Transducer
AT59	24/05/17	20% Clogged Media	Non-Vacuumed Test	Transducer
AT60	25/05/17	20% Clogged Media	Non-Vacuumed Test	Transducer
AT61	31/05/17	20% Clogged Media	Non-Vacuumed Test	Transducer
AT62	01/06/17	Dry Fraction B Sand	Bagged Test	Transducer
AT63	01/06/17	Saturated Fraction B Sand	Bagged Test	Transducer
AT64	01/06/17	5% Clogged Media	Bagged Test	Transducer
AT65	01/06/17	10% Clogged Media	Bagged Test	Transducer
AT66	01/06/17	15% Clogged Media	Bagged Test	Transducer
AT67	01/06/17	20% Clogged Media	Bagged Test	Transducer
AT68	05/06/17	5% Clogged Media [Damp Mix]	Bagged Test	Transducer
AT69	05/06/17	Water & Water in Bag	Bagged Test	Transducer
AT70	05/06/17	5% Clogged Media [Damp Mix]	Bagged Test	Transducer
AT71	05/06/17	5% Clogged Media Deaired	Bagged Test	Transducer
AT72	07/06/17	10% Clogged Media	Bagged Test	Transducer
AT73	08/06/17	Saturated Fraction B Sand Non-Deaired	Bagged Test	Transducer

Continuation of Table C.1				
Experiment Number	Date	Media	Set Up	Transducer or Hydrophone
AT74	08/06/17	Saturated Fraction B Sand Non-Deaired Filled Slowly	Bagged Test	Transducer
AT75	08/06/17	10% Clogged Media Deaired 3 hours	Bagged Test	Transducer
AT76	12/06/17	Saturated Fraction B Sand	Bagged Test	Transducer
AT77	12/06/17	10% Clogged Media	Bagged Test	Transducer
AT78	13/06/17	10% Clogged Media Deaired 16 hours	Bagged Test	Transducer
AT79	13/06/17	10% Clogged Media Deaired 4 hours	Bagged Test	Transducer
AT80	27/06/17	Saturated Fraction B Sand	Bagged Test	Transducer
AT81	27/06/17	Saturated Fraction B Sand	Bagged Test	Transducer
AT82	28/06/17	Saturated Fraction B Sand	Bagged Test	Transducer
AT83	29/06/17	Water	Hydrophone Test	Hydrophone
AT84	29/06/17	Saturated Fraction B Sand [Filled Slowly]	Hydrophone Test	Hydrophone
AT85	04/07/17	Saturated Fraction B Sand Deaired 16 hours	Hydrophone Test	Hydrophone
AT86	04/07/17	Water	Hydrophone Test	Hydrophone
AT87	25/07/17	Water	Hydrophone Test	Hydrophone
AT88	25/07/17	Saturated Fraction B Sand Deaired	Hydrophone Test	Hydrophone
AT89	25/07/17	20% Clogged Media Deaired	Hydrophone Test	Hydrophone
AT90	25/07/17	20% Clogged Media Non- Deaired	Hydrophone Test	Hydrophone

Continuation of Table C.1				
Experiment Number	Date	Media	Set Up	Transducer or Hydrophone
AT91	25/07/17	Saturated Fraction B Sand Non-Deaired	Hydrophone Test	Hydrophone
AT92	05/10/17	Various Media	Hydrophone Sinu- soidal Sweep Test	Hydrophone
AT93 (T29)	03/04/18	Up-Flo [®] Filter Media	ST02 Clean Water Test	Transducer
AT94 (T32)	06/04/18	Up-Flo [®] Filter Media	ST02 Clean Water Test	Transducer
AT95 (T33)	07/04/18	Up-Flo [®] Filter Media	ST02 Sediment Test (Silica Flour)	Transducer
AT96 (T34)	08/04/18	Up-Flo [®] Filter Media	ST02 Sediment Test (Silica Flour)	Transducer
AT97 (T35)	25/04/18	Up-Flo [®] Filter Media	ST03 Clean Water Test	Transducer
AT98 (T39)	01/05/18	Up-Flo [®] Filter Media	ST03 Sediment Test (Fraction E)	Transducer
AT99 (T40)	02/05/18	Up-Flo [®] Filter Media	ST03 Sediment Test (Fraction E)	Transducer
End of Table C.1				

Appendix D

FILTER MONITORING APPENDIX

The following files are available at the following link: <https://goo.gl/K2Do7W>

D.1 Olympus Transducer Calibration Sheets.pdf

D.2 Oscilloscope Settings.set

D.3 Transducer LabVIEW Continuous Signal Programme.vi

D.4 AT42 to AT82 FFT Analysis.m

D.5 AT83 to AT92 FFT Analysis.m

D.6 AT93 to AT99 Integral Code.m

D.7 Conductance Probe Design.pdf

D.8 Sediment Conductance Control File.vi

D.9 Conductance Analysis File.m

Appendix E

FILTER GUIDELINES APPENDIX

The following files are available at the following link: <https://goo.gl/gvBDji>

E.1 China Standards.pdf

The standard presented in this document was taken from the english translation of the standard provided by the Ministry of Ecology and Environment. [125]